Durham E-Theses

Sedimentology, Diagenesis and Reservoir Characteristics of Eocene Carbonates Sirt Basin, Libya

SWEI, GIUMA,HEDWI

How to cite:

SWEI, GIUMA,HEDWI (2010) *Sedimentology, Diagenesis and Reservoir Characteristics of Eocene Carbonates Sirt Basin, Libya*, Durham theses, Durham University. Available at Durham E-Theses Online: http://etheses.dur.ac.uk/491/

Use policy

DEPARTMENT OF EARTH SCIENCES, DURHAM UNIVERSITY

Sedimentology, Diagenesis and Reservoir Characteristics of Eocene Carbonates Sirt Basin, Libya

A thesis submitted to the Durham University
for the degree of Doctor of Philosophy in the
Faculty of Science

Giuma Hedwi Swei

2010

DEDICATION

In the name of Allah, most merciful, most gracious

I would like to dedicate this work to my dear beloved mother, may Allah preserve her. This work is dedicated to the spirit of my beloved father (God have mercy), who was the first encourager and supporter to me in continuing my education and praying Allah to me until the last time I saw him.

I dedicate this work also to all my brothers Hessain, Ali and sisters, who have always encouraged and supported me for further study. I would also like to dedicate this work to my beloved wife, who provides me with unlimited care, support and encouragement that I need to achieve my goal and success. Lastly, I dedicate this work to my dearest children Sara, Siraj, Nawfel, Shayma, Rayan and very little Batoul who were patient and endured living in foreignness and suffered as a result of not spending sufficient time with them during the period of my study.

ABSTRACT

The reservoir quality of Middle Eocene carbonates in the intracratonic Sirt Basin (at the northern margin of the African continent) is strongly influenced by depositional facies and various diagenetic modifications. This thesis investigates the petrography, sedimentology, diagenetic evolution and hydrocarbon potential of the Middle Eocene Gialo Formation in the subsurface of the north-central Sirt Basin based on data from core samples and well logs from five boreholes in the Assumood and Sahl gas-fields. Reducing risk in exploration demands an understanding of reservoir facies development, which is governed by the type and distribution of depositional facies and their diagenetic history. Seven major carbonate facies (and 20 microfacies) have been identified in this study and are interpreted as predominantly deposited under shallow-marine conditions within the photic zone, as indicated from their richness in phototrophic fauna and flora. These include lagoon (back-bank), main bank, fore-bank and open-marine facies, all of which were deposited on a homoclinal ramp type of carbonate platform.

The type and distribution of the Gialo depositional facies were influenced by basin-floor architecture and environmental controls. The basin floor was shaped through pre-Eocene structural development into a series of elevated platforms and deep troughs. Platform facies were deposited across three broad facies belts: (1) inner-ramp, dominated by dasycladacean molluscan wackestone/packstone, nummulitic-bryozoan packstone, bryozoan wackestone; (2) mid-ramp, dominated by nummulitic packstone and *Discocyclina*-nummulitic wackestone; and (3) outer-ramp, dominated by fragmented nummulitic packstone. Troughs were dominated by thick successions of lime mudstone containing rare fine skeletal fragments and nummulites, with deposition taking place in a deeper-marine environment, below the photic zone.

Present-day reservoir characteristics of the Gialo Formation are the net result of modification to the original depositional characteristics caused by diagenesis. This diagenesis took place on the seafloor, under burial, and in the meteoric diagenetic environment. Early marine diagenetic processes affecting the Middle Eocene Gialo carbonates resulted in micritization of bioclasts. Later diagenesis in meteoric to burial environments resulted in dissolution of aragonitic bioclasts, cementation (syntaxial

overgrowths on echinoid grains, and blocky to equant, non-ferroan cements), neomorphism, pressure dissolution, compaction and fracturing. $\delta^{18}O$ and $\delta^{13}C$ values in the Gialo Formation range between -1.06 and -4.16‰ PDB, and 0.76 and 1.89‰ PDB, respectively. These values are mostly marine values, although some alteration is likely. The more negative oxygen of the cements suggests precipitation within the shallow-burial environment under the influence of meteoric water and / or precipitation at higher temperatures during further burial. The carbon isotopic signatures are typical marine values. There is a strong relationship between porosity and the diagenetic processes that-affected the Gialo sediments.

Generally the porosity in the Assumood and Sahl fields is either primary or secondary, enhanced by dissolution and fracturing of the sediments. Reduction in porosity in the investigated sediments is mainly due to cementation and compaction. The common pore-types in the Gialo Formation are intergranular, moldic, intragranular, vuggy and scattered fractures. Porosity ranges from poor to very good (<1% to ~37%) and permeability varies from low to high (<1mD to 100mD). These variations in porosity and permeability are strongly related to facies changes, which were influenced by depositional environment and diagenetic processes. Shallow-water packstones/rudstones containing both primary intergranular and secondary biomouldic porosity have the best reservoir quality. The Gialo Formation is an important gas producing reservoir in the Assumood, Sahl and other surrounding fields. The gas which is generated from the gas-prone Sirt Shale source rock of the northern Ajdabiya Trough possibly migrated onto the Assumood Ridge from the northeast through late Cretaceous, Paleocene and early Eocene carbonates, before being trapped beneath the Augila Shale (Upper Eocene) which is the principal regional seal in the area. This integrated study has helped to understand the reservoir heterogeneity and potential of the Gialo carbonates and based on this current wells are being completed appropriately, as, hopefully, will future wells too.

The facies pattern is different from one well to another, which does suggest that there was a strong tectonic control, that is differential tectonic subsidence and/or fault control, or that deposition was controlled by autocyclic processes. The different vertical positions and numbers of transgressive-regressive cycles in each well make formation-wide correlation problematic. The lack of correlation in terms of cycle thickness, as well as facies, between wells, also suggests autocyclic processes. Third and fourth-order

relative sea-level (RSL) changes do not appear to have been a major control on deposition during this Middle Eocene time.

Table of Contents

Chapter 1.

Chapter 2,

Chapter 3.

Chapter 5.

Chapter 6.

List of Figures

Chapter 1:

Chapter 2:

Chapter 3.

Chapter 5.

List of Tables

ACKNOWLEDGEMENTS

Finally, I would like to thank my family, my wife and my children, for giving me love, happiness and joy; and for their endless support, encouragement and patience.

DECLARATION

No part of this thesis has previously been submitted for a degree at this or any other university. The work described in this thesis is entirely that of the author, except where reference is made to previously published or unpublished work.

Giuma Hedwi Swei
Durham University
Department of Earth Science
September 2010

The copyright of this thesis rests with the author. No quotation or data from it should be published without the author's prior written consent and any information derived from it should be acknowledged.

CHAPTER 1: INTRODUCTION

1.1. General Introduction

Middle Eocene deposition in the Sirt Basin in Libya has been the subject of considerable study in recent years because of the importance of sediments of this age as hydrocarbon reservoirs. This study investigates the sedimentology, diagenesis and sequence stratigraphy of the Middle Eocene Gialo reservoir unit in the Sirt Basin, onshore north-central Libya. The study presented in this thesis concentrates on the Gialo Formation, and includes the analysis and interpretation of data from five exploration wells drilled by Sirte Oil Company within Concession 6. The focus of this study, the Gialo Formation, is the one of the main reservoir targets in the nearby Assumood and Sahl gas fields.

1.2. Reason for Study

Petroleum is the backbone of the Libyan economy. Exploration started in the late fifties and giant oil fields have been discovered in many of the sedimentary basins (Figure 1.1), the most important of which is the Sirt Basin where more than 75% of the country's known petroleum reserves are located. It ranks 15th among the world's petroleum provinces with 43.1 billion barrels of oil equivalent (BBOE) of known petroleum volume (Klett and others, 1997).

Libya produces high-quality, low-sulphur ("sweet") crude oil at very low cost (as low as $1 per barrel in some fields). During the first half of 2003, Libyan oil production was estimated at nearly 1.5 million bbl/d, an increase from 2002 levels but still only about two-fifths of the 3.3 million bbl/d produced in 1970. Total proven oil reserves were 39 billion barrels at the end of 2005.

Continued expansion of natural gas production remains a high priority for Libya for two main reasons. First, Libya has aimed (with limited success) to use natural gas instead of oil domestically, freeing up more oil for export. Second, Libya has vast natural gas reserves and is looking to increase its gas exports, particularly to Europe. Libya's proven natural gas reserves in 2003 were estimated at 46.4 Tcf (17th largest gas reserve in the world) (Ahlbrandt, 2002), but the country's actual gas reserves are largely unexploited (and unexplored), and thought by Libyan experts to be considerably
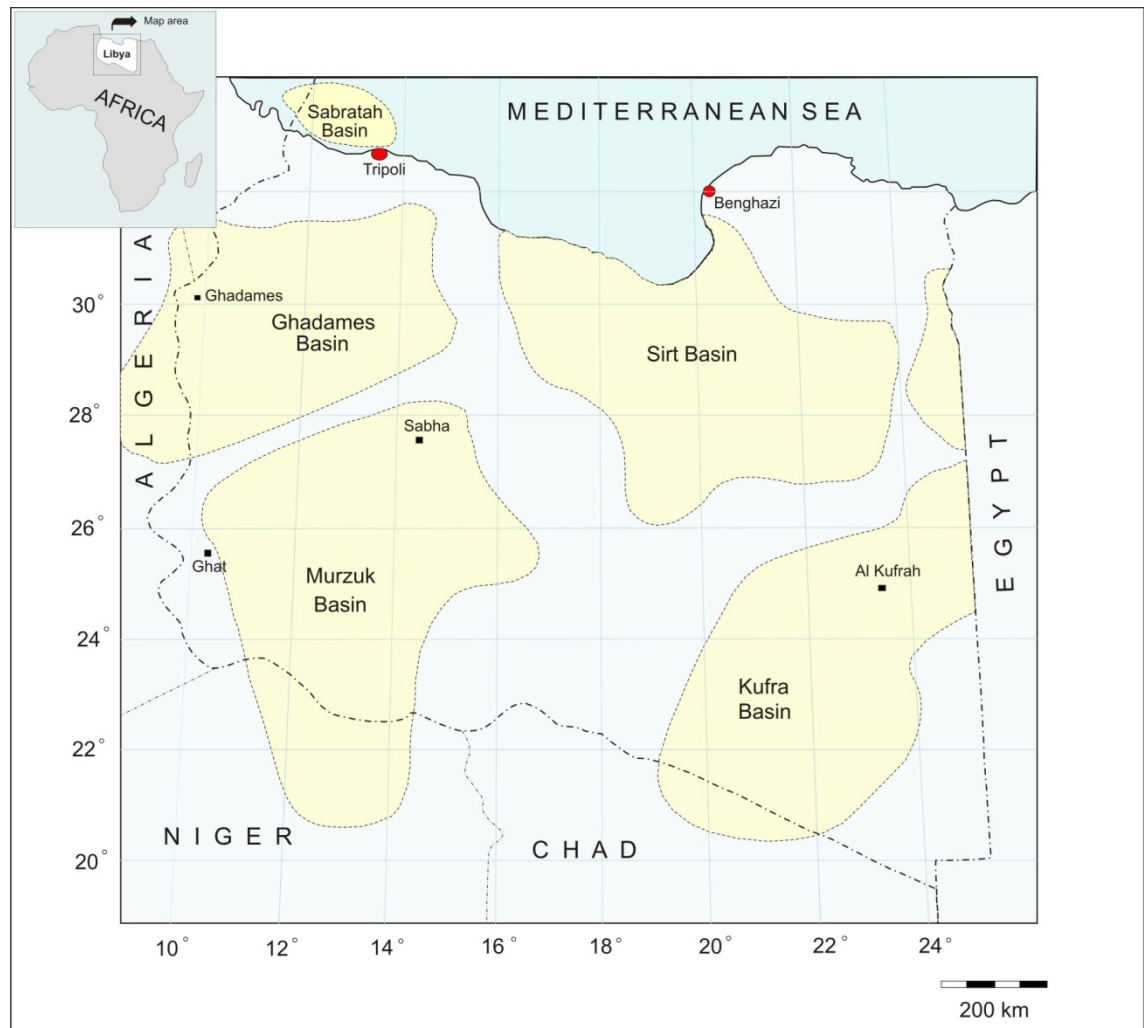
Figure.1.1. Distribution of Sedimentary Basins in Libya.

larger, possibly 50-70 Tcf. Major producing fields include Attahaddy, Defa-Waha, Hatiba, and Zelten, as well as the Sahl and Assumood fields, described in this thesis (Figure 1.2). Although some studies have evaluated aspects of the petroleum system in Libya, still just 37 percent of Libya has been explored for hydrocarbons. Additional studies, such as this, focused on the North Central Sirt Basin, are required to inform future hydrocarbon exploration and production strategies. Carbonates in Libya are major reservoir units, with significant production from Eocene nummulitic deposits (Figure 1.3). Although some of these carbonates have been the subject of sedimentological and diagenetic examination (El-Hawat *et al*., 1986), those in the North Central Sirt Basin have never been studied in detail. This is despite major gas discoveries in the Assumood and Sahl gas fields.
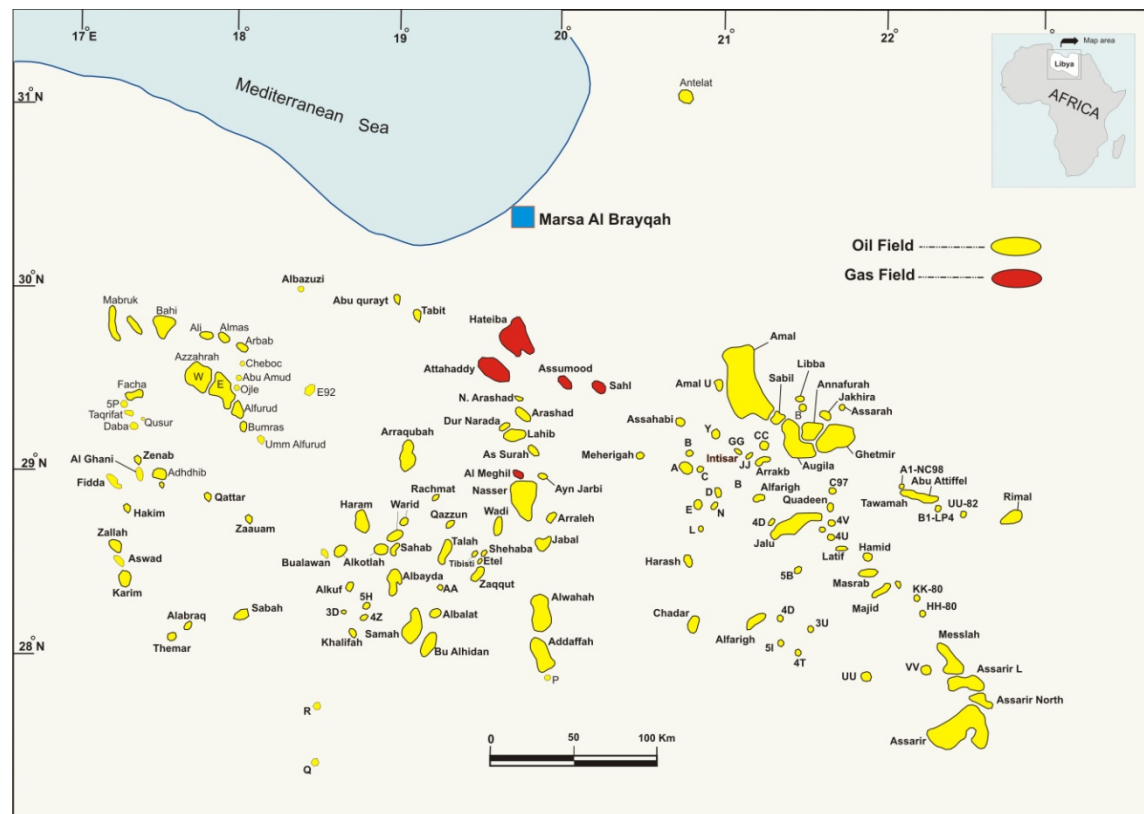
Figure 1.2. Location of oil and gas fields in the Sirt Basin (after Wenneker *et al*., 1996).

Globally, there is considerable variability in the reservoir potential of Eocene carbonates, even within Libya, and within individual fields, reservoir development is usually highly variable. Future research is required to investigate the controls on spatial and temporal reservoir development.

1.3. Aims of study

The general aims of this thesis are: (i) to investigate the primary facies development and architecture of the Middle Eocene Gialo Formation, (ii) to characterize the depositional environment and evaluate controls on sedimentation in this area, (iii) to investigate the depositional and diagenetic factors that influence permeability and porosity, and to determine whether analysis from existing core data may be applied to uncored intervals, (iv) to help develop predictive models to evaluate the use of sequence stratigraphy as a tool to aid in understanding the distribution of important reservoir rocks, in the Assumood and Sahl fields particularly, and (v) to comment on the regional hydrocarbon potential in the light of these findings.

GENERALIZED STRATIGRAPHIC SECTION CONCESSION 6

CENOZOIC	TERTIARY	OLIGOCENE	ARIDA	
		U. EOCENE	AUGILA	
		MIDDLE EOCENE	GIALO	
		LOWER EOCENE	GIR HON EVAP. / FACHA DOL.	MESDAR
			KHEIR / HARASH	
		PALEOCENE	ZELTEN	
			KHALIFA CARB. / KHALIFA SHALE	
			HAGFA SHALE / DAHRA / MEEM/BEDA	
			SATAL	
MESOZOIC		UPPER CRETACEOUS	KALASH	
			SIRTE	
PALAEOZOIC		CAMBRO-ORDOVICIAN	BAHI	
			GARGAF	
		PRECAMBRIAN		
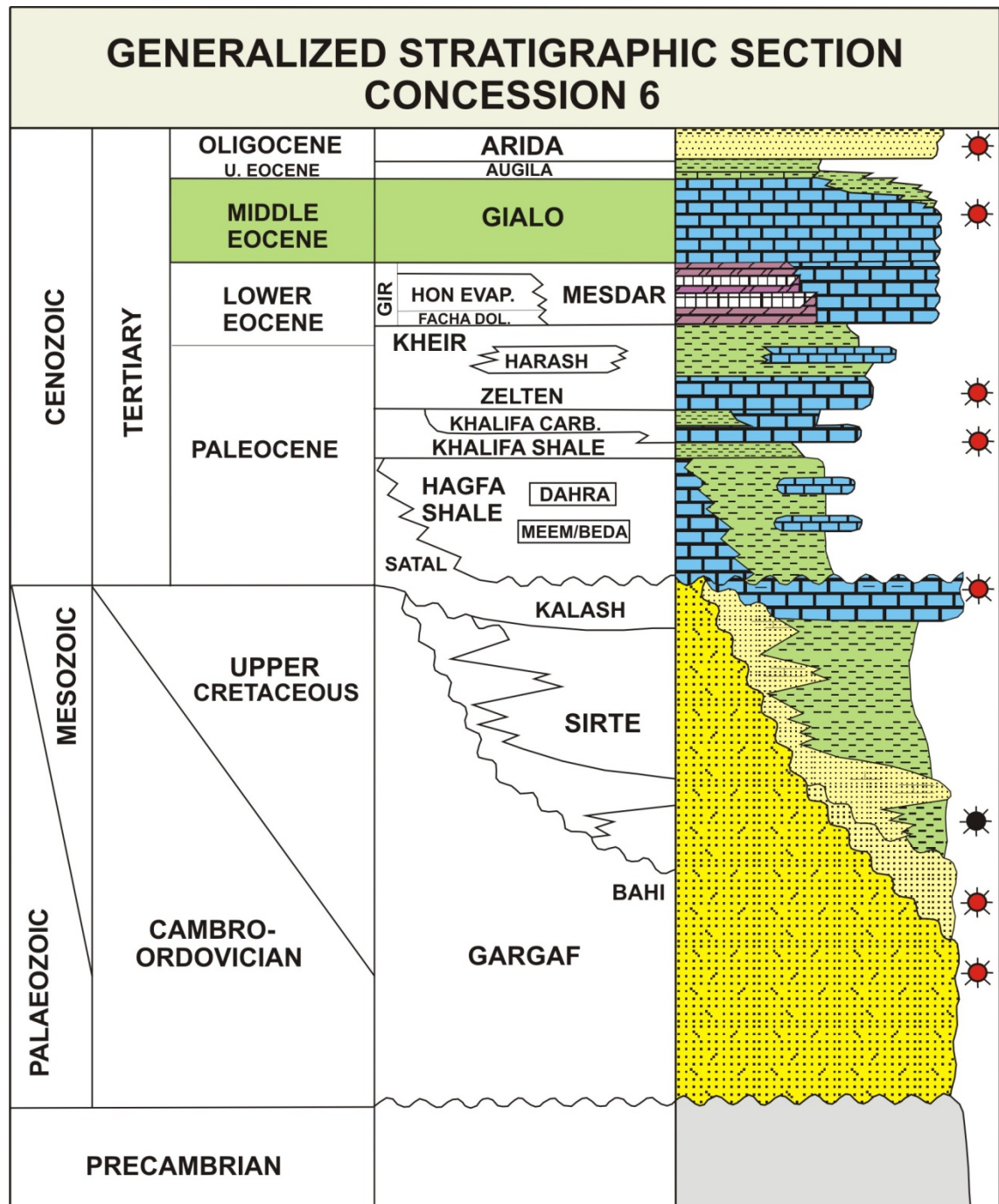
Figure 1.3. Generalized columnar stratigraphic section of Concession 6 (after El Ghoul, 1996).

1.4. Specific Objectives

In an attempt to further our understanding of the geology of Concession 6 (Assumood and Sahl Fields), in the Central Sirt Basin within the general aims of the thesis and constraints imposed by the available database (Appendix II), a number of specific questions will be addressed, as follows.

(1) What are the principal sedimentary facies of the Middle Eocene succession, and what are their chief petrographic and mineralogical characteristics?

(2) How are these facies distributed both spatially and temporally?

(3) What can be deduced from the nature of the facies, their mineralogy and distribution concerning the palaeoenvironments of deposition?

(4) Can a regionally specific depositional framework or model be derived and how does this compare with previous work in the area and with other carbonate depositional models worldwide?

(5) How extensive was the nummulite-dominated depositional system in the areas of study and what is its particular characteristics?

(6) What were the principal controls on sedimentation, including tectonic activity, sea-level changes and sediment supply/production?

(7) What are the specific diagenetic characteristics of the various carbonate facies, what were the processes involved and the relative timing of these changes, and what are the controls on reservoir development?

(8) What are the various features of the sediments, including porosity-permeability characteristics, that help determine hydrocarbon potential in the region? Are the nummulitic bank and other shoal facies good potential reservoirs?

1.5. The area of study

The area of investigation is situated onshore North-Central Libya, in the Sirt Basin in the north-east part of North Concession 6 (Figure. 1.4). Three fields have been chosen (Assumood, North Assumood and Sahl Fields). Geographically, the area is located approximately between latitudes 29° 20' 00" and 29° 40' 00" and longitudes 19° 50' 00" and 20° 15' 00". Assumood is bounded to the north by the Agedabia Trough and to the south by the Wadayat Trough (Figure. 1.5). Assumood discovery well H1-6 was drilled in 1960 to a total depth of 10,284 feet (see note below at end of this section) in Cambro-Ordovician Gargaf Quartzitic Sandstone Formation, and tested commercial gas from the Middle Eocene Gialo Formation. Since then, a total of twelve wells were drilled to outline the field to a depth ranging from 5260 to 10,272 feet (H7-6). These wells penetrated a series of sedimentary rocks ranging in age from the Cambro-Ordovician Gargaf Quartzitic Sandstone Formation to Oligocene. Middle Eocene Gialo Formation is the main proven reservoir interval in the study area. The Sahl Gas Field is

located to the east of the Assumood Field (Fig 1.5 and 1.6). It was discovered in 1962 and is producing gas from Middle Eocene carbonates of the Gialo Formation, which is considered to be the main reservoir in this field. The surrounding gas fields are the Hateiba Field to the north-west and the Attahaddy Field to the west.

*Note: It is the convention in Libya to use feet in the oil industry, and this tradition is continued in this thesis.
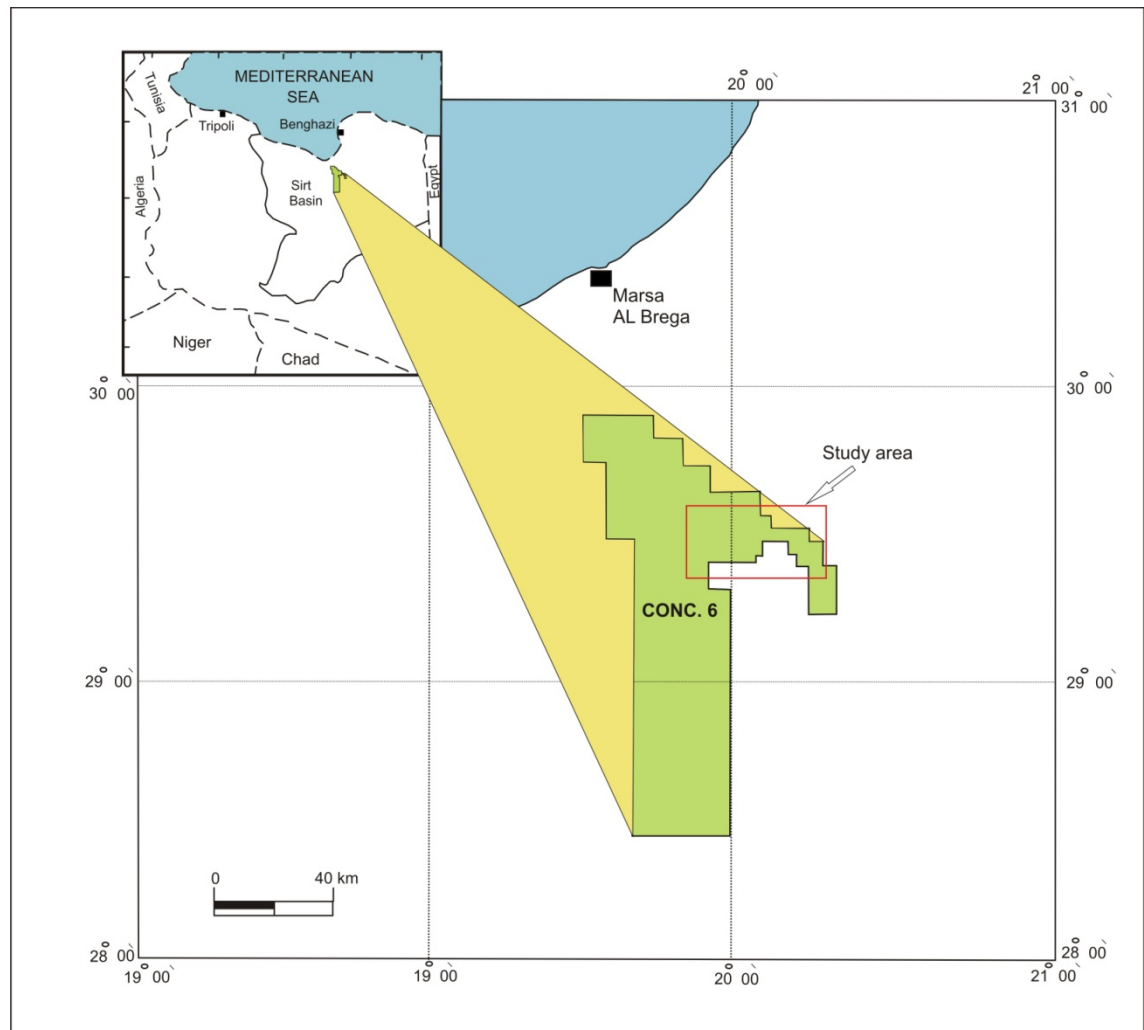
Figure 1.4. Study area location map.
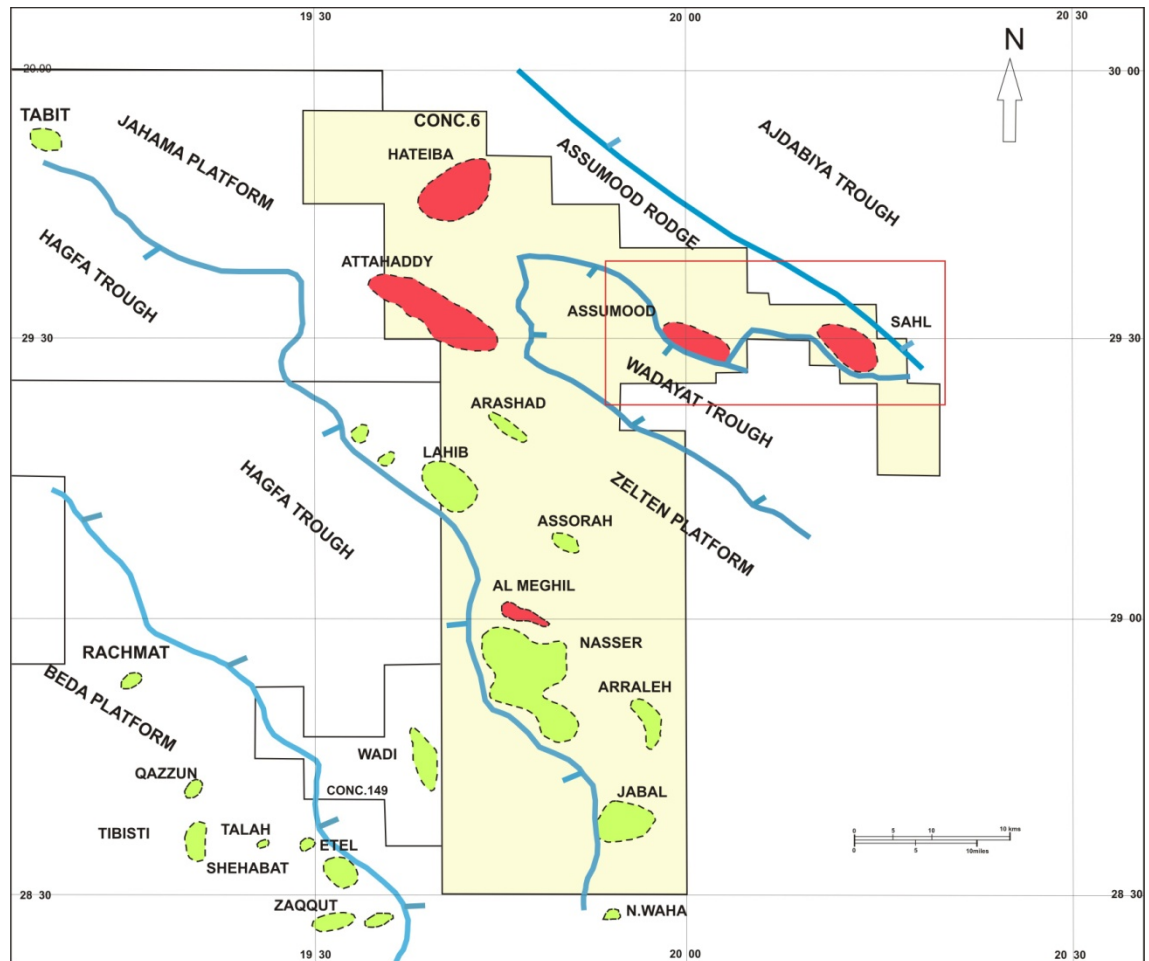
Figure 1.5. The tectonic framework of Concession 6 showing the main subsurface features that developed during Late Cretaceous rifting and the studied fields (after Parrella, 1990).

1.6. Database and methodology

This study is based on the investigation of core samples, thin-sections and wireline logs from five wells from three different gas fields, Assumood, North Assumood and Sahl Fields (OOOO1, O3, H4, H6 and H10-6). The thicknesses of core available are shown in Table 1.1 and Figure 1.7 and the location of the wells are shown in Figure 1.6. The cores all come from the upper parts of the Gialo Formation and since the thickness of the Gialo Formation is up to 1000 feet, it is only the upper fifth (~20%) of the Gialo that is available for detailed study (Figure 1.7). The laboratory investigation included descriptions and logging of approximately 600ft of cores by using a hand lens and binocular microscope. This work was carried out at the Sirte Oil Company laboratory in Brega Libya prior to arrival in Durham. Samples from these cores were

collected every one or two feet, wherever there was a change, and the specific features of interest were photographed.
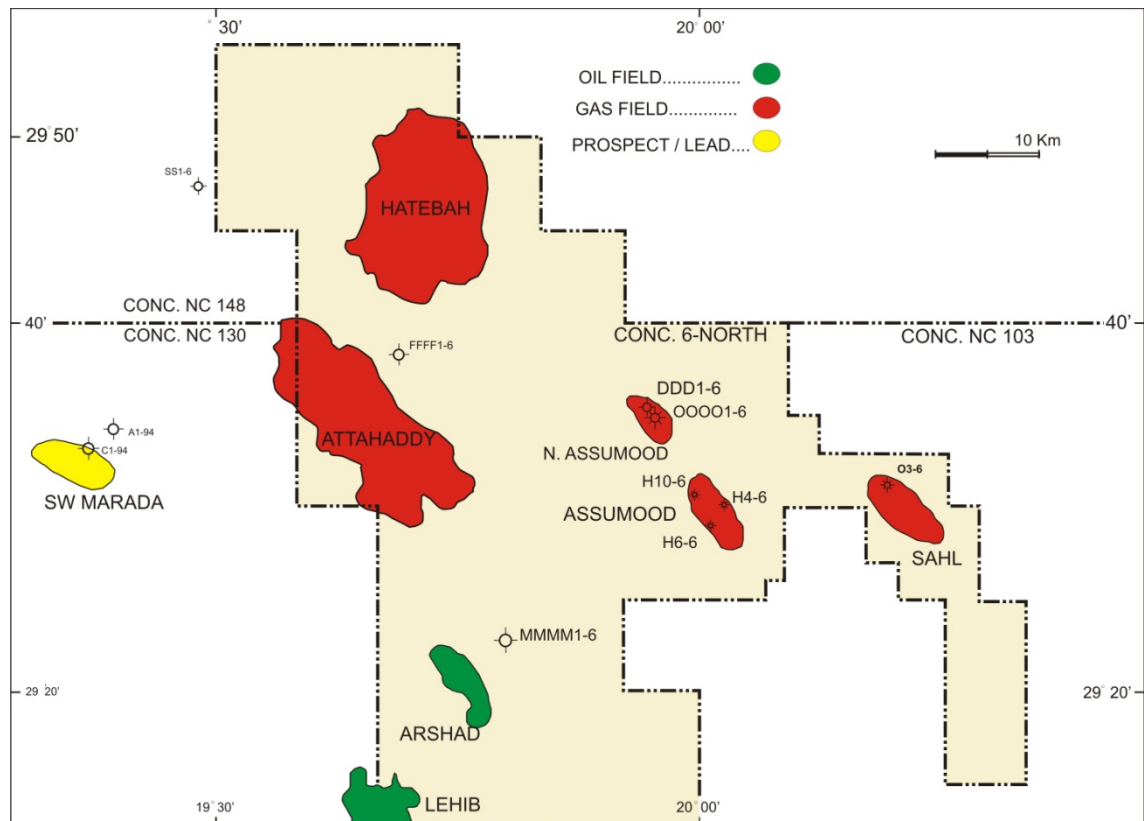
Figure 1.6. Location map of the area showing the location of the fields (Assumood, North Assumood and Sahl Fields) and the wells analysed in this study.

Approximately 175 polished and unpolished thin-sections were prepared in the Earth Science labs at Durham University. These thin-sections were examined petrographically in order to observe rock fabric and to determine the presence and abundance of constituent grains, matrix and cements. Half of each thin-section was stained with alizarin red S and potassium ferricyanide, following the methodology of Dickson (1965, 1966) to distinguish between ferroan- and non-ferroan calcite, dolomite and iron-rich dolomite. The stained thin-sections were covered to protect the sections from damage. Percentages of constituents within the sections were determined using point counting. The terms employed to describe the crystallization fabrics follow Friedman (1965), and those employed in carbonate classification, in principle, follow Dunham (1962). The terms employed in carbonate grain-size measurements follow Wentworth (1922). Determination of the type of porosity uses the descriptive and identification scheme established by Choquette and Pray (1970). Some thin-sections were impregnated with

Well Name	Depth interval of Middle Eocene section (feet)	Interval of cores studied (feet)
OOOO1-6	5105 – 6235	5127 – 5246
O3 - 6	5115 – NDE	5125 – 5373
H4 - 6	4900 – NDE	4905 - 5112
H6 - 6	4879 – NDE	4921 – 5105
H10 - 6	4930 – NDE	4956 – 5084

* NDE – Not deep enough

Table 1.1. Intervals of core studied and the depth of Middle Eocene sections in the investigated wells.
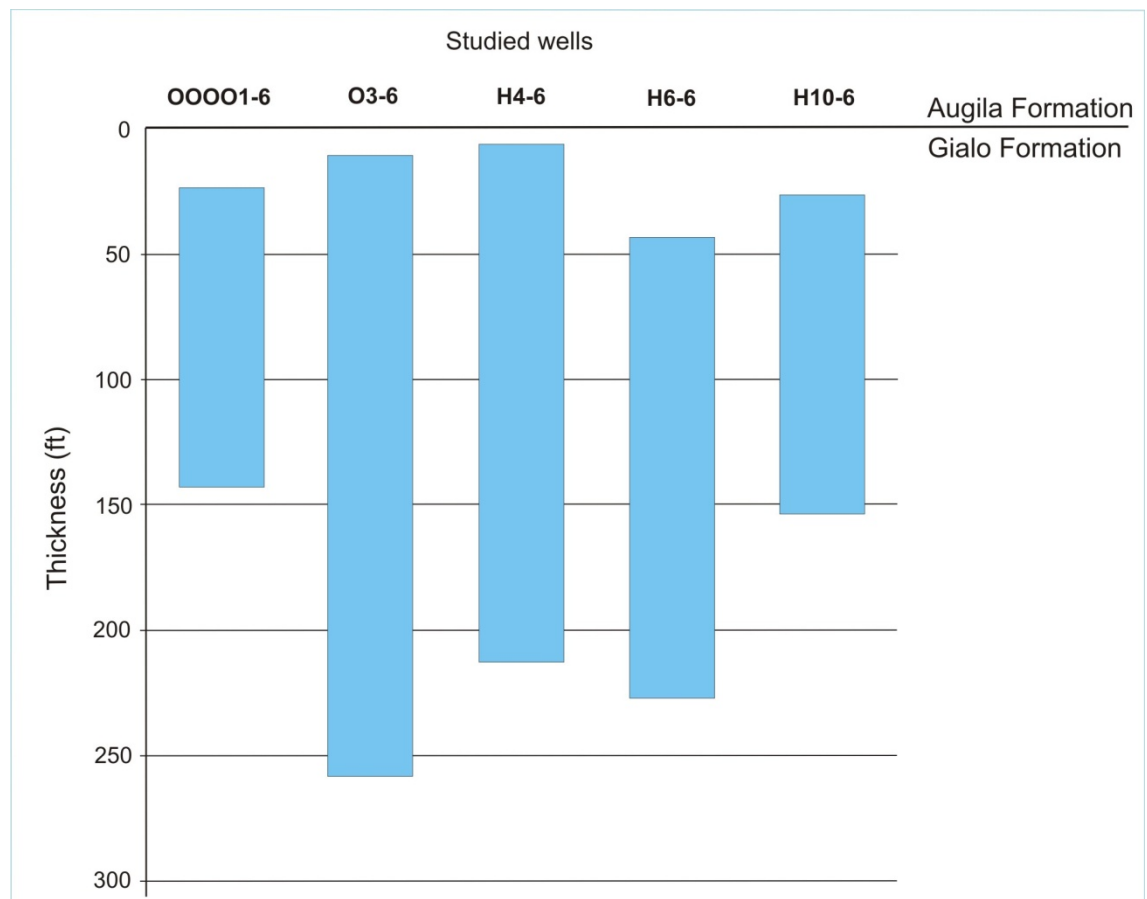
Figure 1.7. Thickness of core studied from the Gialo Formation.

blue-dyed resin in order to determine the relative porosity of the rock. Polished thin-sections were used for petrographic examination by cathodoluminescence. Representative rough surfaces of limestone samples were coated with gold and

examined under SEM to show the different textural features and crystal morphology, as well as the nature of the intercrystalline porosity.

1.7. Thesis layout

This thesis contains a large amount of new data. It was considered necessary to discuss results from one section of the work before moving onto a completely new section. Each of chapters 2-6 contains a summary section, which extracts the principal findings in each case. Further details of this layout are given here so that the results can be clearly identified and separated from the discussion and principal findings.

Chapter 1. THESIS INTRODUCTION

This chapter introduces the general issues, reasons for the study, aims of project, specific objectives and the geographical area of study. The database and methodology also are reviewed; more detail of the data available and the techniques used are found in the relevant chapter and / or in an appendix.

Chapter 2. STRUCTURE AND STRATIGRAPHY OF THE SIRT BASIN

The second chapter summarizes data from previous regional geological studies of the Sirt Basin, Libya including the structural elements and tectonic setting. This chapter also includes the stratigraphy and depositional environments for the formations in the Sirt Basin.

Chapter 3. REVIEW OF EOCENE NUMMULITIC ACCUMULATIONS AND PALAEOENVIRONMENTS

This chapter introduces and describes the general environments of Eocene nummulite deposition and the main factors which controlled the distribution of Eocene nummulitid and other larger benthic foraminifera, the test size and the shape of the foraminifera. Facies models that have been proposed for nummulite deposits and their reservoir quality are also presented.

Chapter 4. FACIES ANALYSIS AND DEPOSITIONAL ENVIRONMENTS OF THE GIALO FORMATION

This chapter discusses the sedimentology of the Gialo Formation (Middle Eocene) in five selected wells for three different fields located in Concession 6, North Central Sirt

Basin, and includes a section on previous work. The main facies and microfacies in the Gialo Formation are described on the basis of core description and petrographic analysis of thin-sections under the transmitted light microscope. Also included are detailed results of laboratory porosity and permeability measurements. There is a section on the subsurface wireline logs, a discussion of the correlation of wireline logs with the identified facies, and a review of the porosity and permeability of the studied sedimentary rocks (based on core analysis and wireline logs). Finally a comparision between the Gialo Formation and other Eocene nummulitic deposits is presented at the end of this chapter for a better understanding of global variations in Paleogene limestones and their reservoir quality.

Chapter 5. DIAGENESIS AND RESERVOIR CHARACTERISTICS OF THE GIALO FORMATION

This chapter provides a brief introduction to carbonate diagenesis, and describes and interprets the main diagenetic features and reservoir quality of the Gialo Formation with data from the scanning electron microscope (SEM), cathodoluminescence (CL) and oxygen and carbon stable isotopes ($\delta^{18}O$ and $\delta^{13}C$). The relative time relationships (paragenetic succession) of the events which have affected the Middle Eocene sediments of north-central Sirt basin during their burial are deduced. The influence of the diagenesis on reservoir equality of the Gialo Formation is discussed and comparison made with other known Eocene Nummulitic reservoirs.

Chapter 6. PETROLEUM GEOLOGY OF THE GIALO FORMATION

This chapter discusses the hydrocarbon potential of Middle Eocene plays in the study area with respect to the source rock, trap types and reservoir rock potential. It also addresses the causes of Gialo reservoir variability across the selected fields in the Sirt Basin, and highlights the importance of integrating wireline log correlations with detailed analysis of the depositional facies and their diagenetic history, for improved exploration potential.

Chapter 7. SEQUENCE STRATIGRAPHY OF THE GIALO FORMATION

This new approach to stratigraphy provides a method for subdividing and describing a succession, which is useful for interpretation and correlation. This chapter includes an

introduction to sequence stratigraphy, definition of some terminology which is used in this study and focuses on the interpretation of the sequence stratigraphy of the Gialo Formation. Since core is only available from the top 20% of the Gialo, it is only this part that can be looked at closely from a sequence stratigraphic point of view. The main objective of this chapter is to assess the vertical variations in the sedimentary succession which may be controlled by relative sea-level change.

The conclusions of this research and recommendations for further work are summarised in *Chapter 8*. Appendices and references used in the thesis follow.

CHAPTER 2: STRUCTURE AND STRATIGRAPHY OF THE SIRT BAIN

2.1. Introduction

Libya is located on the Mediterranean foreland of the African Shield, extends over a platform of cratonic basins that can be divided into two geologic regions, each of which includes a number of sedimentary basins (Figure 2.1). The northern part of the country is situated on a tectonically active subsiding margin (Gumati *et al*., 1991), and includes from west to east the Sabratah Basin, Benghazi Basin, Sirt Basin and Cyrenaica Platform. The southern part of Libya, which lies within a stable cratonic area, includes the Ghadamis and Murzuq Basins to the west, separated by the Tibisti crystalline basement massif from the Al Kufra Basin in the east. As a result of their position at the edge of the African Plate, these basins were affected by successive phases of continental collision and plate divergence (Pickford, 1992). Major hydrocarbon discoveries have been made in the Palaeozoic succession of the Ghadamis and Murzuq Basins, and in the Mesozoic and Cenozoic succession of the Sirt and Sabratah Basins.

The tectonic features of the Sirt Basin were formed by large-scale subsidence and block faulting in response to latest Jurassic/early Cretaceous rifting (Roberts, 1970; Goudarzi, 1980; Guirad and Mourin, 1992; Guiraud, 1998), which controlled the pattern of deposition during the Late Cretaceous and Early Tertiary (Gumati and Kanes, 1985).

2.2. Location of the Sirt Basin and its major structural elements

The Sirt Basin is one of the youngest sedimentary basins of the African Craton, located in the north-central part of Libya (Figure 2.1), with an inshore area of approximately 375,000 Km² and an estimated sedimentary volume of 1.3 million Km³. It contains more than 100 oil and gas fields, including several giants. The basin comprises a broad NW trending embayment. It is bounded to the south by the Tibisti Massif and to the west by the Al Gargaf Uplift and the Ghadamis and Murzuq Basins. To the east, it is bounded by the Cyrenaica Platform and Al Bottnan Basin, and to the north by the Gulf of Sirt (Figure 2.2).
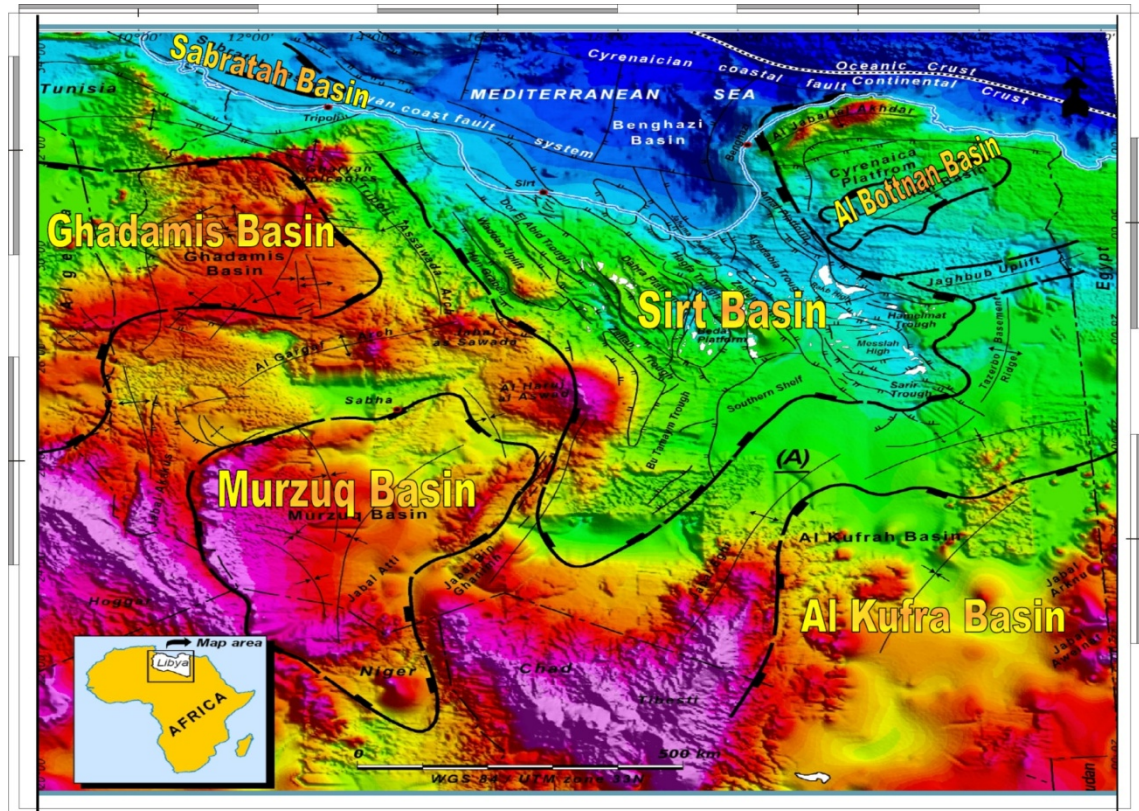
Figure 2.1. Digital topography and the tectonic framework: modified after Mouzughi and Taleb (1981). Digital topography and bathymetry are from GLOBE, NOAA national data centre.

The Sirt Basin comprises four major NW-SE grabens with intervening horsts (Figures 2.1 and 2.3): Hun Graben, Waddan Uplift, Dor El Abid Trough and Zallah Trough, Dahra Platform and Beda Platform, Al Hagfa Trough, Zelten Platform and Al Jahamah Platform, Agedabia Trough and Rakb High. In the southeast, the Agedabia Trough passes into the E-W trending Hameimat and Sarir Troughs. In the southwest, the Dor El Abid Trough continues into the Zallah Trough before swinging S to SSW into the Bu Tumaym Trough. Another important SSW-NNE trending structure is the Kotla Graben, which separates the Beda Platform in the southeast from the Dahra Platform to its northwest. In general, the Sirt Basin displays an asymmetric half-graben style with gentle ENE dipping platforms and steep WSW facing footwalls, so that overall the basin deepens to the ENE.

2.3. Tectonic setting of the Sirt Basin

The Sirt Basin is a major intracratonic rift system on the north central African plate and comprises a complex of horsts and grabens that began to develop in Latest Jurassic time. This complex structure evolved as a rifted embayment on the northern margin of the African Plate. The tectonic evolution of the Sirt Basin includes thermal arching and repeated phases of rifting that culminated in the Late Cretaceous and Paleocene to Early Eocene, and were followed from Late Eocene onward by thermal subsidence. The sedimentary succession of the Sirt Basin reflects its tectonic and structural evolution, which is closely related to the opening of the Atlantic Ocean and the convergence of Tethys in Mesozoic and Tertiary times (Gras and Thusu, 1998).

The Sirt Basin developed following a sequence of tectonic events that led to the break-up of the supercontinent Pangaea. The break-up history of the Gondwana part of Pangaea commenced with the Late Carboniferous and Permian development of the so-called Neo-Tethys and the development of rift systems in Gondwana (Ziegler *et al.*, 2001).

The geological history and the major structural elements of the region were first clearly elucidated by Conant and Goudarzi (1967) and Klitzsch (1970), and further clarified by Massa and Delorte (1984) (Figures 2.2 and 2.4). Early in the geological history, a long period of erosion prevailed throughout North Africa, and by the beginning of the Palaeozoic Era a great part of Libya had been peneplained (Goudarzi, 1980). Precambrian crystalline rocks are exposed in limited and comparatively small areas in south central Libya, west of Jabal Eghi, in the Tibisti area, in the southeastern part near the border with Sudan and Egypt, at Jabal Al Hasawinah north of Brak, and north of Waw an Namus (Figure 2.1).

During the Cambro-Ordovician, up to 1000 m of quartzite sandstone were deposited throughout northern Libya (Anketell, 1996). Thinning of the Silurian succession across the Sirt area, together with alkaline magmatism, presaged the uplift of the Tibisti-Sirt arch (Figures 2.2 and 2.4), during the Hercynian Orogeny (Klitzsch, 1970). Sedimentation continued in the adjacent basins to the east and west, while inversion of the region, together with increased igneous activity, continued during the
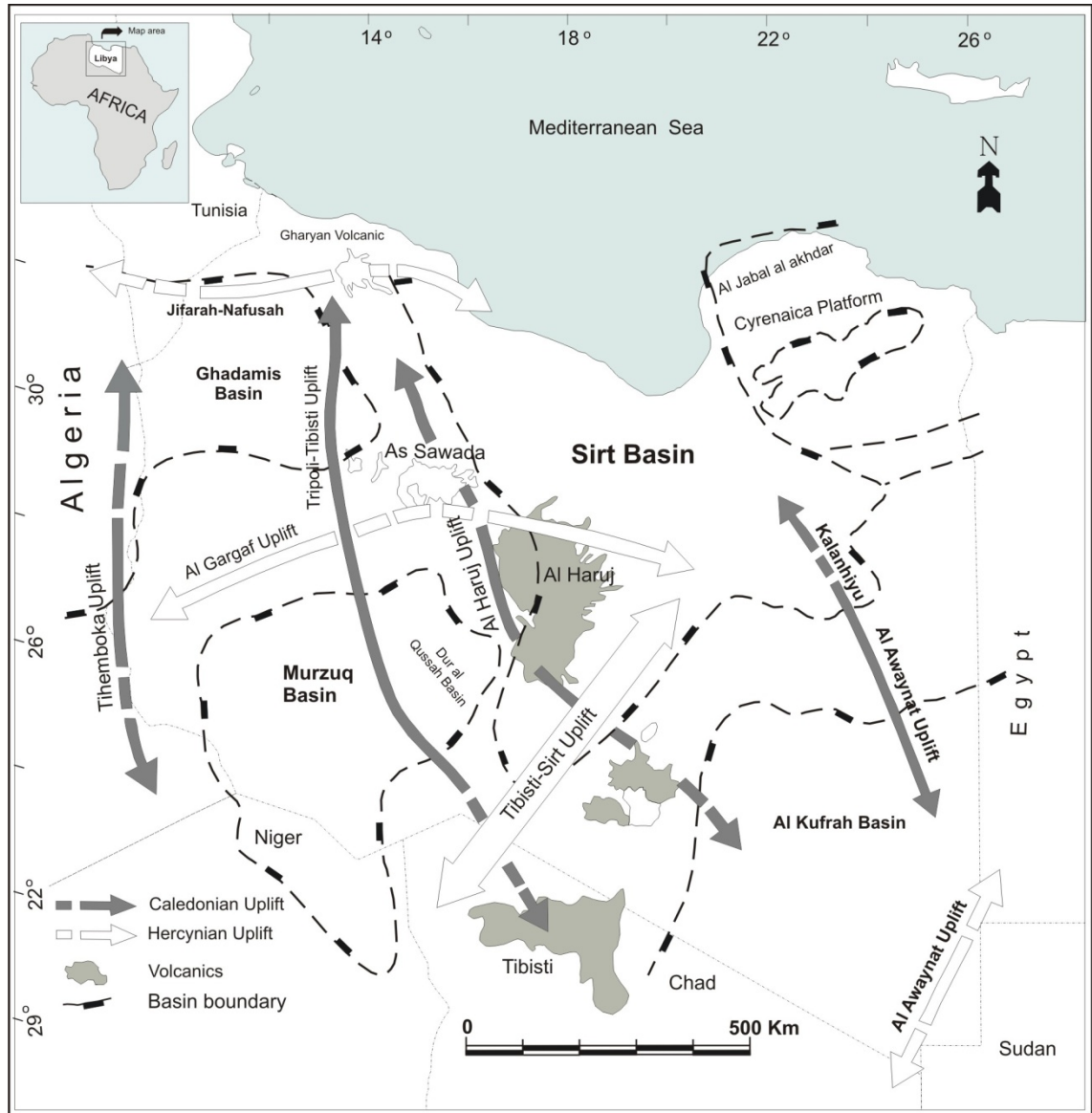
Figure 2.2. Major structural elements of Libya, Caledonian-Hercynian and post-Hercynian volcanics, uplifts and basins (after Klitzsch, 1970; Massa and Delorte, 1984; Bellini and Massa, 1980).

Devonian to reach a maximum during the Permo-Carboniferous. Eruption of basic lava accompanied post-Hercynian movements (Triassic-Jurassic). The Sirt Basin area remained a positive element nearly until the Latest Jurassic (Figure 2.2). The Sirt area gradually submerged, probably for the first time since Early Palaeozoic, as a result of extension that led to the collapse of the pre-existing Sirt arch (Klitzsch, 1970, 1971; Bonnefous, 1972; Burke and Dewey, 1974; Goudarzi, 1980) (Figure 2.2).

The Sirt Basin area experienced stretching and down-faulting during Cretaceous time. Large-scale subsidence and block-faulting began in the latest Jurassic/early Cretaceous. The Basin underwent reactivation, both in the Late Cretaceous (Van Houten, 1983) and Paleocene time and continued into the Early Eocene (Gumati and Kanes, 1985; Van Der Meer and Cloetingh, 1993a, 1993b). Volcanic activity resumed again in post-Eocene time, situated outside the Cretaceous rift at the western side of the Sirt Basin (Guiraud and Belloni, 1995; Wilson and Guiraud, 1998). In general, these volcanic episodes are believed to have been concurrent with movements along deep-seated fractures (major basement fault zones), most likely re-activated during the Alpine Orogeny (Goudarzi, 1980).

Burke and Dewey (1974) suggested that rifting in the Sirt area took place along a weak zone between two African subplates during the Early Cretaceous, as a result of extension that led to the collapse of the pre-existing Sirt arch (Figure 2.2). This event is attributed to the drift of the African Plate, which moved north central Libya over a fixed mantle hotspot during the Early Cretaceous (140-100 Ma; Van Houten, 1983).

According to Gumati and Kanes (1985) and Gumati and Nairn (1991), subsidence of the Sirt Basin reached a climax during the Paleocene-Eocene, corresponding to a period of major crustal extension and reactivation of faults. Anketell (1996) mentioned that the Sirt Basin developed due to inter-and intra plate-movements resulting from the relative motion of the American, African and Eurasian Plates during the opening of the Atlantic Ocean and the development of the Mediterranean on the foreland of the African Plate.

2.4. Previous studies

The Sirt Basin in Libya has been the subject of considerable study in recent years because of the importance of sediments of the discovery of hydrocarbon reservoirs. Despite the enormous amount of geological and geophysical data gained from the exploration activities over more than three decades, published work on the central part of the north Sirt Basin remains limited. Many significant geological contributions achieved by geoscientists, which assist in our understanding of the geology of the central Sirte Basin area, remain as unpublished and confidential internal reports within the operating oil companies. However, only those scientific contributions

that are relevant to the present area of research will be referenced. Others, which have contributed to the understanding of Sirt Basin geology, will be referred to as appropriate. Conant and Goudariz (1967), Burke and Dewey (1974), Van Houten (1983), Anketell and Ghellal (1991) and Gumati and Nairn (1991) have examined and reviewed the main tectonic evolution of the Sirt Basin. The palaeontology and biostratigraphy of the middle Eocene Formation is well known only from outcrop
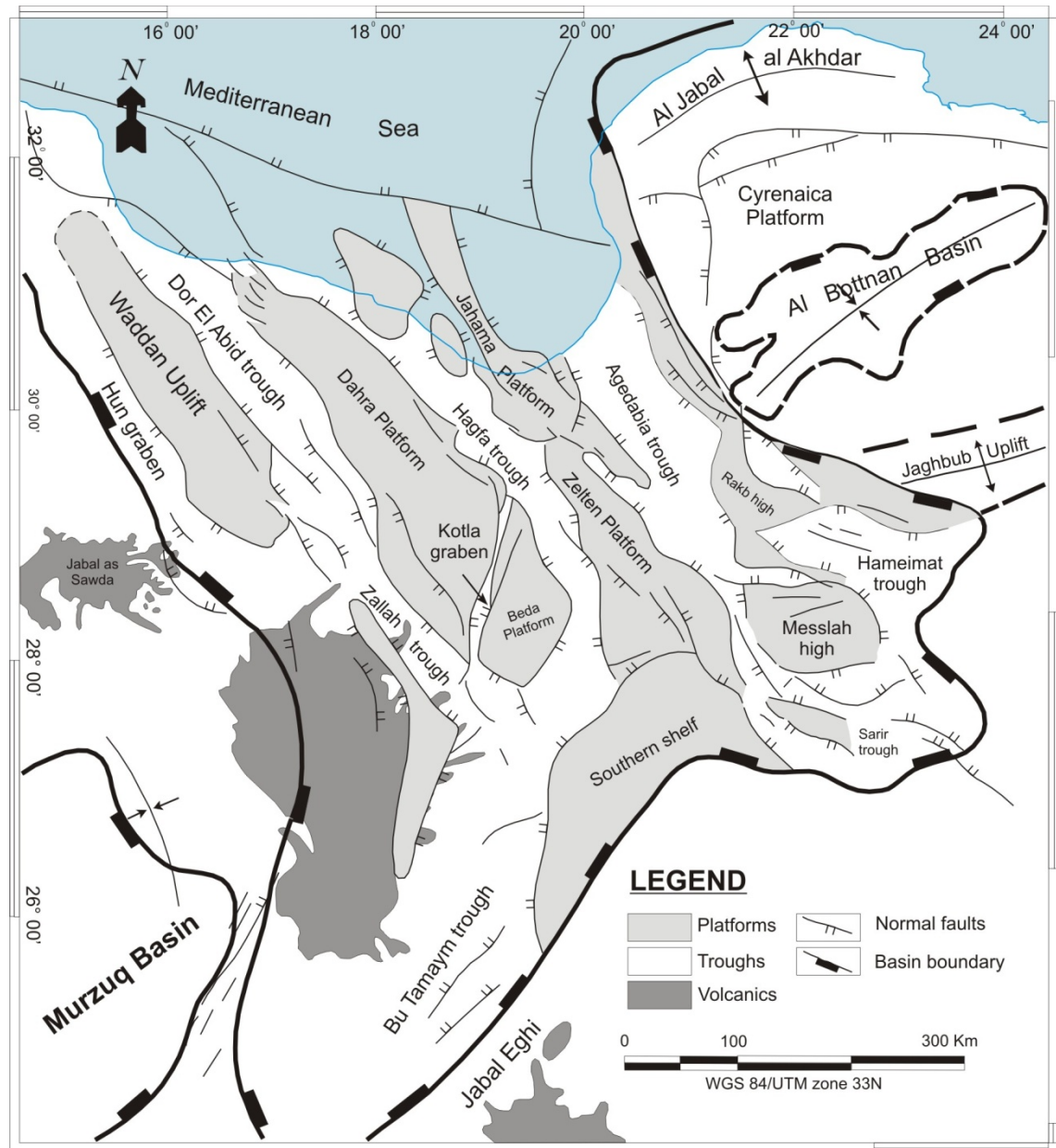
Figure 2.3. The tectonic framework of the Sirt Basin (modified after Mouzughi and Taleb, 1981).
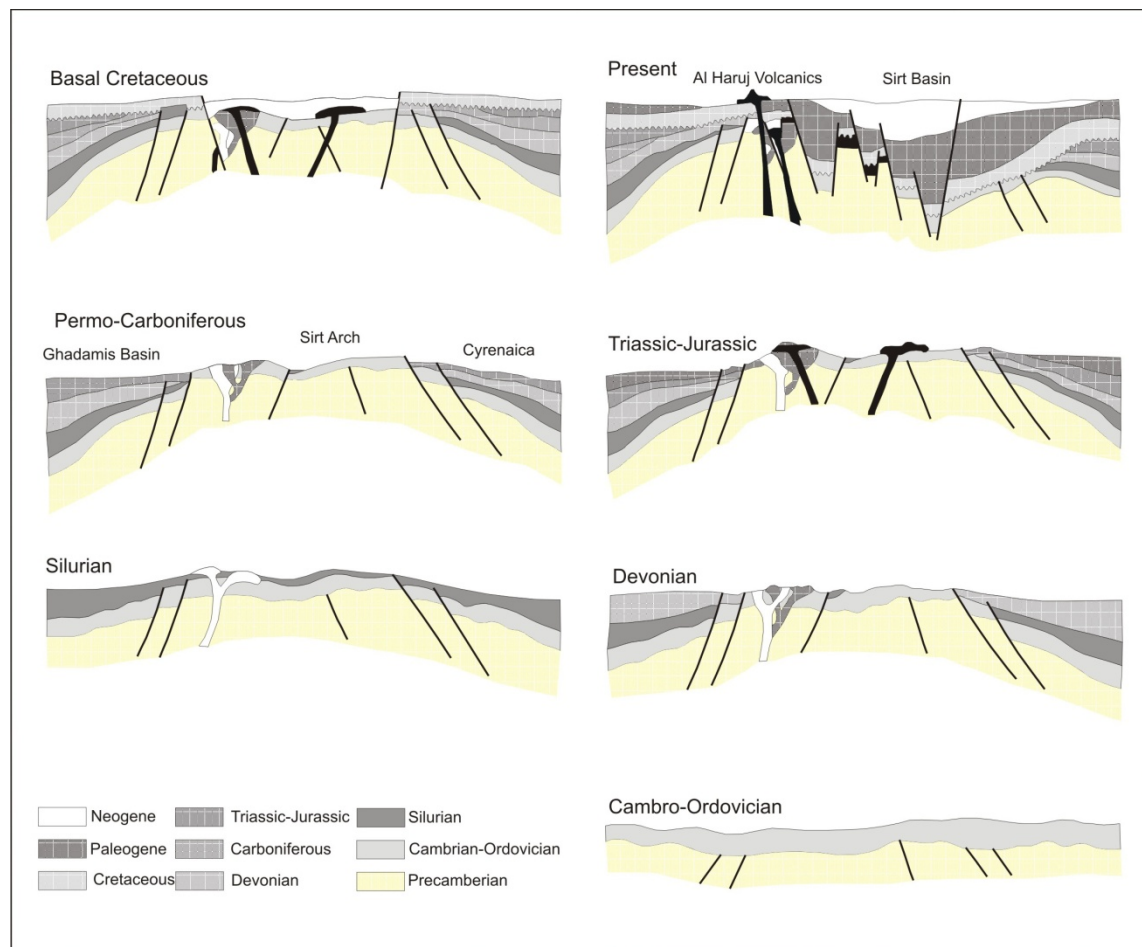
Figure 2.4. Structural development (E-W) of the Sirt region from the Lower Palaeozoic to the present time (modified after Massa and Delorte, 1984).

studies of Barr and Berggren (1980) and Hammuda (1973). El-Hawat *et al.* (1986) described the sedimentary and diagenetic characteristics of the cyclic Middle Eocene Darnah Formation of Jebel Alkdar, in the northeast Sirt Basin. They proposed a tectono-eustatic mechanism with small amplitude sea-level oscillations as the most likely cause of the repetition of carbonate cycles. In comparing to the studies of outcrop, the only comprehensive study based on subsurface data from Nafoora-Augila oil field in Eastern Sirte Basin was carried out by Belazi (1989). He introduced formal formation names based on lithostratigraphic work in the subsurface type section. He focused on the sedimentology, diagenesis, stratigraphy and regional significance of the Tamet Formation as hydrocarbon-bearing and the overlying sedimentary rocks of the Augila Formation. Also he gave little emphasis to the broader sequence stratigraphic framework in terms of using systematic rock fabric changes within the cycle framework for guiding zonation and up-scaling in the subsurface.

2.5. Stratigraphic framework of the Sirt Basin

The sedimentary succession in the Sirt Basin unconformably overlies the igneous and metamorphic rocks of the Precambrian basement. It consists of Cambro-Ordovician clastic sediments and Early Cretaceous sandstones (pre-rift sequence), which are unconformably overlain by Late Cretaceous-Early Tertiary marine sediments (syn-rift) (Van der Meer and Cloetingh, 1993b).

2.5.1. Precambrian (Basement)

The Precambrian basement, consisting of volcanics and granites, crops out in the south Libyan mountains (Jabal Tibisti) and has been penetrated in some deep wells on the basement highs (the Dahra, Beda and Zelten Platforms and the Messlah and Rakb Highs) (Figures 2.3 and 2.5). It is overlain by the Cambro-Ordovician Gargaf Formation with a regional unconformity. The basement-cored wells in the subsurface of the southeastern part of the Sirt Basin represent mainly metamorphic rocks (chlorite schist, phyllites) and crystalline granites. The age of these rocks has been estimated by K/Ar radiometric dating to be Late Precambrian to Early Cambrian (Koscec *et al*., 1996). Wells in the study area did not reach the Precambrian basement.
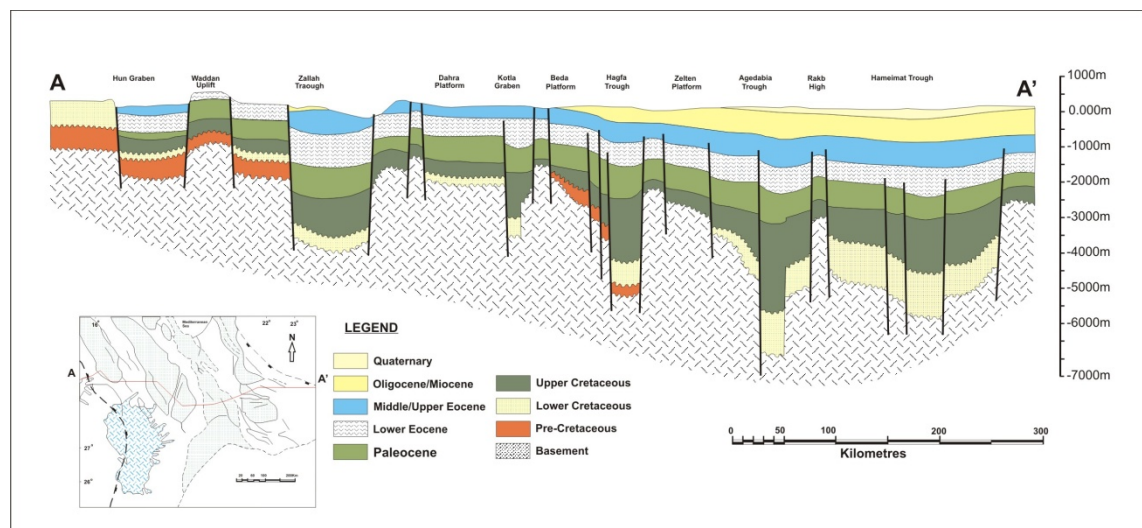
Figure 2.5. Structural E-W cross-section showing the major structure across the Sirt Basin (modified from Roohi, 1996a)

The oil-bearing fractures and weathered zone of the granitic basement of the giant Nafurah/Augila field (Rakb High) are prime examples of the potential of the basement rocks as reservoirs (Williams, 1972; Mansour and Magairyah, 1996).

2.5.2. Cambro-Ordovician (Gargaf Group)

It has been assumed that the basement is unconformably overlain by Cambro-Ordovician arenaceous strata, in part silicified (quartzites), assigned to the Gargaf Group or "Gargaf quartzite". This term is commonly used for the Sirt Basin succession that immediately underlies the undifferentiated continental clastics of the Pre-Upper Cretaceous (Nubian) succession in much of the basin. However, local names, including the Hofra and Amal Formations, are also used.

Barr and Weeger (1972) proposed the name Hofra Formation for a thick succession of relatively clean quartz sandstones with minor amounts of shale and conglomerate, thought to be in part equivalent to the Gargaf Group in the Dahra Platform and other portions of the western part of the Sirt Basin. The Amal Formation or its equivalent is widely spread in the eastern part of the Sirt Basin. The formation consists predominantly of sandstones, usually firmly cemented, and quartzites (Barr and Weeger, 1972). The Amal Formation may be equivalent to the Hofra Formation in the western part of the Sirt Basin. The Samah oil field on the Beda Platform and Attahaddy gas field produce from Cambro-Orovician quartzites.

The Gargaf Formation was deposited over the whole of North Concession 6. It unconformably overlies the Precambrian basement and is overlain by the Nubian and Bahi formations. In the study area, the Gargaf Formation is represented by very hard quartzite with some white weathered feldspar grains.

2.5.3. Triassic

Triassic sediments have very rarely been intersected in the Sirt Basin. In the northeastern part of the basin, near the Amal and Augila fields (Rakb High), middle to upper Triassic sediments are understood to overlie Cambro-Ordovician strata. The Triassic is an intercalation of sands and shales (Ball *et al*., 1996), deposited in a non-marine lagoonal environment (El-Arnauti and Shelmani, 1988).

2.5.4. Late Jurassic-Early Cretaceous (Nubian Formation)

The Nubian 'Formation' is widely distributed in the Sirt Basin. It is particularly well known in the southeastern part of the basin where it is a prolific oil reservoir at As Sarir, Messlah, and many other fields. The 'formation' comprises fluvial and lacustrine

sandstones ranging from very fine-to coarse-grained quartzitic, poorly-sorted, often with a clay matrix. The Nubian 'formation' was deposited during the initial stage of the Sirt Basin; it unconformably overlies basement, Palaeozoic or Triassic/Jurassic graben-fill sediments, and is overlain by the transgressive marine Cretaceous with a maximum thickness of more than 1200 m in the Hameimat Trough.

Overall nearly all facies of the Nubian Sandstone are fluvial, mainly braided river, and lacustrine origin. An exception is part of the variegated shales, which had a marine (lagoonal) influence (El Hawat, 1992).

The Sarir Sandstone is the reservoir of one of Africa's largest oil fields, with 6.5 billion barrels of recoverable oil (Clifford, 1986). It is a prolific producer in the southeastern part of the Sirt Basin (Mansour and Magairyah, 1996). Also the continental Nubian shale is considered to be one of the main hydrocarbon source rocks in the basin (El-Alami, 1996). The Nubian Sandstone forms the main reservoir in the major giant fields (Abu Atiffel, Sarir and Messlah).

In the study area, the Nubian Formation has not been encountered, but most wells have not reached this level.

2.5.5. Upper Cretaceous

2.5.5.1. Cenomanian (Bahi-Maragh Formation)

The formation unconformably overlies the Nubian Formation, the Amal Formation or basement volcanics and granites. The Cenomanian Lidam Formation or other Upper Cretaceous carbonate strata conformably overlie the formation. In the northeastern part of the basin, there is a local basal Cretaceous unit called the Maragh Formation (equivalent to the Bahi Formation in the eastern Sirt basin), which is a transgressive, predominantly clastic unit. The formation was deposited in a littoral or very shallow marine environment during the first transgressive cycle of the Upper Cretaceous (Sghair and El-Alami, 1996). Some oil fields in the eastern part of the Sirt Basin, such as the Amal, an Nafurah and Jakherrah oil fields, are producing from reservoirs in the Maragh Formation.

The Bahi Formation forms the main reservoir in such fields as Haram, Bahi and Attahaddy (Figure 2.6). Also it is a major reservoir for the Nafurah-Augila Waha, Ar

Raqubah and Hateiba fields (Figure 2.7). The boundaries of the Bahi Formation are poor seismic reflectors, especially the lower boundary, so it cannot be differentiated from the Gargaf on seismic sections. Therefore they map as one formation called Bahi/Gargaf (Wennekers *et al*., 1996). In the studied wells the formation has not been penetrated except in well OOOO1-6 Assumood Field.

The Bahi Formation, which is present in the northwestern part of the Sirt Basin, consists of interbedded sandstones, siltstones, conglomerates and shales, with glauconite occurring in the upper part of the formation (Barr and Weegar, 1972). The formation unconformably overlies the Nubian Formation, the Amal Formation or basement volcanics and granites. The Cenomanian Lidam Formation or other Upper Cretaceous carbonate strata conformably overlie the formation. In the northeastern part of the basin, there is a local basal Cretaceous unit called the Maragh Formation, which is a transgressive, predominantly clastic unit. The formation was deposited in a littoral or very shallow-marine environment during the first transgressive cycle of the Upper Cretaceous (Sghair and El-Alami, 1996). Some oil fields in the eastern part of the Sirt Basin, such as the Amal, an Nafurah and Jakherrah oil fields, are producing from reservoirs in the Maragh Formation.

2.5.5.2. Cenomanian (Lidam Formation)

The Lidam Formation is the first distinctive marine formation in many parts of the Sirt Basin overlying the Nubian sandstone. It consists of light brown-grey coloured dolomite, the lower part locally sandy, indicating a local mixing with the underlying sands (Barr and Weegar, 1972). The Lidam Formation has a thickness of up to 600 m in the trough, unconformably overlying the Bahi Sandstone, the Nubian Formation, Palaeozoic strata (Hofra and amal Formations) or igneous and metamorphic basement. The diagenetic history of the Lidam Formation in the northwest Sirt Basin was studied by El Bakai (1996). He concluded that the formation has been greatly affected by diagenesis which began shortly after deposition with the boring activities of microbes, and ended with extensive dolomitization which occured after lithification and compaction.

2.5.5.3. Turonian (Etel Formation)

The Etel Formation consists of thin-bedded carbonates, shale, anhydrite, siltstone and sandstone (Barr and Weegar, 1972). The Formation has a widespread distribution across the central and southern parts of the Sirt Basin, but it is absent on the regionally high areas such as the Dahra, Zelten and Amal Platforms and Rakb High.
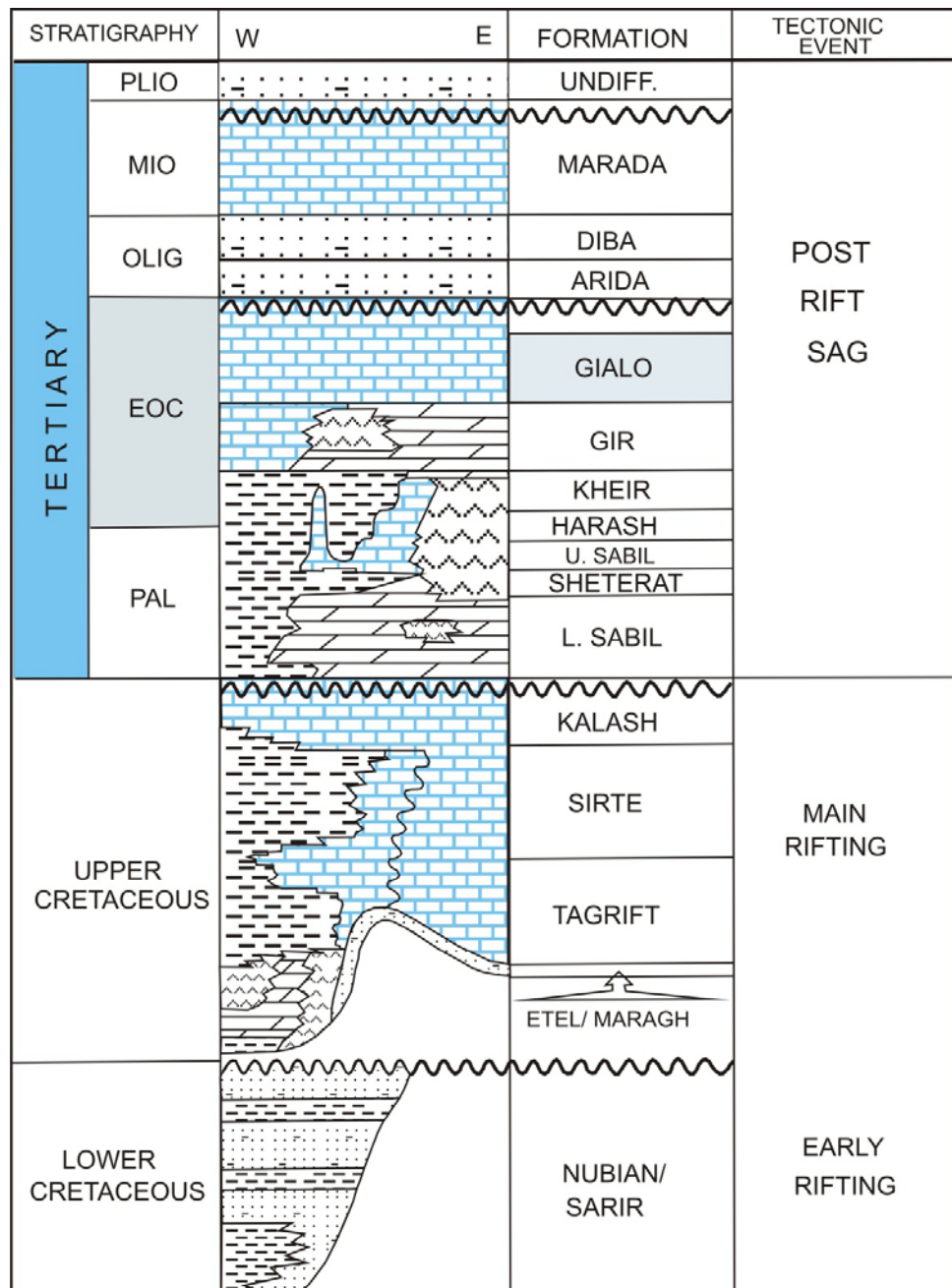
Figure 2.6. Generalized stratigraphic/lithologic correlation chart of the Upper Cretaceous and Tertiary succession of the Sirt Basin (nomenclature after Barr and Weegar, 1972).

The facies vary from evaporitic in the basin centre to carbonate in the north of the Sirt Basin. The typical succession for trough depocentres comprises interbedded black shales and anhydrite, capped by carbonate (El-Alami *et al.*, 1989). The Argub Carbonate is regarded as a basinward equivalent of the Etel Formation, which conformably overlies the Lidam Formation or other Cenomanian rocks and is conformably overlain by the Rachmat Formation in the northwest part of the basin. The shale intervals within the Etel Formation were considered to be the principal effective source rock in the Hameimate Trough (El-Alami, 1996).

2.5.5.4. **Coniacian / Santonian** (Rachmat Formation)

The Rachmat Formation is widespread over much of the Sirt Basin except for the major platform areas such as the Al Hufrah, Zaltan and Amal platforms. It is typical a shale unit, with minor limestone, sandstone and dolomite interbeds. The shales are dominantly grey, fissile to slightly blocky, slightly to non-calcareous, and glauconitic and pyritic in many locations. The limestone interbeds are more frequent in the lower part of the formation (Barr and Weegar, 1972). The formation has a maximum thickness of 600 m in the Agedabia Trough. In the northwest, it conformably overlies either the Argub Carbonate, the Etel Formation, the Bahi Sandstone or the Maragh Sandstone, or the Rachmat Formation rests unconformably on the Amal Formation or granite basement, depending on its position in the basin. At most locations, Sirt Shale conformably overlies the formation.

The Rachmat Formation provides a huge petroleum source for the oil fields located along the crest axis of the basement highs (such as the Augila, Nafoora and Amal field (Belazi, 1989; Roberts, 1970). However, the Rachmat shale is an excellent seal over the Etel Formation, while the Tagrift Limestone is a reservoir in the Augila field.

2.5.5.5. **Campanian** (Tagrift Limestone, Sirt Shale)

The Tagrift Lmestone is restricted to an area along the southeastern margin of the Sirt Basin, including the Rakb High area. The Sirt Shale is widely distributed throughout the grabens of the Sirt Basin. In the south, it contains a shale succession with minor limestone interbeds. Its thickness ranges from 500 m in the Zallah Trough to over 700 m in the Agedabia Trough. The Sirt Shale is conformably overlain by Kalash

Limestone, but underlies the Satal Formation in the Dahra Platform area. Depending on its position in the basin, the basal contact can be gradational or unconformable. In the west of the Sirt Basin, the Sirt Shale sits on rocks as old as the Bahi Formation. To the east, the time equivalent of the Sirt Shale becomes calcareous in the lower part, and the shales grade laterally into and rest upon the Maragh sandstone (Barr and Weegar, 1972). El-Alami *et al*. (1989) concluded that the Upper Cretaceous marine Sirt Shale is the main hydrocarbon source rock in the Sirt Basin.
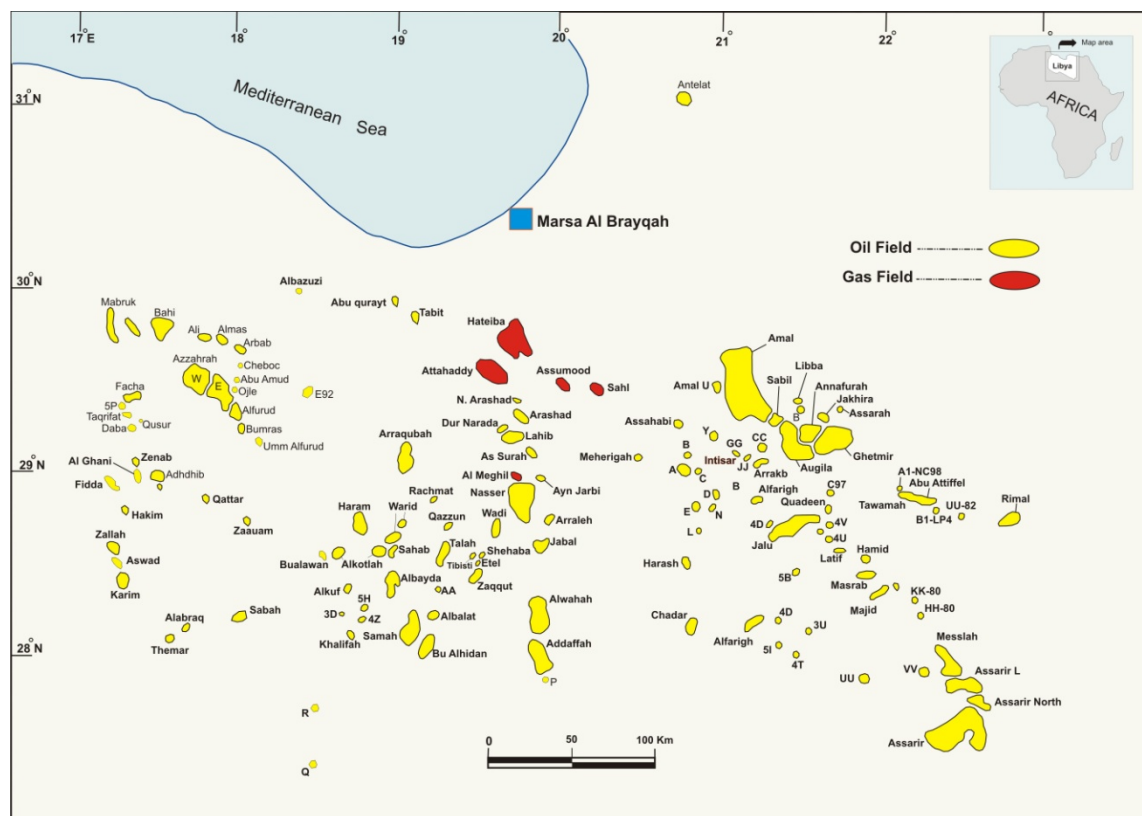
Figure 2.7. Location of oil and gas fields in the Sirt Basin (after Wennekers *et al*., 1996).

2.5.5.6. Maastrichtian (Kalash Limestone, Waha Limestone and Lower Satal Formation)

The Kalash Limestone occurs over much of the Sirt Basin, it has a thickness of up to 600m in the northern part of the Agedabia Trough. The Kalash Formation forms a poor oil reservoir in some areas including the B1-10 area on the Waddan Platform, because of its very low permeability. The limestone is conformably overlain in many places by the Paleocene Hagfa Shale or lower Sabil Carbonate. The Kalash Limestone is

laterally equivalent to the Waha Limestone on the west Zelten Platform and to the Lower Satal Formation on the Dahra Platform. The depositional environment is open marine, probably neritic, as suggested by Barr and Weegar (1972).

The Waha Limestone is the main hydrocarbon reservoir of the Raqubah oil field in the eastern margin of the Dahra Platform and of the Waha field on the Zelten Platform. It represents one of the largest hydrocarbon reserves in the Sirt Basin.

2.5.6. Paleocene

The Paleocene succession occurs over most of the Sirt Basin, and has a thickness of more than 2000 m in the troughs. In the Sirt Basin the Paleocene sequence consists primarily of open-marine calcareous shales and shelf carbonates. The carbonate areas are confined to the platforms, whereas the deeper marine calcareous shale facies is restricted to the subsiding troughs.

2.5.6.1. Danian (Hagfa Shale, Upper Satal Formation, Defa Limestone, Lower Sabil Carbonate)

In the Sirt Basin the depositional pattern of the Danian stage differs according to the basin segments. The Danian strata change laterally from purely shale to totally carbonate. The Hagfa Shale consists of calcareous fossiliferous, rarely glauconitic shales, with local thin stringers of micritic limestone (Barr and Weegar, 1972). The depositional environment of the Hagfa Shale in the central and western parts of the Sirt Basin (Agedabia Trough, Hagfa Trough, southern Zallah Trough) is deep marine, probably outer shelf to upper bathyal (Barr and Weegar, 1972). The Danian shale deposits gradually thin and onlap carbonates of the Upper Satal Formation and the Lower Sabil Carbonate along the shelf margins. The upper member of the Satal Formation is laterally equivalent to the Hagfa shale in the deep troughs, and mostly consists of fine-grained calcilutite and chalky limestone, often dolomitized and containing minor anhydrite intercalations. The Defa Limestone is restricted to the Zelten Platform in the Defa-oil field area. It consists of a variety of interbedded limestone facies and is equivalent to the Satal Formation. The Defa Limestone locally forms the lateral, shallow-marine equivalent of the Hagfa Shale. The Hagfa Shale is conformably overlain by the Beda Formation, and conformably overlies the Kalash Limestone.

The Hagfa Shale is the most important seal in the Zelten Platform, where it encloses the Defa Limestone in the Defa field pool and serves as an overhead seal for the Maastrichtian Waha Formation pool in the Waha field and the various other Maastrichtian and associated pools on the Zelten Platform (Baird *et al.,* 1996). On the Dahra Platform, the Upper Satal Limestone reservoir, which contains giant pools in the Dahra and Bahi fields, is sealed by an uncertain proportion of Hagfa, Beda and Khalifa Shales.

2.5.6.2. Selandian (Beda Formation)

The Selandian succession is well defined in the western part of the Sirt Basin, where it is represented by the Beda Formation (Barr and Weegar, 1972). In the eastern part of the basin, the Selandian is incorporated within the Lower Sabil Carbonates and the Khalifa Shale. The formation consists mainly of various interbedded limestones, with subordinate dolomite and calcareous shales. In the northwest part of the basin, the formation becomes more shaly, and is subdivided into a Lower Thalith Member and an Upper Rabia Member. Over much of the western area, the formation overlies the Danian Hagfa Shale or the upper member of the Satal Formation. The Khalifa Shale or the Dahra Formation conformably overlies the Beda Formation. The formation was deposited in a variety of shallow-marine environments (Barr and Weegar, 1972). The Beda Formation constitutes a reservoir in the Ora, Sabah and Zaggut fields.

2.5.6.3. Thanetian (Dahra Formation)

In the Sirt Basin the Thanetian stage started with a reduction in the areal extent of the carbonate provinces. The restricted shelf environment in the eastern part of the basin retreated and was replaced by open-marine conditions, whereas in the western area carbonate deposition continued. The Dahra Formation is well developed in the western part of the Sirt Basin, and consists mainly of light grey calcarenite, calcilutite and chalk, as well as microcrystalline dolomite and shale interbeds. The Dahra Formation conformably overlies the Beda Formation and is conformably overlain by the argillaceous limestone member of the Khalifa Formation. In the central part of the basin, this formation completely changes laterally to a purely shale section, which is the lower shale member of the Khalifa Formation. The Dahra Formation forms the main reservoirs in the Dahra and Hofra oil-fields.

2.5.6.4. Selandian-Thanetian (Khalifa Formation)

The Khalifa Formation extends over much of the Sirt Basin; it consists of an upper argillaceous limestone unit and a lower shale unit. The lower shale is laterally equivalent to the Dahra Formation, which is covered by a thin, upper argillaceous limestone unit where the Khalifa Formation is present. In areas where the Beda Formation is absent, such as on the Zelten Platform, open-marine conditions prevailed and the areal extent of the restricted environment was reduced. This unit is composed of shales, which are included in the Khalifa Formation. The Khalifa Formation conformably overlies the Dahra and Beda Formations or the Hagfa Shale, and is overlain by the Zelten Limestone. The shales are indicative of open-marine conditions, whereas the upper limestone unit was deposited in a more shallow, marginal-marine setting (Barr and Weegar, 1972). The Khalifa Shale functions as a seal on the Dahra Platform, where it covers the shallow Dahra Formation pool (mainly gas) and some fields elsewhere in the Beda Formation (Baird *et al.,* 1996).

2.5.6.5. Thanetian (Jabal Zelten Group)

The Jabal Zelten Group is usually divided into two formations, the upper Harash Formation and the lower Zelten Limestone. The Jabal Zelten Group is distributed widely across the central and western parts of the Sirt Basin. The Jabal Zelten Group is distributed widely across the central and western parts of the Sirt Basin. It is usually divided into two formations, the upper Harash Formation and the lower Zelten Limestone. The Zelten Limestone Formation is widespread across the central and western parts of the Sirt Basin and consists of argillaceous to shaly, chalky, fossiliferous calcilutite and calcarenite, with subordinate amounts of dolomite. The unit becomes biohermal in aspect in the east of the basin. The Harash Formation is a predominantly chalky, argillaceous and muddy calcarenite, with thin interbeds of fissile shale that are dominant in the lower part of the formation. In some areas, the group cannot be subdivided. This undifferentiated Jabal Zelten Group comprises a dominantly carbonate succession with shale interbeds. The Jabal Zelten Group is conformably overlain by the Facha Dolomite Member of the Gir Formation and the Khair Formation, and conformably overlies the Khalifa Formation. Toward the east, the formation passes into the equivalent Upper Sabil Carbonates. The Zelten Limestone forms the reservoir rock for the Zelten (Nasser) field located on the Zelten Platform.

2.5.6.6. Thanetian (Kheir Formation)

The Kheir Formation is extensively developed throughout much of the Sirt Basin; it overlies the Jabal Zelten Group and in the east the Upper Sabil carbonates. The formation is extremely variable in lithological composition, predominantly shale with some clay, marl and limestone. The lower Eocene Gir Formation conformably overlies it. The open-marine environment, characteristic of this formation, can be correlated over long distances across the Sirt Basin, implying stable conditions of sedimentation during the Late Paleocene to Early Eocene time (Belazi, 1989). The Kheir Shale is one of the most important seals in the basin. It provides overhead seals for the Nasser and Harash oil pools (Baird *et al.,* 1996).

2.5.7. Eocene

Eocene rocks are present in the subsurface throughout the Sirt Basin, where they form major hydrocarbon reservoirs. Eocene rocks outcrop extensively at Jabal Waddan, on the Al Hufrah Platform, in the Zallah Trough, and to the west of Al Haruj al Aswad. Farther south there are extensive outcrops of Eocene littoral rocks which extend as far as the foothills of the Tibisti Massif. In Cyrenaica Eocene rocks outcrop on the northern flank of the Jabal al Akhdar, and continuous outcrops are present along the coast from Tulmaythah to Durnah. In the Sirt Basin the dominant lithologies are shallow-water carbonates, dolomites and evaporites (Megerisi and Mamgain, 1980a).

2.5.7.1. Lower Eocene (Ypresian) Gir Formation

The Gir Formation consists of a succession of interbedded dolomite and anhydrite with subordinate amounts of limestone and shale (Barr and Weegar, 1972). This formation is conformably overlain by the Gialo Formation in most of the Sirt Basin, but in the north-west it is unconformably overlain by the Gedari Formation. The Gir Formation usually overlies either the Upper Paleocene Harash Formation or the Kheir Formation. It is exposed in the western Jabal Waddan area, and extends into the subsurface across much of the Sirt Basin. It comprises shallow-marine carbonates and evaporites, with deeper-marine facies in the northern Agedabia Trough. In some areas the Gir Formation is divided into the Facha Dolomite Member, the Hun Evaporite Member and the Mesdar Limestone Member. The Facha Dolomite Member is a target

for hydrocarbon exploration. It forms the principal reservoir in the western part of the Sirt Basin for the Zallah, Karim, Aswad and Sabah fields, and other fields mainly located in the Zallah Trough and the Dahra and Beda Platforms, where the Hon Evaporite Member is the cap rock for the Facha reservoir.

The Gir Formation has been the subject of several studies. The biostratigraphy of the Gir Formation was examined by Abugares (1996). Based on both planktonic and nannofossil assemblages he demonstrated that the Al Jir Formation in the Sirt Basin is of mid-Ypresian age, and that the contact with the overlying Gialo Formation is unconformable. This formation forms an oil reservoir in some areas in the Sirt Basin, such as the Daba and Facha fields (Figure 1.2).

In the study area, the Gir Formation is present in all wells. Some wells in the Assumood and Sahl fields were not drilled deep enough to reach the Gir Formation. It is represented in the study area by limestone which makes it difficult to differentiate between this formation and the overlying Middle Eocene Gialo Formation. It ranges in depth from 6235 ft in well 4O1-6 (North Assumood) to 6809 ft in well H8-6.

2.5.7.2. **Middle Eocene (Lutetian)** Gialo Formation, Gedari Formation

The Gialo Formation is widely developed in the Sirt Basin, except in the northwest where the Gedari Formation occurs as its lateral equivalent (Figure 2.8). The Gialo Formation consists of a thick succession of shallow-marine nummulite-bearing mudstones, locally developed into highly fossiliferous nummulite bioclastic limestone. Sedimentological studies of the Middle Eocene in Libya are sparse. On the basis of faunal and lithological evidence, El-Hawat *et al.* (1986) concluded that the Middle Eocene facies in the northeast exposures continue to be a complex of shallow and deep water deposits because of Jebel Alkdar tectonism and sea-level fluctuations. Rocks are principally carbonates and represent deep-marine facies in the lower part; and they are generally interpreted to be open-marine, low-energy facies near its base, because of the abundance of plankton and paucity of benthos. Subsequently there appears to have been shallowing upward into facies rich in benthic organisms.

In the area of study, the Middle Eocene Gialo Formation has been found in all wells drilled in the area. It is represented by a thick limestone section (Figure 1.7) and

ranges in depth from 5105ft in well 4O1-6 at the North Assumood to 4900 ft in well H4-6 at the Assumood Field, whereas it is at 5115 ft depth in well O3-6 at the Sahl Field (see Appendix II.vi).
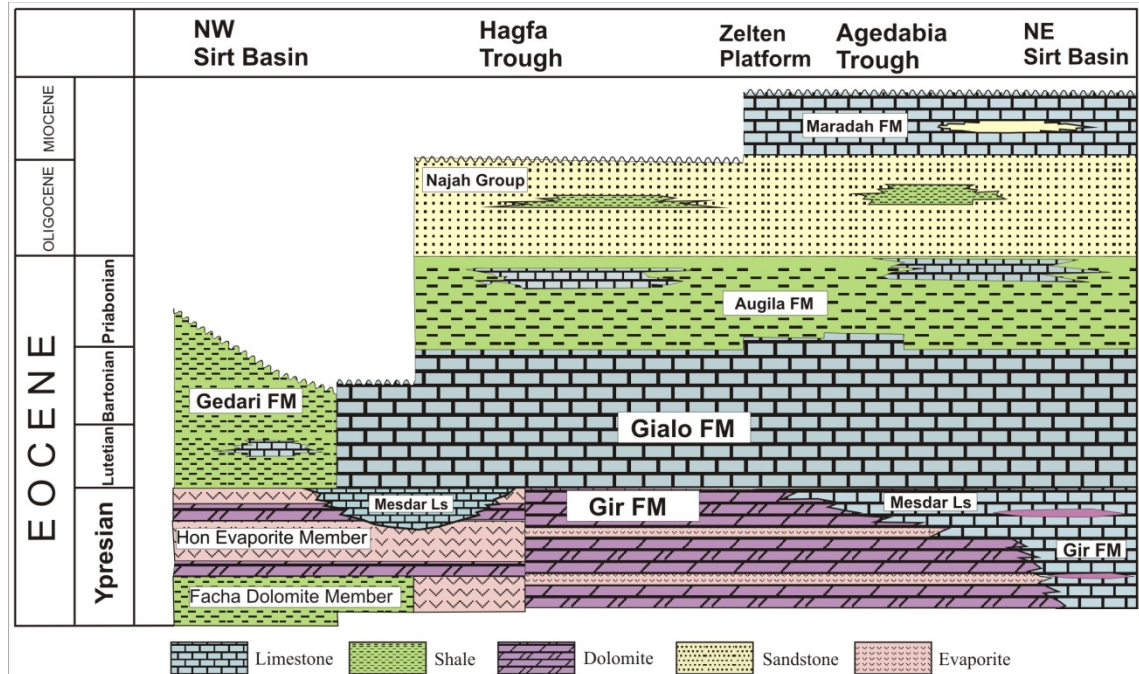
Figure 2.8. Generalized stratigraphic lithologic correlation chart of the Tertiary (Eocene) succession of the Sirt Basin (modified from Barr and Weegar, 1977).

2.5.7.3. Upper Eocene (Bartonian) Augila Formation

The Augila Formation is divided into three lithologic units in the southeast and south central parts of the Sirt Basin. The lower member is soft shale, with thin argillaceous limestone or dolomite interbeds, sand and glauconite at the base. The middle member is friable porous glauconitic quartz sandstone. The uppermost units consist of sandy, slightly glauconitic limestone. The lower part of the Augila Formation locally shows a predominant limestone facies, known as the Rashda Member (Barr and Weegar, 1972), along the eastern margin of the basin. The shale member was probably deposited under inner to outer neritic open-marine conditions, whereas the sandstones and limestones were deposited in shallower, more restricted environments. In the southeast of the basin, the Upper Eocene consists of sandy dolomitic limestone, sandstone and claystone (Clifford *et al.,* 1980). The formation disconformably overlies the Gialo Limestone and is unconformably overlain by sandstone of the Arida Formation. The Augila limestones and sandstones contain some oil on the Rakb High.

In the area of study, the Augila Formation has been found in all wells. It ranges in depth from 4736 ft in well 4O1-6 at the North Assumood to 4440 ft in well H4-6 at the Assumood Field, whereas it is at 4736 ft depth in well O3-6 at the Sahl Field.

2.5.8. Oligocene (Najah Group)

The Oligocene succession of the Sirt Basin is subdivided into the Arida Formation and Diba Formation (Barr and Weegar, 1972), which together form the Najah Group. The Arida Formation is divided into an upper shale unit consisting of soft, light grey to brown, glauconitic shale, and a lower unit composed mainly of sandstone, separated by a thin unit of laminated shale. The Arida Formation exhibits rapid changes in the lithology and facies, ranging from totally continental sandstone in the southeast to marine shale and carbonates in the north of the basin. The sand of the Arida Formation is producing oil in the main Jalu field and some of the small neighbouring fields. It is also producing from well G7-51 in the An Nafurah field (Bezan and Emil, 1996).

The Diba Formation in the south central part of the basin consists of a succession of alternating thick sandstone units and thin shales with sandy limestone at the top. The shale units, also traceable across the Rakb High (Belazi, 1989), indicate that open-marine conditions existed during Middle Oligocene time. The Oligocene regression gave rise to three major types of depositional environment, represented by continental sandstone in the southeast, marine shales and carbonates in the north and northeast, and a complex pattern of facies in the intervening marine/continental interface (Bezan, 1996). The Diba Formation is producing from well 2E1-12 southwest of the Rakb field (Bezan and Emil, 1996) and the shales of the Diba and Arida Formations work as seals, especially in the Jalu fields, where giant fields are involved.

In the study area of the Assumood and Sahl Fields, the Arida Formation was penetrated in all wells and consists of sandstones interbedded with subordinate shales. It ranges in depth from 2770 ft in well H4-6 at the Assumood Field to 2790 ft in well H10-6. Gas shows have been reported in the upper part of the formation. The Diba Formation is believed to exist throughout the area of study, but as this formation has no hydrocarbon prospectivity in the area, it was not logged in all the wells.

2.5.9. Miocene (Maradah Formation)

The Maradah Formation is represented by a large number of lithofacies, including interbedded shales, sandstone, sandy limestone, calcarenite and gypsum (Selley, 1969, 1971; Barr and Weegar, 1972; Benfield and Wright, 1980). Fine-to coarse-grained sands and sandstone are dominant in the western and southeastern parts of the Sirt Basin, but a mixed sedimentary succession occurs farther to the northwest, where individual sand bodies interfinger with sandy shales, shales and sandy carbonate. Gypsum and anhydrite occur widely in association with both clays and carbonates. The depositional environment in the east of the Sirt Basin has been interpreted as fluvial at the basin edge and marginal marine towards the north and northeast. The carbonate and clay succession of the northeast clearly indicates marine shelf conditions (Benfield and Wright, 1980). Gammudi (1996) considered the Maradah Formation Late Miocene in age, with infra-littoral (0-75 m) marine, including some brackish influence.

2.6. Summary

A huge amount of data is available for the Sirt Basin as a result of oil exploration activities extending over more than forty years. Thousands of wells have been drilled and as a result the basin is far better known than any other area in Libya. The oldest rocks in the area are Late Precambrian to Early Cambrian and have been penetrated on the basement highs (Dahra, Beda and Zelten Platforms and Messlah and Rakb Highs). The stratigraphic succession in the onshore Sirt Basin area is dominated by granitic basement, clastics, limestone, dolomite, and evaporites ranging in age from Precambrian to Recent. The tectonic features of the Sirt Basin were formed by large-scale subsidence and block faulting in response to latest Jurassic/Early Cretaceous rifting, which controlled the pattern of deposition during Late Cretaceous and Early Tertiary. The complex tectonic history of the Sirt Basin resulted in multiple reservoirs and conditions that favoured hydrocarbon generation, migration and accumulation.

CHAPTER 3: LITERATURE REVIEW ON EOCENE NUMMULITIC ACCUMULATIONS AND PALAEOENVIRONMENTS

3.1. Introduction

The Eocene corresponds to a prolific period for the development of nummulite carbonate platforms along the continental margins of the Tethyan Ocean (Jorry, 2004). The proliferation of nummulites has produced a significant amount of carbonate sediments, mainly comprising nummulitic grainstones and silt-sized nummulithoclastic packstones. These carbonates compose important hydrocarbon reservoirs in Mediterranean regions, as both in offshore Tunisia (Gulf of Gabès) and Libya (NW offshore zones and Sirt Basin).

The aim of this chapter is to discuss the Eocene nummulitids and other large benthic foraminifera and focuses on the main factors which controlled their distribution and the test size and shape of these foraminifera. The significance of the environmentally influenced life cycle of large benthic foraminifera, and the symbiotic relationship between many large foraminifera and photosynthetic symbionts is discussed. In addition other physical and chemical influences on large foraminifera are summarized including nutrient supply, substrate, water energy, salinity, temperature and taphonomic processes. This chapter also includes a description of some of the facies models that have been proposed for nummulitic deposits and a brief discussion of their reservoir quality.

3.2. Eocene nummulitic deposits

According to Jorry (2004), nummulite accumulations occur in Late Palaeocene to Early Oligocene carbonate deposits, which represent about 30 Ma in the geological record. During this time, the marine microfauna were dominated by nummulites along the Tethys palaeomargins. The morphology of nummulites is characterized by large, lenticular and flat to subglobular tests, which comprise a single planispirally-coiled layer subdivided into numerous simple chambers, separated by septa (Figure 3.1). Nummulite accumulations or "banks" commonly develop in platform or shelf-margin areas and mid to outer ramp settings. These accumulations extend from the West

Pacific, to the Central Mediterranean, and to the Atlantic (Figure 3.2), and form hydrocarbon reservoirs or targets in countries such Tunisia, Egypt, Italy, Oman and Pakistan, as well as Libya (Racey, 2001). The reservoir qualities are mostly induced by the preservation of intraskeletal porosity of nummulite tests.

In general, nummulites have alternating asexual and sexual generations. The asexual generation has a large proloculus (initial chamber) and small test diameter, and is referred to as the megalospheric form, or the A-form. The sexual generation with a small proloculus and large test diameter, is known as the microspheric form, or B-form (Figure 3.3) (Beavington-Penney and Racey, 2004). Many authors have assumed that the asexual and sexual generations alternate, and give rise to an assemblage with an A-to B-form ratio of approximately 10:1 (Blondeau, 1972). However, departures from this ratio may result from environmetal differences and have been used to define a "degree of winnowing". Beavington-Penney and Racey (2004) observed that A-forms dominate fossil communities which result from repeated asexual reproduction and are likely to have formed in the shallowest or deepest parts of the depth range of a particular species. In comparison, sexually produced B-forms are most common in intermediate intervals of a specific depth range. This distribution is partly because sexual reproduction is less likely to be successful in shallow, turbulent water, and the large sexual forms are restricted to deeper environments, below fair weather wave base. They noted that these two environments (shallow and deep) could be distinguished on the basis of test shape and analysis of associated biota, matrix and sedimentary structures.

Nummulite reservoir facies are often associated with muddy and silt-sized facies composed of small debris (nummulithoclasts), which are mainly exported seaward (Loucks et al., 1998; Racey et al., 2001; Jorry et al., 2003; Hasler, 2004; Jorry, 2004). Depending on the platform type (homoclinal ramp, rimmed shelf or platform with sharp slope breaks), the lateral facies variation is generally progressive and other subfacies rich in *Discocyclina* or *Operculina* may occur between nummulite grainstones and nummulithoclastic packstones. In more proximal settings, nummulithoclasts are less abundant in the matrix of restricted/lagoonal muddy facies dominated by *Orbitolites*, *Alveolina*, and miliolids (Middle Eocene Dernah Formation, NE Cyrenaica; Jorry 2004). Nummulithoclasts clearly result from the reworking and the pulverization of nummulites, but fragmentation processes remain unresolved. Loucks et al. (1998) suggested that bioturbation can be an important process for grain breakage. Beavington-Penney (2004) postulated that the fragmentation can also be the result of transportation

of the tests by turbidity currents, storms and/or predation by relatively large bioeroders such as fish and echinoids.

Various depositional models have been proposed (Figure 3.8), and most of them described nummulite accumulations as banks, bars or low-relief banks, in some cases related to palaeo-highs. Previous studies have shown that large benthic foraminifera can be easily reworked by waves and currents (Yordanova and Hohenegger, 2002), and several authors point out that the hydrodynamic behaviour of nummulites is an important factor controlling their distribution (Aigner, 1982; Futterer, 1982; Racey, 2001).

3.3. Previous work on Eocene Nummulites

Numerous sedimentological studies, over the last fifty years have been made on nummulite "banks" and depositional models in order to understand better the geometry of subsurface reservoirs, especially in Tunisia, Libya, Egypt, Italy and Oman (Arni, 1965; Bishop, 1985; Moody, 1987; Bailey et al., 1989; Moody and Grant, 1989; Bernasconi et al., 1991; Loucks et al., 1998; Anketell and Mriheel, 2000; Racey et al., 2001; Jorry et al., 2003a,b; Vennin et al., 2003; Hasler, 2004 and Jorry, 2004). Authors tend to use different terminologies for describing such accumulations (reefs, banks, shoals) or else they emphasise different aspects of nummulite morphology (e.g. large versus small, megalospheric versus microspheric, or thick versus thin forms). Racey (2001) noted that nummulites occupied a broad range of environments in open-marine platform, shelf and ramp settings, though they are invariably absent in more restricted environments. Most of the examples seen in the field and in core possess a sheet-like or very low-amplitude bank-like geometry. In general large flat nummulites tend to be associated with large flat *Assilina* and *Discocyclina* in "deeper" more outer platform/shelf/ramp settings. "Banks" of more robust medium to large sized lenticular to globular shaped nummulites tend to occupy a position intermediate between these two extremes.

Arni (1965) described "nummulite banks" as barriers separating "fore-bank" from more restricted "back-bank" environments, and assumed that the presence of a bank brought about a change in sea-bed morphology. This model was followed with little modification by numerous subsequent authors. Aigner (1983), in a study of Middle

Eocene nummulite build-ups in Egypt, and Moody (1987), in a study of Early Eocene nummulite build-ups in Tunisia, identified shoals and shoal reefs as possible depositional environments. Racey (1988, 1995) studied Middle Eocene nummulite accumulations in Oman, and identified a low-amplitude nummulite bank complex in a mid-ramp setting. Buxton and Pedley (1989) noted that nummulite deposits in the Tethyan Tertiary were generally associated with ramp environments analogous to the coralgal patch reef belt (Figure 3.4). Arni (1965) and Arni and Laterno (1976) also noted that current and wave reworking were important controls on the formation of nummulite accumulations. Subsequent researchers such as Fournie (1975) and Aigner (1983) suggested that nummulite banks formed on pre-existing structural highs.

In a nearby area of study, El-Hawat *et al.* (1986) described the sedimentary and diagenetic characteristics of the cyclic Middle Eocene Darnah Formation of Jebel Alkdar, NE Libya. They proposed a tectono-eustatic mechanism with small amplitude sea-level oscillations as the most likely cause of the repetition of the carbonate cycles. Anketell and Mriheel (2000) also studied the Jdeir Formation, offshore Sabratah Basin (Figure 3.8).
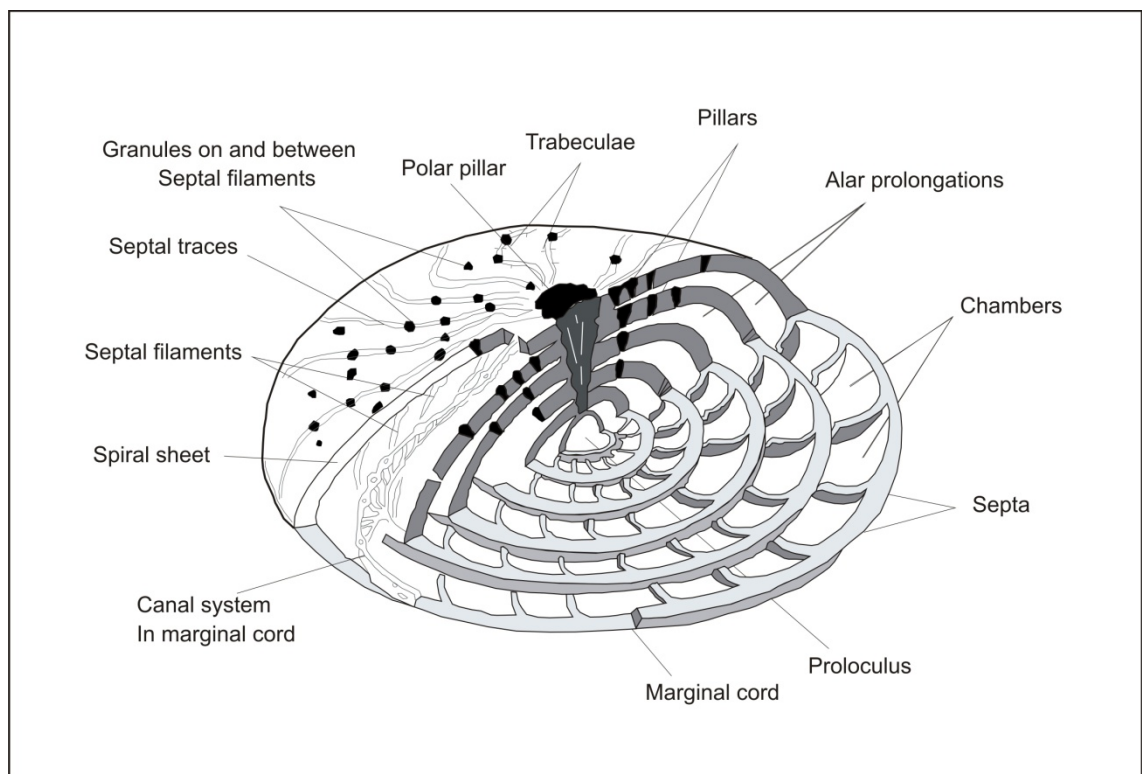
Figure 3.1. Structure and elements of a *Nummulites* test, based on a macrospheric generation (after Racey, 2001).
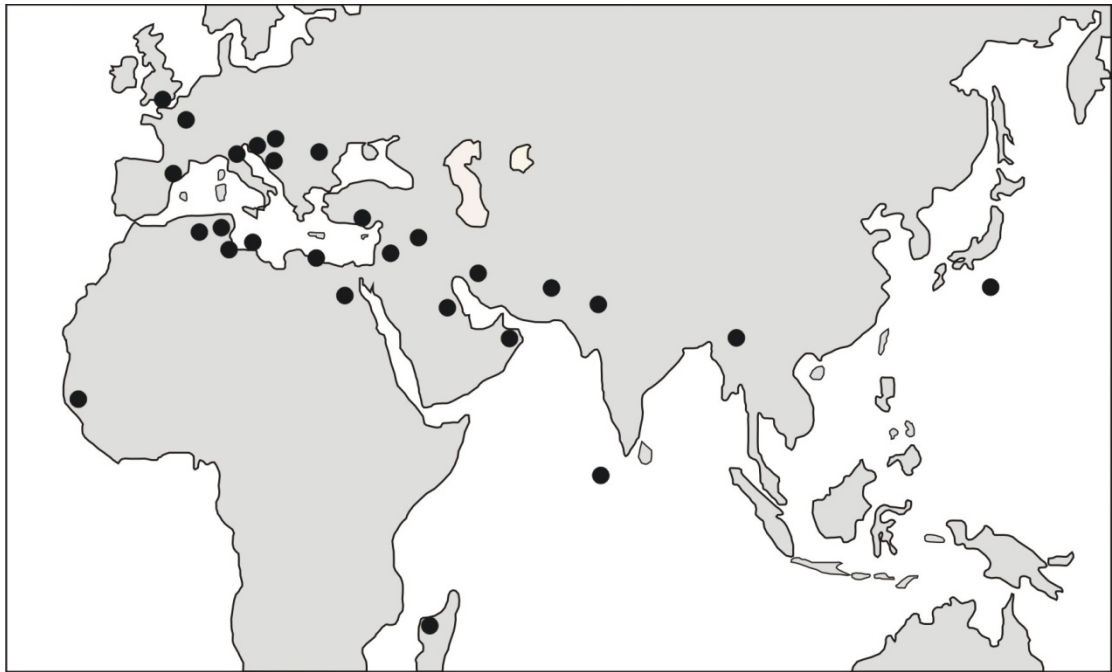
Figure 3.2. Geographic distribution of the Eocene nummulitic carbonate deposits (after Racey, 2001).
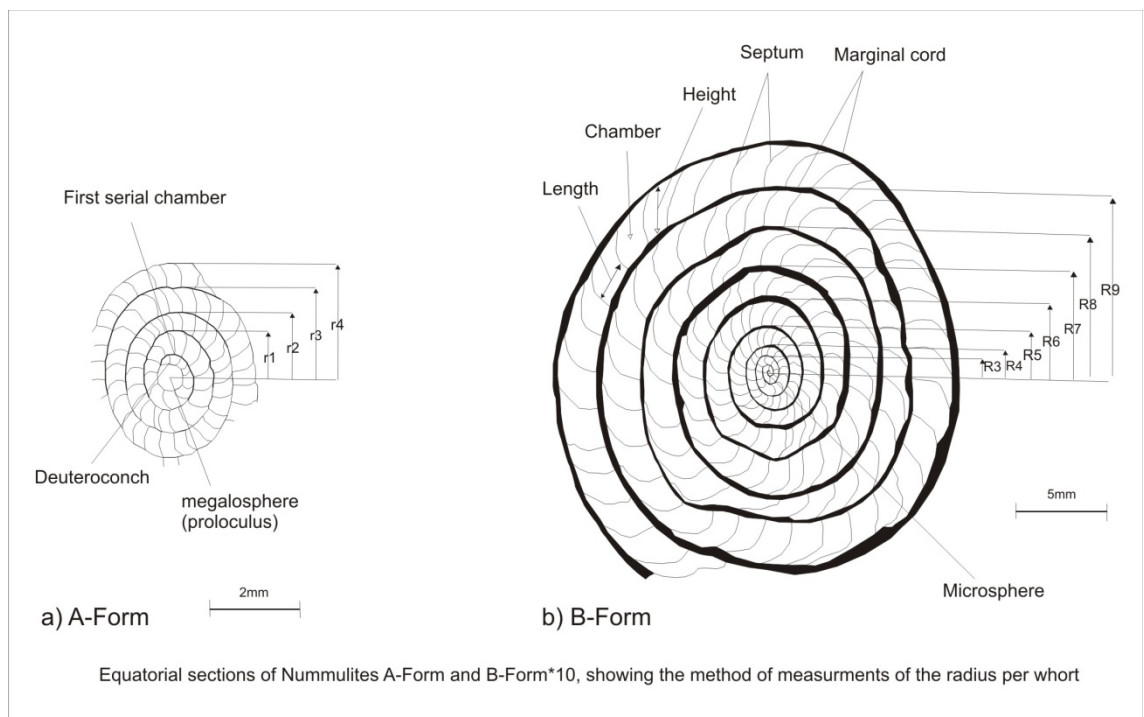
Figure 3.3. Difference between nummulite A-forms (megalospheric generation) and B-forms (microspheric) (after Racey, 2001).

INNER RAMP			SHALLOW SUBTIDAL RAMP		OUTER RAMP	SLOPE TO BASIN
PERITIDAL FACIES Stromolithes, rhizoliths	**LAGOONAL FACIES** Low diversity biogta, with oysters and other pelecypods, rotalid and agglutinated forams.	**BARRIER BEACH FACIES** Unstratified grainstones with ooids and abraded forams, and rare high spired gastropods	**PROTECTED EMBAYMENT FACIES** Seagrass community, with abundant gastropods, miliolid and alveolinid forams, and diverse small infaunal pelecypods	**CORALGAL REEFS OR NUMMULITE BANKS (EOCENE)** **RHODLITH PAVEMNET FACIES** Circumrotary coraline red algae (rhodoliths), codiacean algae, seagrass type miliold forams and encrusting bryozoans	**DEEPER RAMP FACIES** Larger forams common (e.g. Discocyclina) pectrid pelecypods, bryozoans, echinoids, and sparse planktonic forams	**SLOPE TO BASIN FACIES** Dominantly globlgernid planktonic forams, with an associated low diversity small sized biota.

Fig. 3.4. Generalized Tertiary carbonate ramp model showing the main depositional environments and associated faunas (modified from Buxton and Pedley, 1989).

3.4. Ecological Controls on Nummulites Accumulations

3.4.1. Symbiotic Process

Nummulites and other larger foraminifera lived symbiotically with photosynthetic algae and are therefore thought to have been restricted to warm (25°C), clear, shallow (<120m) waters within the euphotic zone (Reiss and Hottinger, 1984). In the symbiotic relationship, the nummulites provide shelter for the algae while the algae produced oxygen and nutrients for the nummulites as a bi-product of photosynthesis (Racey, 2001). Nutrient availability is often linked to temperature and salinity; upwelling adds nutrients whilst reducing temperature; runoff adds nutrients whilst reducing salinity, and evaporation concentrates nutrients whilst raising salinity (Hallock and Schlager, 1986). Nummulites with many other large foraminifera including nummulitids and alveolinids, are characterized by complex internal morphologies. Haynes (1965) related this complexity to the presence of photosynthetic symbionts within the test of many species. This host-symbiont relationship means that most living larger foraminifera are restricted to shallow areas, and if untransported, their presence is generally indicative of water depth less than 130m, i.e., within the photic zone (Hottinger, 1983; Hallock, 1984). Ross (1972) suggested that algal symbiosis in large foraminifera is comparable in terms of growth stimulation and calcium carbonate fixation to that found in hermatypic corals.

3.4.2. Light Intensity and Water Energy

Haynes (1965) proposed that test shape is a compromise between the metabolic requirments associated with algal symbiosis, hydrodynamic factors and light. Many authors have suggested that light availability controls test morphology through symbiotic interaction as illustrated in Figure 3.4 (Haynes, 1965; Hottinger and Dreher, 1974; Hallock and Hansen, 1979). As light intensity decreases with increasing water depth there is a tendency for the test to thin and flatten, resulting in a larger surface area for the photosynthetic symbionts to available light. Hallock (1979) observed that more oblate and thicker tests are found in species inhabiting shallow water where they are more able to withstand higher energies associated with wave or current activity. Trevisani and Papazzoni (1996) identified two nummulite subspecies which occur in the upper and lower facies of shallowing-upward cycles, with the flatter form occurring in base-cycle marls, and the more 'robust' form being restricted to shallower, cycle-top limestones. These differences were attributed to the effects of water energy, light intensity and substrate.
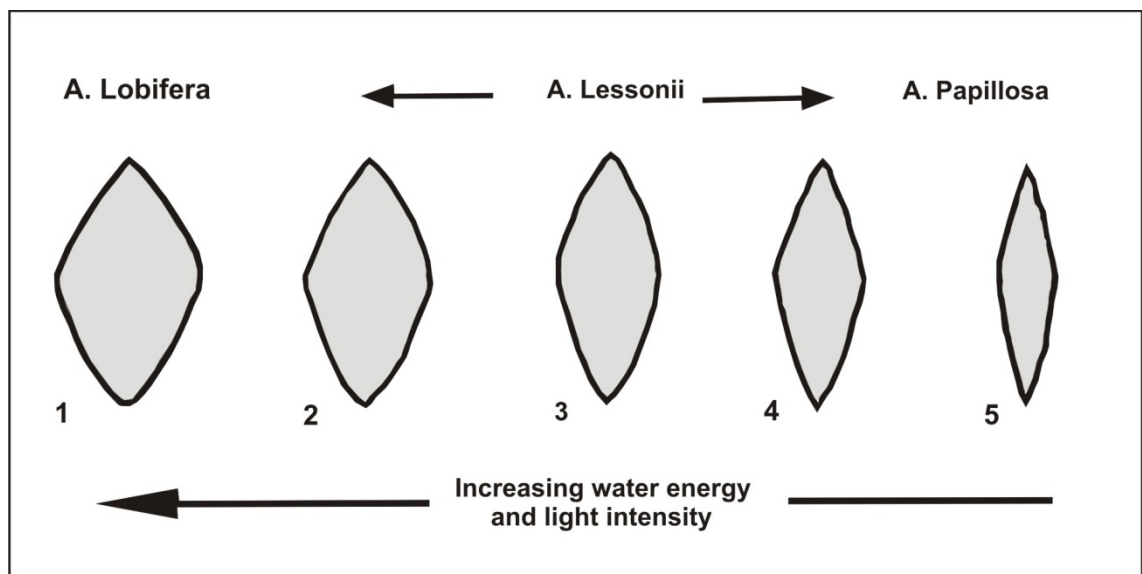
Figure 3.5. The range of shape in three Indo-Pacific species of *Amphistegina* related to water energy and light intensity: (1) *A. lobifera*, high-energy, high-light environment; (2) *A. lessonii*, moderate-energy, high-light environment; (3) *A. lessonii*, low-energy, moderate-light environment; (4) *A. lessonii*, low-energy, low-light environment; and (5) *A. papillosa*, low-energy, very low-light environment (after Beavington-Penny and Racey, 2004).

3.4.3. Substrate

Hohenegger et al. (2000) noted that extant nummulitids from the West Pacific prefer coarse sandy substrates below fair-weather wave base, whilst the deep-dwelling *Planoperculina heterosteginoides* is restricted to poorly illuminated areas of 0.3 to 2.5% surface light intensity, and preferred medium to fine grained sand substrates and calm water. Several authors have attributed variations in test size of fossil nummulites to changes in substrate (often related to changes in water depth). Pomerol (1981) noted that the size of nummulites was inversely proportional to clay content of the surrounding sediments, while Nemkov (1962) concluded that nummulites were larger in shallow-water calcareous and sandy deposits than in deeper water clay-rich sediments. Beavington-Penny (2002) identified two A-form dominated nummulite populations associated with seagrass-vegetated environments in the Middle Eocene Seeb Formation of Oman. Both contained a highly diverse biota typical of shallow-marine, protected environments (including micritic peloids, soritid foraminifera, orbitolites, alveolinids, miliolids, peneroplids, texulariids, probable encrusting foraminifera and dasycladacean green algae), many of which are common in the seagrass environment.

3.4.4. Water Motion

Water motion may influence test shape (Hallock, 1979) (Figure 3.5). Hallock et al. (1986) observed in their study that increased light saturation and water motion produced a thicker wall, and therefore a thicker test. They also noted that, as water motion increased, the test thickens (through increased calcification). Slower growth rates were also noted by Rottger (1972) in *Heterostegina depressa* under conditions of increased water motion.

3.4.5. Salinity

Salinity variations are generally too minor to be ecologically significant in offshore settings, although in nearshore areas with high runoff, salinity variations are marked and may be of considerable importance in controlling foraminiferal distribution (Phleger, 1960). Reiss and Hottinger (1984) reported that the larger foraminifera are abundant and diverse in the Gulf of Aqaba at salinities of 40-41‰. The rotalliid large foraminifera are typically stenohaline, with tolerance limits in the range of 30-45‰ (Hallock and Glenn, 1986).

3.4.6. Temperature

Temperature strongly affects many physical and chemical properties and biological processes within the marine environment (Beavington-Penney and Racey, 2004). Adams et al. (1990), and Jones (1999) observed that temperature also appears to control the diversity of larger foraminifera assemblages: tropical to subtropical, shallow-water assemblages are characterized by more than 10 species, whilst very warm (greater than approximately 31ºC) and warm temperature (less than approximately 20ºC) shallow-water environments generally contain fewer species. Hollaus and Hottinger (1997) suggested that the larger benthic foraminifera distribution limit of 16-18ºC is related to the minimum temperature required for the growth of their endosymbionts. Of the larger benthic foraminifera, amphisteginids and soritids display the widest latitudinal distribution, related to their tolerance of a relatively wide temperature range (Murray, 1991; Langer and Hottinger, 2000), as shown in Figure 3.6.
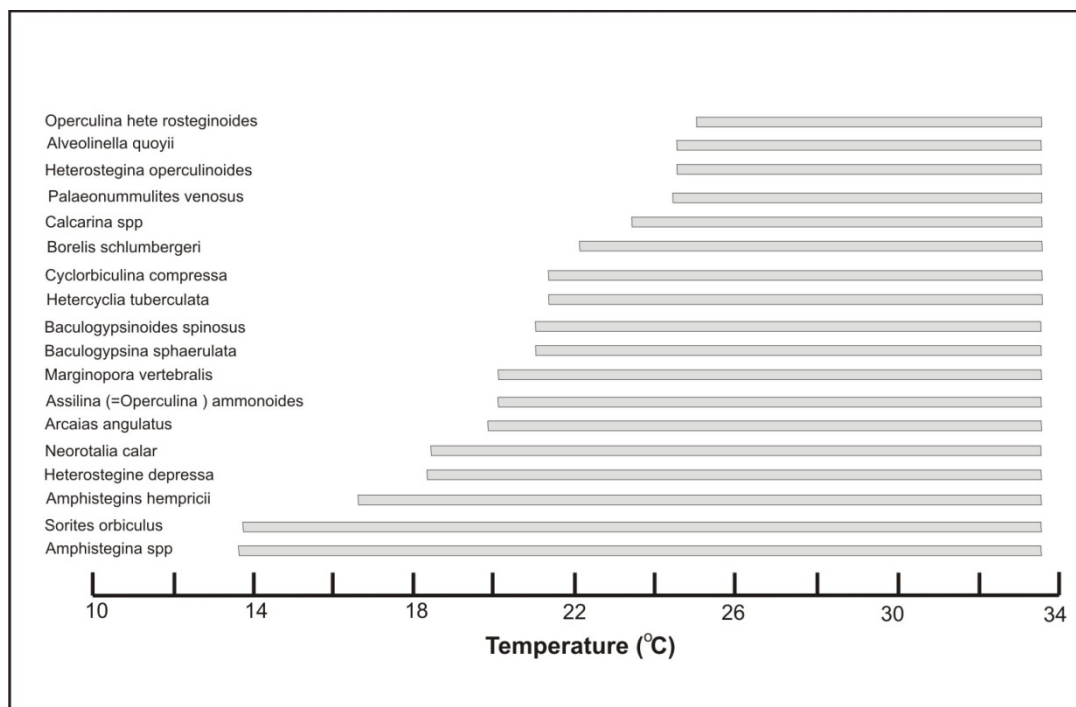
Figure 3.6. Sea-surface temperature ranges of selected larger benthic foraminifera (after Beavington-Penny and Racey, 2004).

3.5. Taphonomic Processes

Beavington-Penney (2004) concluded that possible candidates responsible for the damage observed in Eocene nummulites include predation by large bioeroders, such

as fish and echinoids, and transport within turbidity currents. Other taphonomic factors that have produced or contributed to extra damage (such as micro-scale bioerosion, dissolution, and compaction) are considered to have played only a minor role.

The observations used by Beavington-Penney (2004) to aid identification of in-situ versus transported fossil nummulite tests in thin-section are illustrated in Figure 3.7.

3.6. Depositional models of Larger Foraminifera

In terms of depositional environment, several facies models have been proposed to characterise nummulite-rich deposits (Figure 3.8). Different palaeowater depths are proposed, from 10-60m depth, and different morphologies of sedimentary bodies are described:

- **Nummulite banks:** are convex-up structures. These so-called "bank" structures were described first by Nemkov (1962) and then named by Arni (1965). This sedimentary body is usually characterised by a mono-specific association of nummulites, separating a restricted area (back-bank environment) from an open-marine zone (fore-bank settings). This model has been applied to the Eocene Tatra Formation of Poland (Kulka, 1985), the Middle Eocene build-ups in Egypt (Aigner, 1983), the El Garia Formation in Central Tunisia (Moody, 1987) and the Jdeir Formation in offshore Libya (Anketell and Mriheel, 2000).

- **Shoals:** may form in proximal up-ramp settings or as re-deposited nummulitic material in a deep-water environment (Racey *et al*., 2001). Nummulites were reworked from the proximal up-ramp areas and transported by turbidity or storm currents into deep-waters.

- **Nummulite "bars":** developed in very shallow environments, in front of coralgal reefs bordering a carbonate ramp system (Eichenseer and Luterbacher, 1992)**.** This model has been proposed for the Ager Formation in the south Pyrenees foreland basin (Spain). High-energy hydrodynamic structures forming nummulite bars can be observed in Central Tunisia (after Jorry, 2004). Nummulite-rich sediments are considered as autochthonous deposits or para-autochthonous to

allochthonous deposits, the latter resulting from landward or seaward transportation. Autochthonous deposits are characterized by packstone to
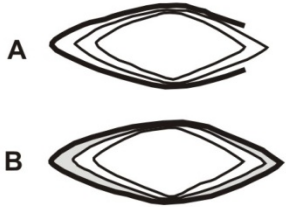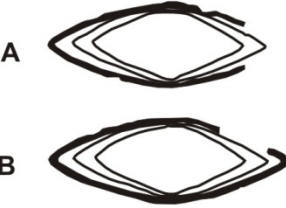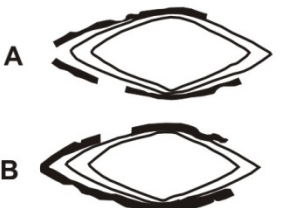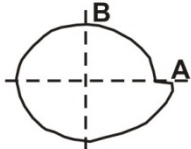
	Axial section	Damage observable in thin-section
In situ	A / B	Test generally undamaged / Outer wall may be missing/damaged on one side of the test in 'A' section
Moderate transport/ wave re-working	A / B	Outer wall may be missing/damaged on one side of the test. / Holes with irregular margins may puncture outer wall on one side of the test. / Shallow 'pits' (which don't penetrate outer wall) may cover entire test surface.
Extensive transport/ wave re-working	A / B	Outer test wall may be missing/damaged on one or both sides. / Hole with irregular margins may penetrate outer wall on both sides of the test. / Shallow 'pits' (which don't penetrate outer wall) may cover entire test surface. / 'Micro-pits' may penetrate outer wall on both sides of the test.
Equatorial section	B A	Diagrammatic representation of megalospheric Nummulites (equatorial view), showing location of axial sections ('A' = section through terminal chamber)

Figure 3.7. Test breakage patterns in *Palaeonummulites venosus* as a guide to the autochthonous versus allochthonous nature of fossil nummulites in thin-section (after Beavington-Penney, 2004).

wackestone textures, in which macrospheric forms (A-form) are much more frequent than microspheric ones (B-form). Tests are rarely abraded and are encrusted on only one side (Jorry, 2004). The fauna associated with nummulite accumulations commonly includes coralline algae, echinoderms, molluscan debris, small benthic foraminifera and larger benthic foraminifera such as *Discocyclina* and *Assilina* (Racey, 2001). In contrast para-autochthonous and allochthonous deposits resulting from transportation or in-situ winnowing are characterised by more or less monospecific assemblages and grain-supported patterns. Sedimentary structures, which should be omnipresent in high-energy deposits, have

been rarely documented in field or core studies (Jorry, 2004). Jorry *et al.* (2003) mentioned the presence of large-scale cross bedding in the Eocene El Garia Formation in Central Tunisia, but most of the grain-supported facies show a rather chaotic pattern and no obvious sedimentary structures.

3.7. Nummulite accumulation reservoirs

Nummulitic limestones form important hydrocarbon reservoirs offshore Tunisia (Racey *et al.,* 2001) (e.g. Ashtart field: 350-400 MMBLS) and Libya (Anketell and Mriheel, 2000) (e.g. Bourri field: 1,000-3,000 MMBLS) and represent potential exploration targets in Egypt, Italy, Oman and Pakistan. Nummulite accumulations may have high porosities ranging from 10-26% and permeabilities ranging from 10-50 mD (Racey, 2001). In the Jdeir Formation, offshore northwestern Libya, porosities reach 40% (Anketell and Mriheel, 2000). According to Racey (2001) the best reservoir development is in nummulite accumulations where there has been little compaction and where nummulithoclastic debris and lime-mud are absent. In these deposits nummulite tests are generally moderately to well sorted and there is minimal or no precipitation of late burial cements. Diagenesis (such as dissolution, dolomitization, cementation and compaction) is the main control on enhancing or destroying the porosity in nummulite accumulations (Anketell and Mrihell, 2000, and Racey, 2001).
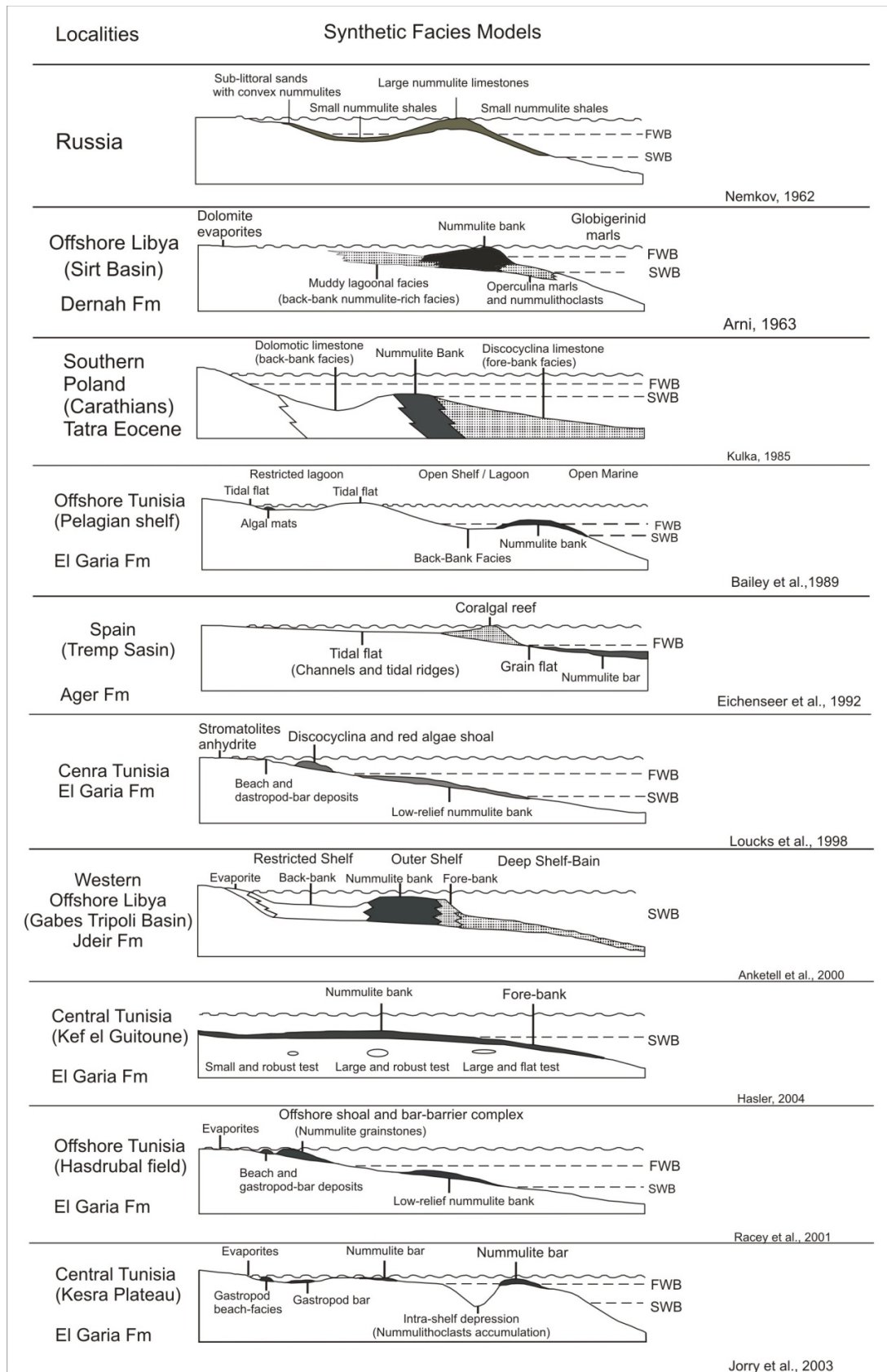
Figure 3.8. Comparison between different models characterising the nummulite palaeoenvironment (modified by Jorry. 2004).

3.8. Summary

Nummulites are Tertiary (Late Palaeocene to mid-Oligocene) benthic rotaliid foraminifera which are particularly common throughout the Tethyan region. Nummulites with other larger foraminifera including nummulitids and alveolinids are believed to have lived symbiotically with photosynthetic algae and are therefore thought to have been restricted to warm (25ºC), clear, shallow waters (<120m) within the euphotic zone. Nummulites had alternating asexual and sexual generations, characterized respectively by small A-forms and large B-forms. In nummulitic banks, B-forms are often dominant in high-energy settings, whereas the A-forms and larger *Discocyclina* are dominant in deeper-water, lower energy settings. The distribution of these two morphotypes is in general controlled by the hydrodynamics of the depositional system. Nummulite tests may display breakage ranging from external damage to complete fragmentation (commonly referred to as nummulithoclastic debris). Studies of modern larger benthic foraminifera suggest that transport-induced abrasion is a likely candidate for the test damage. Larger benthic foraminifera are important contributors to modern and ancient tropical, shallow-marine sediments. Eocene nummulitic limestones are important hydrocarbon reservoirs in North Africa (Tunisia and Libya) with good porosity and permeability. Also they are potential exploration targets in Egypt, Italy, Oman and Pakistan.

CHAPTER 4: FACIES ANALYSIS AND DEPOSITIONAL ENVIRONMENTS OF THE GIALO FORMATION

4.1. Introduction

This chapter presents the description, interpretation and depositional environments of the Middle Eocene Gialo Formation and evaluates the spatial variability in carbonate platform development by using core data and petrographic microscope observations of samples from five selected wells. There is a section on the subsurface wireline logs that have been calibrated by study of the cores and thereby used to facilitate correlation. This chapter also includes detailed results of porosity and permeability measurements made in the laboratory.

4.2. Introduction to Gialo Formation

The Gialo Formation consists of lime wackestone interbedded with packstone, locally grading to grainstone, much of which is nummulite-rich that developed during the Middle Eocene over the central and eastern portions of the Sirt Basin. Towards the west, the formation passes laterally into a series of mixed shales, dolomites and evaporites of the Gedari Formation. To the northeast, in the vicinity of the Agedabia Trough, it gives way to a thick succession of deeper marine shales (Wennekers *et al.*, 1996; Hallett, 2002) (Figure 4.1). The total thickness of the Gialo Formation in the type section (well E91-59) is 1585 ft. In this study, 1130 ft was recorded in well 4O1-6 and only the upper part of the formation was penetrated by wells O3-6, H4-6, H6-6 and H10-6. The Gialo Formation conformably overlies the Gir Formation, whereas the upper contact with the overlying Augila Formation is sharp and possibly disconformable. It is the main oil reservoir in the Gialo Field and several neighbouring fields. It is gas productive in the Sahl and Assumood fields.

4.3. Previous work on the Gialo Formation

The Gialo Formation in the Sirt Basin in Libya is a thick limestone unit of Middle Eocene age. It has been the subject of considerable study (mainly outcrop) during the last decade because of the importance of sediments of this age as

hydrocarbon reservoirs. The sedimentology of the Eocene formations at outcrop was essentially documented by El Hawat (1985, 1986a), and El Hawat and Shelmani (1993). These studies give important information to understand the relationships between the different sedimentary processes, taking place on the platform, the slope and the basin. The description of the three main type-sections in NE Cyrenaica was decisive for the characterization of the facies heterogeneities of the Dernah Formation (Middle Eocene). Three principal depositional environments were recognized by the authors: a) Lagoonal and inner bank facies, dominated by large *Orbitolites, Alveolina,* miliolids and red algae, and these crop out-along a roadcut near Cyrene, b) nummulite bank and outer bank facies, dominated by nummulites and lime mudstone (roadcut near Ain ad-Dabusseyah), and c) coralgal and dolomite facies, dominated by coral, nummulites, *Discocyclina* and red algae (west Dernah roadcut). Recent studies were undertaken on the Dernah Formation (Abdulsamad, 1999; Abdulsamad and Barbieri, 1999), in order to correlate outcrop sections to subsurface wells. The authors used the determination of nummulite species to establish guidelines for correlation.

Belazi (1987) carried out the only comprehensive sedimentological study based on subsurface data from the Nafoora-Augila oil fields in the Eastern Sirt Basin. He introduced formal formation names based on lithostratigraphic work in the subsurface type-section. He focused on the sedimentology, diagenesis, stratigraphy and regional significance of the hydrocarbon-bearing Tamet Formation and the overlying Augila Formation. He placed little emphasis on the broader sequence stratigraphic framework in terms of using systematic rock-fabric changes for guiding zonation and up-scaling in the subsurface.

4.4. Facies classification and descriptions

A facies is defined as a body of rock characterized by a particular combination of lithology, and physical and biological structures that bestow an aspect (facies) different from the body of rock above, below and laterally adjacent (Walker, 1992). Accordingly, a depositional facies reflects a variety of biological, physical and chemical processes that were active in the depositional environment. Although facies are often given brief descriptive names it is generally understood that they are units which will ultimately be given an environmental interpretation (Middleton, 1978; Walker, 1992).

Based on the core description of five wells (OOOO1, O3, H4, H6 and H10-6) and the petrographic study of 175 thin-sections, seven main facies and twenty microfacies within the Gialo Formation have been distinguished during this study. These seven major facies are described and interpreted below, and the facies scheme is summarised in Table 4.1.
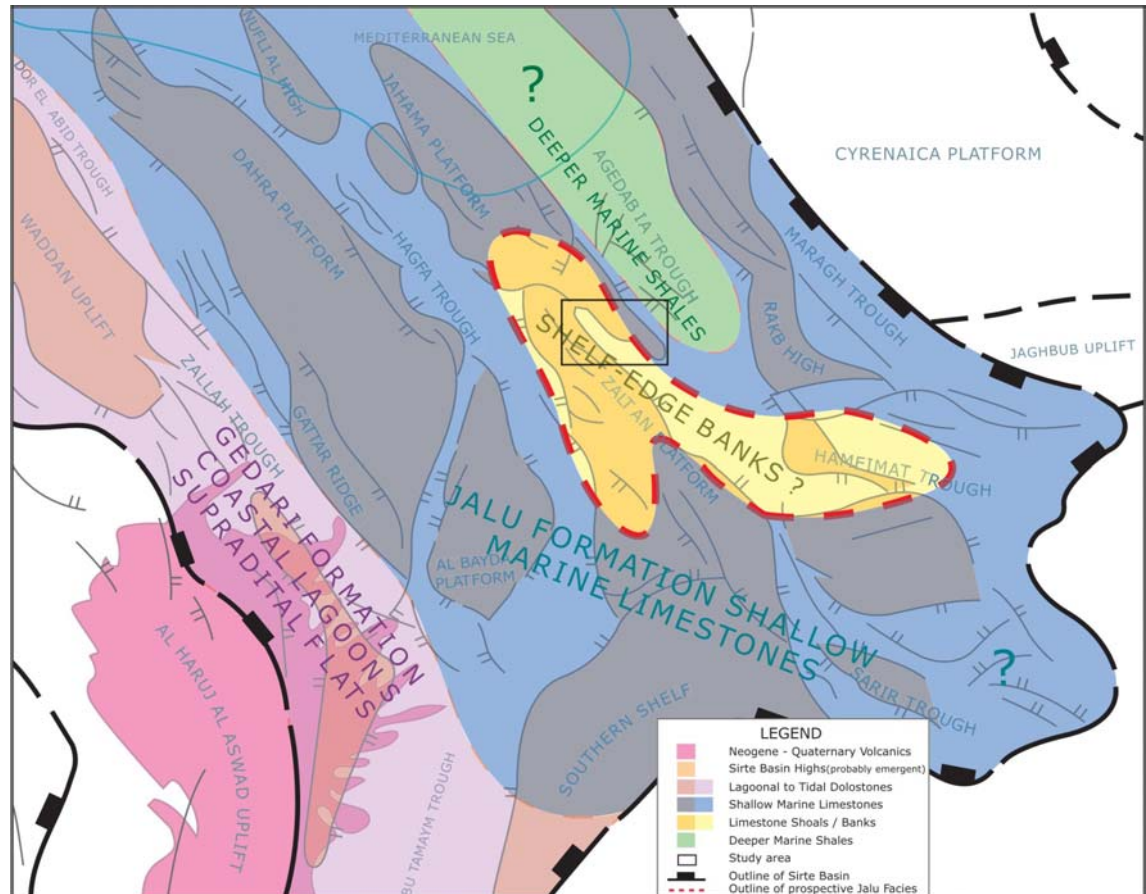
Figure 4.1. Structural elements and facies distribution (after Hallett, 2002).

Lithologies, presented as petrographic summary charts in Appendix I, are described as informatively as possible in terms of their texture, structures and faunal content. Carbonate lithologies are described in terms of Dunham's (1962) textural classification (see Appendix III). Lithologies named as two (or more) textural types are on the border of the textural types as defined by Dunham (1962) and often contain areas of both (or all) textural types in one thin-section. For example, beds which are described as wacke/packstones include areas of both wackestone and packstone texture. Bioclastic lithologies are those composed of whole or fragmented bioclasts of which no fossil group constitutes ≥15% by volume. Fossil names prefixed to lithological names indicate

that the lithology includes ≥15% by volume of the aforementioned fossil. For example, a *Discocyclina* and nummulite bioclastic wacke/packstone is a wacke/packstone which contains ≥15% of both *Discocyclina* and nummulites, and <15% of other bioclast types.

4.4.1. Nummulite facies (NF):

Microfacies: **Nummulitic Packstone/Rudstone (NP/R) Nummulitic Wackestone/Floatstone-Packstone (NW/F-P)**

Nummulitic Wackestone-Packstone/Floatstone (NW-P/F)

Nummulithoclastic Wackestone/Floatstone (NCW/F)

Nummulithoclastic Wackestone/Packstone (NCW/P)

This facies is widespread in the study area. It occurs in the upper and middle parts of wells H4, H6, H10 and 4O-6 while in O3-6 it occurs only in the middle part underlying the *Operculina-Discocyclina* bioclastic facies (Figures 4.9, 4.10, 4.11, 4.12 and 4.13). The facies is generally characterized by a creamish brown and brownish grey colour and, soft to medium hardness; unit thickness varies between 5-80 feet; small and large nummulites (whole <30% and fragments <40%) are abundant. Other common components are echinoid fragments and spines, both commonly rimmed by syntaxial calcite overgrowths. Minor bryozoan, and scattered skeletal grains of smaller foraminifera (rotaliids), rare *Discocyclina* and brachiopod fragment also occur. Molluscan fragments and coralline red algal fragments are very rare. All are in a fine to medium coarse skeletal grain wackestone/packstone matrix of bioclastic hash. Lime mud matrix is rare and patchily distributed, since much of it was removed by winnowing. The sorting of the bioclasts is moderate to poor.

The Nummulitic Packstone/Rudstone microfacies is observed in the upper part of wells 4O1, H10 and H6-6. The grains of this microfacies are represented by robust, sub-globular small nummulites (A-forms with scattered large, flattened B-forms), echinoid fragments, and *Discocyclina* (Figures 4.2 and 4.3a); bryozoans, coralline algae and peloidal grains are rare. The nummulite chambers are partially to completely filled by sparry calcite (Figure 4.3a).

The Nummulitic Wackestone/Floatstone-Packstone microfacies is observed in most of the wells. It consists of robust sub-globular small A-forms and scattered

flattened large B-forms with minor echinoid, *Operculina*, mollusc fragments and scattered bryozoans.

Core photograph and photomicrograph of nummulite facies (NF) showing the common occurrence of small A-form (N-AF) and large flattened B-form (N-BF) nummulities, well 4O1-6, 5134'.

Thin-section photomicrograph of nummulitic packstone/rudstone microfacies showing robust, small A-form and flattened large B-form nummulites, with scattered *Discocyclina* (D), well 4O1-6, 5134', PPL.

Figure 4.2. Nummulite facies (NF), Gialo Formation.

The Nummulithoclastic Wackestone/Floatstone and Wackestone/Packstone microfacies are observed in most of the studied wells and are composed mainly of whole and fragmented large and small benthic foraminifera, nummulites, echinoid plates, bryozoans and mollusc fragments in varying amounts, with high contents of micrite (Figure 4.3C&D). Most fragmented grains are angular and moderately to poorly sorted, which together suggest the material was reworked from the shallow-water nummulite platform and then redeposited in a low-energy environment. The matrix is dominantly composed of sand-sized nummulite debris, and organic matter (Figure 4.3D). Nummulites are tightly packed in parts and locally grain contacts are sutured or stylolitic. The stylolite seams are not generally common; they have a low amplitude and are usually filled by black organic matter. Microfractures are observed in some places, partially to completely filled by calcite cement. Bored nummulites are rarely present (Figure 4.5B). Authigenic minerals are dominated by non-ferroan calcite cements and

scattered disseminated pyrite. Observed porosity in this facies is poor to very good (5-26%) and includes intergranular, intragranular, vuggy, moldic and rare microfracture, with poor to good permeability.

Facies interpretation

Aigner (1983) summarized that nummulites commonly occur in association with other large foraminifera in neritic and shelf-ramp environments in many parts of the Mediterranean Palaeogene successions and are considered to have formed as banks or 'reefal' build-ups. The occurrence of well-preserved, abundant large perforate foraminifera and echinoids indicates that normal-marine conditions prevailed during the deposition of this facies. The large size, nature and sorting of the large nummulite tests and grain-supported texture of the nummulite rudstone are all indicative of a moderate to high-energy bank environment. Nummulites may have lived originally on a relatively soft lime-mud substrate (Blondeau, 1972), although the sedimentary texture and the biofabric of the nummulite bank facies suggest that considerable amounts of mud have been winnowed away and that the foraminiferal tests have been concentrated by physical processes (Aigner, 1983). The Nummulitic packstone has a dense concentration and imbrication of nummulites. This is indicative of winnowed lags caused by short hydrodynamic events (Aigner, 1983). He also suggested that the reworking of nummulites must have occurred without large-scale lateral transport by in-situ winnowing and in shallow waters subjected to storm events. Large flat nummulites tend to be associated with similarly shaped *Assilina* and *Discocyclina* in relatively deep-water facies, whilst smaller, lenticular nummulites occurred in shallower-water. Lenticular to globular-shaped nummulites tend to occupy intermediate environments. Outer-wall damage of some nummulites in the Nummulithoclastic Floatstone/Rudstone microfacies may indicate moderate transport and wave re-working (Beavington-Penney, 2004). The occurrence of abundant nummulithoclastic debris in the Nummulithoclastic Wackestone/Floatstone (NCW/F) and Nummulithoclastic Wackestone/Packstone (NCP/W) microfaces indicates extensive transportation. It is suggested that periodic high-energy events resulted in redeposition in inter-bank or back-bank areas. Abundant micrite is indicative of deposition in lower energy conditions. Anketell and Mirheel (2000) suggested that high-energy conditions caused fragmentation of nummulites in the Jdeir Formation, carrying them towards the back-bank setting. From a study of the

Al Garia Formation of Tunisia Beavington-Penney *et al.* (2005) concluded that nummulites on palaeohighs were transported into surrounding deeper water. They suggested that ocean and storm currents swept the platform top, producing a nummulitic sediment package that thickened and became increasingly fine-grained and fragmented into the outer-ramp environments.

Racey (2001) documented the complex relationships between large benthic foraminifera typical of Early Tertiary carbonate platforms, and concluded that nummulites occupied a broad range of open-marine environments on both the ramp and shelf, and were generally absent from more restricted waters.

A — Thin-section photomicrograph of nummulite packstone/ rudstone (NP/R) microfacies shows compacted robust-flattened A-form nummulite. Blocky to drusy calcite cements have partially filled porosity (red arrow),well H6-6,4930', PPL.

B — Large nummulite grain exhibits partial boring, filled by equant calcite cement (b1), and lime mud (b2), well 4O1-6, 5225', PPL .

C — Well H6-6, 4973', PPL

D — Well H10-6, 4989', PPL

Thin-section photomicrograph of nummulithoclastic wackestone/packstone (NCW/P) of poorly sorted skeletal fragments, predominantly of nummulite tests, as well as a few whole tests of nummulites. Calcite cement partially occludes the porosity (red arrow).

Figure 4.3. Thin-section photomicrographs of nummulite facies, Gialo Formation.

4.4.2. *Discocyclina*-Nummulite facies (DNF):

> Microfacies: *Discocyclina* Nummulite Wackestone/Packstone
>
> (DNW/P)
>
> *Discocyclina* Nummulite Wackestone/Floatstone (DNW/F)

This facies is recognized in the upper, middle and lower parts of most of the studied wells (Figures 4.9, 4.10, 4.11, 4.12 and 4.13). Units range in thickness from 10-60 feet and have a light-grey to greenish-grey colour. Poorly sorted, fragmented and whole robust, flattened *Discocyclina* comprise between 15-25% of this facies, and are associated with whole (mainly small A-forms) and fragmented nummulites (15%) (Figure 4.4A). Less common bioclasts are echinoid plates, bryozoa and small benthic foraminifera. The matrix is dominantly composed of finely fragmented bioclasts. Equant sparry calcite cement fills pore-space between some bioclasts and results in a pack/rudstone texture. There is a variation in the abundance of large benthic foraminifera. Abundant (≤60% by volume) and common (≤20% by volume) large benthic foraminifera give rise to packstone and wackestone textures respectively. Pressure dissolution seams and micro-stylolites were the only structures seen in this facies. Poor to good visible porosity (3-13%) includes small vugs and intragranular pores. The permeability is low due to poor interconnections.

Facies interpretation

The abundance of larger perforate benthic foraminifera in this facies indicates deposition under normal-marine conditions within the photic zone. Previous studies have interpreted *Discocyclina* as having lived in a broad spectrum of environments in the photic zone, including shallow fore-reef and back-reef environments (e.g., Racz, 1979; Anketell and Mriheel, 2000) and deeper, outer-ramp (e.g., Gilham and Bristow 1998). Other authors have noted an environmental control on test morphology, with *Discocyclina* in very shallow photic-zone settings having small, robust tests, whilst those living in lower-light, deeper settings have large flattened tests (e.g., Ghose, 1977; Loucks *et al*., 1998; Sinclair *et al.,* 1998; Geel, 2000). The presence of abundant elongate *Discocyclina* suggests deposition in the photic zone, but below FWWB (Beavington-Penney *et al*., 2005). A low to moderate energy environment of deposition is inferred from the muddy or marly matrix, wacke/packstone texture and well preserved nature of the thin, rather delicate tests of large benthic foraminifera. Whole

and fragmented nummulites are interpreted to have been reworked from higher energy areas.

4.4.3. Nummulitic- *Discocyclina* facies (NDF)

Microfacies: **Nummulitic- *Discocyclina* Wackestone/Floatstone (NDW/F)**

Nummulitic- *Discocyclina* Wackestone-Packstone (NDW-P)

This facies occurs in the middle parts of wells H6 and H10-6, while in 4O1-6 it occurs only in the upper part underlying the Nummulite Facies (Figures 4.11, 4.12 and 4.13). Unit thickness of this facies varies between 5-35 feet.

The Nummulite-*Discocyclina* Facies is characterized by light grey to brownish grey, poorly sorted, small and large nummulites (whole and fragmented), associated with robust whole and fragmented, flattened large and small *Discocyclina* (Figure 4.4B). Other less common bioclasts are small echinoid fragments; syntaxial calcite spar overgrowths and micrite envelopes are observed. The chambers of the foraminifera are partially to completely filled with sparry calcite and locally by micrite, rarely by pyrite. The matrix is composed of micrite, fine bioclastic fragments and rare equant calcite. Poor visible intergranular, intragranular and mouldic porosity is present.

Facies interpretation

The biota in this facies indicates deposition under normal-marine conditions within the photic zone. Whole and fragmented nummulites are interpreted to have been reworked from medium-higher energy areas. Deposition in a low-moderate energy regime, fore-bank environment is suggested by the abundance of micrite (average 20-45%) and thin flattened *Discocyclina* (Henson, 1950).
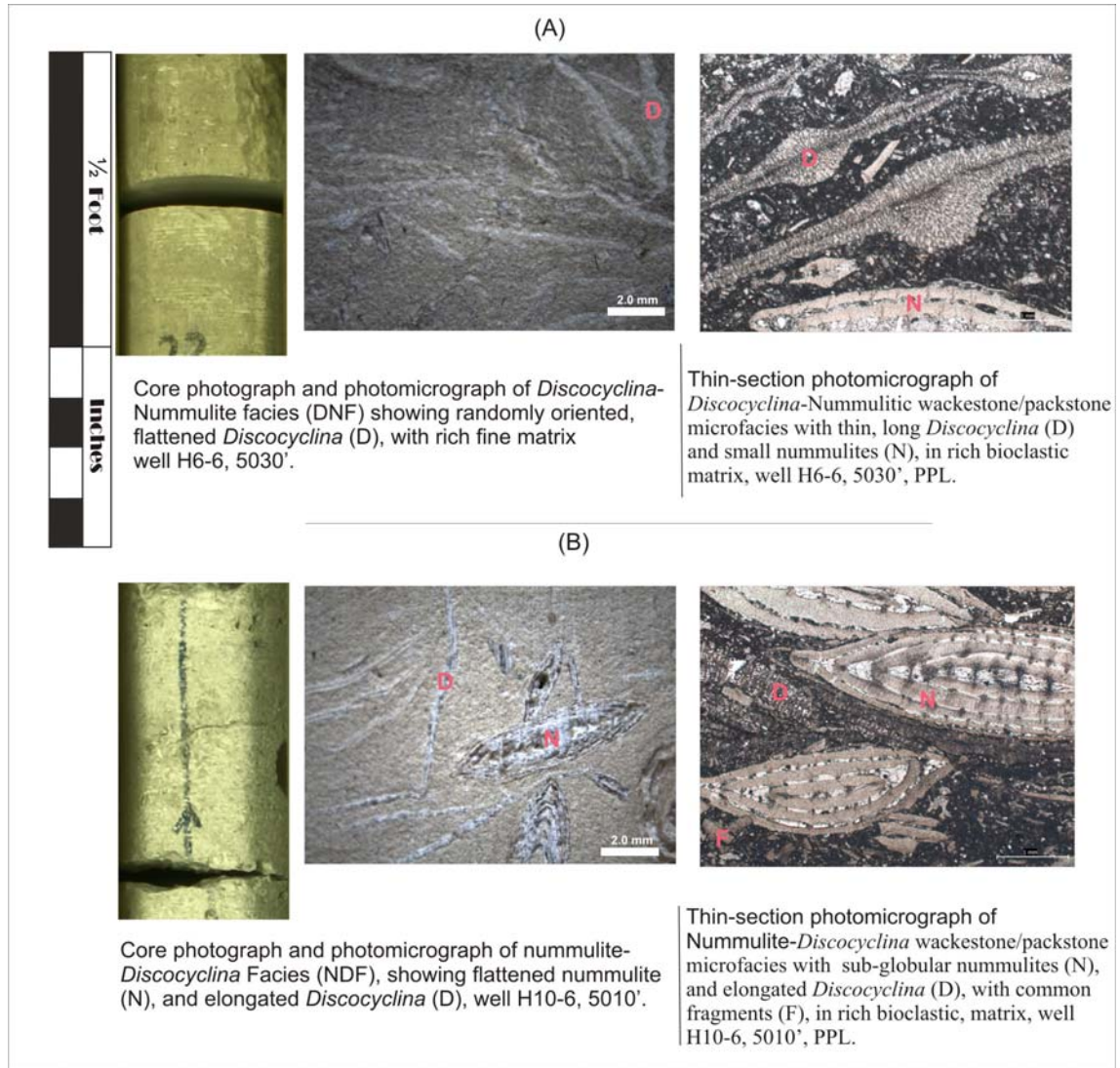
Figure 4.4. *Discocyclina*-Nummulite and Nummulite-*Discocyclina* facies of the Gialo Formation.

4.4.4. Molluscan facies (MF):

Microfacies: Molluscan Bioclastic Wackestone/Packstone (MBW/P)

The molluscan bioclastic wackestone microfacies is identified only in the lower part (5ft thick) of well H4-6 overlying the nummulite facies (Figure 6.9). The molluscan facies is composed mainly of brownish grey to light grey, poorly sorted medium-coarse grained mollusc fragments (bivalves, gastropods and scattered scaphopod fragments, 15-30%), with less common echinoid plates, brachiopods and whole and fragmented small nummulites. Other bioclasts include small foraminifera (rotaliids and textularia). This facies has wackestone/packstone locally grading to mudstone/wackestone depositional textures. Micritic envelopes are occasionally noted. The original mollusc

shells have been partially to completely dissolved and only the outer micritic envelope remains, especially in wackestone/packstone microfacies (Figure. 4.5). Subsequently, these envelopes are filled by blocky and drusy calcite and the original structure of the bioclasts is lost. Syntaxial calcite overgrowths are rare around echinoid plates in the packstone lithologies. The matrix in this microfacies is dominantly composed of micrite (partially recrystallized to microsparite). Rare pressure dissolution seams and stylolites also occur. Poor to good (2-12%) vuggy and mouldic porosity is present. Sedimentary structures were not observed in this facies

Facies interpretation

The fauna present in the molluscan bioclastic wackestone facies (bivalves, brachiopods, gastropods and scaphopods) provides evidence of a restricted environment (Wilson, 1995). Associated bioclasts of echinoid fragments indicate normal marine environments. The internal microstructure of molluscs is composed of coarse drusy sparite with rare porosity. This suggests that the unstable original aragonite was completely dissolved and the void filled by drusy sparite. Sbeta (1991) interpreted the presence of wackestone and packstone facies rich in bivalves, foraminifera and ostracods within the Harshah Formation (Middle-Upper Eocene) in offshore western Libya as having been deposited in a shelf lagoon environment. Deposition in lagoonal areas is the inferred environment of formation of these sediments.

Core photograph and photomicrograph of mullscan facies showing large brachiopod (B) and scattered bivalve (V) fragments, well H4-6, at 5059'5" depth.

Thin-section photomicrograph of molluscan bioclastic wackestone, H4-6 well, 5059'5".

Molluscan bioclastic wackestone/packstone microfacies showing bivalves (V), echinoid (E) fragments and broken nummulites (N), in fine bioclastic matrix, H4-6 well, 5060', PPL.

Figure 4.5. Mollusc facies (MF), Gialo Formation.

4.4.5. *Operculina*-Nummulitic Facies (ONF):

Microfacies: *Operculina*-Nummulite Wackestone (O-NW)

Operculina-Nummulite Wackestone/Packstone (O-NW/P)

This facies is observed in the middle part of well O3-6, with about 5 feet thick overlying the nummulite facies (Figure 4.10). The *Operculina*-Nummulite facies consists of medium grey to brownish grey wackestone-packstone, and is poorly sorted. It contains abundant thin and flat whole and fragmented *Operculina* (up to 40%) (Figure 4.6). *Operculina* are associated with small whole and mainly fragmented nummulites and other small benthic foraminifera (Textulariidae). Another less common component is echinoderm debris; the fine matrix contains a high proportion of nummulithoclastic debris. Stylolite structures are rarely present. Observed porosity is poor to good (4-12%), and includes small vuggy and rare intragranular pores.
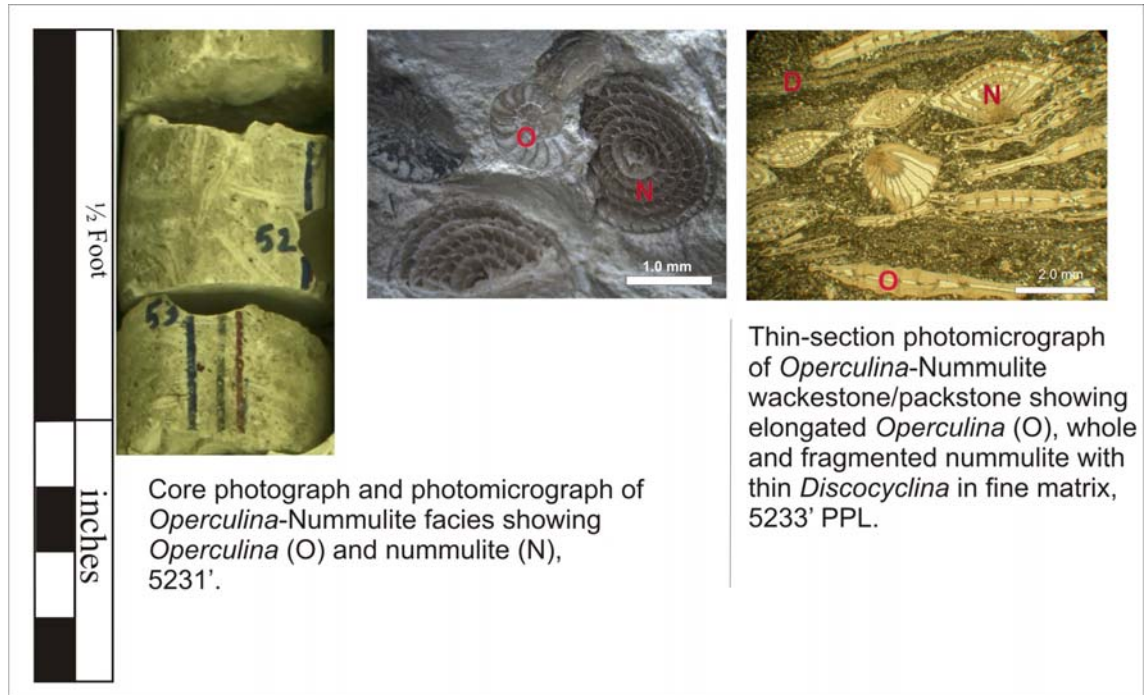
Figure 4.6. *Operculina*-Nummulitic Facies (ONF), Gialo Formation, well O3-6.

Facies interpretation

Based on previous studies in Tunisia (Loucks *et al*., 1998; Racey *et al*., 2001), in Libya (Arni, 1965), in Spain (Eichenseer *et al*., 1992) and in Yugoslavia (Bignot, 1972), the *Operculina* facies characterizes a deeper-water environment than the nummulite facies. However, in modern environments, the foraminifera *Operculina* can occur with thin nummulites in deep-water (Hohenegger *et al*., 2000). Thin and flat *Operculina* forms suggest moderate to deep water but still within the photic zone.

4.4.6. *Operculina-Discocyclina* bioclastic facies (O-DBF):

Microfacies: *Operculina-Discocyclina* **Wackestone/Rudstone**

Operculina-Discocyclina **Bioclastic Wackestone /Packstone**

Operculina-Discocyclina **Mudstone**

Glauconitic Bioclastic Wackestone/Packstone

This facies has been penetrated in four wells, H4, O3, H6 and H10-6. The maximum thickness of 53 ft was encountered in well O3-6 and the minimum thickness of 15 ft was penetrated in well H10-6 (Figures 6.9, 6.10, 6.11 and 6.12). This facies consists predominantly of a thick succession of medium grey and tan to buff,

poorly sorted, medium hardess, wackestone-packstone, with intercalated levels of packstone and mudstone. The fauna is characterized by the presence of abundant thin, flat, fragmented and whole *Operculina* and *Discocyclina* (15 to 35%) (Figure 4.7). These are associated with small whole and mainly fragmented nummulites and other small benthic foraminifera (Textulariidae). Another less common component is echinoderm debris, all in a fine matrix containing a high proportion of nummulithoclastic debris. Stylolite structures are rarely present. Observed porosity is poor (2-7%) and includes small vuggy and rare intragranular pores. *Operculina-Discocyclina* bioclastic mudstone is chiefly composed of intensely bioturbated mudstone and wackestone with local floatstone. It is characterized by a diverse foraminiferal assemblage dominated by either nummulites or *Discocyclina* and *Operculina*. Other bioclasts include echinoid and bivalve fragments. The packstone texture is developed with tightly packed, flat *Discocyclina* and *Operculina*, which are variably imbricated.

The Glauconitic Bioclastic Wackestone/Packstone microfacies with abundant glauconite forming individual crystals or filling chambers is present in well O3-6 (Figure 4.7). Glauconitic bioclastic packstones contain up to 30% subrounded, platy green glauconitic grains as well as fragmented shallow to deep water bioclasts (nummulites, *Operculina* and *Discocyclina*).

Facies interpretation

The presence of the bioclasts in this facies indicates open-marine conditions. Abundant thin *Discocyclina, Operculina* and the presence of micrite suggest that these deposits formed in low to moderate energy conditions, below FWWB, within the photic zone. The variation in foraminiferal assemblage reflects the different water depths encountered in the middle ramp setting, with the sediments containing nummulites reflecting shallower waters than those containing *Discocyclina* and *Operculina*. The localized development of packstone with scoured bases is interpreted as the result of storm reworking and winnowing of the middle ramp. Arni (1965) and Arni and Lanterno (1972) have proposed that the association of abundant fossil fragments with *Discocyclina sp.*, *Assilina sp*. and *Operculina* can be regarded as characteristic of a fore-bank setting. The presence of glauconite in some samples of this facies is thought to be as a result of slow sedimentation rates or concentration due to reworking.
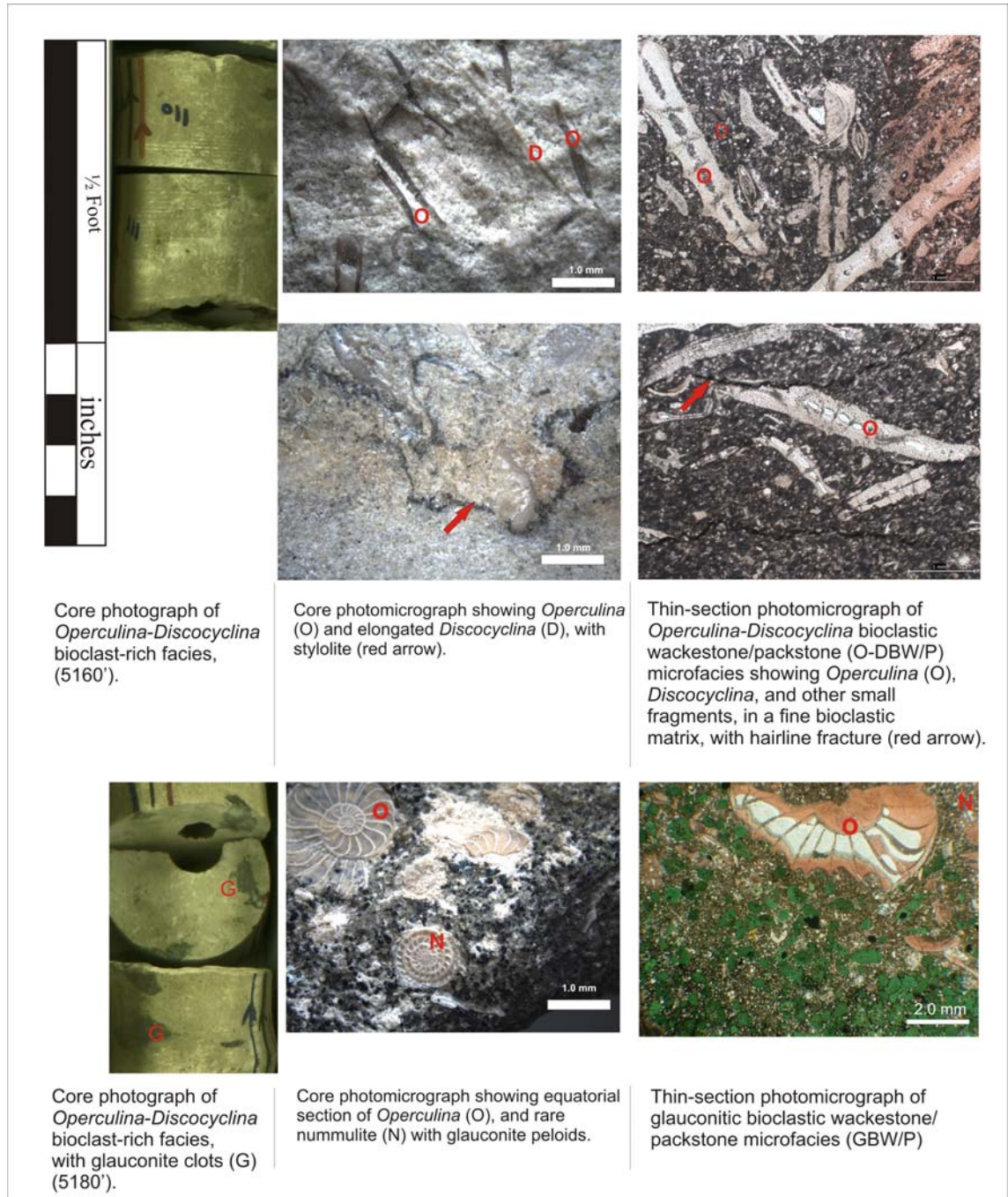
Figure 4.7. *Operculina-Discocyclina* Bioclastic facies (O-DBF), Gialo Formation, O3-6 well.

4.4.7. Lime mudstone facies (LMF):

Microfacies: Lime Mudstone/Wackestone (LM/W)

This often chalky-textured limestone is recorded in the lower part of all the studied wells (except H4-6) (Figures 6.10, 6.11, 6.12 and 6.13). Bed thickness of this facies is about 5-15ft. Petrographically, it is a lime mudstone containing planktonic foraminifera and a sparse (Figure 4.8), low-diversity benthic assemblage dominated by

whole and fragmented flat *Discocyclina*, small nummulites and rare *Operculina* fragments. Organic debris is locally abundant. The sediments are locally burrowed. Horizontal, laterally discontinuous, microstylolites and dissolution seems, enclosing argillaceous material are common, and tend to enhance bed contacts.

Facies interpretation

The dominance of fine-grained sediments and the lack of abraded detritus indicates a very low energy depositional environment (the low energy setting may be due to deposition in an area protected from wave or current activity, perhaps by a barrier, or below the zone of wave or current activity), with the presence of planktonic foraminifera and the benthic assemblage indicative of relatively deep-water, outer-ramp conditions. The presence of barren horizons and the preservation of organic detritus indicate periodic anoxia, though the general presence of benthic organisms indicates that the sediments were usually oxygenated.

Core photograph and photomicrograph showing fine-laminated and bioturbated lime-mud, composed of planktonic foraminifera and reworked benthic foraminifera, well H4-6, 5100 ft.

Thin-section photomicrograph of lime mudstone/wakestone microfacies (LM/W), showing very fine planktonic foraminifera and reworked benthic foraminifera (D and N), H4-6 well, 5100 ft, PPL.

Thin-section photomicrograph of lime mudstone/wackestone microfacies, locally mudstone, burrowed sediments and rare fine skeletal material, well H6-6, at 5040 ft, PPL.

Thin-section photomicrograph of planktonic mudstone/wakestone microfacies (PM/W), with planktonic foraminifera (P) and echinoid fragments, H6-6 well, 5040 ft, PPL.

Figure 4.8. Lime mudstone facies, Gialo Formation.
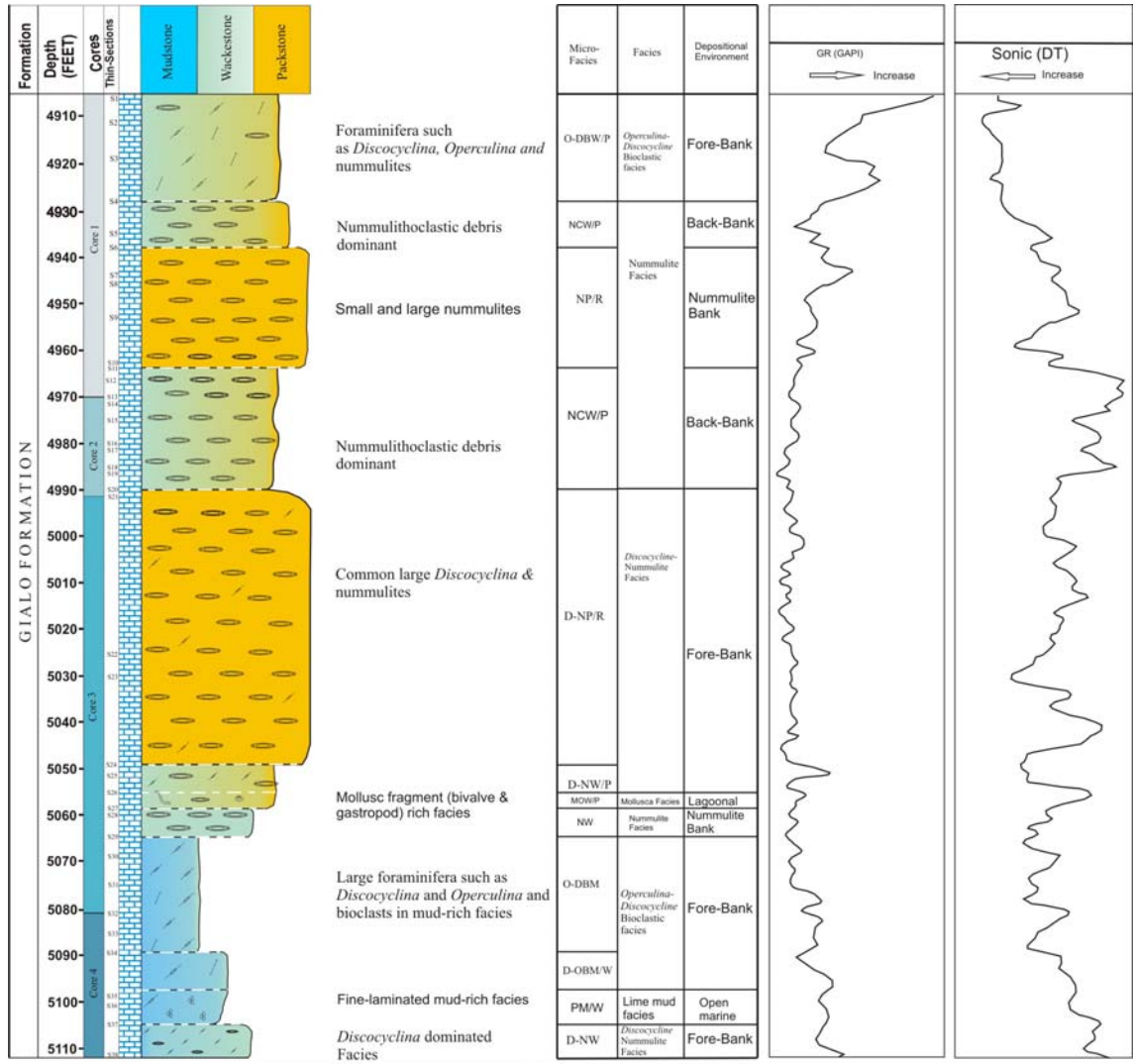
Figure 4.9. Gialo Formation depositional facies and petrophysical characteristics, Well H4-6.
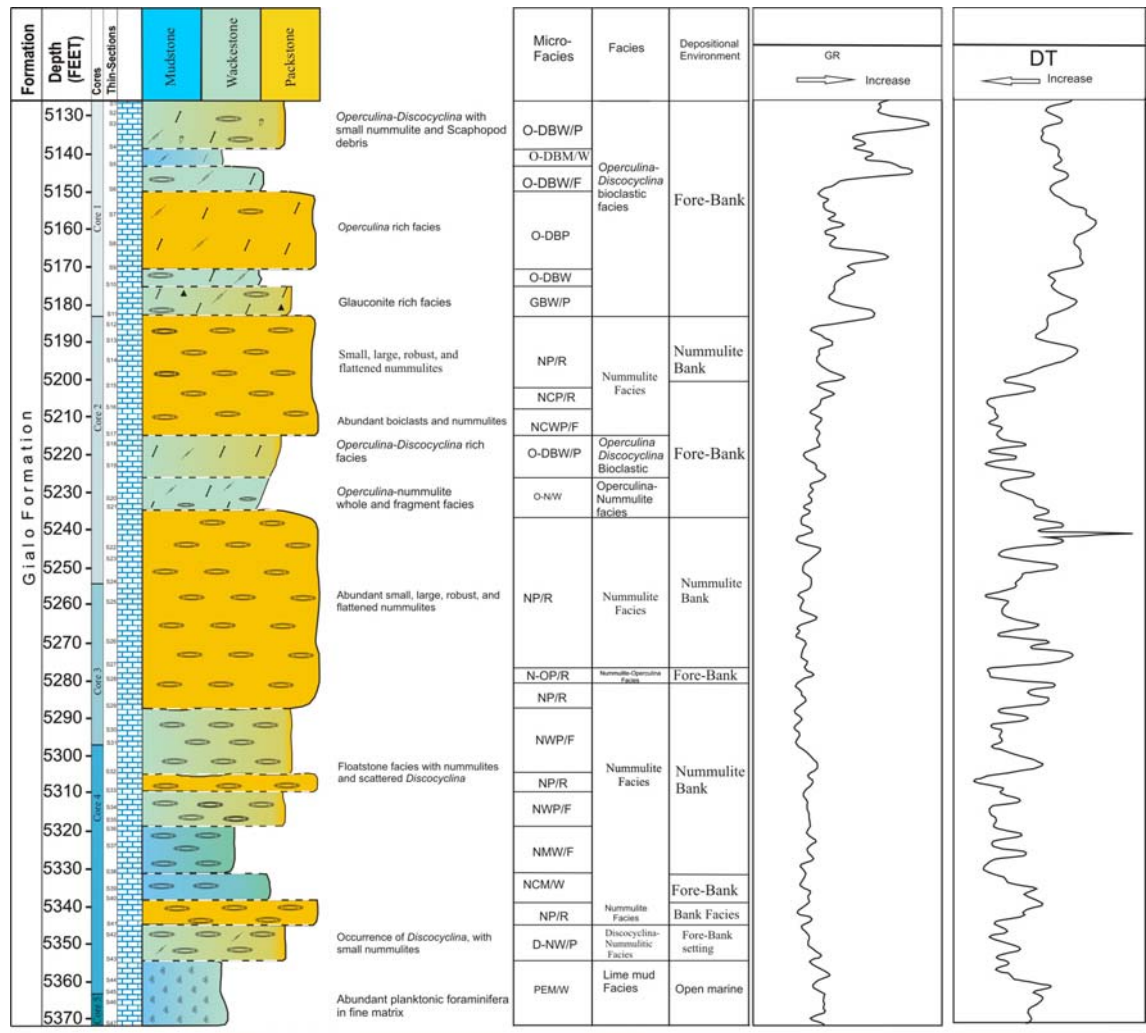
Figure 4.10. Gialo Formation depositional facies and petrophysical characteristics, Well O3-6.

Facies	Microfacies	Grain Types	Environment
Nummulite Facies (NF)	Nummulitic Packstone/Rudstone (NP/R) Nummulitic Wackestone/Floatstone-Packstones (NW/F-P). Nummulitic Wackestone-Packstone/Floatstone (NW-P/F Nummulithoclastic Wackestone/Floatstone (NCW/F) Nummulithoclastic Wackestone/Packstone (NCW/P) Nummulite-Echinoid Wackestone (NEW)	Nummulites (A&B-forms) Nummulithoclastic debris Echinoid fragments Brachiopod fragments Bryozoan Rotaliids Intraclasts	Bank, back-bank setting
Discocyclina-Nummulitic Facies (DNF)	*Discocyclina* Nummulite Wackestone/Packstone (DNW/P) *Discocyclina* Nummulite Wackestone/Floatstone (DNW/F)	*Discocyclina* Nummulites Echinoid fragments	Fore-Bank setting
Molluscan Facies (MF)	Molluscan Bioclastic Wackestone/Packstone (MBW/P)	Molluscan fragments Echinoid fragments Nummulites, Rotaliids	Back-Bank Lagoon Environment
Nummulitic-*Discocyclina* Facies (NDF)	Nummulitic *Discocyclina* Wackestone/Floatstone (NDW/F) Nummulitic *Discocyclina* Wackestone-Packstone (NDW-P)	Nummulites *Discocyclina* Echinoid fragments	Fore-Bank
Operculina-Nummulitic Facies (ONF)	*Operculina*-Nummulite Wackestone (O-NW) *Operculina*-Nummulite Wackestone/packstone (O-NW/P)	*Operculina* Nummulite *Discocyclina* Echinoid fragments	Fore-Bank
Operculina-*Discocyclina* Bioclastic Facies (ODBF)	*Operculina*-*Discocyclina* Wackestone/Rudstone (O-DW/R) *Operculina*-*Discocyclina* Bioclastic Wackestone/Packstone (O-DBW/P) *Operculina*-*Discocyclina* Mudstone (O-DM) Glauconitic Bioclastic Wackestone/Packstone (GBW/P)	*Operculina* *Discocyclina* Nummulites, echinoids	Fore-Bank
Lime mudstone Facies (LMF)	Lime Mudstone/Wackestone (LM/W)	Planktonic foraminifera Echinoid fragments	Open marine environment

Table 4.1. Facies of the Gialo Formation in studied wells, north-central Sirt Basin.
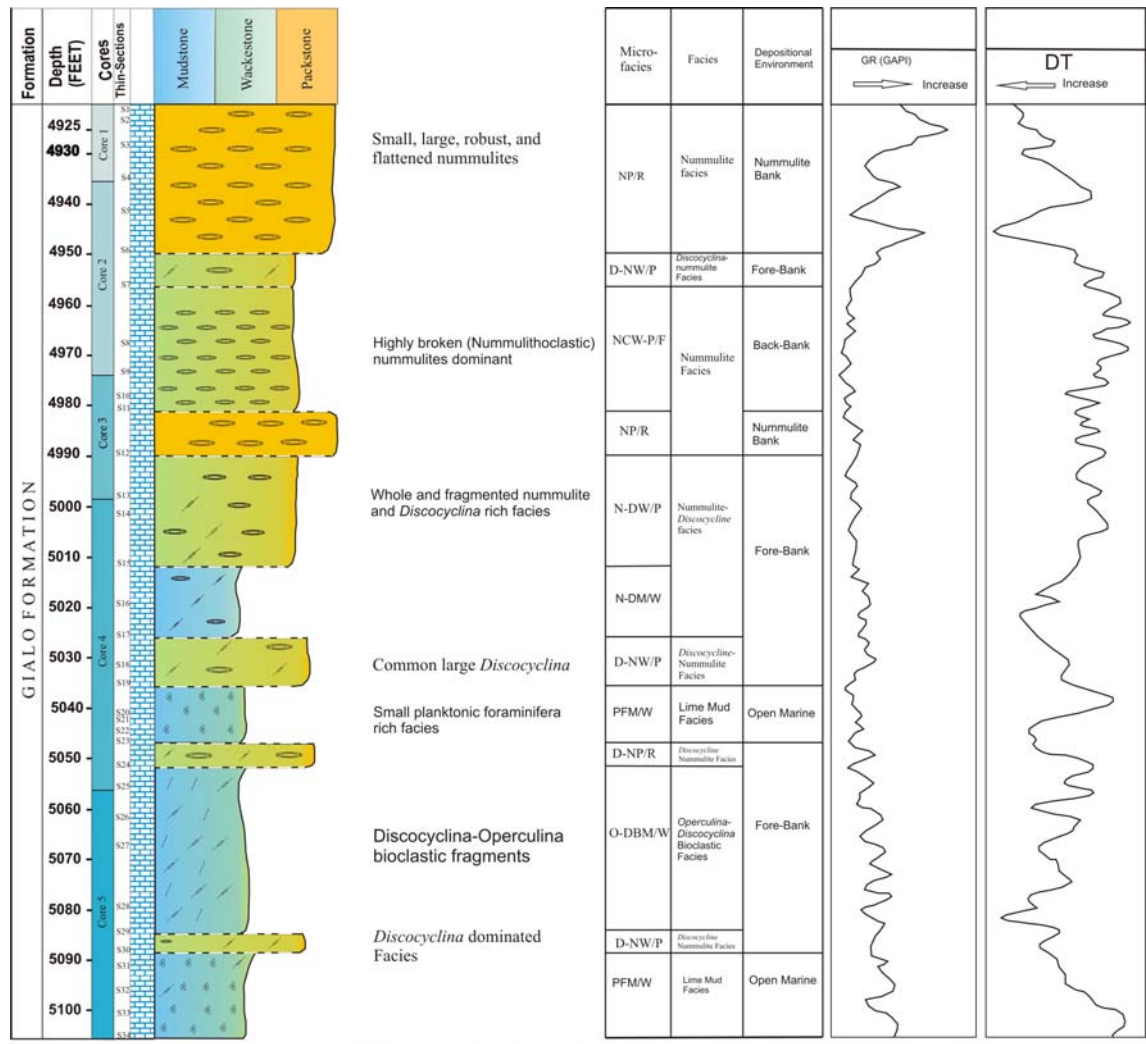
Figure 4.11. Gialo Formation depositional facies and petrophysical characteristics, Well H6-6.

4.5. Wireline Log Characteristics

4.5.1. Introduction

Wireline logs are a continuous recording of the electrical, sonic or nuclear properties of the formation. Logs are extremely important in the characterization of subsurface formations. However, logs are not capable by themselves of providing full and perfectly accurate reservoir characterization; the best characterizations occur when logs are combined with cores and their associated analysis.

Well logs have been used to facilitate correlation, but their patterns can also provide information relevant to the depositional history and sequence stratigraphy of deposits (e.g., Emery and Myers, 1996).

Vertical log profiles can be used to infer changes in depositional energy and patterns of sedimentation. Thus, a decrease in the GR log reflects a decrease in natural radiation levels that is typically related to clay content; consequently this implies an increase in grain size and therefore also of depositional energy levels, to which a relative lowering of sea level may be inferred (Rider, 1986; Emery and Myers, 1996).

The quality of the wireline data was checked. The calliper logs look acceptable as their response matches other logs in shaley intervals. The GR log is in agreement with the response of density, neutron, sonic and PEF logs. The logs-to-core correlation is checked in the depth track, and gives a satisfactory result in most cases.

4.5.2. Gamma Ray Logs

The gamma ray log measures directly the natural radioactivity of the formation, which comes essentially from the radioactive elements thorium, uranium and potassium. In the study wells, the gamma ray logs show a high signal response in the mudstone/wackestone microfacies compared with packstone microfacies (excluding some intervals from both microfacies, see Figures 4.10 and 4.12). This suggests an increased abundance of clay minerals in the slope facies association compared with the other facies. Overall GR values are indicative of a relatively cleaner (less micrite/clay matrix) lithology. Gamma ray log character is used to construct models in which vertical trends in cycle thickness (fining or thickening upward) occur and this alternation can be used to determine the larger sequence framework and its response to changing water depth. Gamma ray is measured in API (American Petroleum Institute) units and ranges from very few units (in packstone microfacies, locally grainstone) to over 200 API units in shales.

Many facies and microfacies in the studied wells can be correlated with depositional energy and thus to gamma-ray response. Grain-dominated packstone/rudstone was deposited in moderate-high energy environments and typically has low gamma-ray activity compared with mud-dominated mudstone and wackestone which was deposited in low energy environments and typically has higher gamma-ray response (Figures. 4.10 and 4.12)

4.5.3. Sonic Logs

The sonic log is a porosity log that measures interval transit time (Δt) of a compressional sound wave travelling through the formation. Geologically this capacity varies with lithology, rock texture and, in particular, porosity. Known sonic log values for pure carbonate are given as 46 ms/ft (Rider, 1986; Crain, 1986). Porosity has a strong effect on sonic values, but the porosity effect in this interval is likely to be insignificant relative to the effect of lithologic variation. The information on a sonic log is recorded as interval transit time in microseconds per ft. Sonic log information from Gialo Formation normal-marine rocks predominantly reflects variations in density. High interval transit time (Δt) values on the log are interpreted as particularly organic-rich layers (wackestone-mudstone) which correlate with most of the facies (Figures 4.9, 4.10, 4.11 and 4.12).

4.5.4. Density Logs

The density log is a continuous record of a formation's *bulk density*. This is the overall density of a rock including solid matrix and the fluid enclosed in the pores. Geologically, bulk density is a function of the density of the minerals forming a rock (i.e. matrix) and the volume of free fluids which it encloses (i.e. porosity) (Rider, 1996). Density logs give similar information to that provided by sonic log measurements in the context of this research. Density of Gialo Formation rocks is strongly correlated with facies type (Figure 6.13).

4.5.5. Discussion

In general the study of wireline logs from a number of wells in the area show that: (I) gamma ray logs have a high signal response in the Lime mud, *Discocyclina-Operculina* bioclastic wackestone and Mollusc facies; this suggest an abundance of clay minerals in the outer-ramp facies compared to the other facies. (II) The sonic and gamma ray logs have low signal responses in the nummulite facies (packstone). This is a reflection of the low amounts of argillaceous material. (III) Some facies and microfacies in the studied wells can be correlated easily with depositional energy and thus to gamma-ray response.
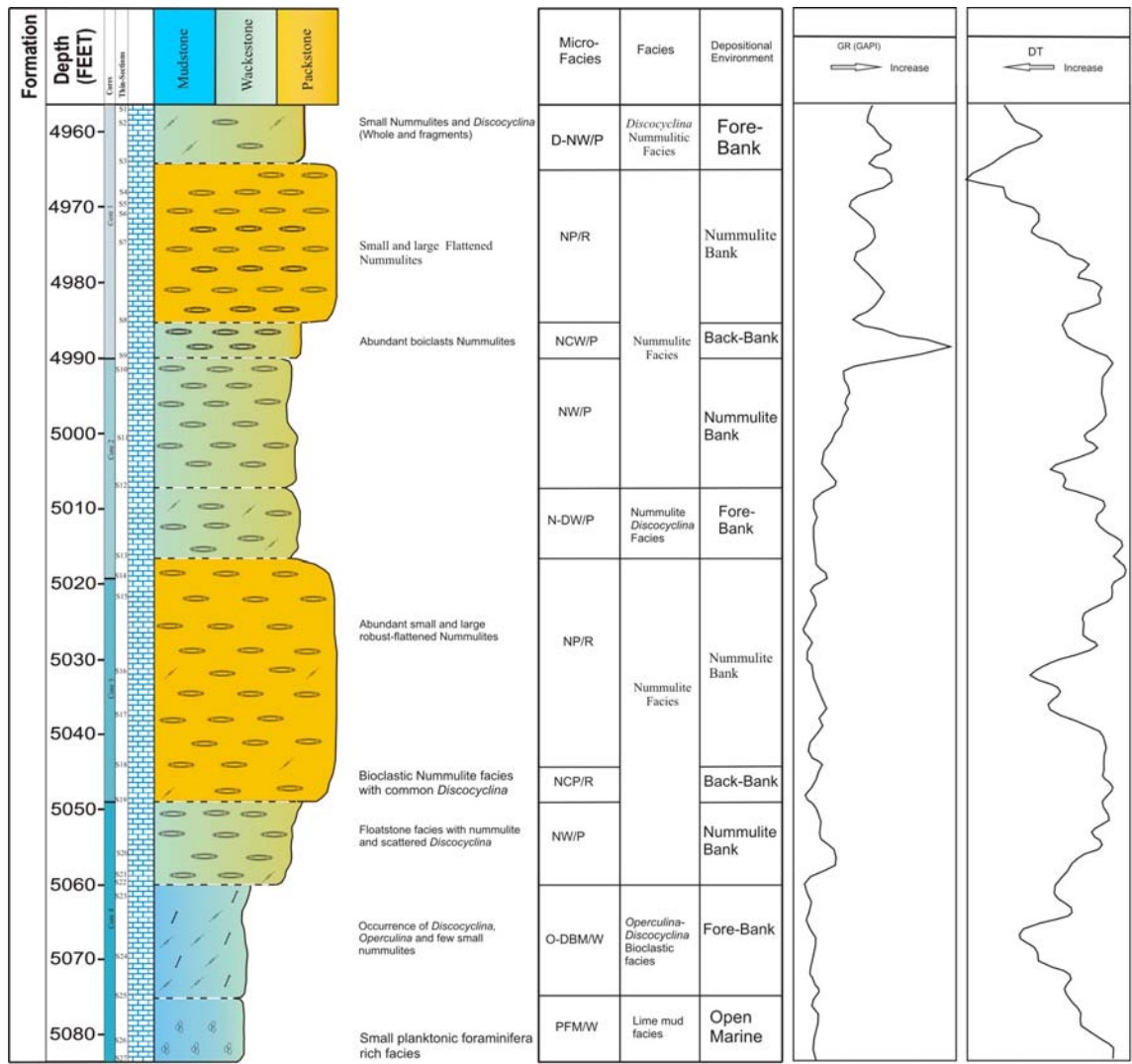
Figure 4.12. Gialo Formation depositional facies and petrophysical characteristics, Well H10-6.
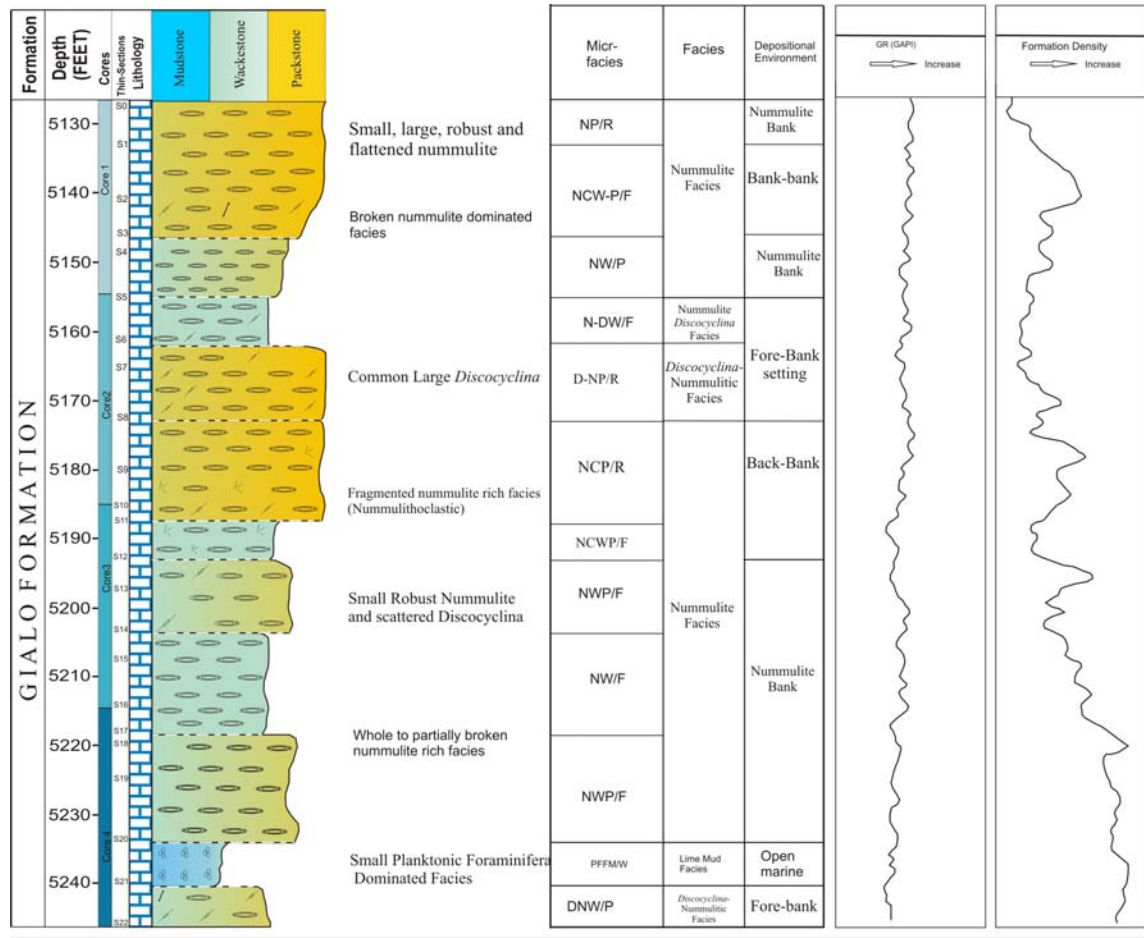
Figure.4.13. Gialo Formation depositional facies and petrophysical characteristics, well OOOO1-6.

4.6. Porosity and permeability measurements

Porosity and permeability are usually obtained either from core analysis or alternatively, where cores are not available, from wireline log analysis (e.g. sonic, neutron, density and resistivity logs). This section presents both the laboratory measurements of porosity and permeability, as well as porosity obtained from thin-sections.

4.6.1. Thin-section investigation

The petrographic investigation shows that the porosities in the samples analyzed are either primary, formed during the deposition of the sediment (e.g. especially in the Nummulite facies) or secondary, caused by dissolution and fracturing (e.g. as in the Molluscan facies). They include intergranular, intragranular, mouldic and fracture porosity types. The petrographic investigation also indicates that the porosity inherited

from the depositional environment and / or diagenetic processes (e.g. dissolution and fracturing) has then been reduced by compaction and cementation, especially by calcite. The porosity calculated from thin-section by point counting shows that the Nummulitic packstone facies generally has higher porosities than the other facies (Table 4.2).

Facies	Porosity Types	Range (%)	Average (%)
Nummulite Facies (NF)	Inter-intragranular and mouldic	5-26	15.5
Discocyclina-Nummulite Facies (D-NF)	Inter-intragranular	3-13	8
Nummulite-*Discocyclina* Facies (N-DF)	Inter-intragranular and mouldic	2-15	8.5
Lime mud Facies (LMF)	Rare intergranular	1-5	3
Discocyclina-Operculina Bioclastic Facies (D-OBF)	Inter-intragranular and mouldic	2-7	4.5
Molluscan Facies (MF)	Inter-intragranular	6-20	13
Operculina- Nummulitic Facies (ONF)	Inter-intragranular	4-12	8

Table 4.2. Porosities calculated from thin-sections of the different facies from the studied wells.

4.6.2. Laboratory Determination of Porosity and Permeability

In general it is considered that the true porosity and permeability of rocks are probably greater than the results obtained from laboratory porosity and permeability measurements. This is because the small core plugs may completely miss the larger pores like vugs and fractures. In the present study, porosity and permeability measurements were conducted in the laboratory of Sirt Oil Company on ~200 core plugs (2.5 cm in diameter) from wells 4O1, O3, H4, H6 and H10-6. These results are listed in Appendix II and illustrated in Figures 4.14 and 4.15. A summary of porosity and permeability values in various facies is given in Table 4.3.

Facies	Well	Porosity (%)		Permeability (mD)	
		Range	Mean	Range	Mean
Nummulite Facies (NF)	4O1-6	17-36	26.5	1-410	205.5
	H6-6	8-35	21.5	1-67	34
Discocyclina-Nummulite Facies (D-NF)	4O1-6	13-34	23.5	1-225	133
	H6-6	19-27	23	1-4	2.5
Nummulite-*Discocycline* Facies (N-DF)	4O1-6	30-32	31	11-38	24.5
	H6-6	10-36	23	1-5	3
Lime mud Facies (LMF)	4O1-6	17-19	18	1-2	1.5
	H6-6	12-27	19.5	1-4	2.5
Discocyclina-Operculina Bioclastic Facies (D-OBF)	H6-6	14-32	23	1-7	4
Molluscan Facies (MF)	H4-6	15-30	22.5	6-8	7

Table 4.3. Porosity and permeability range in various wells based on laboratory core analysis.
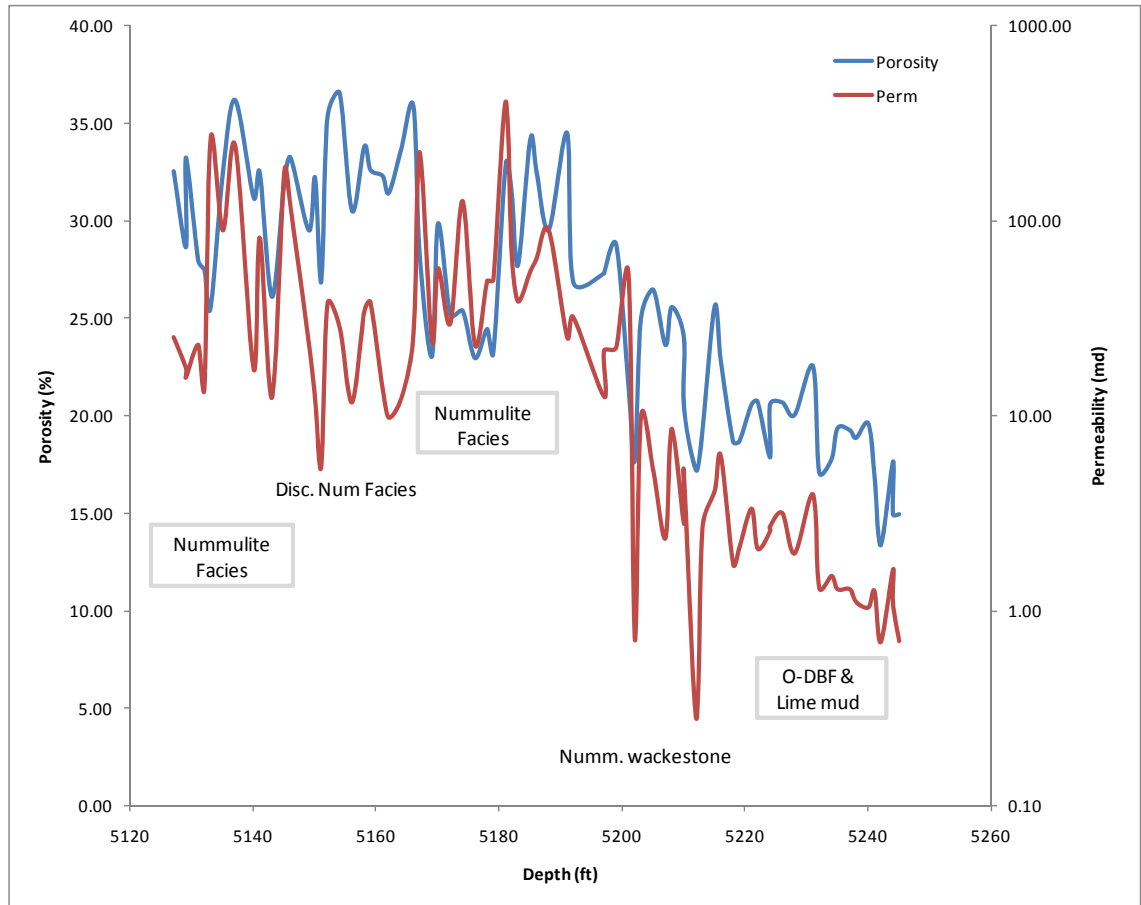
Figure 4.14. Porosity and permeability values of the Gialo depositional facies in well 4O1-6, NW Assumood Field.
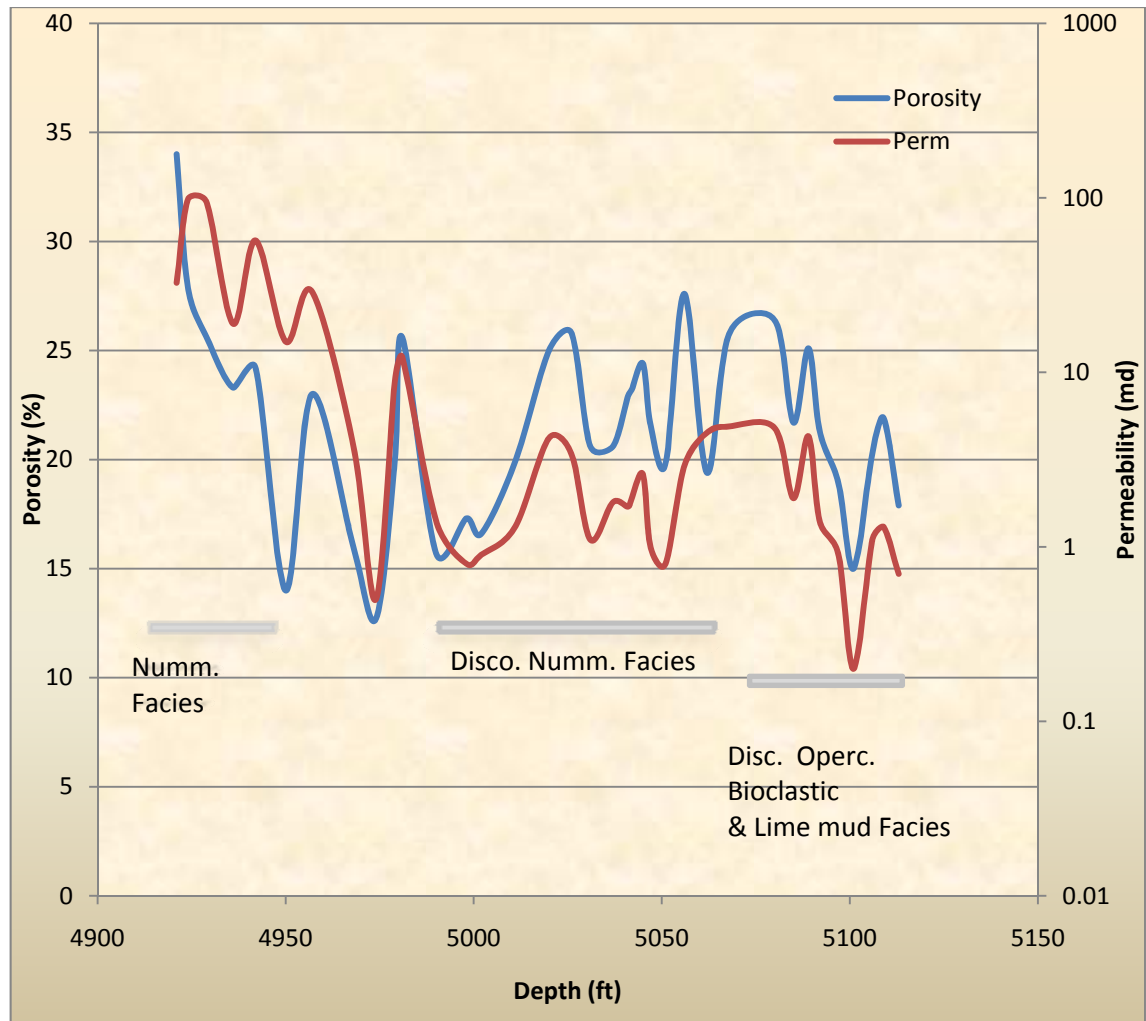
Figure 4.15. Porosity and permeability values of the Gialo depositional facies in well H6-6, Assumood Field.

The present results indicate a large range of both porosity and permeability in the investigated sediments. In general the nummulite facies has poor to fairly good porosity and permeability, with very favourable inter-intraparticle and mouldic porosity. Drilling activity in the study area indicates the presence of significant hydrocarbon accumulation in the Middle Eocene Nummulite facies of well 4O1-6. The *Discocyclina* nummulite facies has fairly good porosity but poor permeability. *Discocyclina –Operculina* bioclastic and Lime mud facies have a lower porosity and permeability than the other facies (Figures 4.14, 4.15 and Tables 4.2 and 4.3).

4.7. Discussion and overall depositional interpretation

Seven facies and eighteen microfacies have been recognized based on the petrography of the bioclastic components and foraminifera assemblages. These facies and microfacies can be interpreted as having accumulated in open-marine, fore-bank, bank and back-bank settings.

The Nummulite facies is the main facies in the Gialo Formation and occupies most of the upper and middle parts of wells 4O1-6, H6-6, H10-6 and H4-6, while occurring only in the middle parts of wells O3-6 and H4-6, underlying the *Operculina-Discocyclina* Bioclastic facies. The distribution of the various facies and microfacies in the five studied wells is shown in Figures 4.9, 4.10, 4.11, 4.12 and 4.13. The nummulites are very well preserved and both generations (A and B) are present, though the assemblage is dominated by the smaller A-forms and they show variable imbrication in a dark matrix with localized peloids. This facies represents the development of nummulite shoals or banks in an inner-ramp setting and was deposited around FWWB (Fig. 4.16). Currents were sufficient to concentrate the bioclasts but insufficient to cause significant abrasion or remove all the lime mud matrix. Packstone/rudstone and locally grainstone indicates local higher-energy conditions, probably above FWWB. The lack of abrasion of the benthic foraminifera indicates that these were autochthonous accumulations, winnowed in-situ by oscillatory currents (Racey, 1990), similar to those interpreted from Tertiary foraminiferal banks of Oman and Egypt (Aigner, 1982, 1983, 1985; Racey, 1990). The interbedded mudstones and wackestones represent the development of more protected intershoal areas. The nummulithoclastic microfacies observed in most of the studied wells consists mainly of wackestone, wackestone/packstone and wackestone/floatstone with fragmented nummulites dominating and minor amounts of echinoid and rare mollusc fragments. The occurrence of nummulithoclastic debris with minor echinoid and rare mollusc (bivalve, gastropod) fragments suggests deposition in a low-energy, back-bank to lagoonal environment. Beavington-Penney and Racey (2005) concluded that transport of sediment from the palaeohighs resulted in abrasion and fragmentation of nummulites and produced packages that gradually thicken and become increasingly fine-grained into mid and outer ramp environments. The *Operculina-Discocyclina* Bioclastic facies is recorded in the upper-most part of well O3-6 overlain by the Nummulite facies and the lower parts of wells H4, H6 and H10-6 and has not been recorded in 4O1-6 well. This might

suggest that the Gialo Formation changes gradually to deeper-water deposits to the south and southeast. Mudstone to wackestone, locally lime mudstone, contains a low-diversity benthic assemblage dominated by flat *Discocyclina, Operculina* and rare planktonic foraminifera. The dominance of organic debris, burrowed sediments and lack of abraded detritus indicate a very low energy depositional environment, with the presence of planktonic foraminifera and the benthic assemblage indicative of relatively deep-water outer ramp conditions.

The *Discocyclina*-Nummulite facies is observed in most of the studied wells. The presence of elongate *Discocyclina* in this facies may reflect an increase in water depth, although they may also be allochthonous (Beavington-Penney and Racey, 2004). This facies was deposited in low-energy conditions, below FWWB in a middle-ramp setting. The variation in foraminiferal assemblage reflects the different water depths encountered in the middle-ramp setting, with the sediments containing nummulites reflecting shallower waters than those containing *Discocyclina.*

The mollusc facies is observed in the lower part of well H4-6. Bioclasts and the high amount of carbonate mud in the mudstone/wackestone microfacies within this facies suggest deposition in low energy lagoonal environments. The lime mud facies is observed in the lower part of most of the studied wells, overlain by *Operculina-Discocyclina* bioclastic facies in well H10, *Discocyclina*-nummulite facies in well H6, O3 and nummulite facies in well 4O1-6. The presence of planktonic foraminifera suggests deposition in an open-marine environment. The gradual variation in facies from shallow to deep photic zone deposits in the five wells as shown below, is more compatible with a ramp model than any other depositional model (Figure 4.16).

The porosity and permeability in the investigated sediments are variable from one facies to another, and from one well to another. This variability reflects multiple interbedding of more or less porous and permeable intervals with poroperm controlled by a combination of depositional facies, diagenetic history and tectonic overprint. The reduction of porosity and permeability in some Gialo Formation sediments can be attributed to the development of sparry calcite, the presence of high amounts of micrite matrix, and the mechanical and chemical compaction of these rocks.
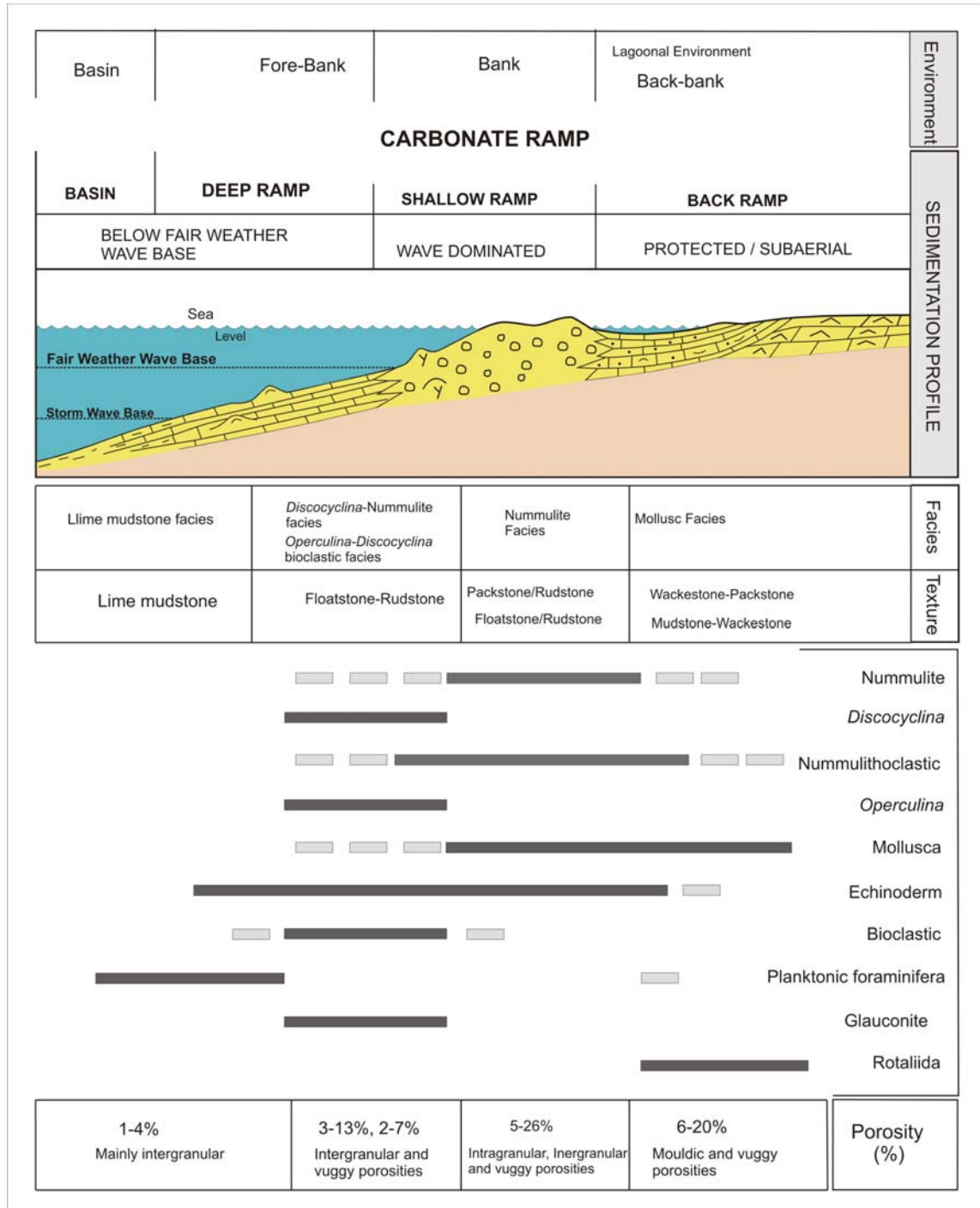
Figure 4.16. Schematic distribution of facies, texture and bioclasts along the facies model for the Gialo Formation.
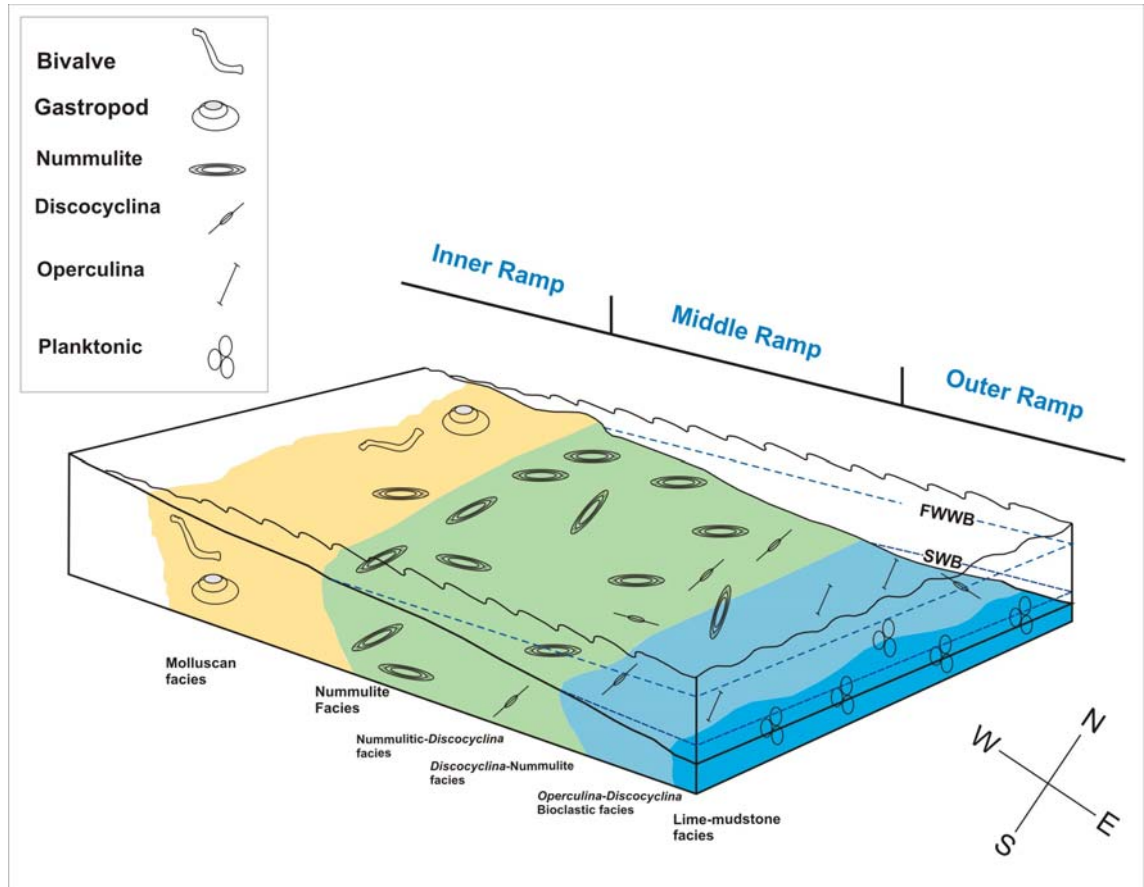
Figure 4.17. Depositional model of the Gialo carbonates. The model shows a well-defined ramp with the main accumulation of nummulites occurring in a mid-ramp position.

4.8. Comparison with nummulite carbonates from Oman (the Seeb Limestone):

The Seeb Formation developed during Middle Eocene time similar to the Gialo Formation. It crops out on the Batinah Coast of northern Oman and is also locally present on the west flank of the Oman Mountains (Figure 4.18). It has been the subject of a series of studies, focusing mainly on the type section at Wadi Rusakl (Figure 5.29), e.g., Racey (1995, 2001) and Beavington-Penney *et al*. (2006). These studies suggested that the Seeb Formation was deposited on a storm-influenced ramp and the authors noted that for much of its extent it is characterized by a transgressive package of limestones up to 350m thick. This displays a vertical trend in foraminiferal content, with alveolinids and miliolids dominating basal sections, whilst younger sections are characterized by an association of nummulitids (nummulites and *Assilina*) and the orthophragminid *Discocyclina*. The nummulites generally occur in packstones-

grainstones which form distinctive low-amplitude banks (1-10m thick). These are often dominated by B-form nummulites and show evidence of physical processes (scouring, test abrasion). The topographic relief on these nummulite banks was low; frequently, the banks take the form of a series of amalgamated nummulitic sheets which are slightly convex upwards. Within the nummulite "bank" facies, test borings and encrustation by oysters are rarely observed, whilst burrows are occasionally recorded. *Alveolina* in shallower waters and *Assilina* in deeper waters form generally similar, but significantly smaller, low-amplitude bank complexes.
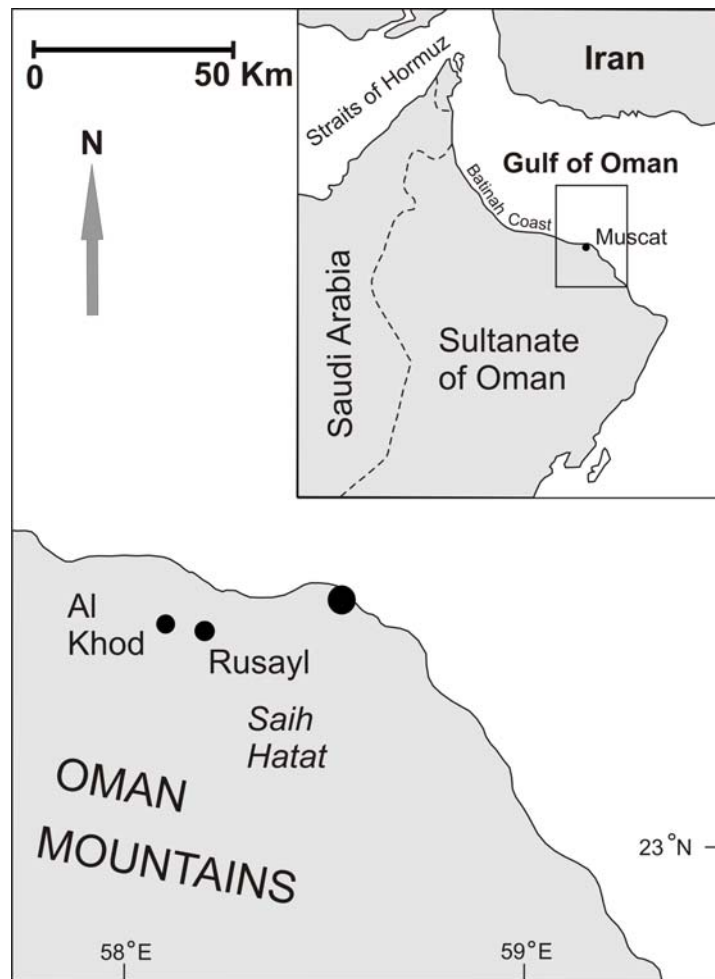
Figure 4.18. Map of north-east Oman showing the location of the Al Khod. Location of the main map is shown on the inset. (after Beavington-Penney, *et al*., 2006).

Porosity and permeability, which are generally affected by limited diagenesis, range from 0.7-14.5% and 8-95mD, respectively.

4.9. Summary of Gialo depositional environments

The Middle Eocene Gialo Formation has been studied in five wells in the Assumood and Sahl fields, Concession 6, Sirt Basin. Detailed core description and petrographic study show that the Gialo Formation consists mainly of shallow-water carbonate and is characterized by facies and thickness variations between the five wells. The vertical and lateral variation of the Gialo depositional facies was influenced by basin-floor architecture and other environmental controls. Sedimentological and petrological investigation of 175 thin-sections to document the main components (nummulite, *Discocyclina*, *Operculina* and planktonic foraminifera), distinguished seven separate sedimentary facies and twenty microfacies, including Nummulite facies, *Discocyclina*-nummulite facies, Mollusc facies, Nummulite-D*iscocyclina* facies, *Operculina*-nummulite facies, *Operculina-Discocyclina* bioclastic facies and Lime mudstone facies. These facies were predominantly deposited under shallow-marine conditions, within the photic zone, as indicated from their richness in phototrophic fauna and flora, and can best be ascribed to a carbonate ramp (Figure 4.16). Open-marine, fore-bank, main bank and lagoon (back-bank) environments are recognised.

The nummulite packstone/rudstone facies dominated by A-forms with minor to common B-forms forms the upper part of the bank. Fragmentation and abrasion of sediments resulted in the transport of sediments from the palaeohigh and redeposition in back-bank environments. The *Operculina-Discocyclina* bioclastic facies accumulated in a fore-bank setting. There is a pronounced gradation from coarser to finer debris down the ramp. Towards the north and northwest of the Sahl Field (towards the open Tethyan sea), mid-ramp shallow-marine moderate-high energy environments prevailed and low relief nummulitic shoals developed in the Assumood area. Sediments from the shoals and mid-ramp environment were fragmented and later transported during storms and strong currents to a relatively deeper marine location in the outer ramp environment near the Sahl field.

Petrographic and petrophysical studies indicate that porosities and permeabilities in the Gialo Formation are strongly related to the depositional environments. Porosity is at a maximum in the nummulitic bank facies and lowest in the lime mud facies.

CHAPTER 5: DIAGENESIS OF THE GIALO FORMATION

5.1. Introduction

This chapter describes and interprets the main diagenetic features which have been recognized from petrographic half-stained thin-sections, cathodoluminescence microscopy (CL), scanning electron microscopy (SEM) and oxygen and carbon stable isotope analysis ($\delta^{18}O$ and $\delta^{13}C$). Also discussed here are the relative time relationships (paragenetic sequence) of the events which have affected the Middle Eocene sediments of the north-central Sirt basin during their burial. The influence of the diagenesis on porosity and permeability of the Gialo Formation is also discussed.

5.2 A brief review of the carbonate diagenetic environments

5.2.1 Introduction

Diagenesis refers to the sum of physical, chemical and biochemical changes that affect a sediment after deposition and during or after lithification (e.g. Bates and Jackson, 1980). It includes all post-depositional processes excluding metamorphism and surface weathering. There is an extensive literature on carbonate diagenesis which has been reviewed recently in Bates and Jackson (1980), James and Choquette (1983, 1984), Mcllreath and Morrow (1990), Tucker and Bathurst (1990), Tucker and Wright (1990) and Tucker (1991 and 1993). In carbonates there are many complex processes that act upon sediments during and after transformation into rock. The main processes leading to diagenetic alteration are either physical, chemical or physiochemical (Chilingar *et al.*, 1979). Diagenetic processes include the dissolution, neomorphism and replacement of unstable minerals, the compaction of grains and lithification by the precipitation of void-filling cements. Three diagenetic environments which pass vertically and laterally into one another can be distinguished: the marine, near-surface meteoric and burial environments (James and Choquette 1990b; Tucker and Wright 1990) (Figure 5.1). This section focuses on the key diagenetic aspects related to this thesis and provides a brief introduction to carbonate diagenesis. The three principal diagenetic environments are briefly discussed and the summary is designed to provide the reader with an introduction which is relevant to the interpretations of this study.

5.2.2 Marine Diagenesis

Marine diagenesis takes place on or just below the sea floor, and on tidal flats, tidal channels and beaches. It generally operates over short time-spans (only years to thousands of years) in most cases by comparison with meteoric and burial diagenesis. In the open-marine environment, the processes operating depend very much on water depth and latitude; along the shoreline climate is a major factor. In low-latitude, shallow-marine environments the main processes involved in sea-floor diagenesis are: (a) the precipitation of cements, and (b) the alteration of grains by the biological borings of organisms (James and Choquette, 1990b). Cementation is most widespread in areas of high current activity, such as along shorelines and shelf margins, where sea-water is pumped through the sediments, but it also occurs in areas of evaporation, such as on tidal flats and beaches (Tucker, 1993). Micritization of grains by algae, fungi and bacteria takes place almost everywhere but it is most prevalent in quieter water locations
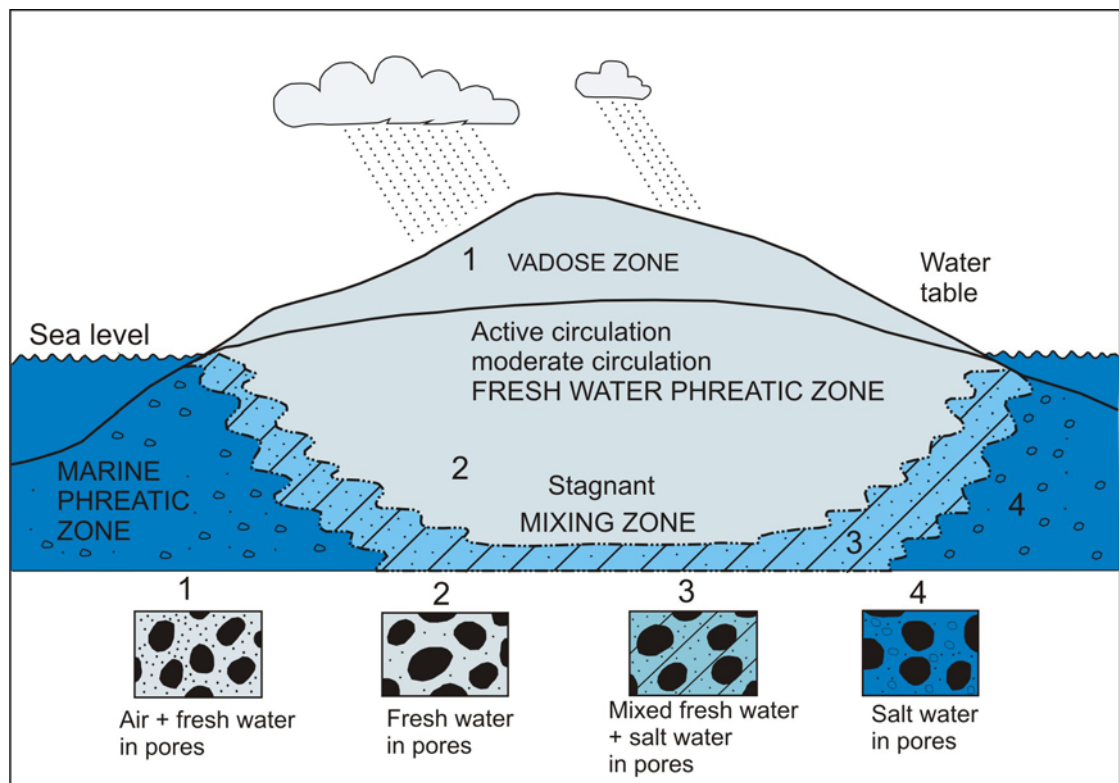
Figure 5.1. Distribution and relationship of major diagenetic environments in the shallow subsurface (after Longman, 1982).

where there is little sediment movement (James and Choquette 1990b). Thus in the shallow-marine realm, it is possible to distinguish three zones: (1) the active marine phreatic, where pore-waters are constantly being replenished and cementation is common (e.g. reefs and sand shoals); (2) the stagnant marine phreatic, where there is little sediment or pore-fluid movement, microbial micritization of grains is ubiquitous and cementation is limited (e.g. on-shelf lagoons); (3) the marine vadose, where cementation chiefly occurs through evaporation of sea-water and there may also be some evidence of microbial effects (e.g. beaches, tidal flats) (Tucker and Wright, 1990). In mid-high latitudes, shallow-marine carbonates are rarely cemented. Shallow sea-water becomes undersaturated in $CaCO_3$ away from the subtropics, and carbonate grains are thus more liable to suffer dissolution (Alexandersson, 1978).

Marine cements have a large variety of morphologies and are essentially formed of only two minerals: aragonite and high-Mg calcite (Tucker and Wright, 1990). The common types of aragonite cement are acicular crystals occurring as isopachous fringes, needle meshworks and botryoids, and micron-sized, equant crystals (micrite). High-Mg calcite cement occurs as acicular-bladed isopachous fringes, equant crystals, micrite and peloids (Tucker and Wright, 1990). Geochemically, trace element analysis of modern marine aragonite cements reveals that they typically contain 8000-10,000 ppm strontium, with sodium concentrations around 2000 ppm, and magnesium values of 1000 ppm or less. Magnesium calcite cements generally have between 12 and 19 mole % $MgCO_3$, with relatively low strontium values of around 1000 ppm (James and Ginsburg, 1979; Tucker and Wright, 1990).

Stable isotopic studies show that the oxygen isotopic signatures of shallow-marine cements and sediments depend largely on the sea–water $\delta^{18}O$ composition and temperature (Milliman, 1974; James and Ginsburg, 1979; Anderson and Arthur, 1983). With marine cements, the values are commonly those predicted for precipitation in equilibrium with sea-water or they are slightly heavier, or more enriched than would be expected (Gonzales and Lohmann, 1985). The $\delta^{18}O$ range is typically -0.5 to +3‰, and high-Mg calcite cements display a slight enrichment in $\delta^{18}O$ compared to aragonite, due to fractionation effects (Tucker and Wright, 1990).

5.2.3. Meteoric Diagenesis

The meteoric diagenetic environment is the zone where rainfall-derived ground-water is in contact with sediment or rock, and two distinct zones are recognized vadose and phreatic. Each zone has characteristic processes and products (Steinen, 1974; Allan and Mathews, 1982) which enable their recognition in ancient limestones (Beeunas and Knauth 1985). These environments are dynamic and small fluctuations in sea-level can create significant differences in the diagenetic stratigraphies.

The water-table is the surface where atmospheric and hydrostatic pressures are equal (James and Choquette, 1990b). The water-table is the critical interface in meteoric diagenesis. It separates the zone of intermittent saturation and drying (vadose zone) from the zone of permanent saturation (phreatic zone). Transitional between the vadose and phreatic zone is the capillary-rise zone (or capillary-fringe zone) where water is drawn up by capillary action. There are such marked differences in processes and products above and below the water-table that its position can be recognized in ancient subaerially-exposed sequences (Wright 1982, 1986).

In the vadose zone the pores periodically contain water or air or both. Water drains under gravity, and this can be relatively rapid in the case of conduit flow (water movement via joints and fractures) compared to the case of diffuse flow (water movement though inter-and intra-granular pores). Two sub-zones can be identified: the upper zone of infiltration and the lower zone of percolation. The three most important processes in the vadose zone are (1) gravitational drainage, (2) desiccation by evaporation, and (3) evapo-transpiration (James and Choquette, 1990b). Water passing through this zone contains both atmospheric CO_2 (and other 'acidic' gases), soil-derived CO_2 and organic acids. Not only does this increase the acidity of the fluid, but also adds dissolved organic carbon to the ground-water, and increases the ability of the fluid to dissolve the limestone wall-rocks (Tucker and Wright, 1990). In contrast to the vadose zone, pores in the phreatic zone are always filled with water, so that calcite crystals can grow unimpeded by water-air interfaces until they come into contact with neighbouring carbonate grains or cement crystals (Morse and Mackenzie, 1990).

In the shallow subsurface, where the marine and meteoric waters interface, there is a mixing-zone (Back *et al*., 1979, 1984). This environment was once considered important in studies of dolomitisation, but now the mixing zone model has been

generally discarded. The geometry of the mixing-zone varies along a shoreline, depending on the hydrostatic head, rock porosity-permeability and presence of confined / unconfined aquifers (Tucker and Wright, 1990). Limestone dissolution can take place in the mixing zone.

Cement morphologies in the vadose and phreatic zones are different due to the different nature of the water-wetted surfaces in these regimes. In the case of the vadose zone, downward percolation of water is not uniform, and thus cements are distributed irregularly throughout the fractures and pores within the wall-rocks. These calcite cements are concentrated at grain boundaries and commonly exhibit a curved surface, reflecting growth outward towards the curved interfaces of partially water-filled pores (meniscus cement; Dunham, 1971). In the deeper regions of the vadose zone, where more fluid is available, droplets of water can accumulate at the bottom of grains, or at the top of fractures, joints and cavities. This leads to formation of pendant cement shapes (microstalactitic cement; Longman, 1980), reflecting the shape of the gravity-induced, convex-downward and elongated water-air interface. Vadose silt, which is composed of fragments of cement detached from pore ceilings and from fine-grained detritus infiltrating with water from above, may line the bottom of pores to form geopetal layers (Dunham, 1969).

Phreatic meteoric cements may grow faster than vadose cement, because new dissolved constituents may be brought rapidly and in larger quantities by flowing and continuous phreatic freshwater to sites of cement nucleation and growth. Freshwater phreatic cements form isopacous layers around grains or occur as blocky calcite. The calcite cement generally is of larger size than the fine-grained calcite spar found in the vadose zone, and commonly coarse crystals abut directly against grain boundaries (Morse and Mackenzie, 1990).

Geochemically, the vadose and phreatic meteoric cements in carbonate rocks are composed of low-magnesium calcite (Morse and Mackenzie, 1990). Observations of the compositions of waters bathing modern near-surface sediments and experimental evidence show that low-magnesium calcite is the phase anticipated to form from such waters (Morse and Mackenzie, 1990). Meteoric waters in carbonate sediments have low salinities, low Mg^{2+}/Ca^{2+} ratios, low SO_4^{2-} concentrations, variable, but measurable,

concentrations of PO_4^{3-} and generally low dissolved organic carbon concentrations (Lohmann, 1988).

Stable isotopic studies have shown that the $\delta^{18}O$ composition of meteoric ground-water is largely constant at individual geographic sites (Craig, 1961). Variations in the amount of dissolved soil gas CO_2, and in the extent of rock-water interaction, produce a distinct geochemical trend for diagenetic alteration and precipitation products. This pattern of invariant $\delta^{18}O$ coupled with variable $\delta^{13}C$, is termed the meteoric calcite line, and serves as the baseline relative to which chemical variations can be distinguished (Lohmann 1988). Since the composition of meteoric water can vary geographically with individual systems possessing unique values, the $\delta^{18}O$ signature of the meteoric calcite line must be determined individually for each sequence and locality studied (Lohmann, 1988). The $\delta^{13}C$ compositions of meteoric cements are distinctly lower than those of the depositional sediments. The main features are a more negative $\delta^{13}C$ caused by the addition of light carbon (^{12}C) from the soil, although variations in $\delta^{13}C$ are not simply a function of distance below an exposure surface (Tucker and Wright, 1990).

5.2.4. Burial Diagenesis

Burial processes, particularly cementation, compaction and pressure dissolution, operate over a considerable range of depths, pressures and temperatures. As a result pore-fluids vary greatly in terms of salinity, chemistry and origin (James and Choquette 1988). Burial diagenesis is generally taken to begin below the depth where sediments are affected by near-surface processes of the marine and meteoric environments, and continue to the zone where metamorphic dehydration reactions occur (Choquette and James, 1987; Morse and Mackenzie, 1990). The early diagenetic history of carbonate sediment usually takes place in meteoric waters that are oxic to only slightly reducing. Waters in the deeper burial environment generally have elevated salinities that usually increase with depth. These waters are reducing owing to their long isolation from the atmosphere and because of burial diagenesis of organic matter (Morse and Mackenzie, 1990).

Both higher temperatures and longer time periods associated with cement formation in the deep-burial environment, result in the formation of cements which have

distinctive compositions and morphologies (Morse and Mackenzie, 1990). Cements precipitated in the burial environment are commonly composed of clear, coarse calcite spar. According to Tucker and Wright (1990) there are four main cement textures: 1) Drusy, equant calcite, 2) Poikilotopic calcite, 3) Equant-equicrystalline mosaics of calcite spar, and 4) Syntaxial calcite spar.

Compared with marine cements, burial spar is typically depleted in Mg, Sr and Na, but it may have significant amounts of Fe and Mn (Choquette and James, 1987). Many burial cements are ferroan (>0.30 weight % FeO), as shown by staining and geochemical analysis. These cements are usually the result of precipitation from negative Eh pore-water with Fe^{2+} in solution derived from clay minerals and shales. An important consequence of the reducing conditions is that redox sensitive metals such as iron and manganese are mobilized and can co-precipitate with the carbonate cements (Morse and Mackenzie, 1990). Manganese concentrations typically reach many hundreds of ppm. Burial spar contrasts with near-surface meteoric calcite cement since shallow groundwater is well oxygenated and therefore does not contain these elements in solution (Tucker and Wright, 1990).

Stable isotopic compositions are distinctive in deep-burial carbonate cements, typically composed of carbon and oxygen isotopic ratios that are light, or depleted. A wide range of $\delta^{18}O$ values is commonly seen in successive burial cement generations, due to fractionation effects and the elevated temperatures present in the burial environment (Dickson and Coleman, 1980; Moore, 1989).

5.3. Diagenesis of the Gialo Formation

5.3.1. Introduction

Present-day reservoir characteristics of the Gialo Formation are the net result of modifications to the original depositional textures caused by diagenesis. Diagenesis has greatly altered the Gialo Formation with extensive alteration in marine, fresh-water and burial environments. Instability of component minerals such as aragonite, as well as the high initial permeability of carbonate sediments, make them very susceptible to diagenetic processes. However, some of the diagenetic processes are known to be common only in particular environments and hence provide a tool for better understanding of the depositional history. This section discusses the main diagenetic

processes and their products and the relative time relationships (paragenetic sequence) of these events which have affected the Middle Eocene Gialo sediments during their burial. It also includes discussion of the porosity-diagenesis relationships of the investigated sediments.

5.3.2. Diagenetic processes

175 half-stained thin-sections were examined for their petrographic fabrics, chips from 10 samples were examined using scanning electron microscopy (SEM) and thirteen polished thin-sections were studied using the cathodoluminescence (CL) microscope. The main diagenetic processes which have affected the Gialo Formation are micritization, dissolution, cementation, neomorphism, pressure dissolution, compaction and pyrite growth.

5.3.2.1. Early marine diagenesis

5.3.2.1.1. Micritization

Micritization is a common process in shallow-water environments and has been interpreted to result from boring by microorganisms including endolithic algae, bacteria and fungi (Bathurst, 1975; MacIntyre *et al*., 2000; Reid and MacIntyre, 2000). Micritic envelopes are present on some bioclastic grains, but in some cases they were difficult to distinguish from external (matrix) micrite (Figures 5.2 and 5.3). Micritization of bioclasts occurs on or just below the sediment-seawater interface and is most prevalent in quieter-water locations where is little movement of sediment (Tucker and Wright, 1990). This occurred soon after deposition and predates all other diagenetic features. In this study micritization was only observed in the molluscan grains of the inner ramp facies, in the outer portions of the grains (Figures 5.2 and 5.3). The micrite envelopes are important during diagenesis because they maintain the shape of the grains after the dissolution of the aragonitic grain itself. Repeated micritization may lead to complete reconstruction of grains, leaving no evidence of their original nature. This may explain the texture of completely micritized clasts.

5.3.2.1.2. Probable marine-vadose rim calcite cement

Clear marine cements are rare in the Gialo Formation. They would be expected to be isopachous fibrous or bladed cement coatings around or within grains or inclusion-rich overgrowths on echinoderm fragments. However, non-ferroan asymmetric calcite cements do occur within bioclast cavities, nummulites especially, observed rarely in the upper part of well 4O1-6 (Figures 5.4 A&B) and are believed to be early precipitates in the shallow marine environment. The rims are up to 100 microns in thickness and mostly occur on the undersides of shell material, as well as locally lining whole cavities and surrounding grains. The cements are well seen in concave areas of substrate where they form crusts which thin and taper in thickness. The crystals themselves are acicular, grey or cloudy in appearance, and oriented normal to the grain substrate. These cement crusts have been fractured (Figure 5.4 A), clearly showing their early diagenetic origin.

On the basis of the acicular nature of the crystals, and their contrast with clear, equant calcite, also occurring in the sections, these rim cements are interpreted as marine in origin. The geometry would suggest a vadose environment, with air-water filled cavities (Tucker, 1991), and so precipitation beneath a tidal flat for example. An alternative interpretation could be that these cements are some sort of stalactitic-type precipitate from meteoric water, but then they might be expected to be more extensive, and associated with more evidence of dissolution.

5.3.2.2. Meteoric and early burial diagenesis:

5.3.2.2.1. Dissolution

Dissolution is a diagenetic phenomenon that has been observed in some facies of the Gialo Formation and resulted in the formation of secondary porosity. This occurs as a result of the interaction between the grains and undersaturated fluids, generally freshwater, which may have entered the sediments from small islands and exposed sand shoals on the shallow sea-floor. Dissolution may have affected the Gialo Formation during an early meteoric phase and also possibly during a late burial phase. The first phase of dissolution probably occurred during the exposure of the Gialo Formation to subaerial conditions as a result of a eustatic sea-level fall during early Middle Eocene time, which has been recorded in other sections (e.g. Haq et al., 1987). However, no
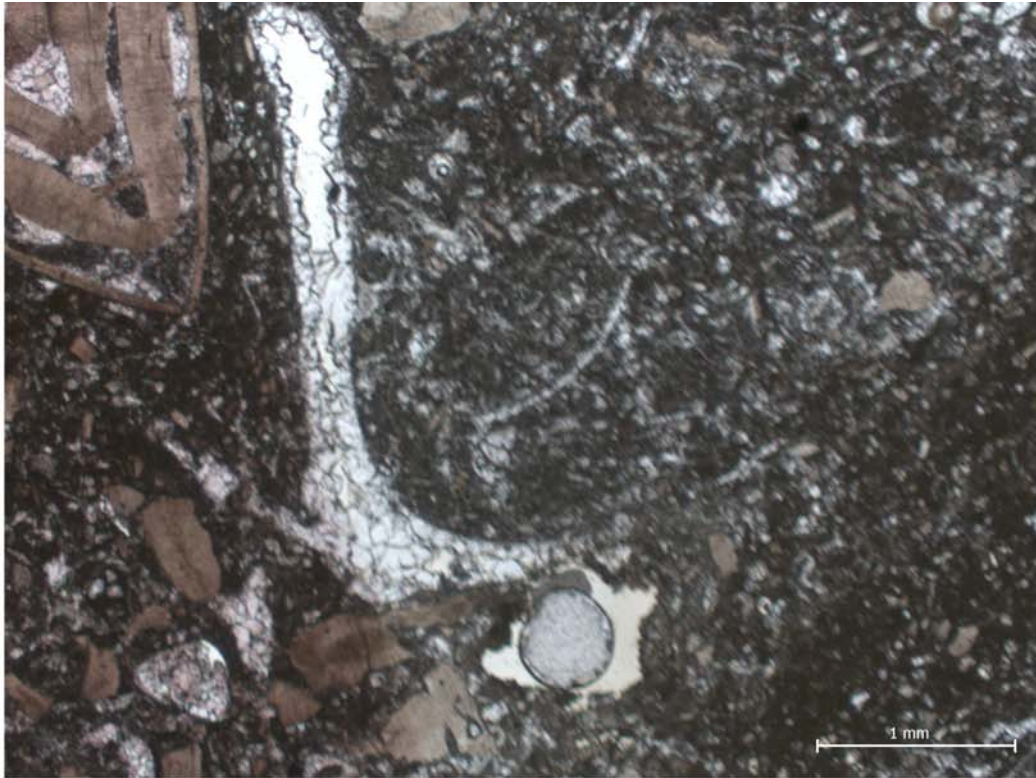
Figure 5.2. Photomicrograph shows mollusc fragments (bivalves). Aragonite has dissolved and completely to partially filled by drusy calcite cement (micrite-envelope was difficult to distinguish from external micrite. well H4-6, Depth 5058 ft., PPL.
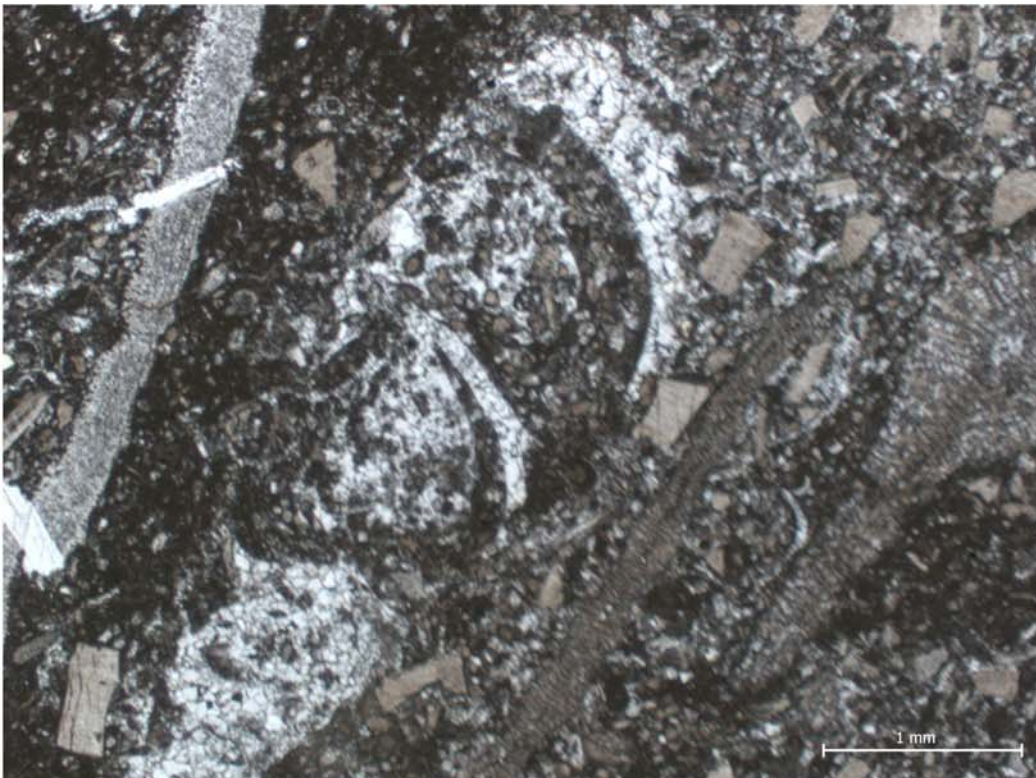
Figure 5.3. Photomicrograph shows large aragonitic grain (gastropod), underwent marine diagenesis followed by extensive meteoric and burial alteration. Well H4-6, Depth 5058 ft., PPL.
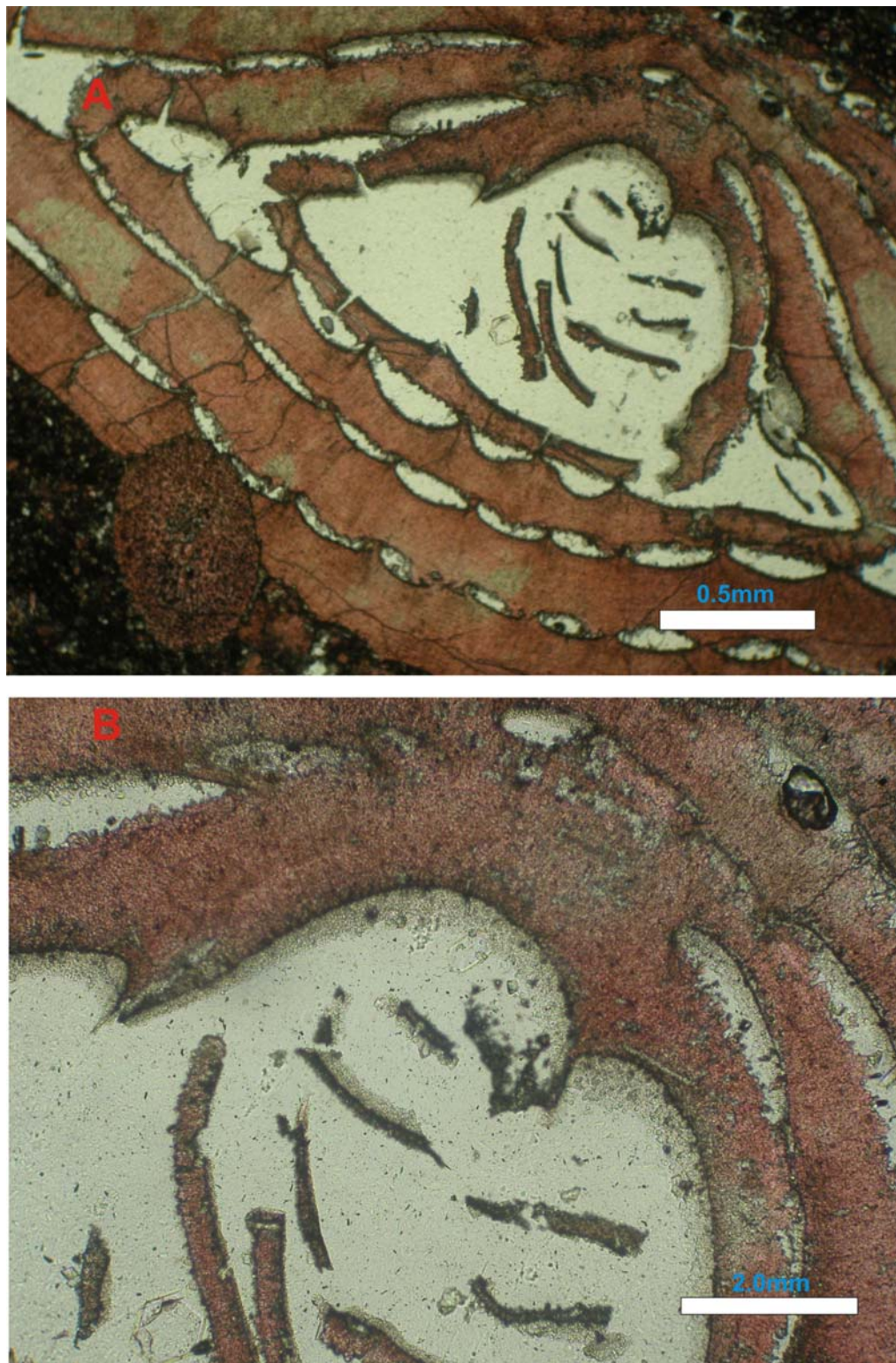
Figure 5.4. Photomicrographs (A&B) show early rim cement probably of marine origin in nummulitic packstone. These photomicrographs illustrate the importance of early rim cement in preventing compaction and the subsequent obliteration of primary porosity. Note porosity is in white.

clear evidence of subaerial exposure was seen in the studied cores of the Gialo Formation. The exposure event could have been responsible for the creation of large volumes of vuggy and some mouldic porosity, which has enhanced the reservoir potential of the Gialo Formation. Aragonite has not been recognised in the investigated sediments, either because of leaching or stabilisation to low Mg-calcite (Figures 5.5, 5.6 and 5.7).

The second phase of dissolution occurred as a result of increasing burial resulting in the formation of dissolution seams in association with late-stage cementation. Dissolution enhanced porosity along microfractures (Figure 5.25) developed during burial compaction. Secondary porosity greatly enhanced primary intergranular porosity and is mainly responsible for the formation of high reservoir potential (Figures 5.12 and 5.13). In some samples, 20% of the rock may be porous due to dissolution. Many of the biomoldic pores are partially or completely filled by drusy, non-ferroan calcite, particularly in the middle part of the Gialo Formation (Figures 5.5 and 5.7).
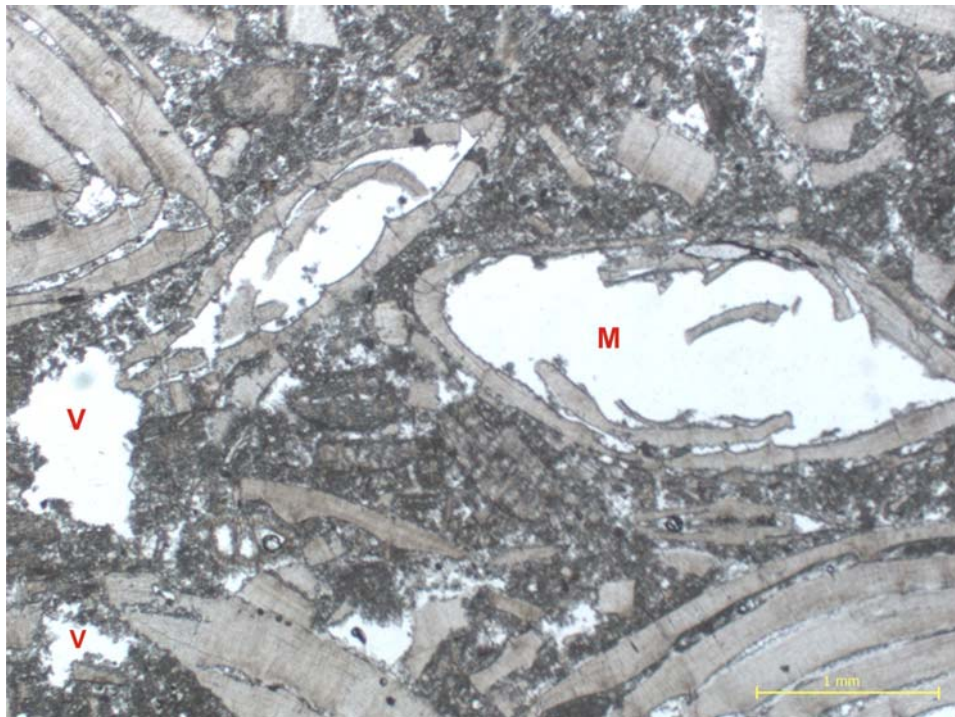
Figure 5.5. Photomicrograph shows dissolution, small vuggy (V) and mouldic porosity (M) produced by selective leaching Well 4O1-6, Depth 5180 ft., PPL.
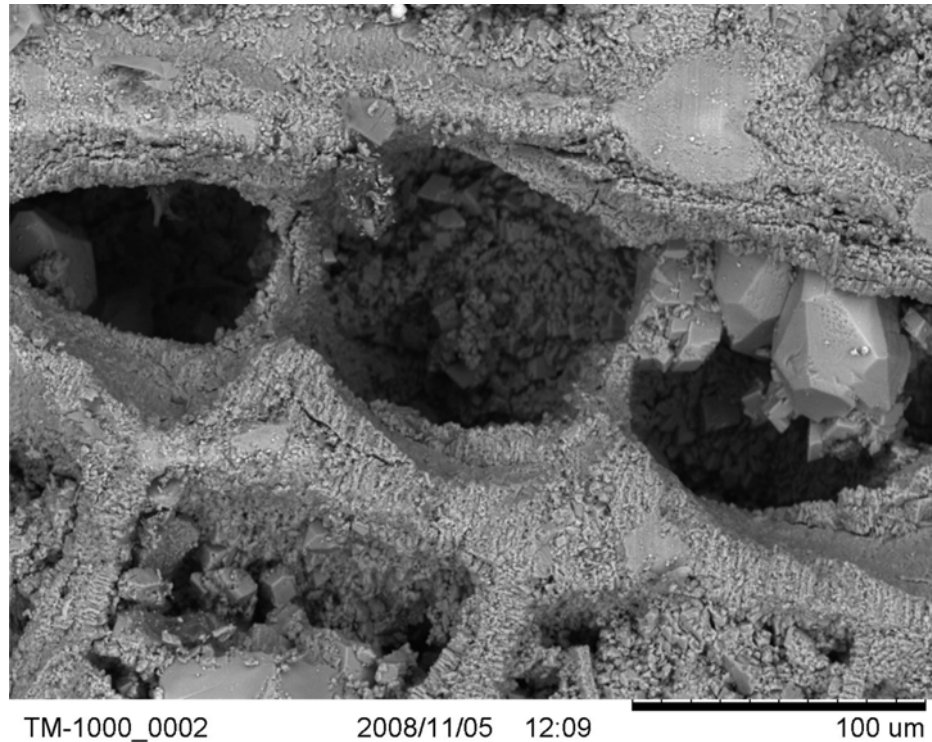
Figure 5.6. SEM showing well developed euhedral calcite crystals partially filled foraminifera chambers. Well H10-6, Depth 4946 ft.
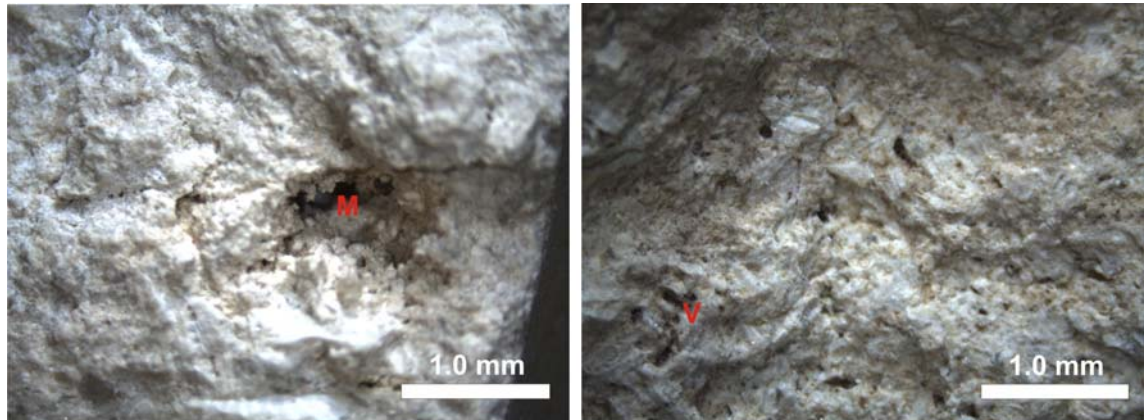
Figures 5.7. Core photomicrographs showing partial infill of fully dissolved bioclasts by drusy/ blocky calcite cement and left mouldic porosity (M). Scattered small vuggy (V). Well O3-6, Depth 5185 ft.

5.3.2.2.2. Cementation

The petrographic investigation indicates that the drusy calcite, blocky calcite and syntaxial overgrowths are the most common cement types observed in the Gialo Formation and these formed during different stages of the diagenetic history (Figures

5.8 to 5.17). The determination of a burial origin for calcite spar can usually be made on the basis of textural criteria and the timing of spar precipitation relative to compactional features (Tucker and Wright, 1990).

5.3.2.2.3. Non-ferroan drusy, equant and syntaxial overgrowth calcite cements

Non-ferroan sparry calcite cement occurs mostly as void fillings of different kinds (intergranular, intragranular and mouldic porosity). The lack of association of this non-ferroan calcite with burial-indicative textural criteria indicates it developed at a relatively early stage of diagenesis probably in the meteoric phreatic environment. It was formed after the dissolution diagenetic phase, as indicated by its relationship to the host-rock. The precipitation of non-ferroan drusy calcite spar is the main cause of porosity reduction in the Gialo Formation and usually takes the form of drusy mosaic, equant and syntaxial overgrowth cements. Drusy calcite crystals increase in size towards the centre of the original pore-space (Figures 5.8, 5.14, 5.16 and 5.17). Drusy calcite post-dates the formation of the micrite envelopes and it has been commonly reported from meteoric phreatic zones (Wilson, 2002; Scholle and Ulmer-Scholle, 2003). Also, calcite spar is usually better developed within intergranular space than within moulds derived from dissolution of skeletal particles. This suggests that the dissolution of bioclasts, probably aragonitic, occurred near contemporaneously or slightly post-dating the precipitation of some drusy cement (Tucker and Wright, 1990; Wilson and Evans, 2002). Equant calcite cements are present throughout most thin sections and microfacies; they reduce or completely fill pore space and have planar intercrystalline boundaries.

Syntaxial calcite overgrowths on echinoderm and crinoid fragments (Figures 5.11, 5.12 and 5.13) are less common in the Gialo Formation within the nummulite facies but are only a minor feature in the *Discocyclina* and *Operculina* facies. The calcite grows in optical continuity with the echinoderm fragments, generally surrounding the grains, and it is elongated along the C-axis. Syntaxial overgrowths can form in several diagenetic environments; Longman (1980) suggested that, although syntaxial overgrowths form most commonly in fresh-water phreatic environments, they may also form, but rarely, in vadose and deeper subsurface diagenetic environments. Flügel (2004) pointed out that overgrowth cements from near-surface marine and
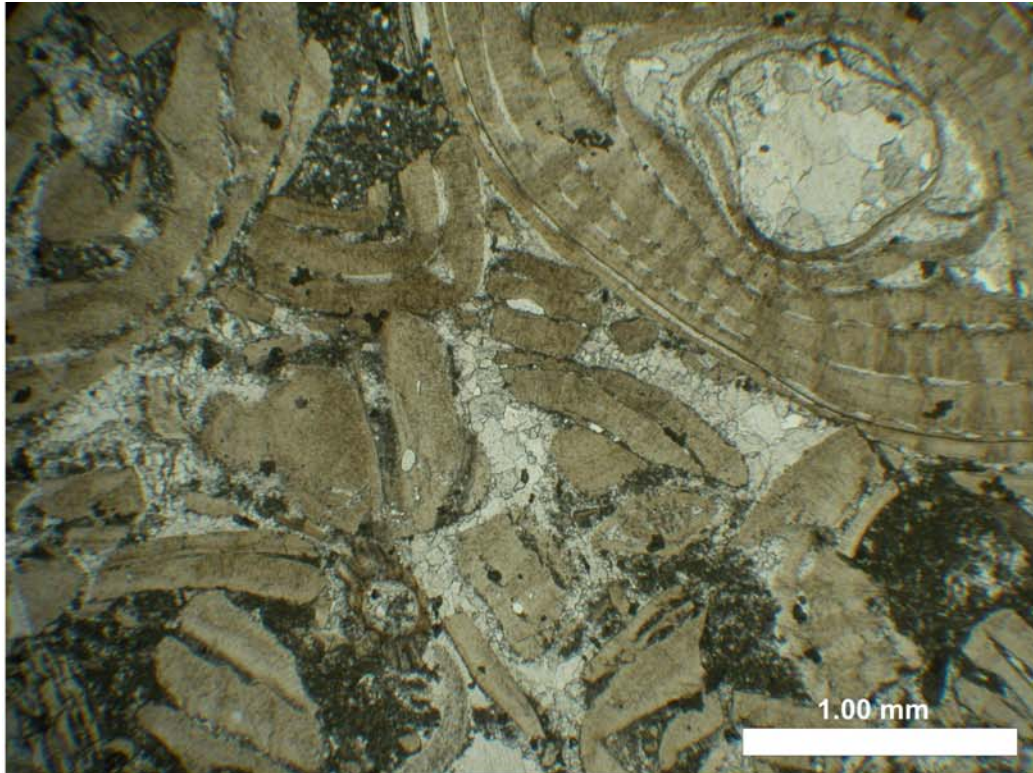
Figure 5.8. Thin-section photo from the middle part of the formation, where drusy calcite has filled porosity. Well H10-3-1, Depth 5022 ft., PPL.

TM-1000_0001   2008/11/05   11:58   100 um
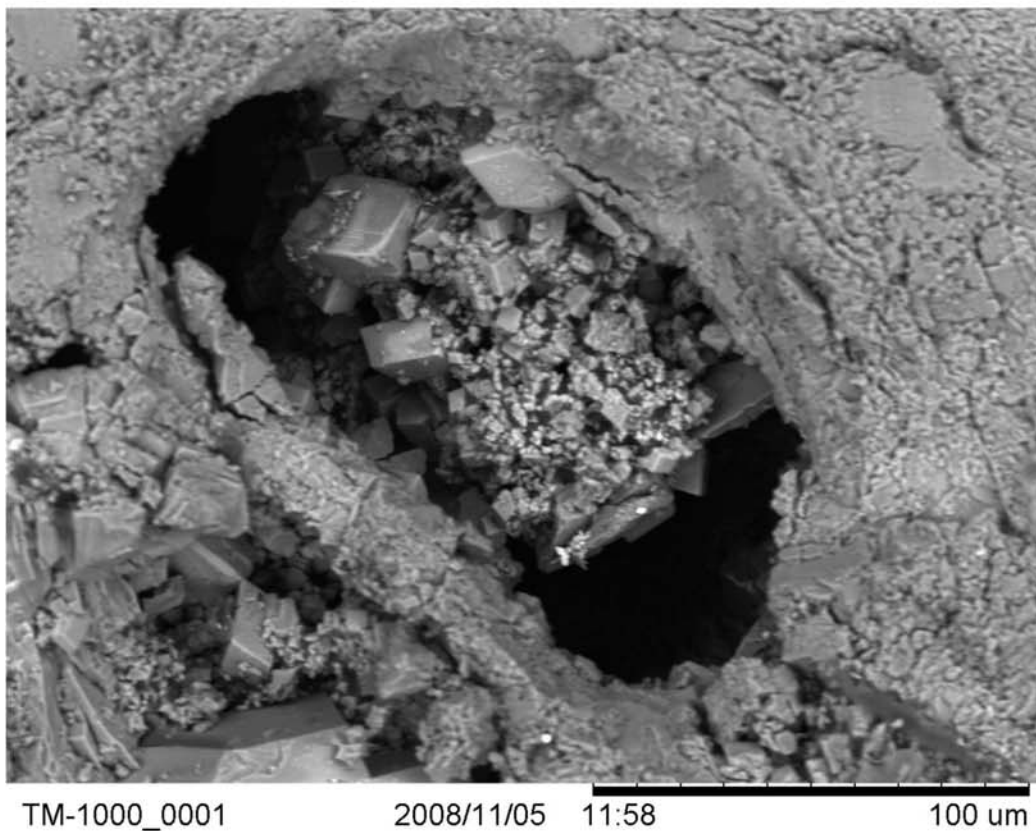
Figure 5.9. SEM photomicrograph shows calcite crystal growth within a foraminifera chamber. well H10-6, Depth 4956 ft.

vadose-marine environments are cloudy and inclusion-rich, in contrast to the clearer overgrowths from burial environments. Thin cloudy overgrowth cements often represent the first generation of overgrowth on echinoderm grains followed by continued growth under meteoric conditions (Flügel, 2004). In some samples within the nummulite facies, syntaxial overgrowths alone have reduced porosity by more than 15% (Figures 5.11 and 5.12). Many of the syntaxial overgrowths in the nummulite facies are clear cements, but in other facies they are cloudy, and may be inclusion-rich.

Source of calcium for early calcite cement: Since the cementation of sediment grains requires the input of an enormous amount of $CaCO_3$ and an efficient fluid-flow mechanism for complete lithification (Tucker & Wright, 1990), sea water and/or aragonite dissolution of carbonate grains would likely have been the source of the early cement during the shallow burial.

5.3.2.2.4. Neomorphism

Neomorphism in the Gialo Formation resulted in enlargement of micrite crystals (Figure 5.10), a process by which crystals that measure only a few microns in diameter may enlarge to a size measuring tens of microns in diameter. This creates a neomorphic product similar to sparry cement in crystal size. Neomorphic replacement of micritic matrix by microsparite is observed just in the upper-middle part of well H6-6 (Figure 5.10).
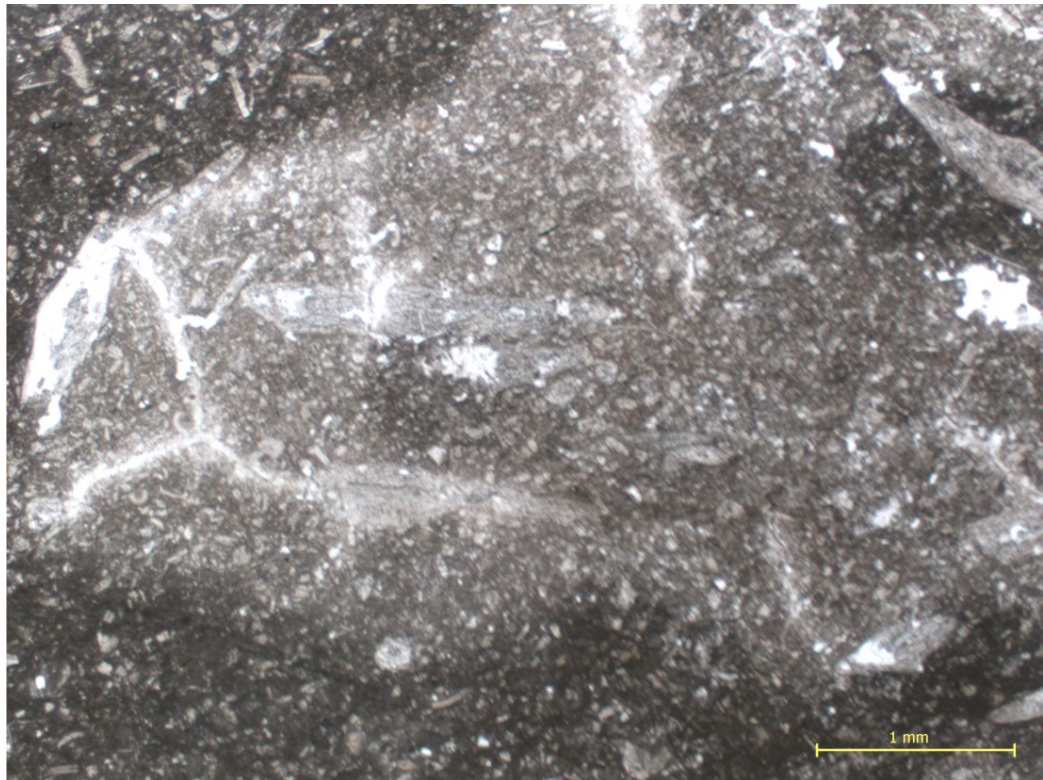
Figure 5.10. Photomicrograph shows aggrading neomorphism of carbonate mud (micrite) Well H6-6, Depth 5009 ft., PPL.
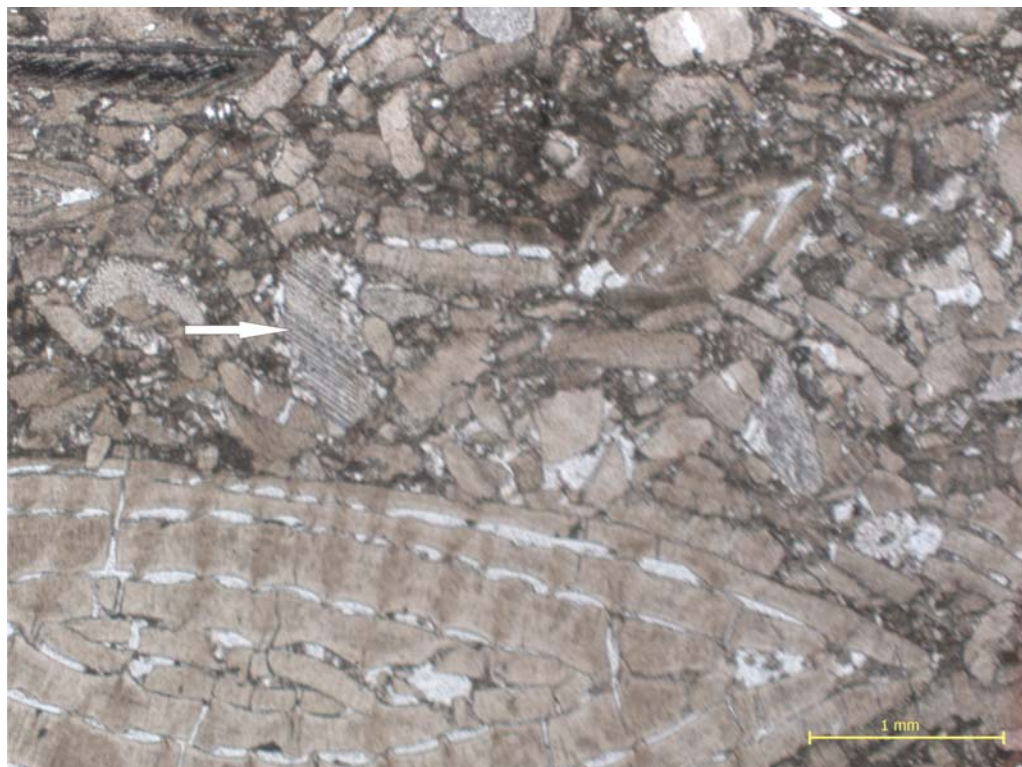
Figure 5.11. Primary porosity has been reduced by compaction and syntaxial overgrowth cements (arrow). Well H4-6, Depth 4935 ft, PPL.
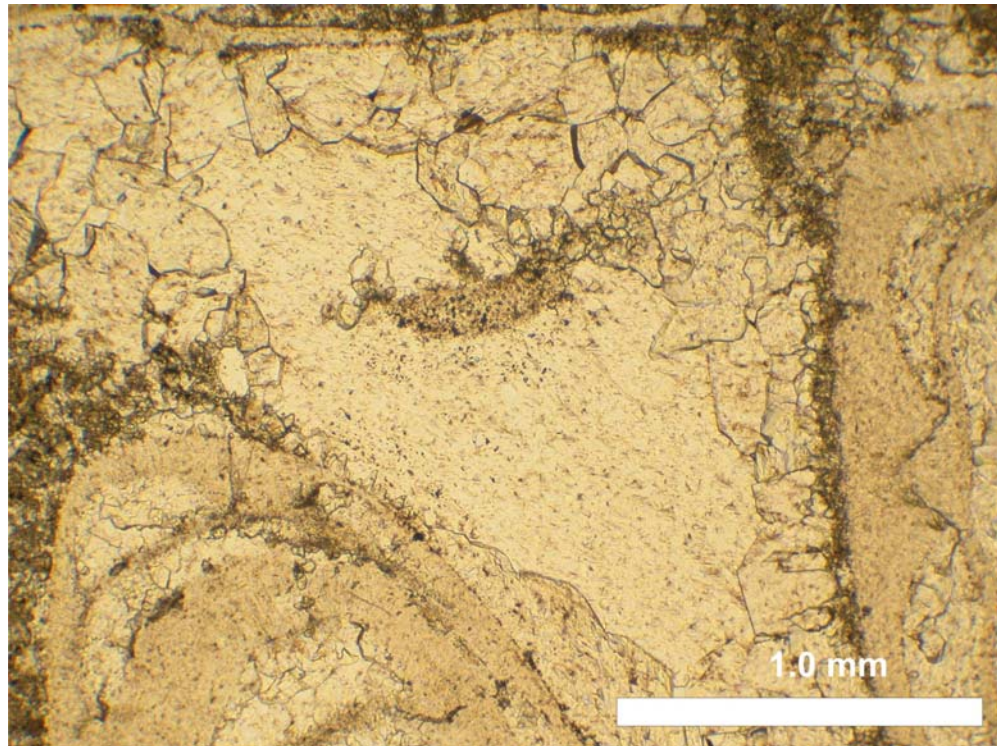
Figure 5.12. Photomicrograph shows cement around echinoderm fragments (syntaxial overgrowth). Well 4O1-6, Depth 5180 ft., PPL.
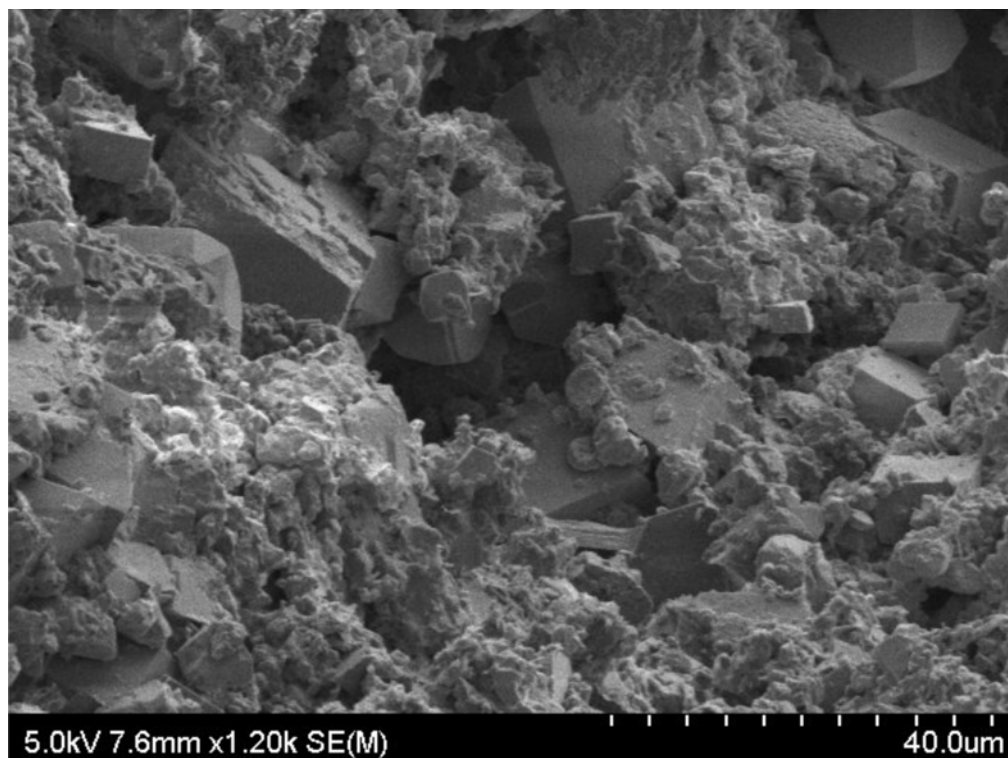
Figure 5.13. SEM photomicrograph shows blocky to drusy calcite crystals growth and partially to completely filled porosity. Well OOOO-1-6, Depth 5193 ft.
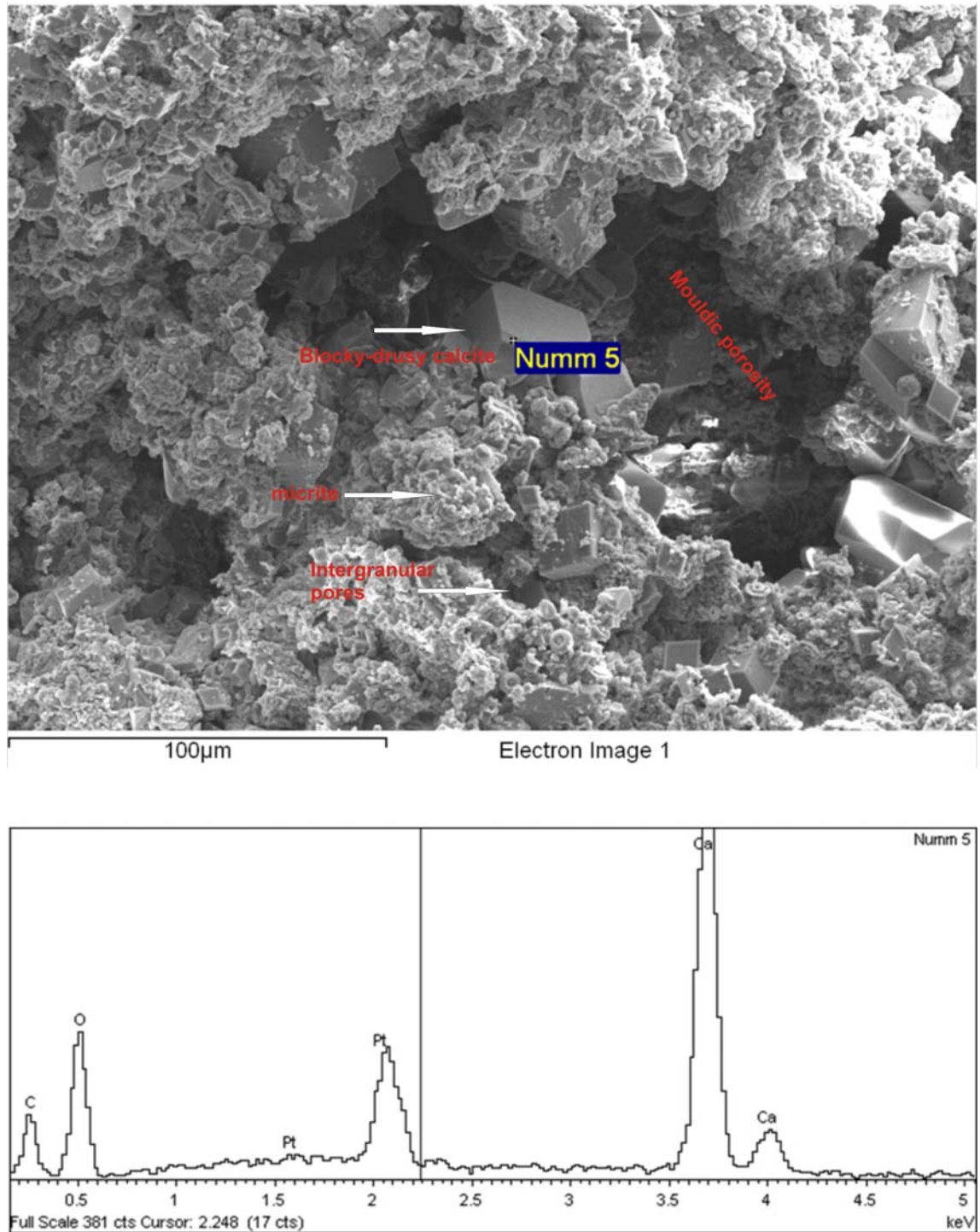
Figure 5.12. SEM micrograph showing former mouldic pores that have been partially filled by equant to drusy calcite spar. well developed intercrystalline porosity within microspar matrix. EDX spectrum of the same sample showing the composition of the calcite crystals. Well 4O-6, Depth 5127 ft.
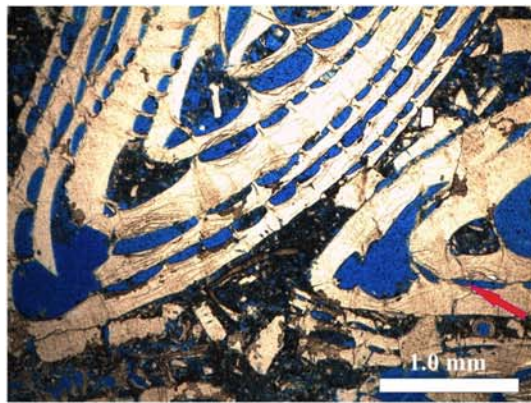
(A) Well OOOO1-6, Depth 5127'
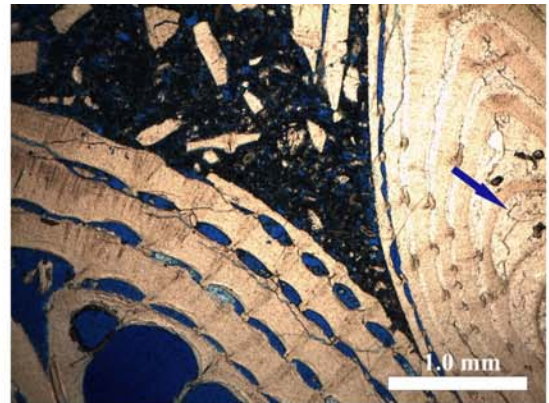
(B) Well OOOO1-6, Depth 5127'
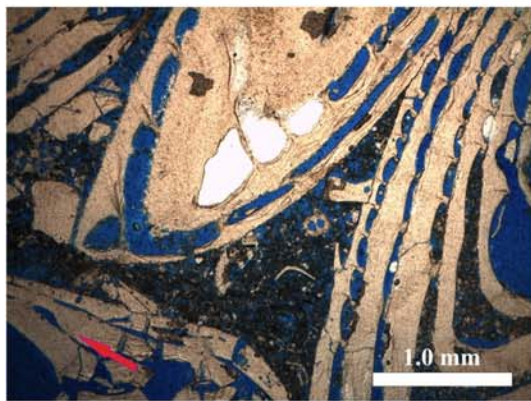
C) Well OOOO1-6, Depth 5127'
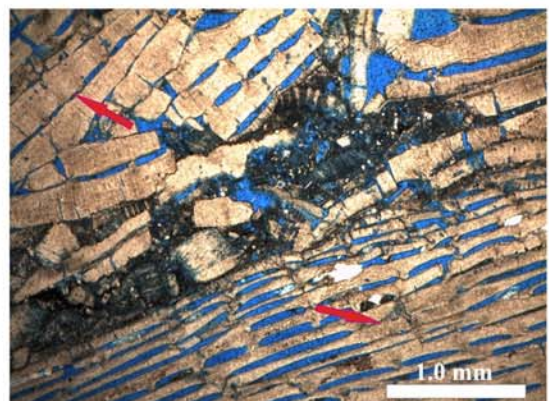
(D) H6-6 Depth 4942'.

(E) Core sample, well OOOO1-6, Depth 5153'.
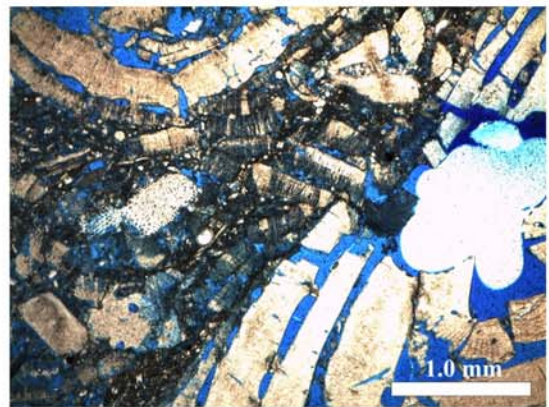
(F) H6-6 Depth 4942'.

Figure 5.13. Inter-and intrapartical porosities of good visible primary porosity (mainly within foraminifera chambers) have been reduced by mechanical compaction crushed many of these nummulite tests (red arrows). Interconnection between pores is generally limited, except in some fracture porosity connects intraparticle pores to the effective interparticle pore network. Cementation is generally limited (blue arrow). Photograph of core sample (E) of Nummulite facies showing small and large nummulite moulds.

10.0kV 16.6mm x1.20k SE(M) 40.0um
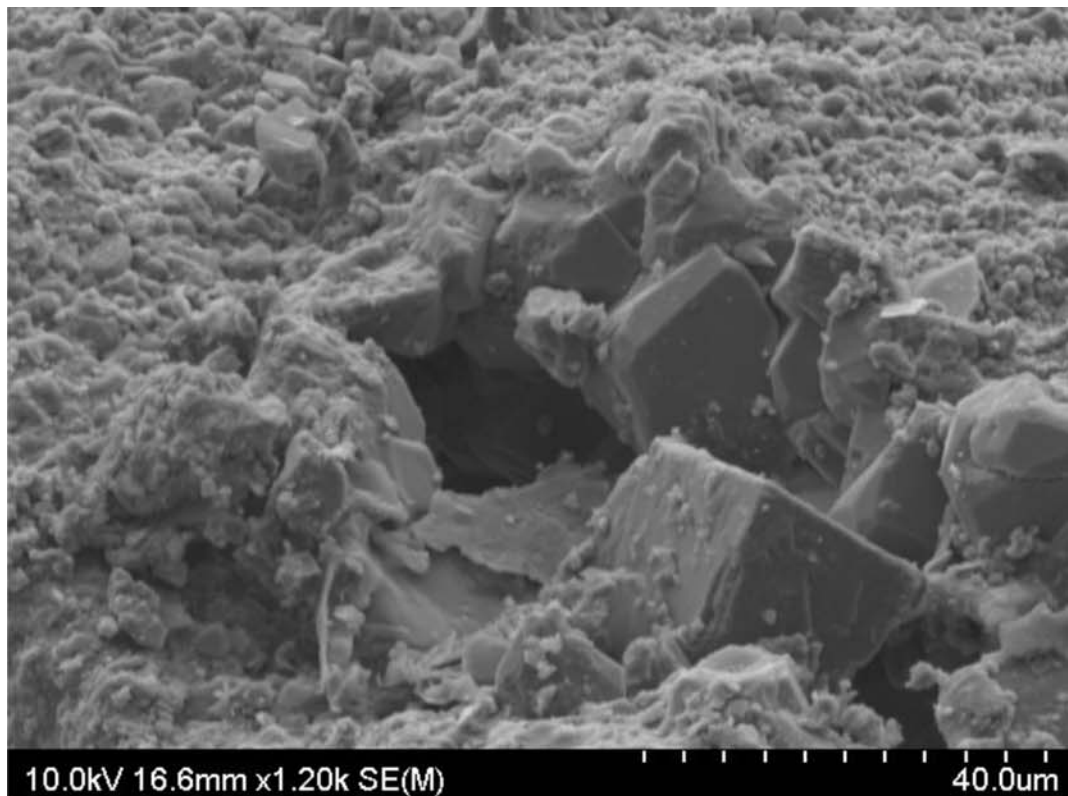
Figure 5.16. SEM photomicrograph shows blocky to drusy calcite crystals growth within porosity. well H4-6, Depth 4944 ft.

12.0kV 15.3mm x2.00k SE(L) 20.0um
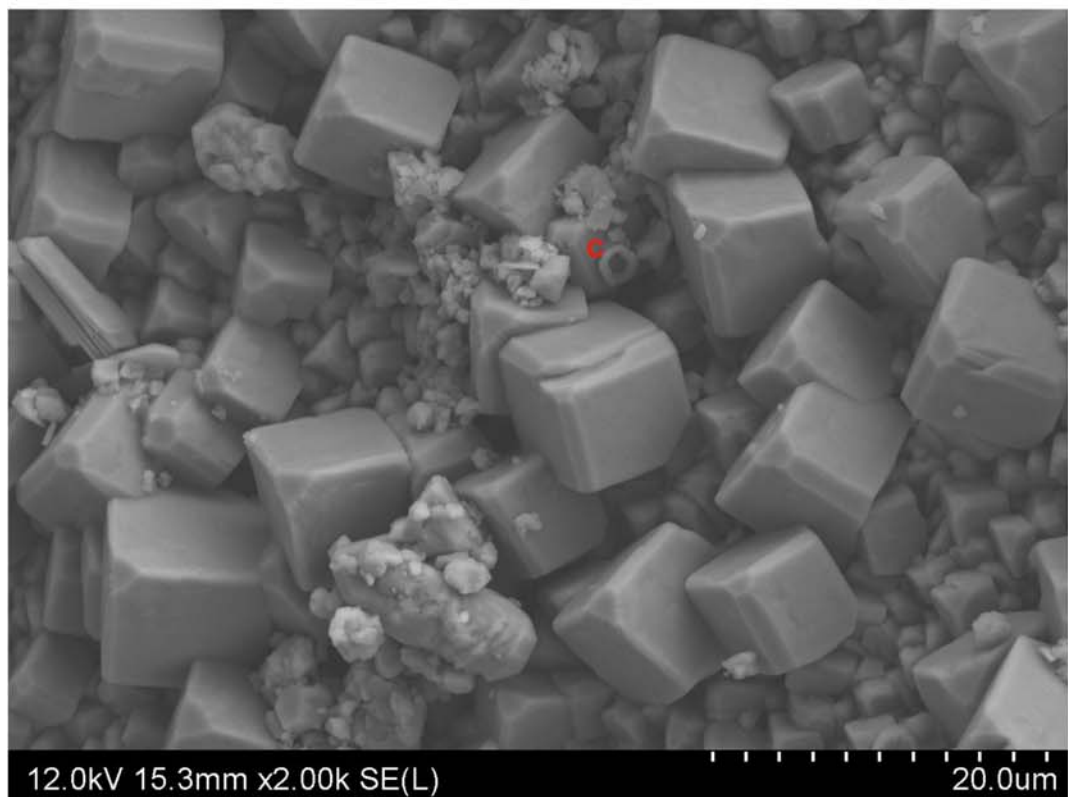
Figure 5.17. SEM microphotograph showing well developed interlocking euhedral calcite crystals with intercrystalline porosity. scattered well-preseved coccoliths C and micrite. Well H10-6, Depth 4991ft.

5.3.2.3. Late burial diagenesis

Burial diagenesis is generally taken to begin below the depth where sediments are affected by near-surface processes of the marine and meteoric environments. The burial diagenetic zone is characterized by a mix of physical and chemical diagenetic processes, most leading to porosity destruction. Many features have been recognized in the study area which represent evidence for late burial diagenesis. These include compaction, pressure dissolution and microfractures. Burial cements are often coarse grained and locally show poikilotopic textures. They are usually formed from relatively reducing pore fluids and, thus, may have elevated Mn^{2+} and Fe^{2+} contents.

5.3.2.3.1. Compaction and pressure dissolution

Compaction is a common and important diagenetic process in carbonate rocks and refers to any process that decreases the bulk volume of the rocks. Many carbonate sediments lose some of their original porosity as a result of compaction during burial. The effects of compaction are most pronounced in rocks in which early cements, such as marine and near-surface meteoric cements, are poorly-developed or absent. The compaction processes and products generally split into two categories: mechanical and chemical (pressure dissolution). Mechanical compaction begins as soon as there is overlying sediment with simple dewatering, re-arrangement of particles and closer grain packing, whereas chemical compaction mostly requires several hundred metres of burial (Tucker, 1993). Evidence for mechanical compaction in the Gialo carbonates is provided by crushed and broken fossils, deformation and truncation of bioclasts, alignment of elongated grains, and tight interlocking of grains (Figures 5.18 and 5.19). The petrographic investigation indicates that mechanical compaction is more evident in the nummulitic floatstone/packstone than the other microfacies (e.g. mud-supported limestones). This is shown where the lime-mud content increases and the rock changes from wackestone to mudstone but grain breakage is rarely recognised.

As a result of increasing overburden (several hundred to a thousand metres or more), chemical compaction (pressure dissolution or solution transfer) replaces mechanical compaction and further reduction of pore space takes place. Chemical compaction and pressure dissolution also results in the dissolution of grains and sediment, and this may be a significant source of $CaCO_3$ for burial cementation (Tucker, 1993). Pressure

dissolution arises from the increased solubility of material at grain contacts and along sediment interfaces as a result of applied stress. Chemical compaction in the investigated limestones is indicated by the presence of dissolution seams, fitted fabrics (micro-stylolites between grains) and through-going stylolites (Figure 5.20), but they are not abundant. Therefore, this suggests that early near-surface cementation was common and prevented this fabric from developing extensively (e.g. Bathurst, 1986). Microstylolites and mechanical compaction features are common in the nummulitic bank facies, suggesting a general lack of early cementation there.

Several generations of stylolites affect the Gialo Formation. Throughout most of the studied sections there are horizontal stylolites with a simple wave-like form. Concentrated along dissolution seams there is usually an insoluble residue of dark organic matter or bituminous substance. Stylolitization significantly affects carbonate reservoir quality by providing pathways for hydrocarbon migration. The stylolites have clearly acted as pathways for hydrocarbon migration since bitumen is still present as a residue along most stylolites (Figure 5.20).

5.3.2.3.2. Ferroan sparry calcite cement

This calcite is quantitatively very minor and observed only in some intervals of the *Discocyclina* microfacies, H10-6 well. It occurs as a pore-filling cement, occupying either whole or parts of foraminifera chambers and occurring between bioclasts (Figure 5.21). Incorporation of Fe^{2+} in the calcite lattice takes place usually during the late stage of burial when there are reducing conditions with low sulphide activity (Evamy, 1969). The Fe^{2+} is thought to be derived from compaction of the intercalated shale during burial and this will have facilitated the expulsion of iron-rich fluids (Oldershaw and Scoffin, 1967).

Source of calcium for late calcite cement: There has been much discussion of the origin of the $CaCO_3$ for burial calcite spar cementation in limestones, but little agreement (see Bathurst, 1975). Pressure dissolution is commonly invoked as the major source of $CaCO_3$ for many limestones lacking in early cement (Tucker and Wright, 1990). This is also likely to have been the mechanism to provide the $CaCO_3$ for late calcite cement in the Gialo carbonates. The predominance of non-ferroan calcite as the main burial cement could indicate that there was no source of Fe in the system. This
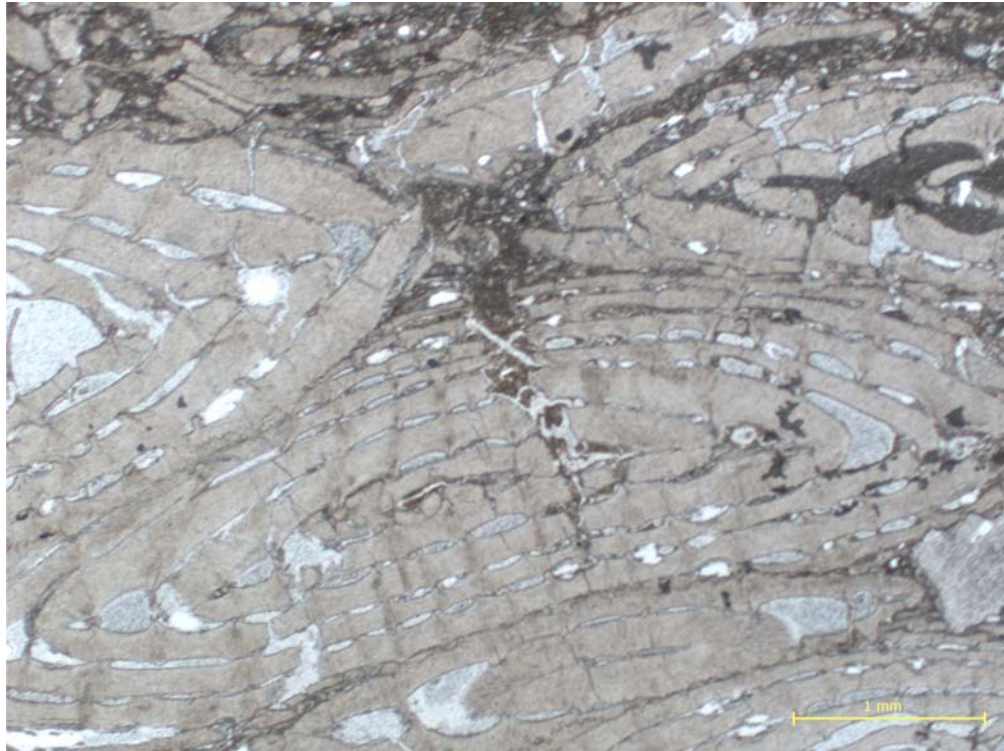
Figure 5.18. Photomicrograpg shows compactional fracturing of robust nummulite, lack of early marine cement enhancing mechanical compaction and grain deformation within nummulitic packstone. Well H6-6, Depth 4950 ft., PPL.
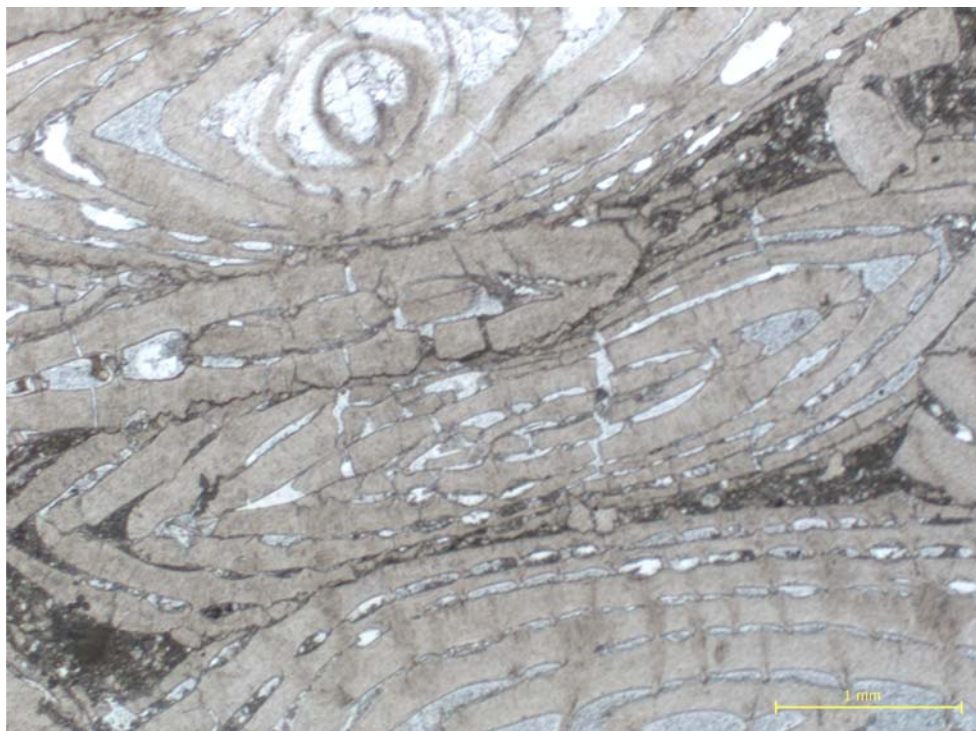
Figure 5.19. Porosity is partially occluded by late calcite cement whilst compaction related partially fractures and associated pressure solution at grain boundaries and development of micro-stylolites between tests are clearly visible. Well H6-6, Depth 5450 ft., PPL.
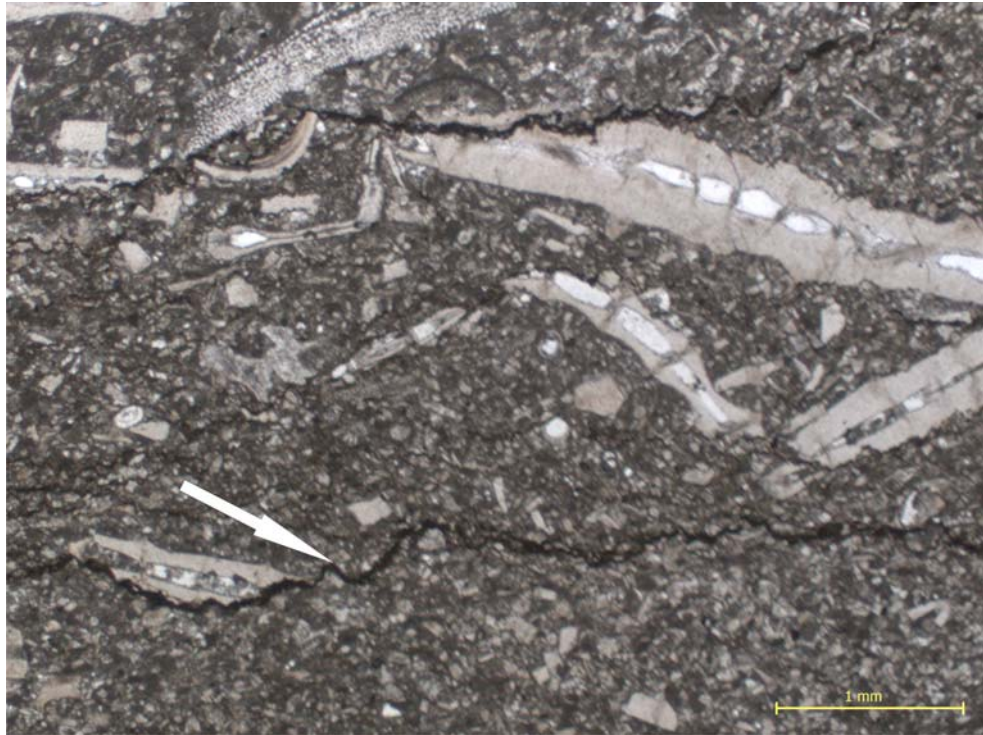
Figure 5.20. Well Well developed dissolution seams (arrow "micro-stylolite") with common benthic and minor planktonic foraminifera. Dark material (bitumen) is concentrated along along the micro-stylolite. Well O3-6, Depth 5234ft.,PPL.
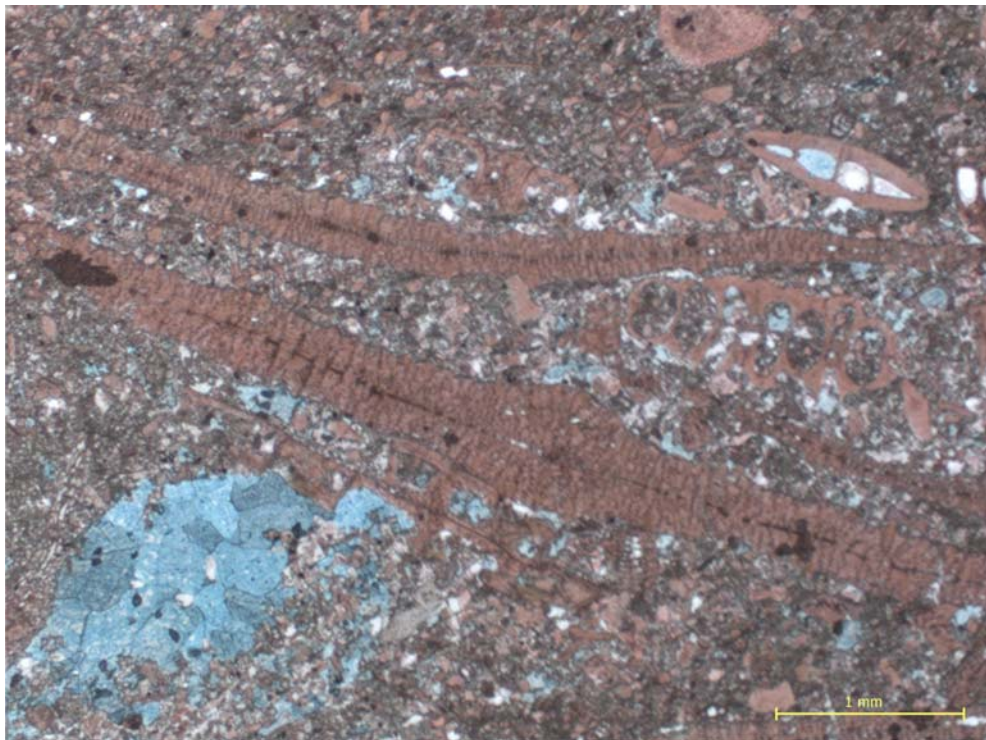
Figure 5.21. Ferroan calcite cement (blue) filling porosity with common elongated Discocyclina. Well H10-6, Depth 4956 ft., XPL.

could have been a result of the early formation of pyrite, which is common in the Gialo carbonates, which would have removed any available Fe leaving the remaining pore fluid depleted in Fe ions (similar to the interpretation of Allan and Wiggins, 1993).

5.3.2.3.3. Silicification

Silicification of some bioclasts and precipitation of authigenic silica in voids is observed in a few samples (Figure 5.22) within the nummulitic facies in the Gialo Formation. Two different petrographic types of chert are recognized, microquartz and chalcedonic quartz (Flügel, 2004), occurring in the nummulitic facies, particularly in wackestones. However, as these crystals are small and appear to be scattered, their influence on the cementation of the rocks, and on porosity and permeability, is very limited. Moody *et al.* (1992) interpreted silica replacement in the 'Compact Micrite' immediately above the El Garia Formation, to be a product of meteoric diagenesis in a near-surface mixing zone; however, clear evidence of subaerial exposure was not observed in Gialo strata. The source for the silica is probably from dissolved siliceous microfossils (Robertson, 1977).

5.3.2.3.4. Crystalline dolomite

Very fine to fine crystalline dolomite rhombs were observed in a few samples within the middle part of well OOOO1-6, particularly in the nummulite facies (Figure 5.23). Dolomite crystals developed across boundaries of compacted grains, indicating that it is a syn-compactional or post-compactional feature formed during burial. Dolomite rhombs also occur lining dissolution vugs and pores. Tucker and wright, 1990 pointed out that scattered rhombs, dolomite crystals along stylolites and pressure dissolution seams, and late cavity-filling dolomite cements are all common forms of burial dolomite, occurring in many limestone. In the Gialo the dolomite does not contribute significantly to porosity reduction.

5.3.2.3.5. Pyrite

Pyrite is observed in some facies of the Gialo Formation, but it is most common in wackestone-mudstone of the Nummulite and *Discocyclina*-nummulite facies in the lower part of well O3-6. Pyrite is usually scattered in cubic shaped crystals in the micrite matrix or fills bioclastic cavities (Figure 5.24). Authigenic pyrite commonly

forms under reducing conditions and may replace carbonate or organic material, or be in close proximity to organic material (Flügel, 2004). In modern sediments the sulphur required for pyrite formation is derived from seawater (Hudson and Palframan, 1969), whereas iron is usually transported to the basin attached to clay minerals, from which it is then released under reducing conditions (Carroll, 1958). According to Berner (1970) the sulphide for the precipitation of pyrite comes mainly from bacterial reduction of dissolved sulphate in pore waters, producing H_2S which reacts with Fe^{2+} in solution. Other sources of H_2S are from thermal maturation of kerogen or crude oil (Machel *et al.*, 1995).

5.3.2.3.6. Microfractures

Microfractures cross-cutting micrite and bioclasts have been recognized in some units of the Gialo Formation. They are locally partially to completely filled by non-ferroan calcite (Figure 5.25). The partially-filled microfractures represent a significant contribution to porosity and permeability development. In the molluscan facies, some fractures are partially filled by organic material. These fractures are up to several centimetres in length and reach up to 1mm in width.
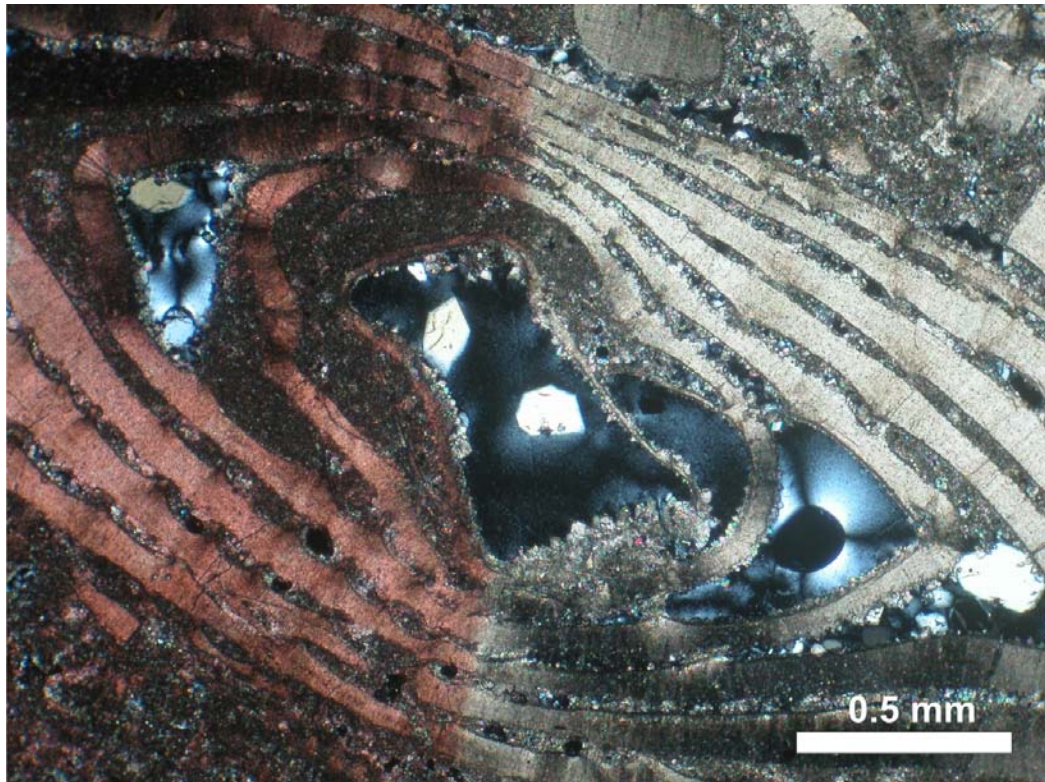
Figure 5.22. Megaquartz crystals in nummulite chamber, well 4O1-6, Depth 5180ft., XPL
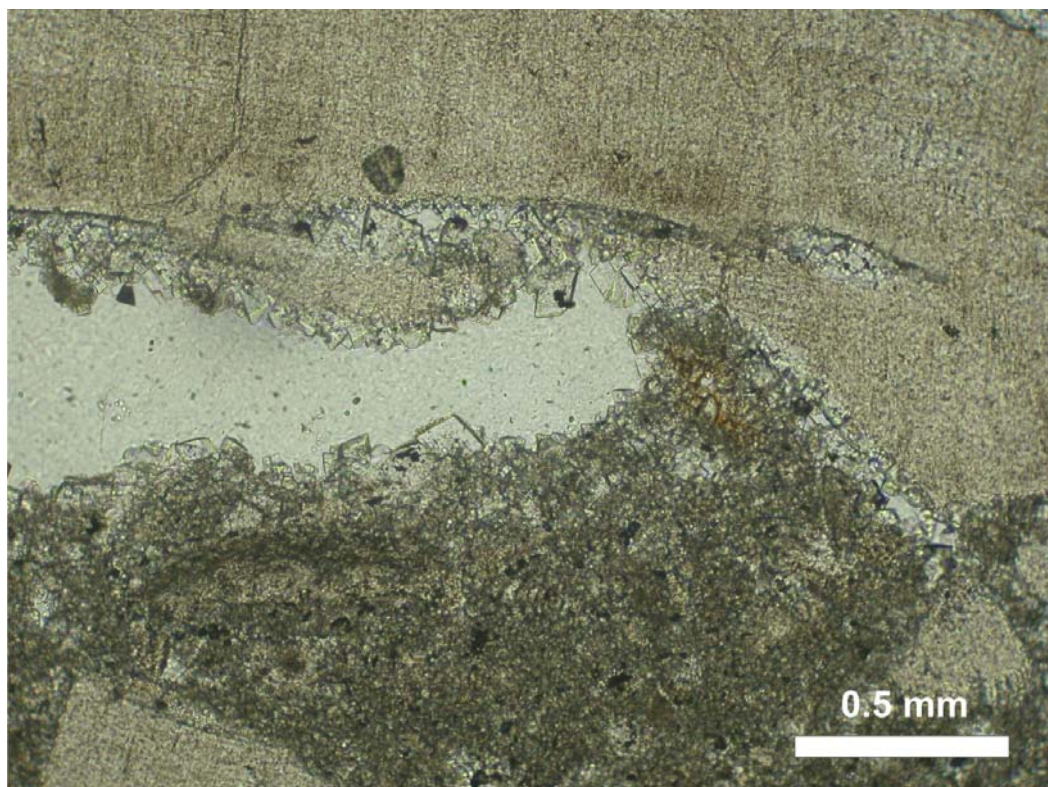
Figure 5.23. Very fine to fine crystalline dolomite rhombs occurring within a nummulite cavity and upon internal sediment. Well 4O1-6, Depth 5180ft.
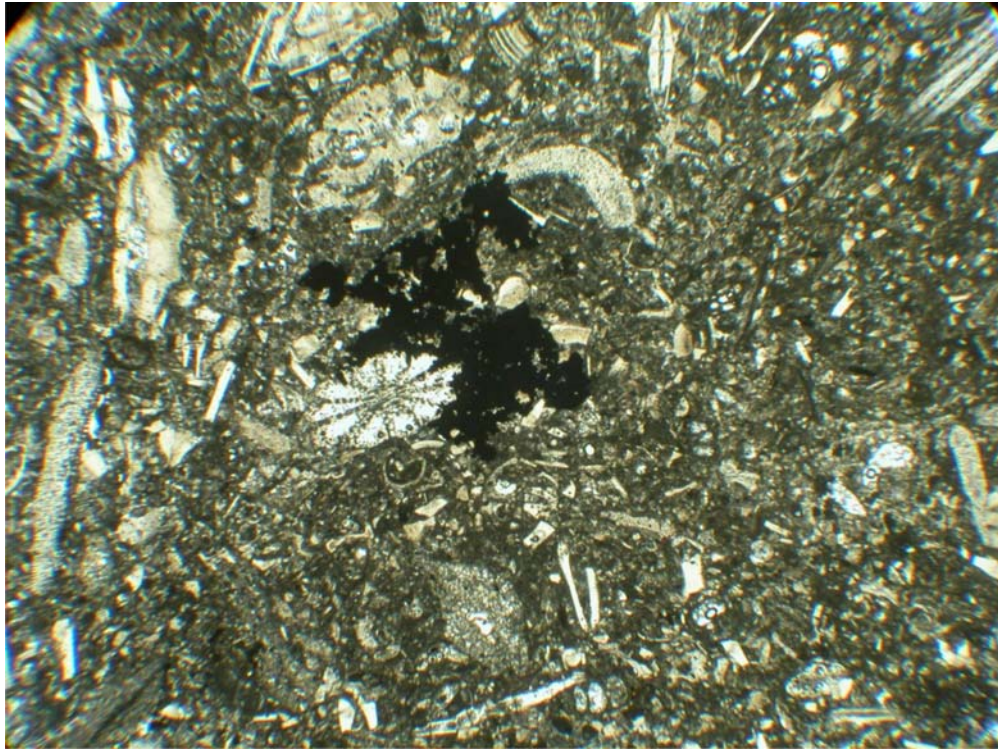
Figure 5.24. Photomicrograph shows pyrite (black) filling bioclast fragment cavities within micrite matrix. Well O3-6, Depth 5257 ft., PPL.
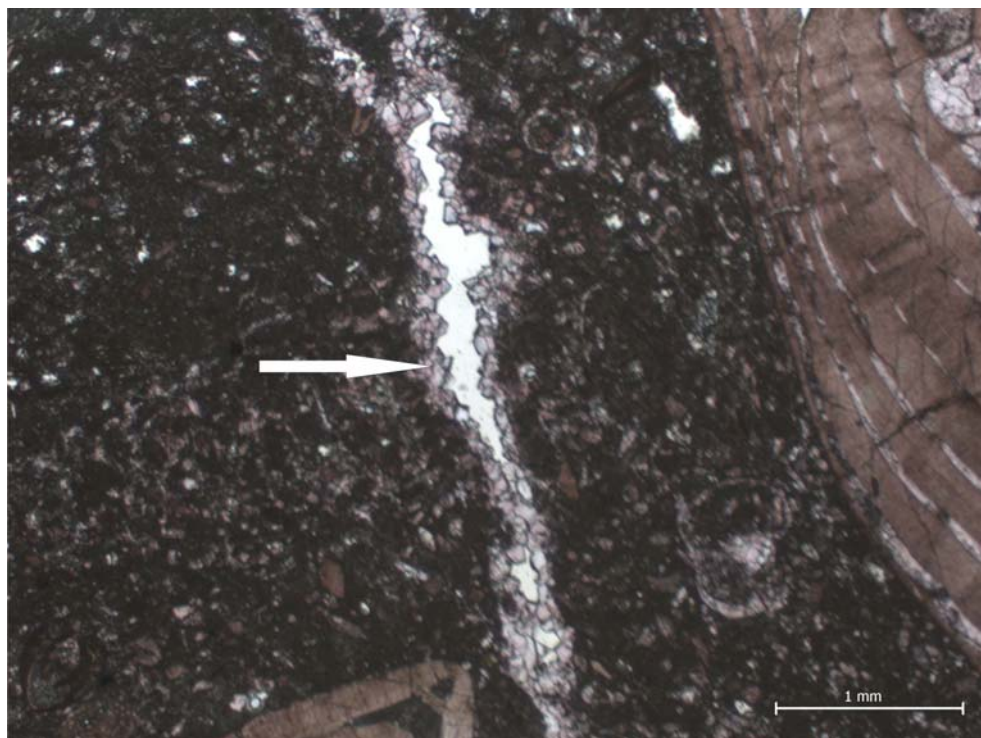
Figure 5.25. (A&B) Micro-fracture parially filled with calcite cement (arrow) in micrite matrix. Well H4-6, Depth 4992 and 5058 ft. resectively, PPL.

5.4. Cathodoluminescence

The use of Cathodoluminescence (CL) to examine carbonate sediments has provided much additional information about the diagenetic processes (Amieux, 1982). The most common application of CL in carbonate rocks is in revealing successive stages or zones of void-filling cements that cannot be seen using transmitted light microscopy (Miller, 1988).

Cathodoluminescence features of calcite have generally been attributed to variation in the concentration of Mn which is the main activator and to Fe, the main quencher (Machel and Burton, 1991). According to Miller (1988) the intensity of luminescence in calcite can be grouped into three categories: non-luminescence (dead, extinguished or black), dull (brown-orange-red) and bright luminescence (bright yellow, orange and red). The variation between bright and dull cement luminescence generally indicates a change from oxidizing to more reducing conditions in the fluid (Meyers, 1991). Non-luminescent calcite is normally the result of a low content of an activator (Fairchild, 1983). Non-luminescent calcite is suggested to be precipitated from oxidizing pore-water, whereas bright and dull luminescence indicates a more reducing pore-fluid (Meyers, 1978; Tucker, 1991).

In this study ten uncovered and polished thin-sections from different facies of the Gialo Formation were examined for their CL in order to investigate the effect of the chemistry of the pore-fluid on the cementation. Two generations of cement in terms of their CL character have been observed in the studied limestones: early bright orange luminescence and a later dull luminescence (Figures 5.26). Bright pink to orange zones are seen within the microcrystalline calcite matrix (micrite-microspar), as well as in the early stages of syntaxial overgrowth calcite on echinoid fragments (Figure 5.26 A&B). The dull luminescent calcite includes much of the sparry (mainly drusy) cement, occurring between grains and filling bioclastic cavities (e.g. nummulite chambers). It also forms the late syntaxial overgrowth calcite cement (Figure 5.26 A&B) (Wilson and Evans, 2002). Bioclasts (especially nummulites) are commonly luminescent with a quite bright orange colour, similar to the early calcite cement. This suggests they have picked up manganese and this is probably the result of some recrystallization and alteration. The dull sparry calcite cement which fills nummulite chamber (Figure 5.26 C&D) is probably a burial cement.
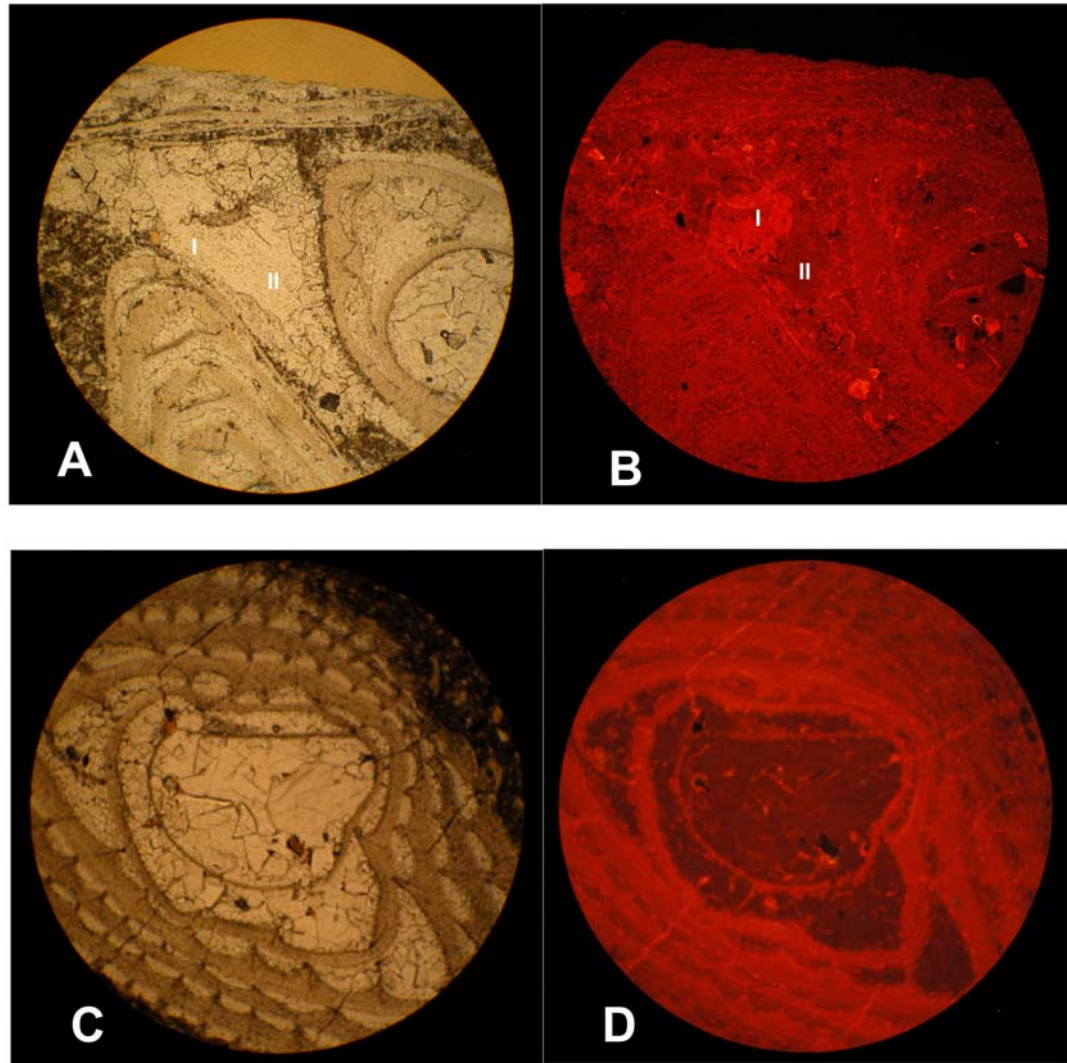
Figure 5.26. Thin-section microphotographs taken under normal light (PPL) and CL. A &B showing growth-zones in a syntaxial cement, two growth-zones (I and II) can dimly be seen: zone I is older and zone II the younger. These zones are more distinct under CL (B) and comprise: a brightly luminscence earlier generation (I), forming a thin "border" around the crinoid, and dull luminscent later generation (II) occupying most of the inter-granular porosities. Well 4O1-6, Depth 5180 ft. C&D sparry calcite (within foraminifera chambers) has a dull luminescent zone (D) whereas the nummulite shell has bright luminscence. well H6-6, Depth 4921 ft.

5.5. Stable oxygen and carbon isotopes ($\delta^{18}O$ & $\delta^{13}O$)

The stable isotope signatures for oxygen and carbon are useful for assisting with the interpretation of sedimentary and diagenetic conditions (Hudson, 1977; Anderson and Arthur, 1983; Marshall, 1992; Corfield, 1995 and Sharp, 2007). The two most naturally abundant isotopes of oxygen, ^{18}O and ^{16}O, and of carbon, ^{13}C and ^{12}C, are normally used. Variations in $^{18}O/^{16}O$ and $^{13}C/^{12}C$ ratios between samples are measured by high-precision mass spectrometry (Fairchild *et al*., 1988). The abundance

of ^{18}O and ^{13}C in a sample is conventionally reported as the per mil (=mg/g or ‰) difference in delta (δ) notation ($\delta^{18}O$ and $\delta^{13}C$) between isotope ratios in the sample and those in the international Pee Dee Belemnite (PDB) standard which, by definition, has $\delta^{18}O$ and $\delta^{13}C$ values of 0‰ (Hudson, 1977). Increasingly negative, or more depleted, δ values with respect to VPDB imply a relative increase in the lighter isotopes (^{16}O, ^{12}C) in the analysed samples, while more positive, or enriched, values indicate a relative increase in the heavier isotopes (^{18}O, ^{13}C). The $\delta^{18}O$ of a carbonate precipitated from water depends chiefly on the $\delta^{18}O$ composition and temperature of the water. Increasingly lighter (more negative) values tend to be associated with decreasing salinity and with increasingly higher temperatures (Hudson, 1977). The $\delta^{13}C$ composition of precipitated carbonates reflects the source of bicarbonate dissolved in the waters, which can include sea water ($\delta^{13}C$ near 0‰), marine shell dissolution ($\delta^{13}C$ near 0‰), soil weathering processes ($\delta^{13}C$ near -10‰), bacterial oxidation or sulphate-reduction of organic matter ($\delta^{13}C$ near -25‰), bacterial methanogenic fermentation ($\delta^{13}C$ near +15‰), oxidation of methane ($\delta^{13}C$ from -50 to -80‰), or biotic reactions associated with thermal cracking and decarboxylation ($\delta^{13}C$ from -10 to -25‰) (Hudson, 1977; Irwin *et al*., 1977; Mozley and Burns, 1993).

On a $\delta^{18}O$ and $\delta^{13}C$ cross-plot, Hudson (1977) distinguished a number of characteristic isotope fields for carbonates having different origins. His diagram has been followed, adapted, and extended by many subsequent workers (Choquette and James, 1987; Moore, 1989; Morse and Mackenzie, 1990).

5.5.1. Results of isotopic analyses

Twenty-two specimens were sampled for carbon and oxygen isotope analysis from different facies of the Gialo Formation after detailed petrographic study. A microscope and drill assembly was employed to extract 0.2 to 0.5mg of powdered carbonate (including bioclasts, cements and micrite) from carefully selected areas of core chips. These included 14 samples of carbonate skeletons (nummulites, echinoid, brachiopods, bryozoa, *Discocyclina*, *Operculina* and mollusc) and 6 samples of different cements. The results of this analysis are shown in Table 5.1 and Figure 5.27, and simplified in Figure 5.28 where the general results and interpretations have been summarized.

Most of the dominant cements in the studied succession of the Gialo Formation show closely similar isotopic signatures. They all show negative oxygen values (Table 5.1) with $\delta^{18}O$ values between -2.68 to -4.16‰ and positive $\delta^{13}C$ values (0.90‰ to 1.05‰ PDB). Equant calcite cement within nummulite tests also has moderately depleted $\delta^{18}O$ values (-3.81‰ to -3.98‰ PDB) and positive $\delta^{13}C$ values (0.92‰ PDB). Based on petrographic observations, these calcite cements show some association with burial diagenetic features (i.e. compaction). The majority of the calcite cements within the Gialo Formation have more negative oxygen than the fossils, suggesting precipitation within the shallow burial environment under the influence of meteoric waters and/or precipitation from seawater at higher temperatures during burial. The carbon isotopic signatures are typical marine values (e.g. Tucker and Wright, 1990).

Well name	Depth Feet	Skeleton/Cement type	$\delta^{18}O$‰ (PDB)	$\delta^{13}C$‰ (PDB)	
4O1-6	5133	Echinoid	-1.22	1.17	
4O1-6	5133	Nummulite skeleton	-1.06	1.09	
H10-6	5022	Nummulite cement	-3.98	0.92	*
H4-6	5112	*Discocyclina*	-2.08	0.86	
H4-6	5098	Nummulite	-2.09	0.76	
H4-6	5089	Matrix	-2.23	0.79	
H4-6	5058	Drusy cement	-4.16	0.90	*
H4-6	4963	Nummulite cement	-3.81	0.92	*
O3-6	5257	Brachiopods	-1.96	0.76	
O3-6	5250	*Operculina*	-2.29	1.06	
O3-6	5232	Mollusc	-2.25	0.89	
H6-6	4921	Nummulite skeleton	-3.93	0.98	
H6-6	4929	Nummulite skeleton	-3.22	1.05	
H6-6	4974	Drusy cement	-2.68	1.05	*
H6-6	4975	Drusy cement	-2.72	1.03	*
H6-6	5031	*Discocyclina*	-2.17	1.00	
H6-6	6001	Glauconite	-1.92	1.89	
O3-6	5126	Nummulite skeleton	-2.81	1.03	
H4-6	4938	*Discocyclina*	-2.51	1.19	
H6-6	4956	Bryozoa	-2.51	1.17	
H6-6	4957	Nummulite skeleton	-2.15	1.00	
H6-6	4970	Matrix	-2.02	0.91	

Table 5.1. The results of oxygen and carbon isotope analysis of carbonate cements and skeletons of the Gialo Formation (* Cement).
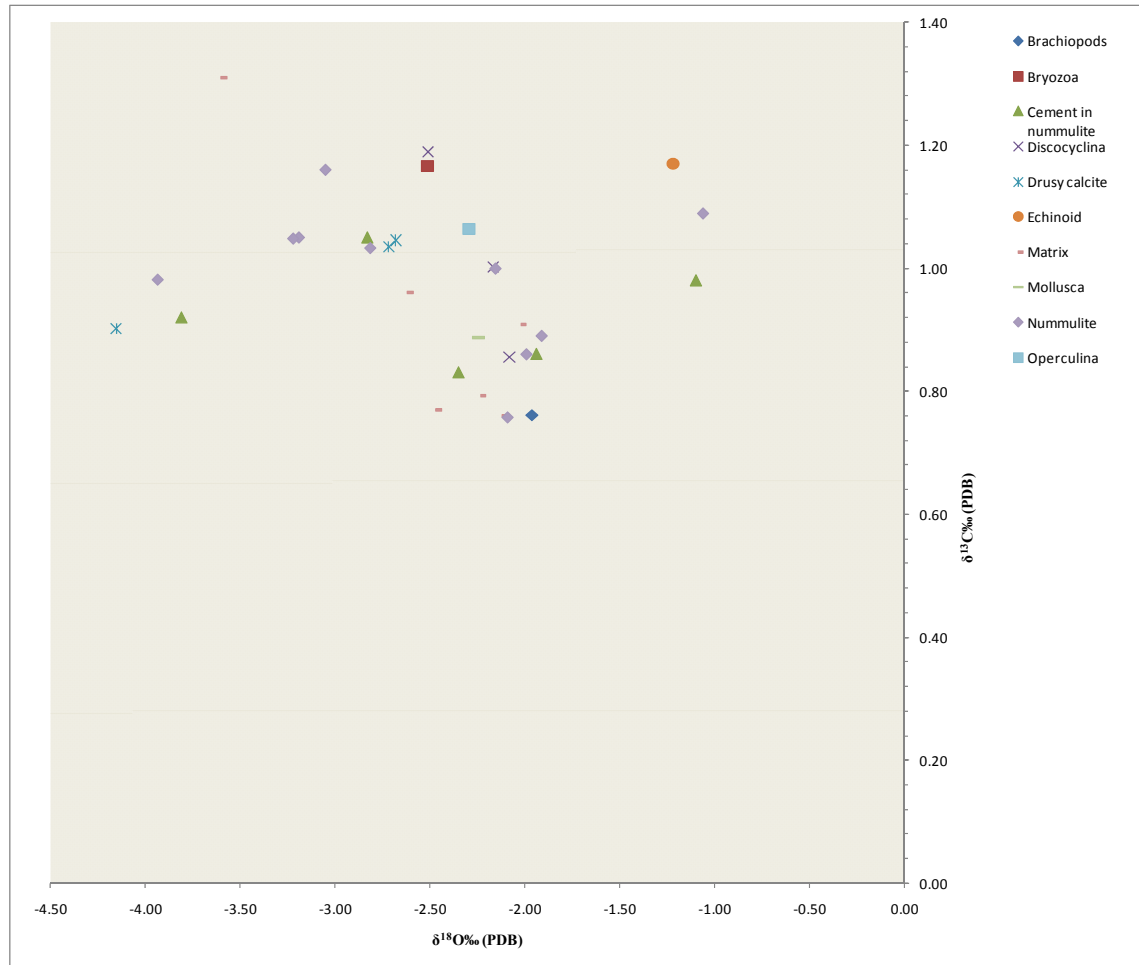
Figure 5.27. δ^{18}O- δ^{13}C plots for some Gialo Formation carbonate skeletons and cement samples.

For the fossils, nummulites have negative δ^{18}O values (-1.06‰ to -3.93‰ PDB) and positive δ^{13}C values (0.98‰ to 1.09‰ PDB). *Operculina* has negative δ^{18}O value (-2.29‰ PDB) and positive δ^{13}C value (1.06‰ PDB). *Discocyclina* has negative δ^{18}O values (-2.08 to -2.51‰ PDB) and positive δ^{13}C values (0.86 to 1.19‰ PDB). The mollusc fragment has a negative δ^{18}O value (-2.25‰ PDB) and positive δ^{13}C value (0.89‰ PDB).

δ^{18}O values from -4 to -6‰ were recorded for cement thought to be precipitated from meteoric-derived ground water by Lawrence and White (1991). The relatively depleted δ^{18}O values of the fossil particles within the Gialo indicate that their fabric may have suffered some neomorphic alteration from a fresh-water dominated fluid (Shaaban, 2004). The least negative δ^{18}O for the fossils (-1.06‰) could be a

marine signature. All the δ^{13}C values of the bioclasts could be original unaltered marine values.

The Gialo isotope results can be compared with Middle Eocene "nummulite bank" limestones of the Giza Pyramids Plateau (Egypt) (Figure 5.28) which is a time equivalent and similar unit to the Gialo Formation. Holail (1994) concluded that the texturally well-preserved non-dolomitized nummulite grains from the Giza Pyramids succession were originally calcitic. He obtained δ^{18}O values ranging from -0.8 to -2.1‰ PDB and δ^{13}C values ranging from +0.4 to +2.8‰ PDB. For the whole-rock limestone, δ^{18}O values range from -2.0 to -3.6‰ PDB, and δ^{13}C values range from -0.5 to 2.0‰ PDB. Average δ^{18}O in the nummulite grains is 1.1‰ higher than that of the limestone matrix and differences in δ^{13}C between nummulite grains and the limestone matrix are less distinct. The nummulite grains and the limestone matrix samples appear to preserve a primary δ^{13}C signature. The relative depletion of δ^{18}O values of the limestone matrix suggests some degree of diagenetic alteration under the influence of ^{18}O-depleted pore-waters. Matrix-replacive dolomites (δ^{18}O ~ -0.6 to 1.2‰ PDB) are significantly enriched, and carbon isotopes (δ^{13}C ~ 0.8 to 3.0‰ PDB) are similar to the marine Eocene values. The wide range of the δ^{13}C values (-0.1 to -6.1‰ PDB) observed for calcite spars may simply reflect precipitation from fluids which have undergone different degrees of water/rock interaction (Meyers *et al*., 1985).
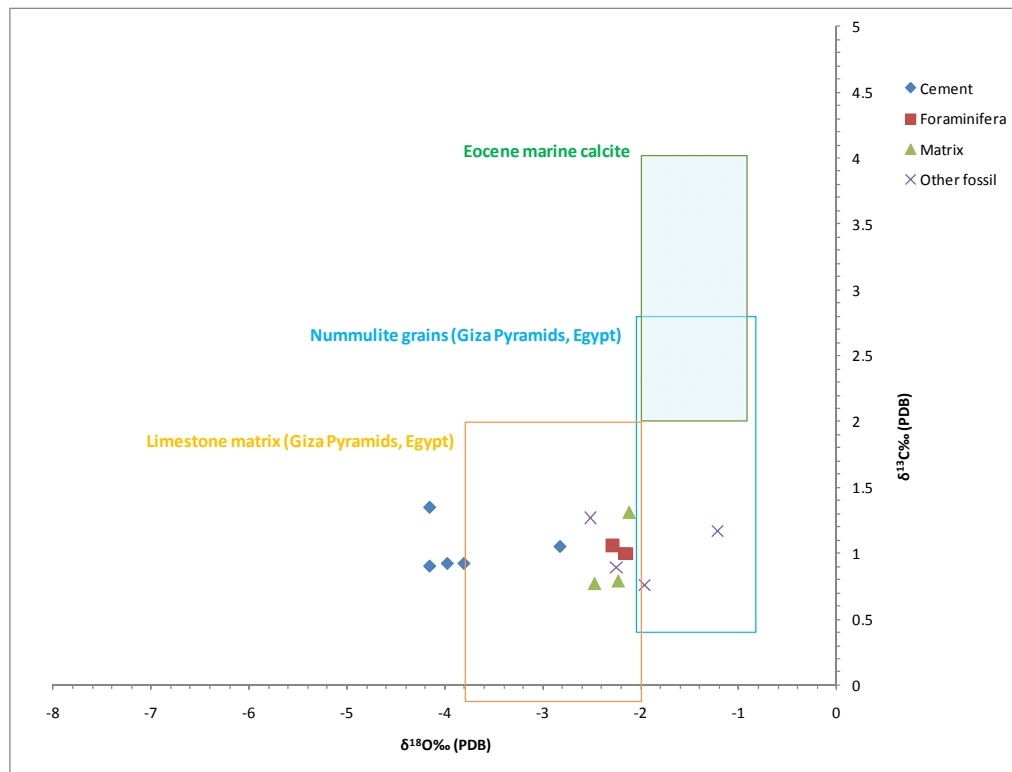
Figure 5.28. $\delta^{18}O$-$\delta^{13}C$ cross-plot (simplified from Figure 5.27) for the Gialo Formation and the Middle Eocene carbonate from Egypt (Holail, 1994).

5.6. The diagenetic sequence

Combining detailed petrographic descriptions of the cements and bioclasts with the interpretation of the diagenetic environment, based on geochemical data, it is possible to establish a diagenetic history for the Gialo carbonates. The paragenesis of the carbonate facies of the Gialo Formation in the studied wells is summarized in Figure 5.29, which shows the diagenetic processes and their relative timing:

Marine diagenesis: marine phreatic diagenesis involved early micritization of grains. Micrite envelopes developed around some mollusc fragments. During this stage, early compaction gradually decreased primary porosity.

Meteoric diagenesis: this stage began with meteoric vadose diagenesis during which metastable skeletal grains were dissolved, generating a secondary fabric with selective porosity. Subsequently, phreatic diagenesis occurred when pores spaces were filled by meteoric waters. Cements with a variety of fabrics were precipitated (drusy and syntaxial overgrowths) and they progressively occluded primary pore spaces. Zoning

was rarely observed under CL. Aggrading neomorphism occurred in mud-supported limestones.

Burial diagenesis: This stage was characterized by increasing overburden stress and development of dissolution seams, stylolites and fractures. Primary and secondary porosity was occluded through compaction in the absence of cementation in most places. Shallow-burial diagenesis, represented by slight mechanical compaction, resulted in the breakage of some shells, cracking of crystals, and also neomorphism of some shell components as indicated by depleted $\delta^{18}O$ values. Some burial dissolution created local vuggy porosity-filled with ferroan calcite. Also scattered dolomite rhombs were precipitated.

5.7. Diagenetic History and Porosity Development

The previous discussion of the diagenesis of the various mineralogical constituents of the Middle Eocene section in the Assumoud and Sahl fields indicates that the pore system was dramatically influenced both by the original depositional environment and by the later diagenetic history. Porosity obtained by visual estimates from thin-section ranges from poor to very good (<1% to ~37%) and permeability varies from low to high (<1mD to 100mD). The variations in porosity and permeability are strongly related to depositional environment as well as diagenetic processes (Figure 5.30). In general the porosity in the studied area is either primary, formed during deposition of the sediment or secondary, enhanced by dissolution and fracturing of sediments. Primary porosity is rare to common and patchily distributed and now partially to completely occluded by calcite cement. The secondary porosity formed by selective dissolution of some grains such as aragonite and calcite has resulted in the development of mouldic, vuggy and intercrystalline porosity in most of the sedimentary facies in the study area. Cementation by drusy calcite and syntaxial overgrowths has greatly reduced porosity. The porosity-permeability relationship of different facies is slightly complex because of the great variability of pore types (Figure 5.30). Pore connectivity appears to be variable with total porosity and, particularly, permeability showing a slightly weak trend of decreasing with increasing depth.

Microfractures are interpreted as mechanical fractures that developed after lithification, probably during localized uplift or compression. It is, however, difficult to

assess the potential contribution of these microfractures to porosity. An example of good permeability resulting from fractures in carbonate rocks is documented in the Tertiary Asmari Limestone in Iran (McQuillan, 1973). In the present study visual core descriptions and thin-section investigations indicate the development of microfractures in some parts of the identified facies but in many cases these are partially to completely filled by calcite cement.

Figure 5.30 summarizes the relationship between measured core porosity and permeability of selected facies encountered in the studied area. This figure shows the superior reservoir quality of the packstones compared with most of the other facies, which may show a high porosity (18-36%) but generally with a low permeability. The lowest porosity values observed are in the open-marine (lime mud facies) and *Discocyclina*-nummulite facies (>12-25%). The diagenetic processes appear to be having a negative influence on the development of porosity in some of the sedimentary facies. This is attributed to late cementation by calcite and compaction processes. Late meteoric and burial cementation, and compaction, are the main reasons for the reduction in porosity, whilst dissolution of grains and sediment within the Gialo Formation was the reason for porosity generation.
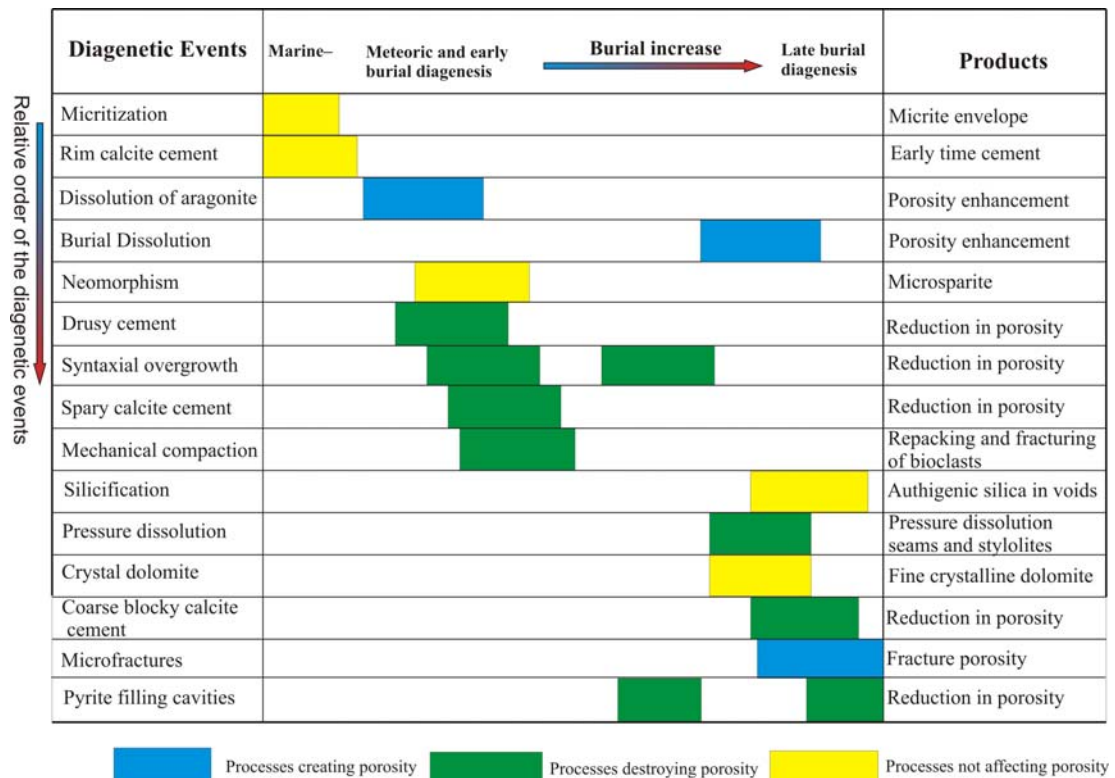
Figure 5.29. Paragenetic sequence of the diagenetic events observed in the Gialo Formation.
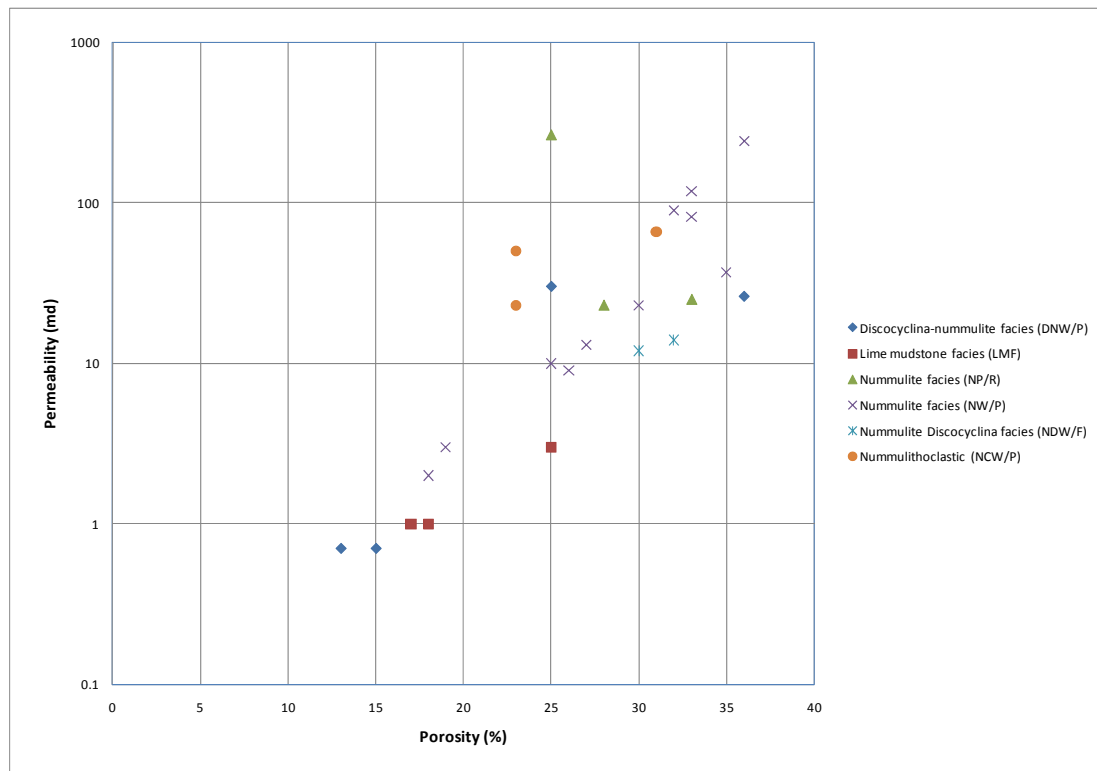
Figure 5.30. Relationship between core measured porosity and permeability of selected facies, Gialo Formation, Assumood and Sahl fields.

5.8. Summary

Present-day reservoir characteristics of the Gialo Formation are the net result of modifications to the original depositional characteristics caused by diagenesis. The diagenetic processes took place on the seafloor, in the meteoric environment and under burial conditions. Rare micritization is recorded and micrite envelopes, when present, preserved mouldic pores from collapsing. Lack of early seafloor cementation may have preserved intergranular porosity in the early burial stage, but then porosity was reduced through burial compaction. Grain breakage, grain penetration, plastic deformation and a few fine fractures were produced by mechanical compaction. Amongst these products, fracturing would have improved permeability, especially in mud-supported facies. Chemical compaction is more evident in grain-supported facies, causing partial grain dissolution and forming localized horizontally-discontinuous stylolites. Both of these processes are a source for burial calcite cement. Porosity in the lower parts of the Gialo

Formation in Assumood and Sahl fields is partially to more than partially filled with burial ferroan and non-ferroan calcite cement. Meteoric and early burial diagenesis includes dissolution, drusy calcite and syntaxial overgrowth cements and neomorphism. Localized neomorphism enlarged the crystal size of lime mud (< 4μm) to microspar (< 10μm). Syntaxial overgrowth cements have developed and are mainly associated with crinoids fragments. These processes generally reduced matrix porosity in some facies.

Two generations of cement are revealed by cathodoluminescence (CL), dull luminescent and bright orange cement. The dull luminescent zone includes sparry (mainly drusy) calcite cement between grains and filling bioclastic cavities (e.g. nummulite chambers) and late syntaxial overgrowth calcite cements. Bright pink to orange zones represent mainly the microcrystalline calcite (micrite), early syntaxial overgrowth cements and bioclasts (nummulites). The cathodoluminescence behaviour of syntaxial overgrowth calcite shows two cement stages, an early overgrowth cement which is bright luminescent and probably formed in a meteoric to shallow-burial environment with manganese present, then a later overgrowth that is dull and therefore probably contains iron and less Mn which reduces the luminescence. Bright luminescence of the syntaxial overgrowths is indicative of precipitation from waters changing from oxic to suboxic/anoxic in character. Bioclasts (nummulite) have picked up manganese to become luminescent as a result of some early recrystallization and alteration. Dull sparry calcite cement which fills nummulite chambers is probably a burial cement.

The oxygen isotope values of the bioclasts vary from marine values to more negative values as a result of some alteration. The more negative oxygen of the cements suggests precipitation within the shallow-burial environment under the influence of meteoric water and / or precipitation at higher temperatures during further burial. The carbon isotopic signatures are typical marine values.

There is a strong relationship between porosity and the diagenetic processes that have affected the Gialo sediments. Generally the porosity in the Assumood and Sahl fields is either primary or secondary, enhanced by dissolution and fracturing of the sediments. Reduction in porosity in the investigated sediments is mainly due to cementation and compaction.

CHAPTER 6: PETROLEUM GEOLOGY

6.1. Introduction

The Sirt Basin belongs to the top 15 among the world's petroleum provinces, having known reserves of 43.1 billion barrels of oil equivalent (Ahlbrandt, 2002). The Sirt Basin formed as a result of extensional tectonics. There are large areas of uplift and subsidence associated with normal faulting, while the absence of compresional folds is noticeable (Brady, *et al.*, 1980). Most of the faults cutting the Mesozoic and Tertiary section are normal faults. Intensive basement block faulting occurred in central Libya during the Mid-Cretaceous and continued through the early Tertiary. This faulting resulted in the development of the horsts (platforms) and grabens (troughs) of the Sirt basin. Some of these faults are mappable on the surface; others were detected by geophysical methods. The nature of the faults which control the Sirt Basin grabens is important, particularly in respect of oil migration. Eocene nummulitic limestones form important hydrocarbon reservoirs offshore Tunisia (Racey *et al.,* 2001) (e.g. Ashtart field: 350-400 MMBLS) and Libya (Anketell and Mriheel, 2000) (e.g. Bourri field: 1,000-3,000 MMBLS). They are potential exploration targets in Egypt, Italy, Oman and Pakistan. The Middle Eocene Gialo Formation is widely developed in the Sirt Basin, except in the northwestern part where the Gedari Formation occurs as its lateral equivalent (Figure 6.1). Deposition was varied in both thickness and lithofacies on the platforms and in the troughs (Figure 6.2). The southern Jahama Platform has gas-bearing Gialo reservoirs currently in production. The Hateiba field, located on the north-central platform is a gas reservoir developed mostly in thick Waha sandy limestone. Along the southern platform margin, the Assumood and Sahl gas-fields are developed in the uppermost beds of the regional Gialo carbonate platform.

The objective of this chapter is to evaluate further the hydrocarbon potential of Middle Eocene plays in the study area with respect to the source rock, trap types and reservoir rock potential. The causes of Gialo reservoir dissimilarities across the selected fields in the Sirt Basin are discussed to highlight the importance of integrating wireline log correlations with detailed analysis of the depositional facies and their diagenetic history, for improved exploration potential.
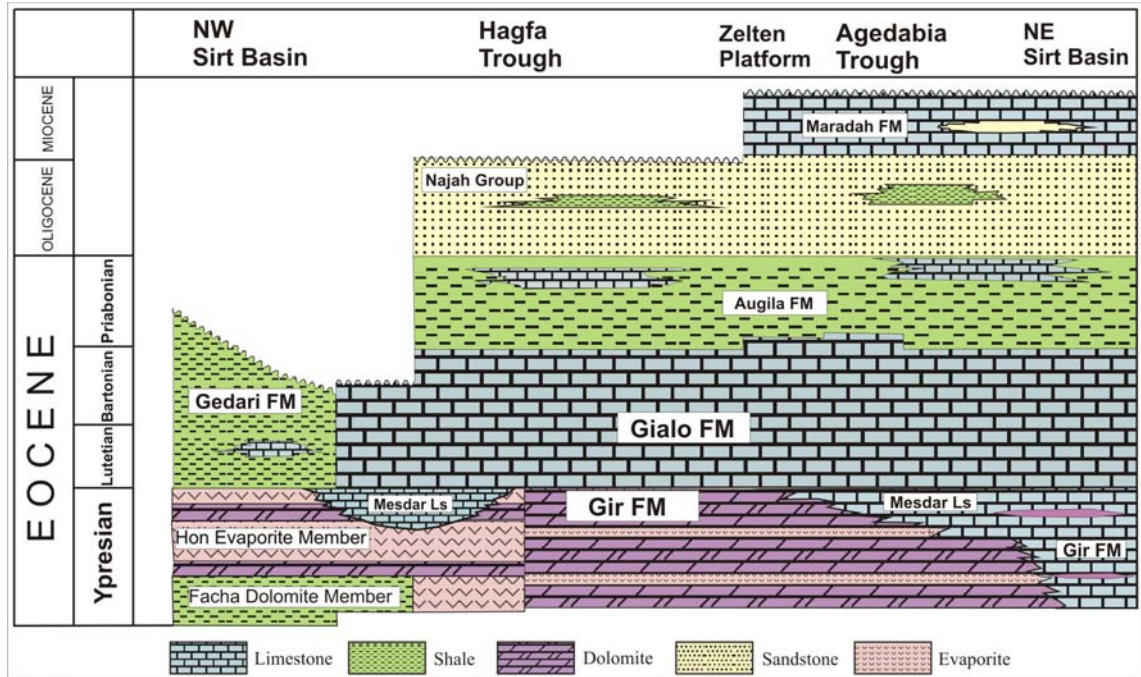
Figure 6.1. Generalized stratigraphic lithological correlation chart of the Tertiary (Eocene) succession of the Sirt Basin (modified from Barr and Weegar, 1972).
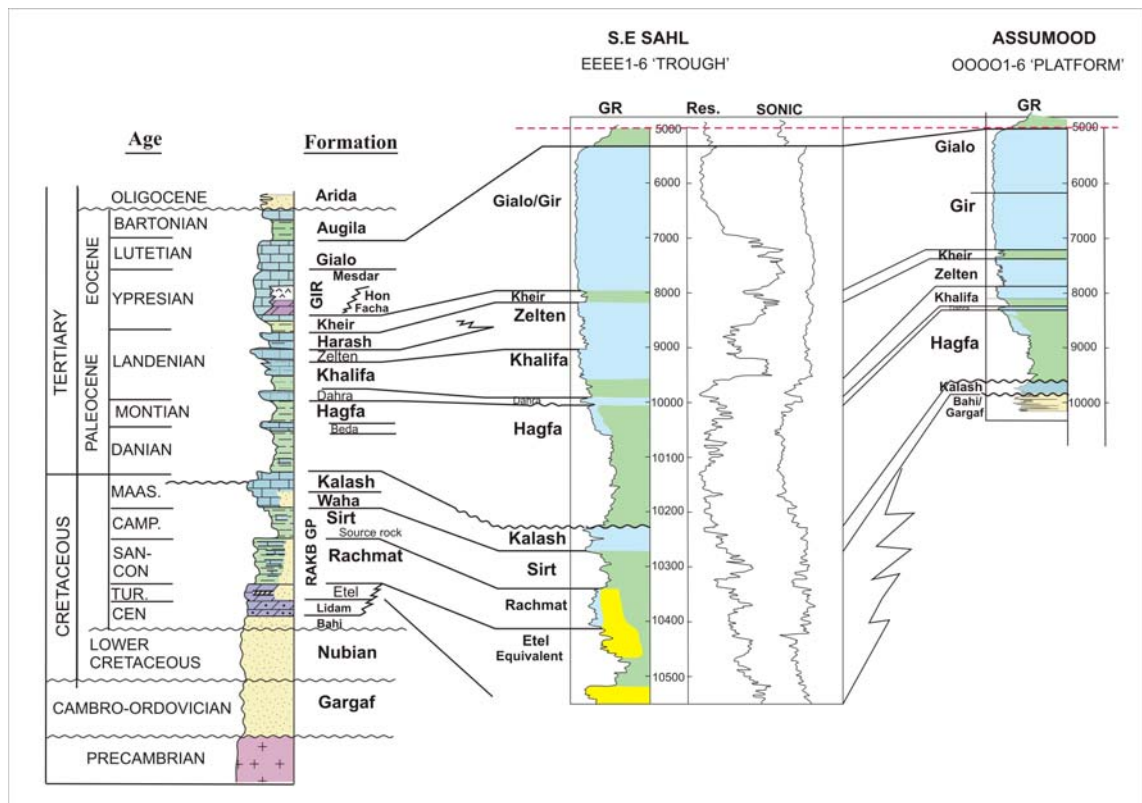
Figure 6.2. Stratigraphy of the study area (Sahl and Assumood fields).

6.2. Seismic of Gialo Formation

The top Gialo horizon has a strong response on the seismic sections across the whole area due to the good acoustic impedance contrast at the contact between the overlying Augila Formation (shale) and the Gialo Formation (carbonate) (Figure 6.3). The depth of the Middle Eocene Gialo Formation ranges from 4736 ft sub-sea in the H4-6 well to 5009 ft sub-sea in the OOOO1-6 well in the Assumood Field area and 4969 ft sub-sea in the O3-6 well in the Sahl Field. Its thickness ranges from 1130 ft in well OOOO1-6 in the Assumood Field to 1680 ft in well H7-6 in the Sahl Field. The most distinctive feature on this horizon is the channel, which was interpreted on some lines (Figures 6.3 and 6.4). The channel has a north-south direction and might separate gas contained within the Gialo reservoir in the Assumood gas-field area from possible gas accumulations in the same formation on the other side of the channel. This can provide encouragement for further study of the northern Assumood area for structural closures (Figure 6.5).

The two-way time (TWT) values of the top Gialo horizon were obtained from the Sirt Oil Company, and then posted on the seismic base map. The TWT values range from 1133 ms to 1250 ms, with the lowest values being located on the Assumood Field in the south and the highest values being located in the Sahl Field and Wadayat Trough, south Sahl Field. The TWT values were hand-contoured with a contour interval of 20 ms. The complete map (Figure 6.5) shows topographic lows located along the Wadayat Trough and also shows the high structure of the Assumood Field. Both faults strike NW-SE which is the regional trend in the Sirt Basin. The contour density increases towards the north of the area, indicating steeper dips representing a carbonate bank in the middle Eocene.
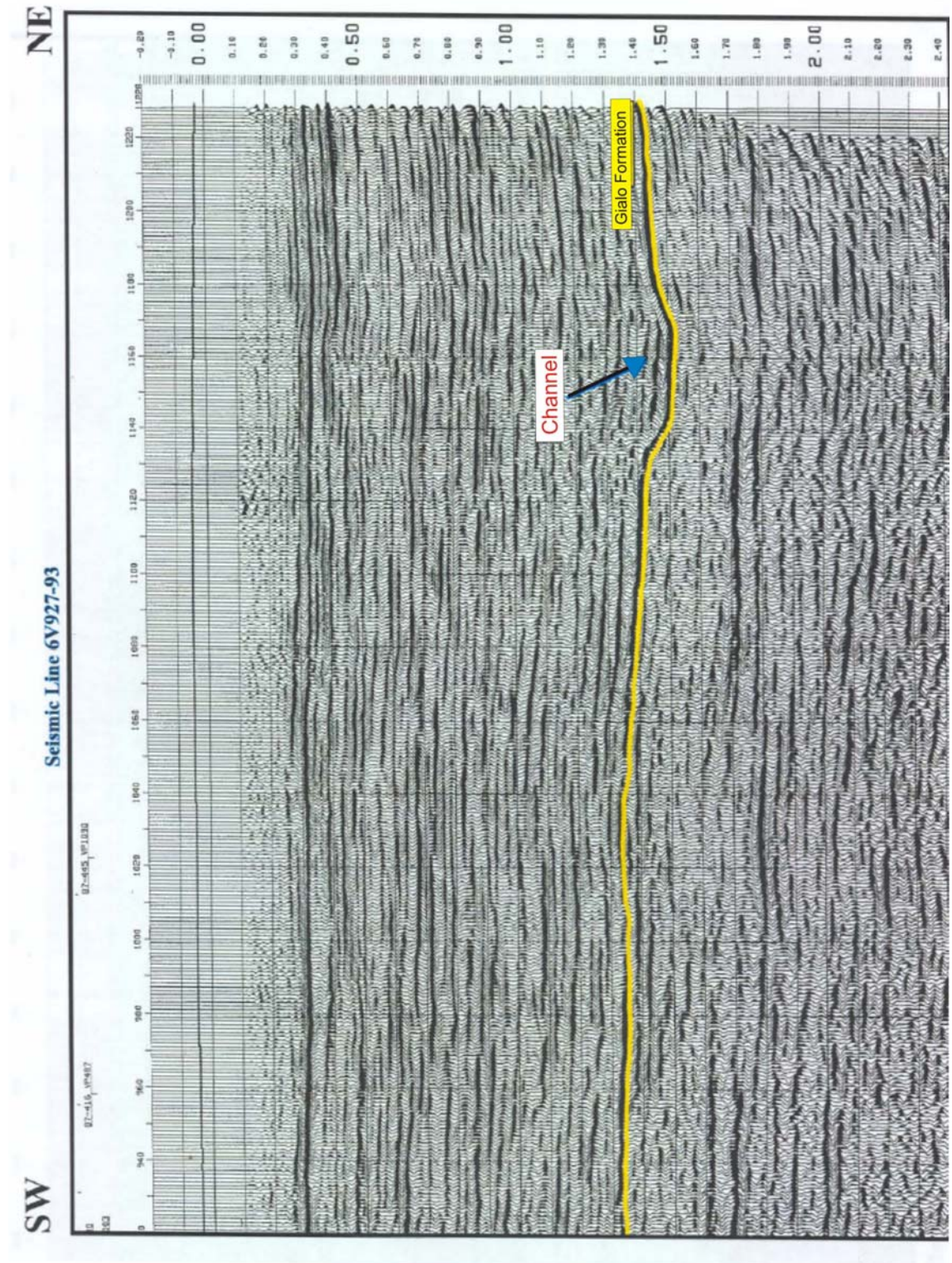
Figure 6.3. The Middle Eocene Gialo Formation channel on line 6V927-93.
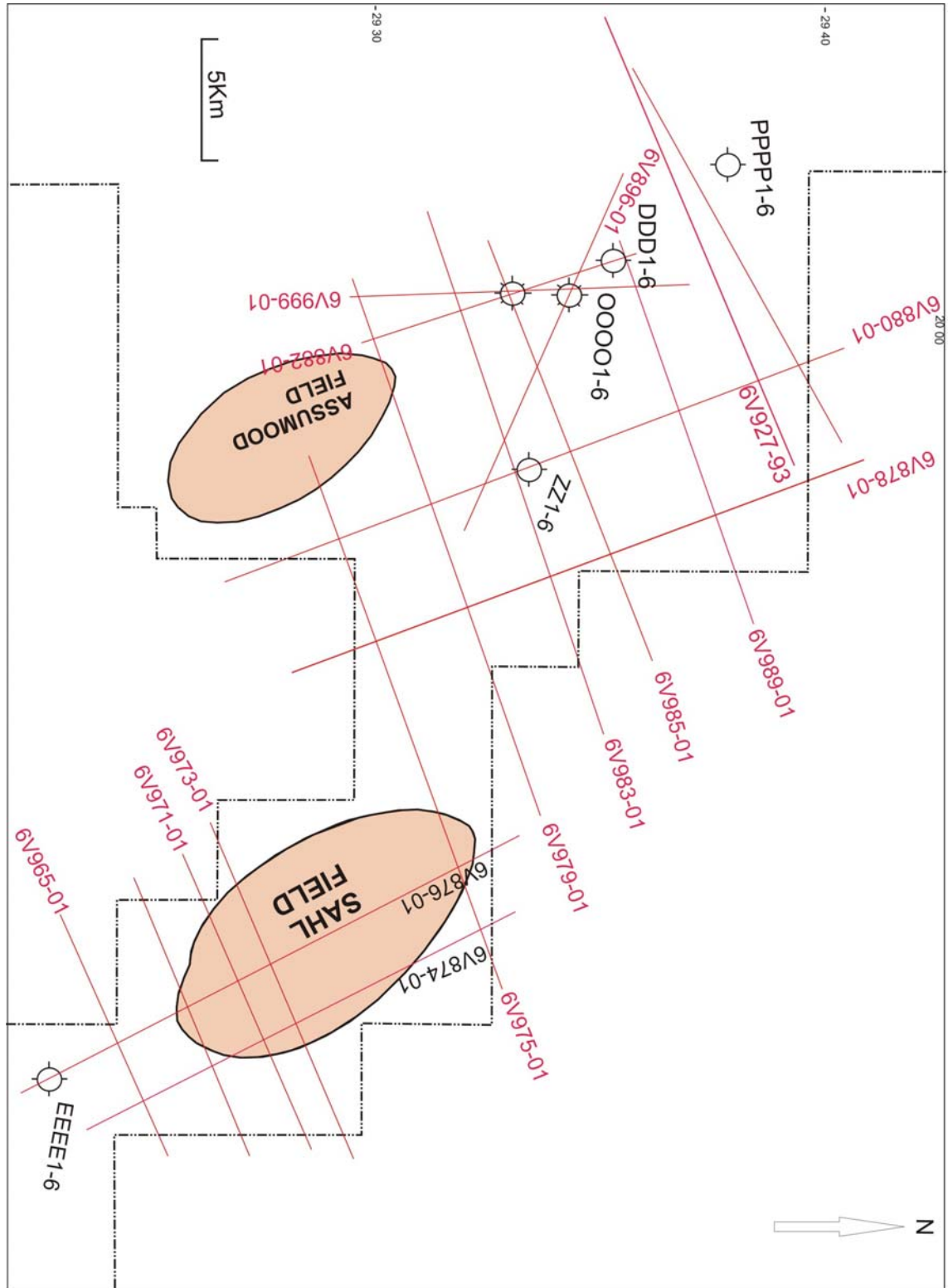
Figure 6.4. Seismic base map
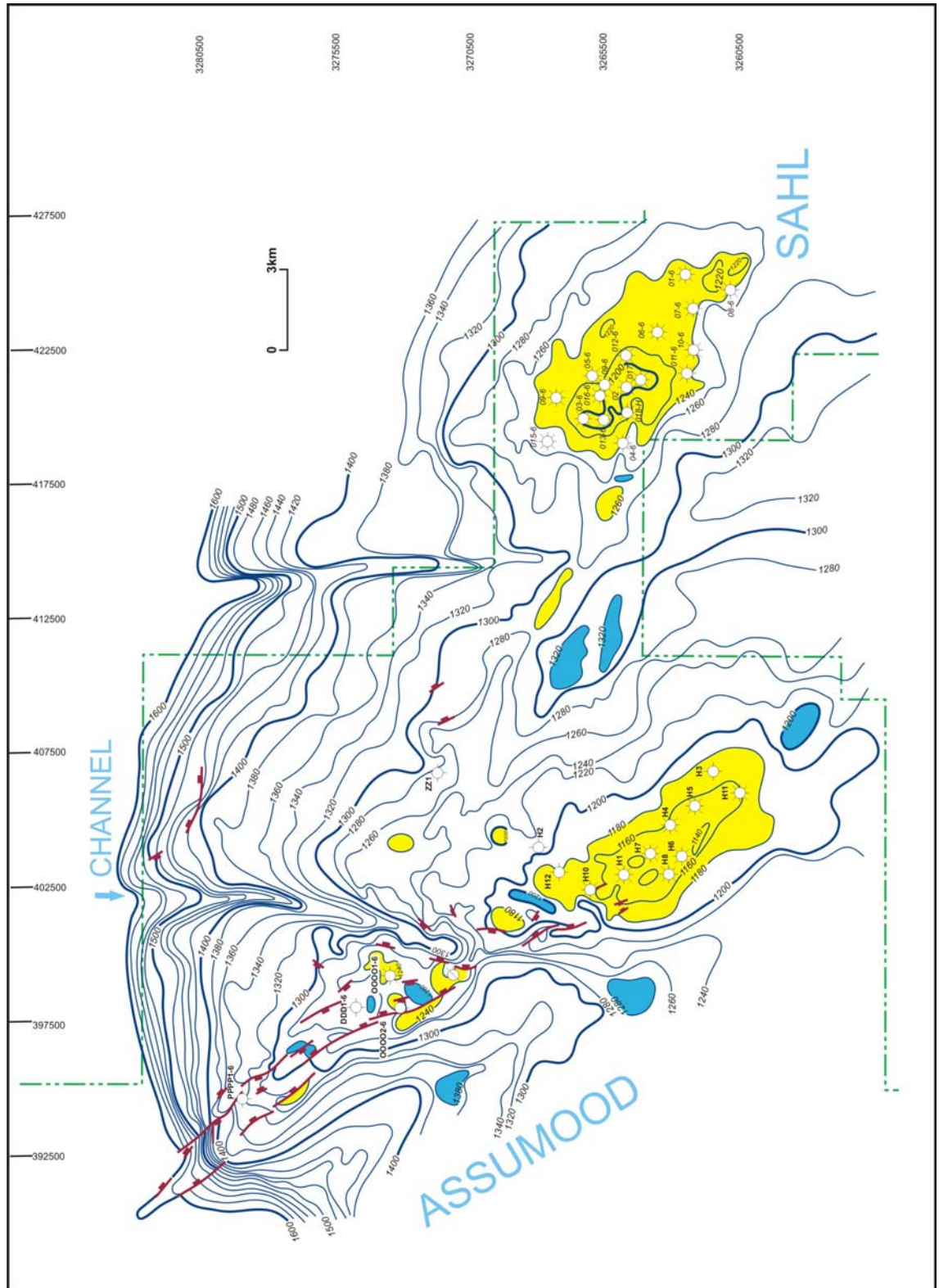
Figure 6.5. Middle Eocene Gialo Formation time-structure map.

6.3. Depth Structure on Gialo Formation

Structural closures at the top Gialo level were mapped across the Assumood and Sahl field areas (Figures 6.6 and 6.7). The map indicates that there are two areas with unproved exploration potential within the original gas/water contact at –5227 ft. The larger area is a closure above the –5150 ft structural contour. The smaller area is above the -5000 ft structural contour. A small area of possible structural closure was mapped along the northern flank of the Assumood field. The previously proposed test of the OOOO-6 structure is located north of this closure. The OOOO-6 structure is separated from the Assumood field by an erosion channel cut into the Gialo surface (Figure 6.7). By looking at the map in Figure 6.6, it can be seen that the dry hole DDD1-6 missed the top of the structure in the Gialo Formation. The crest of the structure is represented by a closure (marked in yellow) and located south-southwest of the DDD1-6.

6.4. Source and migration of hydrocarbons

Recent petroleum geochemistry data confirm the dominance of the Upper Cretaceous Sirt Shale as the source of hydrocarbons in the Sirt Basin (Ghori and Mohammed, 1996; Baric *et al*., 1996). The principal Upper Cretaceous source rocks have an average of 1.9% total organic carbon (TOC; Parsons *et al*., 1980). Maturation data show that the top of the oil window (time-temperature index [TTI; Lopatin, 1971] = 15, vitrinite reflectance [R_0] = 0.7%) in the east and central Sirt Basin grabens is encountered between approximately 8858 and 11,155 ft (Ahlbrandt, 2002).

The Ajdabiya Trough (north of the study area) has probably generated more hydrocarbons than any other comparable size area in Libya (Hallett, 2002). Hallett and El Ghoul (1996) suggested that the Sirt Shale in the Wadayat Trough is gas-prone and probably sourced the gas-fields of Sahl, Assumood and perhaps Attahaddy too. Meanwhile Roohi (1996) argued that the asymmetrical shapes of the troughs in the western Sirt Basin and the regional structure of downward slopes of both platforms and troughs towards the axis of the Ajdabiya Trough suggest that hydrocarbon migration trends had to be mainly WSW. Therefore, the hydrocarbons generated in the Ajdabiya Trough could have been trapped in the Zelten Platform and high areas, whereas hydrocarbons generated in the Al Hagfa Trough could have been trapped in the Az Zahrah-Al Hufrah Platform (Futyan and Jawzi, 1996 and Roohi, 1996). In conclusion,
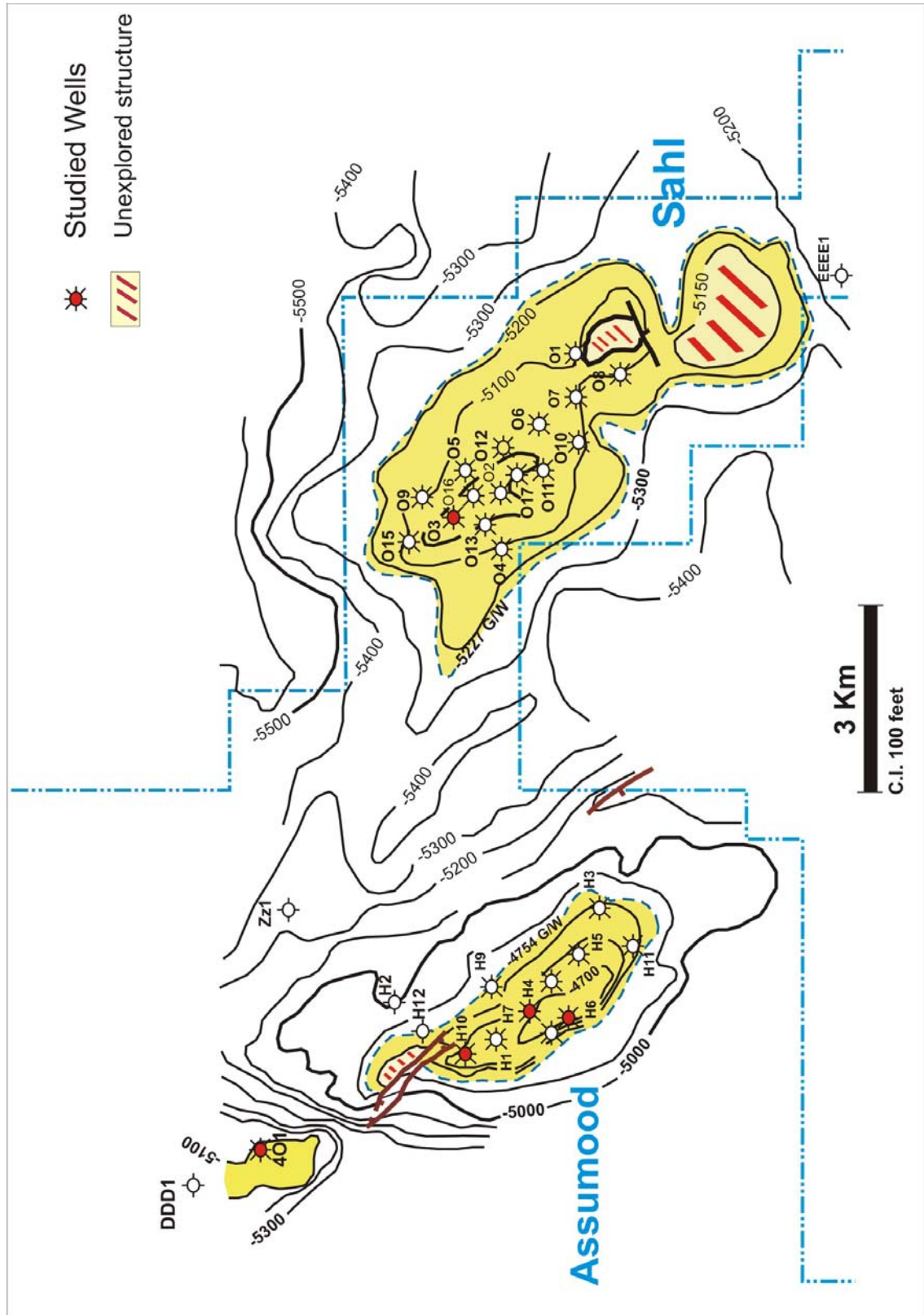
Figure 6.6. Middle Eocene Gialo Formation depth structure map.
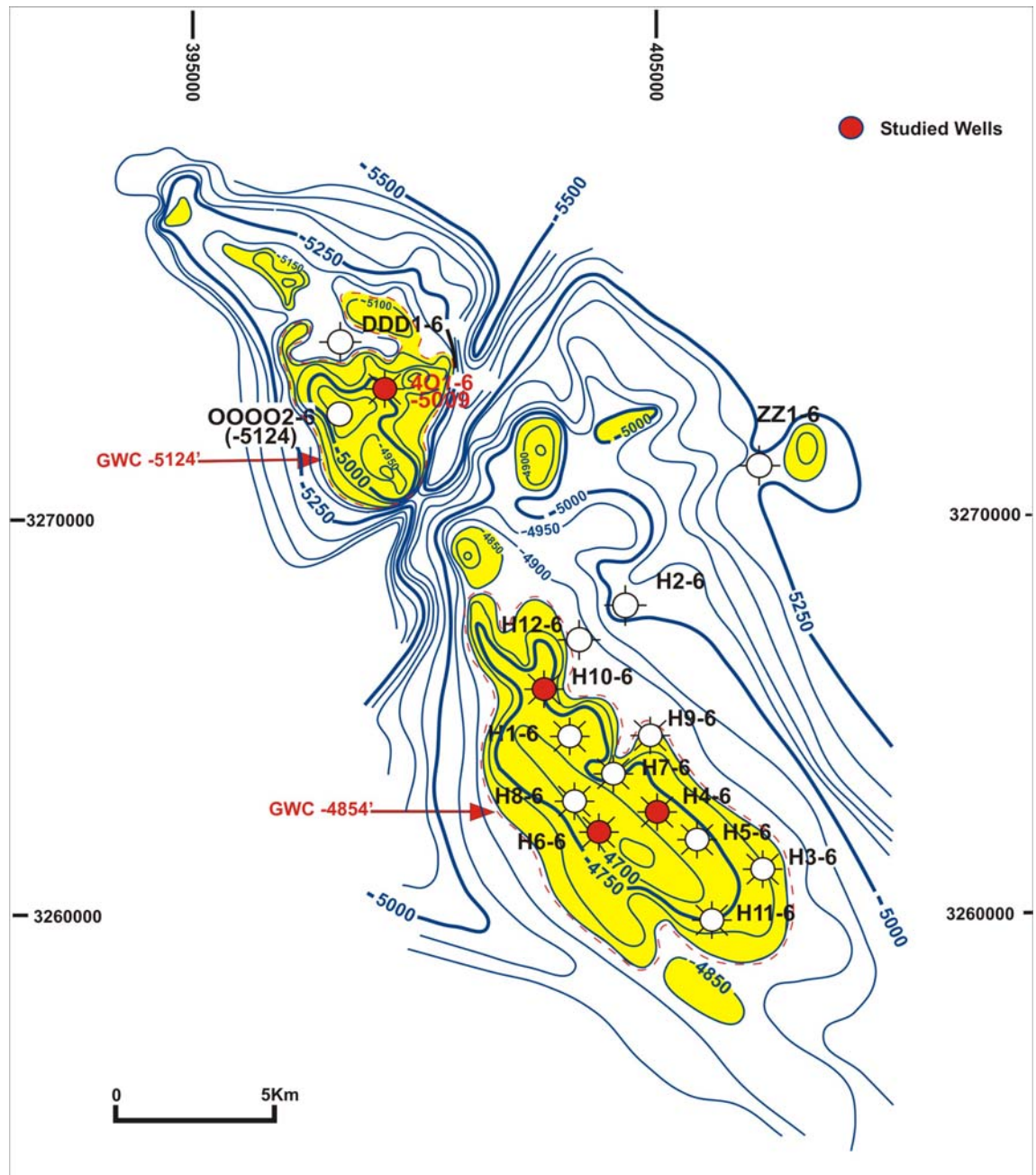
Figure 6.7. Middle Eocene Gialo Formation depth structure map.

either or both the Ajdabiya and Wadayat troughs may have contributed to the hydrocarbon accumulations in the Jahama and Zelten Platforms.

Guiraud and Bosworth (1997) pointed out that strike-slip rejuvenation was particularly important for vertical migration. Hydrocarbon expulsion and migration have occurred from the Tertiary up to the present-day (Gumati and Schamel, 1988; Ahlbrandt, 2002). The gas which is generated from the gas prone Sirt Shale source rock of the northern Ajdabiya Trough possibly migrated onto the Assumood Ridge from the

northeast through late Cretaceous, Palaeocene and early Eocene carbonates before being trapped beneath the Augila Shale (Upper Eocene) which is the principal regional seal in the area. The Sahl and Assumood gas pools were put on production in 1991 and 1993 respectively. Most of the discoveries are restricted to the platforms, whereas the troughs remain largely undrilled. Hallett and El Ghoul (1996) suggested that more exploration activity should be undertaken in the troughs. Only 100 wells have been drilled in the troughs and this is less than 10% of the total.

6.5. Hydrocarbon potential and reservoir quality

Eocene rocks are of economic importance and form reservoirs in lower and middle Eocene carbonates, which contribute about 15% to the total reserves of the Sirt Basin (Wenneker *et al*., 1996). Porosity and permeability investigations of numerous samples suggest that the nummulitic limestone and some intervals of the *Discocyclina-Nummulitic* and *Operculina-Discocyclina* Bioclastic facies have good reservoir potential but that the lime-mud facies is less promising due to generally low permeabilities and porosity. The common pore-types in the Gialo Formation are intergranular, moldic, intragranular, vuggy and scattered fractures. Porosity ranges from poor to very good (<1% to ~37%) and permeability varies from low to high (<1mD to 100mD). These variations in porosity and permeability are strongly related to facies changes, which were influenced by depositional environment and diagenetic processes. Moderate to good porosity and permeability occur in wackestone/packstones and packstones (Figure 5.28), deposited in moderate to high-energy, shallow-water settings. In general the porosity in the studied area is either primary, formed during deposition of the sediment or secondary, enhanced by dissolution and fracturing of sediments. Primary porosity is rare to common and patchily distributed, and now partially to completely occluded by calcite cement. Secondary porosity formed by selective dissolution has been recorded in many areas.

The Gialo Formation is an important productive reservoir in the Assumood, Sahl and other surrounding fields. The porosity log and the average absolute porosities from core analysis indicate that higher porosities developed at structurally-higher levels. The reservoir quality is good in the top stratigraphic layers but progressively decreases towards the base of the reservoir (Figure 6.7). The restriction of good secondary porosity to the upper parts of the formation may indicate that tectonism caused

emergence of the formation into subaerial conditions. The Gialo carbonate reservoir in the Assumood and Sahl fields is about 1130 ft thick (well OOOO1-6) and overlain by Augila shale, with a gas column of 80-100' in thickness. The low formation resistivities in the gas-bearing zones are attributed to the high formation water salinity (Figure 6.8). Assumood and Sahl fields are surrounded by gas-fields which suggest that any prospective location found in this area is more likely to contain gas.

6.6. Seals

The top seal for the Gialo reservoir on the Assumood Ridge and Jahama Platform is provided by the thick calcareous shale of the upper Eocene Augila Formation (Figure 6.1). This unit provides a thick regional seal which extends over most of the platform (Wennekers *et al.*, 1996).

6.7. Gialo reservoir facies in the Sirt Basin

Reservoir facies in the south Jebel and Nasser fields (Figures 6.9 and 6.10, wells BBBB1, BBBB2 and C228-6) are hosted in three depositional facies: a) dasycladacean-molluscan lime wackestone/packstone (upper-most depositional facies "near the formation top") (Figure 6.11), b) bioclastic packstone, and c) echinoidal-benthic foraminifera wackestone (Sirte Oil Company internal report). Porosity values in the dasycladacean reservoir (main reservoir) are locally good, generated by meteoric dissolution of the patchily distributed dasycladacean fragments.

Permeability, however, is low due to the heterogeneous pattern of pore distribution. The other two, relatively thin, reservoir facies were not recorded in the Nasser Field. Other depositional facies, like the widely-spread nummulitic lime packstone, are present in this area but contain poor reservoir characteristics due to complete occlusion of the intragranular porosity by calcite cement.

Farther north, in Assumood's OOOO1-6 wildcat well, a thin *Discocyclina*-nummulitic wackestone occurs at the base, followed by a nummulitic wackestone/packstone in the middle part of the succession and a thin nummulitic packstone/rudstone at the top (Figure 6.11). In contrast to Jebel and Nasser fields, the nummulitic packstone in OOOO1-6 accommodates very good reservoir characteristics.
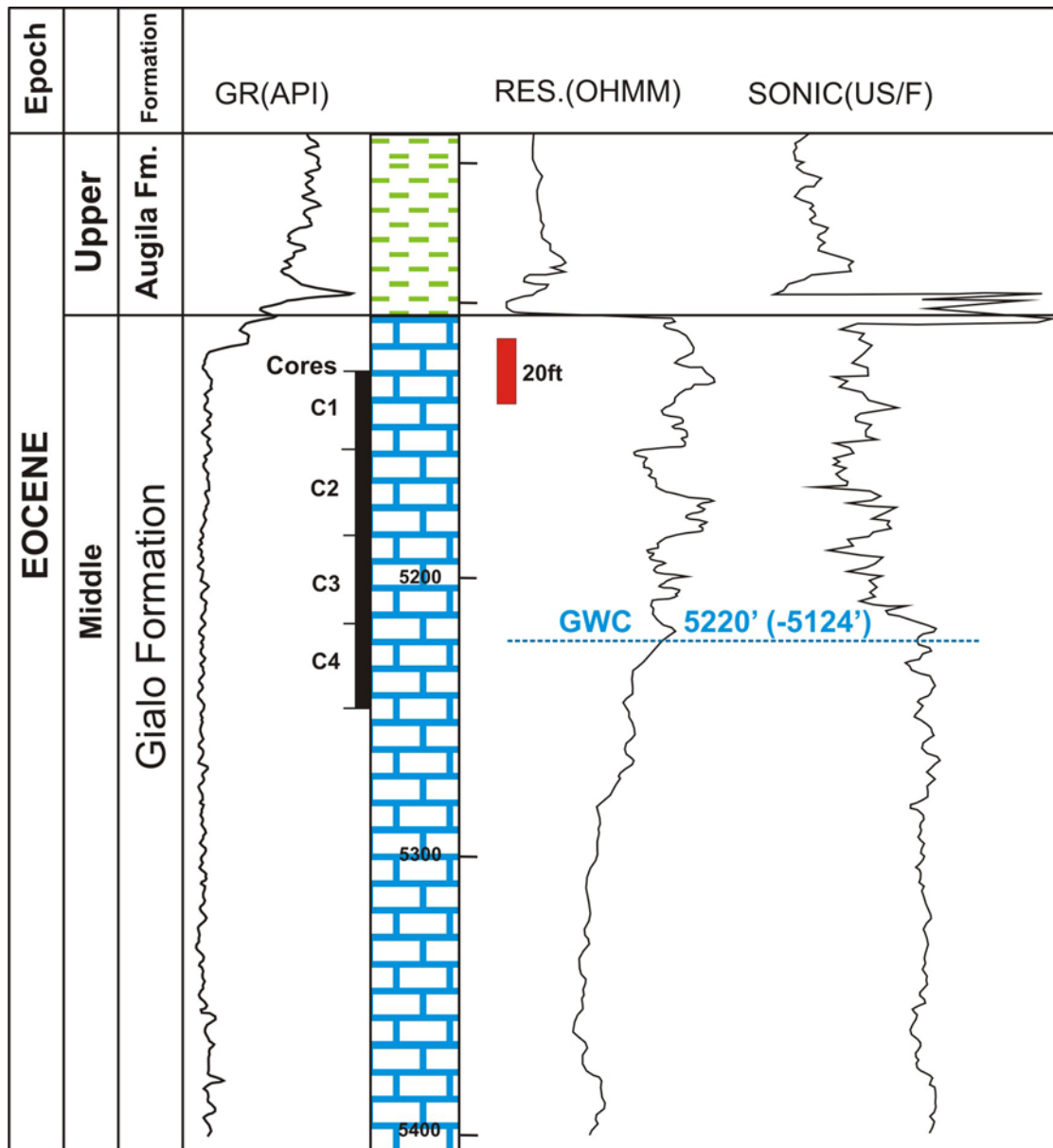
Figure 6.8. Log characteristics and general lithology, well OOOO1-6. The well was completed as a vertical gas producer from the Gialo Formation and had an initial production of 14 MCFG/D.

Porosity-destructive diagenesis was minimal, and characterized by rare cementation, rare chemical compaction and stylolitization. Porosity is good, well connected, homogeneously distributed, and permeability is high. Pore-types are dominated by open intragranular within nummulite tests and matrix porosity.
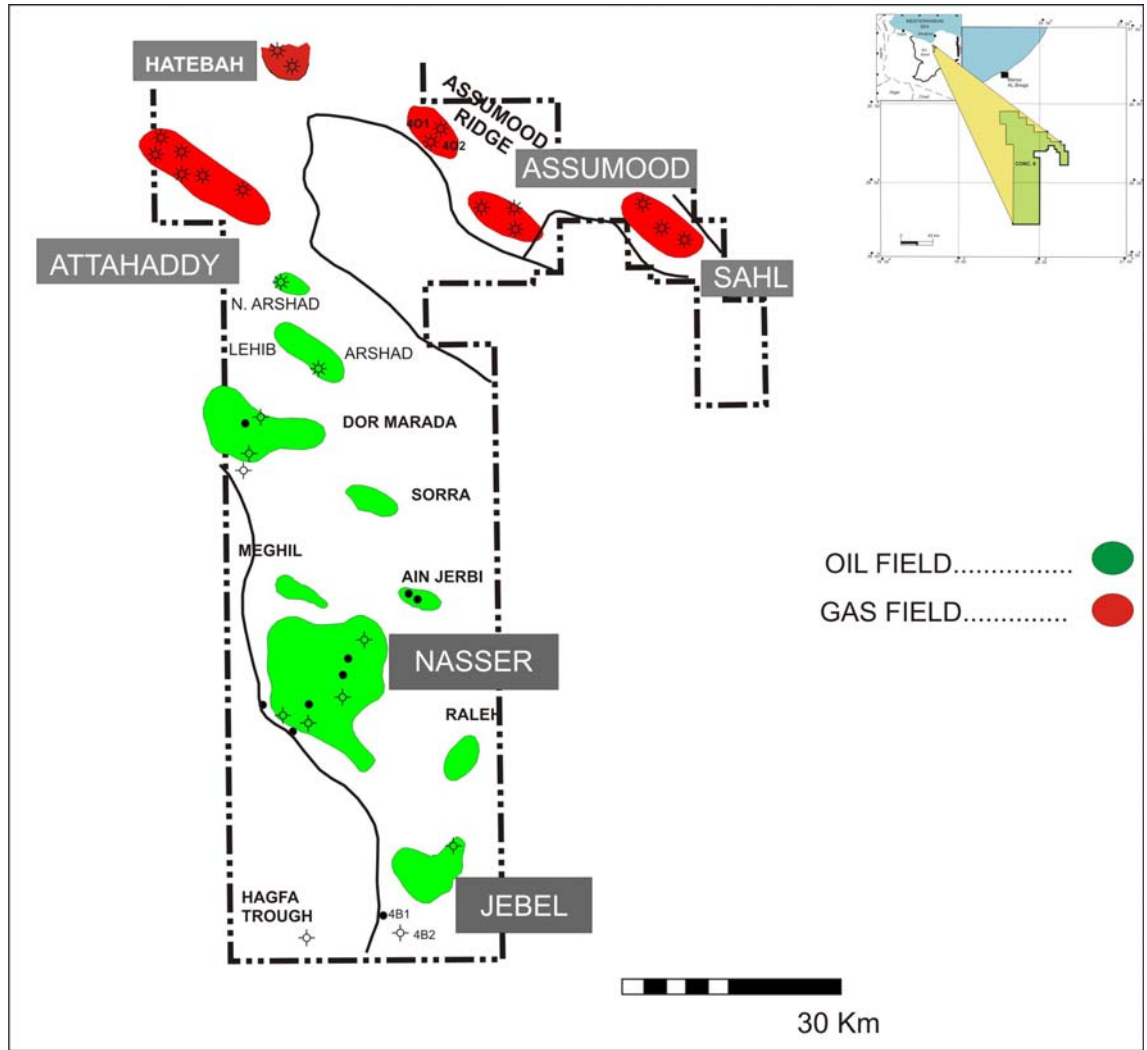
Figure 6.9. Location map of studied fields (Assumood and Sahl fields) and other gas and oil fields in Concession 6 – Sirt Basin.
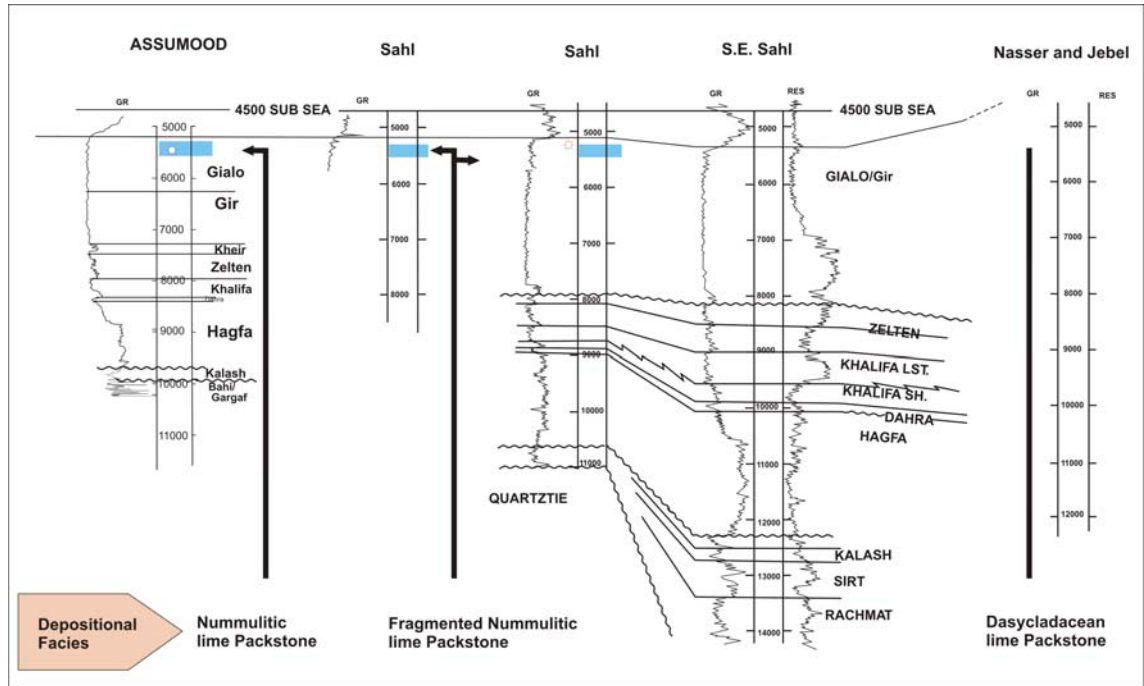
Figure 6.10. Correlation of the Gialo reservoir facies in selected fields in Concession 6. Sirt Basin.

In the Sahl Field (well O3-6), the reservoir facies are hosted in *Operculina-Discocyclina* bioclastic wackestone/packstone and fragmented nummulitic packstone. This depositional facies was not well developed in the other studied fields (Figure 6.11). Most of the lime mud was winnowed out due to high-energy levels in the depositional environment. Primary inter- and intragranular porosity is good, well connected, homogeneously distributed and permeability is high. In summary, this study reveals that the Gialo reservoir facies are dissimilar across the basin due to dissimilarities between their host depositional facies and their diagenetic history.
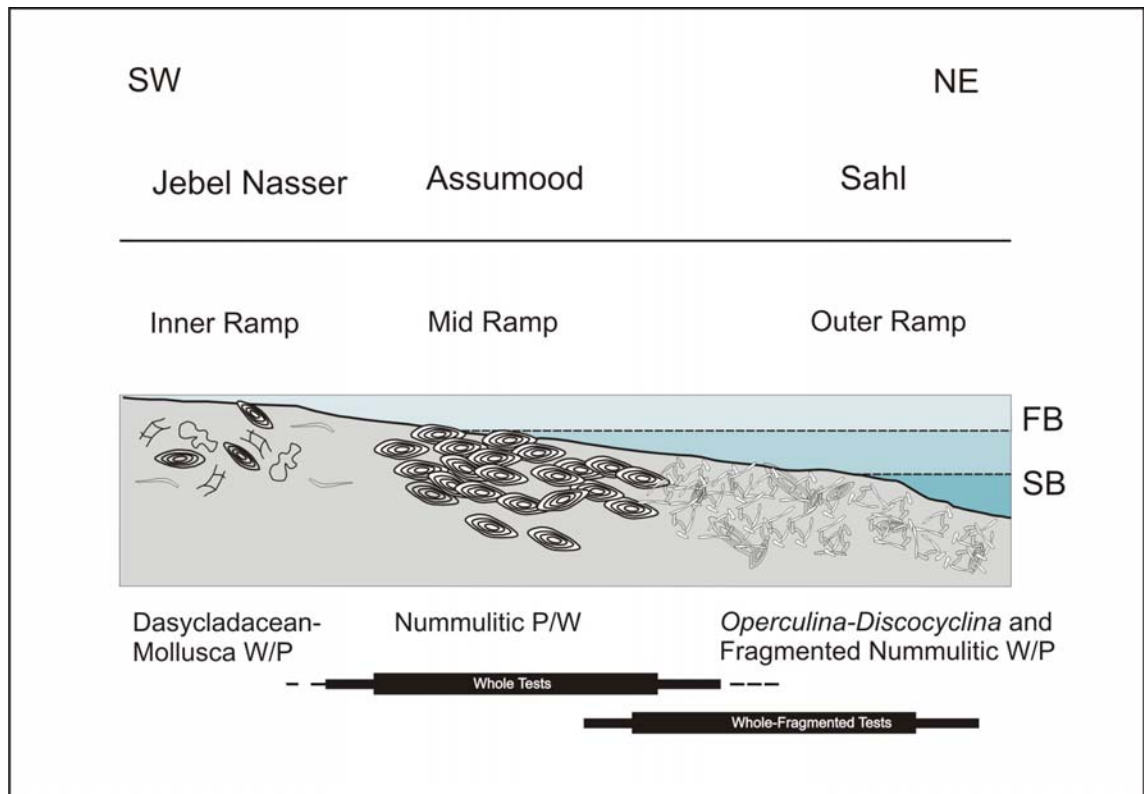
Figure 6.11. Schematic diagram representing the upper-most depositional facies (near formation top) in the studied wells and Jebel and Nasser fields (Sirte Oil Company internal report). In Jebel and Nasser fields, a dasycladacean-molluscan wackestone/packstone was deposited. In Assumood (well OOOO1-6), whole tests of nummulites dominate the nummulitic packstone. In Sahl (well O3-6), a fragmented nummulitic packstone was deposited. Such facies belts are typical of deposition in inner-, middle-, and outer- ramp environments.

6.8. Comparison with nummulite carbonates from Tunisia (El Garia Formation):

The El Garia Formation developed during the Lower Eocene and has been the subject of a series of studies (e.g. Loucks *et al*., 1998; Racey, 2001; Jorry *et al*., 2003; Beavington-Penny *et al*., 2005) and also forms a major carbonate reservoir interval similar to the Gialo Formation. In the Hasdrubal field (Figure 6.12) two distinct depositional environments are proposed for the El Garia. Nummulites accumulated in shallow-water depths, forming nummulite shoals. The reworking of these shallow sediments leads to nummulite-rich sediment transportation downdip off the platform, forming low-relief nummulite-banks (Racey et al., 2001). Jorry et al., 2003 studied the

El Garia in central Tunisia (Kesra Plateau) (Figure 6.12) and concluded that nummulites are concentrated on palaeohighs and nummulithoclast-rich facies accumulated within intra-shelf depression and/or within the basin. In Kef el Guitoune (Central Tunisia) nummulite bank facies in the El Garia Formation consists of coarse-grained sediments, poor in muddy matrix, accumulated near SWB. The fore-bank deposits are characterized by an abundance of nummulite debris. Successive storm events may have contributed to successive stacking of the nummulite bank deposits (Hasler, 2004). These differences in depositional settings are probably the result of available palaeogeography and palaeoenvironments in the basin. *Discocyclina* facies were concentrated landward of the nummulitic facies and are interpreted as shoal deposits (Loucks *et al*., 1998). In comparison, in the Gialo Formation the *Discocyclina* facies lies seawards of the nummulite facies and are inferred to have formed in a fore-bank setting. The back-bank lagoonal environment of the molluscan facies in the Gialo Formation is absent from the El Garia Formation.

Racey (2001) stated that primary porosity in the El Garia Formation in the Ashtart Field is occluded by fringing and blocky calcite cements, whilst intraskeletal porosity within nummulite tests is often preserved but is ineffective. Leaching and much later dissolution enhanced porosity and postdated fractures and stylolites. Porosity is generally high (range 1 to 35%) with an average permeability of 1,700 mD (range 0.01 to 3,400 mD). Moody et al., 2001 stated that typical meteoric cements are absent in the El Garia Formation and much of the cement appears to have precipitated after compaction during a burial environment, except for some early syntaxial cement around echinoderm fragments. Nummulite tests are recrystallized to microcrystalline calcite with abundant associated microporosity. Sediments in the El Garia Formation underwent extensive compaction with burial. Compaction destroyed large amounts of effective interparticle porosity. Locally, compactionally fractured nummulites connected some intraparticle pores to the remaining interparticle pore system. Where echinoderm fragments are common, syntaxial overgrowth cement is a major feature that occludes porosity. In some areas, dolomitization produced pore networks composed of intercrystalline and mouldic porosity that are quite permeable. Most lime packstone and grainstone have moderate to high porosity (15-25%) with an average permeability of 5mD, but much of this porosity is ineffective and does not add to permeability.
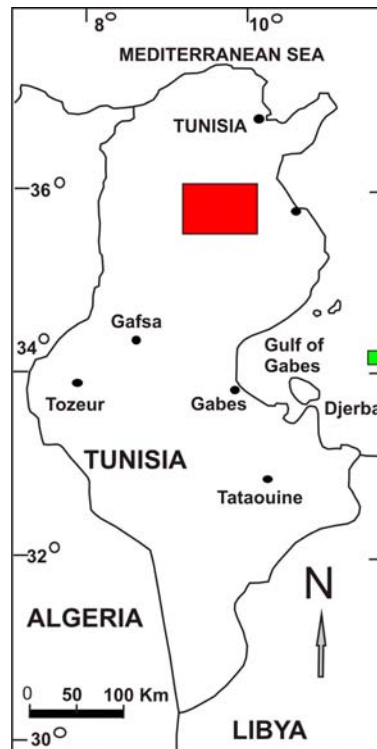
Figure 6.12. Location map of the Kesra Plateau, Central Tunisia (red square) and Hasdrubal Field (green square).

6.9. Summary

The complex tectonic history of the Sirt Basin resulted in multiple reservoirs and conditions that favoured hydrocarbon generation, migration and accumulation. The gas was generated from the gas-prone Sirt Shale source rock of the northern Ajdabiya Trough and this migrated onto the Assumood Ridge from the northeast through late Cretaceous, Palaeocene and early Eocene carbonates before being trapped beneath the Augila Shale (Upper Eocene), which is the principal regional seal in the area. The time-structure map shows that the contour density increases towards the north of the area, indicating steeper dips representing a carbonate bank in the Middle Eocene. The OOOO-6 structure (north part of the Assumood Field) is separated from the Assumood field by a channel structure cut into the Gialo surface.

Dissimilarities in the type and quality of the Gialo reservoir facies across the Sirt Basin are attributed to vertical and lateral variations in depositional facies and their diagenetic history. Vertical and lateral variations of the Gialo depositional facies were governed by basin-floor architecture and environmental variables. Two broad facies groups are distinguished: (1) Platform facies: comprising shallow-marine

dasycladacean, bryozoan, and nummulite-rich packstone and wackestone, which were deposited in inner to outer ramp facies belts. (2) Trough facies: comprising relatively deeper-marine, fine skeletal, rarely nummulitic, lime mudstone. Each platform facies belt hosted distinctive reservoir facies: (a) inner-ramp dasycladacean-rich facies were affected by mineral-controlled meteoric dissolution, which brought about good, but patchy, moldic porosity in Jebel and S. Nasser Fields. (b) Mid-ramp nummulitic packstone facies are rarely cemented and contain good, well-connected, matrix and intragranular porosity in whole tests of nummulites in the Assumood Field. (c) Outer-ramp fragmented nummulitic lime packstone facies, with rarely cemented inter-and intragranular porosity, are good reservoirs in Sahl Field.

Reservoir quality in the Gialo Formation is a function of grain types, pore types, grain size, sorting, cementation and compaction, and it is difficult to predict areas of high reservoir quality; exploration should be oriented to positioning a well into the main trend of the mid-ramp, nummulite accumulation. Different nummulite facies can be reservoirs depending on their diagenetic history. A diagenetic decrease in porosity must be distinguished from a lack of porosity because of an unfavourable depositional environment, so that exploration options can be adequately assessed. This integrated study has shown that the presence of good reservoir rocks, hydrocarbon traps and the close proximity of potential source rocks, and this is significantly encouraging for further hydrocarbon exploration in the area. The study also helps with our understanding of the reservoir heterogeneity and its potential, on the basis of which current wells have been completed appropriately and successfully; the information should also aid in completing future wells productively.

CHAPTER 7: SEQUENCE STRATIGRAPHY OF THE GIALO FORMATION

7.1. Introduction

The sequence stratigraphic evaluation here of the Gialo Formation is based on integrating the facies and wireline log (GR) data from the five wells (OOOO1, O3, H4, H6, and H10-6) which have been described in detail in chapters four and five. This chapter presents a short introduction to sequence stratigraphy, including definitions of some terms which are used in this study, and then a consideration of the sequence stratigraphy of the Gialo Formation. However, since cores are only available from the upper part of the Gialo Formation, it is only this part of the section that can be considered from a sequence stratigraphic point of view. Unfortunately the wireline logs of the Gialo do not reveal any trends or patterns which could be interpreted confidently in terms of coarsening or fining upwards, nor any surfaces or discontinuity zones which could be sequence/cycle boundaries. In some cases high-frequency cyclicity can be inferred from well-logs which can then contribute towards a sequence stratigraphic model. A lack of correspondence of facies and cycles to well logs is quite typical for carbonates and contrasts with logs from clastic successions where they can be very useful for cycle-sequence analysis. In addition, little information can be obtained from the seismic data since the Gialo strata are flat-lying and lap-out geometries (offlap, onlap etc) are not developed (Chapter 6). The main objective of this chapter then is to assess the vertical variations in facies in the sedimentary succession, as deduced from studies of the core material, and then determine whether this information can be considered in a sequence stratigraphic framework.

7.2. Introduction to sequence stratigraphy

Sequence stratigraphy is defined as the analysis of the sedimentary response to changes in base level, and the depositional trends that emerge from the interplay of accommodation (space available for sediments to fill) and sedimentation (Catuneanu, 2006). Much of the current research in carbonate depositional systems has been oriented towards the application of sequence stratigraphic techniques to the carbonate rock

record. The study of sequence stratigraphy began with Sloss (1963). Brown and Fisher (1977) Mitchum (1977) and Vail *et al*. (1977b) used seismic data to identify genetically related packages bounded by unconformities, i.e. depositional sequences. The application of sequence stratigraphy to carbonate depositional systems was a topic of debate in the late 1980s, particularly with respect to how a sequence framework developed essentially for clastic systems could be adapted to reflect the realities of carbonate environments (Sarg, 1988; Schlager, 1989). Following on from these early contributions, significant progress was made in the early 1990s when the fundamental principles of carbonate sequence stratigraphy, as well as the differences between the clastic and carbonate stratigraphic models, were elucidated (James and Kendall, 1992; Jones and Desrochers, 1992; Schlager, 1992; Hunt and Tucker, 1993; Loucks and Sarg, 1993; Tucker *et al*., 1993; Schlager 2005). More recently there have been attempts to standardize the sequence stratigraphic approach through the work of Catuneanu (2006) and Catuneanu *et al*. (2009).

Depositional sequences are created by changes in accommodation space, which is controlled by the rate of subsidence, rate of eustatic sea-level change, and sedimentation rate (Handford and Loucks, 1993). Depositional sequences include shallowing-upward (regressive) and deepening-upward (transgressive) units, and distinctive surfaces, namely sequence boundaries and flooding surfaces. In a sequence stratigraphic framework, depositional sequences are predictable and can be used to help identify source, reservoir and seal lithologies (Handford and Loucks, 1993). High-resolution stratigraphy incorporates outcrop, core and wireline logs to construct a sequence stratigraphic framework (Van Wagoner *et al*., 1990).

The terminology of sequence stratigraphy is complex (see Figure 7.1). Eustasy is defined as a change of sea level in all the oceans, which may be caused by changes in ocean-basin volume or ocean water volume. A relative change in sea level means that the sea level is rising or falling with respect to the land on a local or regional scale. Sequence boundaries are often unconformities with evidence of subaerial exposure related to the maximum fall in sea level. Read (1995) described how unconformities can be identified in carbonates: 1) drastic changes in lithology (e.g. carbonates overlain by conglomerates, red-beds, green shale, and/or sandstone), 2) karstified surfaces and breccias, 3) palaeosols and calcretes, and 4) biostratigraphic gaps and hardground surfaces.
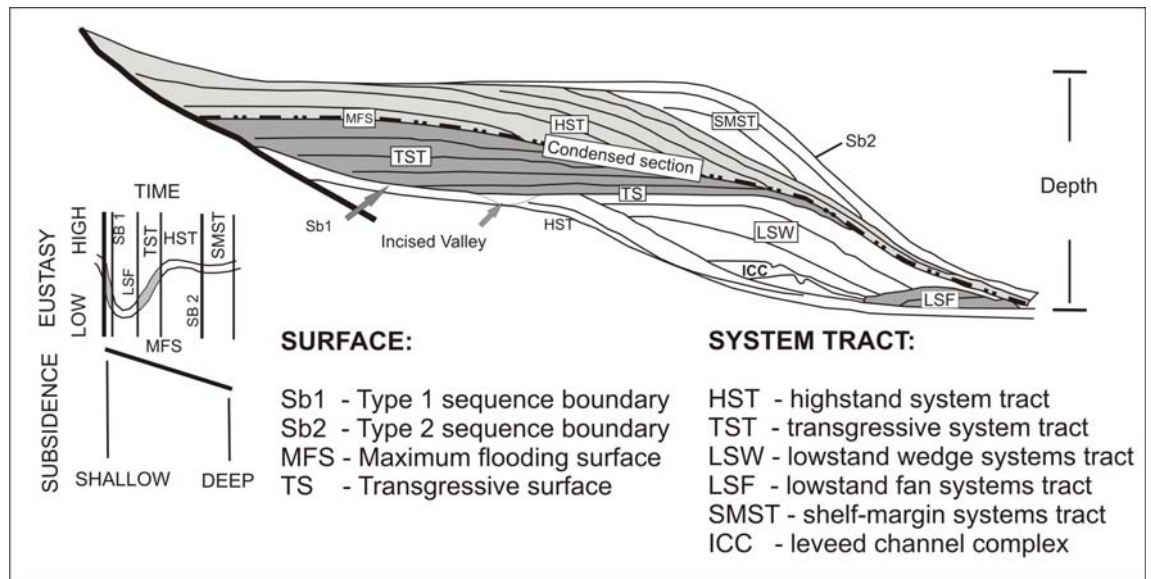
Figure 7.1. Various components of the systems tract model (after Handford and Loucks, 1993).

There are several orders of cyclicity used in sequence stratigraphy (Vail *et al*., 1977a; Goldhammer *et al*., 1990), in terms of duration of sea-level rhythms and of sediment packages. First-order cycles are approximately 200 to 300 m.y. long, and are related to changes in ocean-basin volume related to global tectonics (Pitman, 1978). This includes break-up of supercontinents and formation of ocean basins. Second-order cycles are 10 to 50 m.y. long, and represent changes in basin evolution, such as changes in the rates of subsidence or uplift. Third-order cycles, superimposed on second-order cycles, are approximately 0.5 to 5 m.y. long, and result in the formation-scale cycles, termed sequences, observed in the rock record. Third-order cycles are formed when changes in sea level are often less than 50 m and sedimentation rates are a few cm k.y^{-1}. Many believe that the origin of these cycles is eustasy, related to changes in ice volume, driven by Milankovitch rhythms (Miall, 1986; Miall and Tyler, 1991; Vail *et al*., 1991; Catuneanu, 2006). Fourth and fifth-order cycles are 10 to a few 100 k.y. long, and are referred to as parasequences, also driven by high-frequency, climatically-driven (orbital forcing) changes in sea level (Heckel, 1985; Goldhammer *et al*., 1990) or productivity/oxygenation rhythms (Fischer and Bottjer, 1991). They can also be the result of autocyclic, sedimentary processes, such as tidal-island migration, tidal-flat progradation, and bioclastic sand-bank migration. Formation by syn-sedimentary tectonic processes, mostly extensional fault movements, can also give rise to parasequences. See Bosence *et al.* (2009) and Tucker and Garland (2010) for recent

reviews of parasequence formation. Parasequences are the fundamental building blocks of a depositional sequence and are defined as 'a relatively conformable succession of genetically-related beds or bedsets (1 to 10m thick), forming shallowing-upward cycles bounded by flooding surfaces' (Van Wagoner, 1995). This definition has been modified and extended by Spence and Tucker (2007). The stacking patterns of parasequences, their lateral and vertical thickness and facies variations, enable the larger-scale sequences to be defined and their constituent systems tracts.

Systems tracts (Brown and Fisher, 1977; Mitchum, 1977; Handford and Loucks, 1993) are inferred on the basis of stratal stacking patterns, position within the sequence, and types of bounding surface. Figure 7.1 illustrates the various components of the systems tract model. The definition of systems tracts has been gradually refined from the earlier work of Exxon scientists (Posamentier and Vail, 1988; Van Wagoner *et al*., 1988, 1990), based on the contributions of Galloway (1989), Hunt and Tucker (1995) and Plint and Nummedal (2000). See Catuneanu *et al*. (2009) for a review.

The early Exxon sequence model included four systems tracts: the lowstand, transgressive, highstand and shelf-margin systems tracts. The lowstand systems tract, as defined by the Exxon school, includes a "lowstand fan" (falling sea level) and "lowstand wedge" (sea level at a lowstand; Posamentier *et al*., 1988). The lowstand fan systems tract consists of autochthonous (shelf-perched deposits, offlapping slope wedges), and allochthonous gravity-flow (slope and basin-floor fans) facies, whereas the lowstand wedge systems tract includes the aggradational fill of incised valleys, and a progradational wedge which may downlap on to the basin-floor fan (Posamentier and Vail, 1988). Hunt and Tucker (1992) redefined the lowstand fan deposits as the "forced regressive wedge systems tract", also known as the "falling stage systems tract" (Plint and Nummedal, 2000). The lowstand systems tract (LST) is deposited in the basin and on the slope during maximum lowstand of sea level. Karstification, soil development, and dolomitization may all occur on exposed areas of a carbonate platform and siliciclastics may be deposited in the basin at this time.
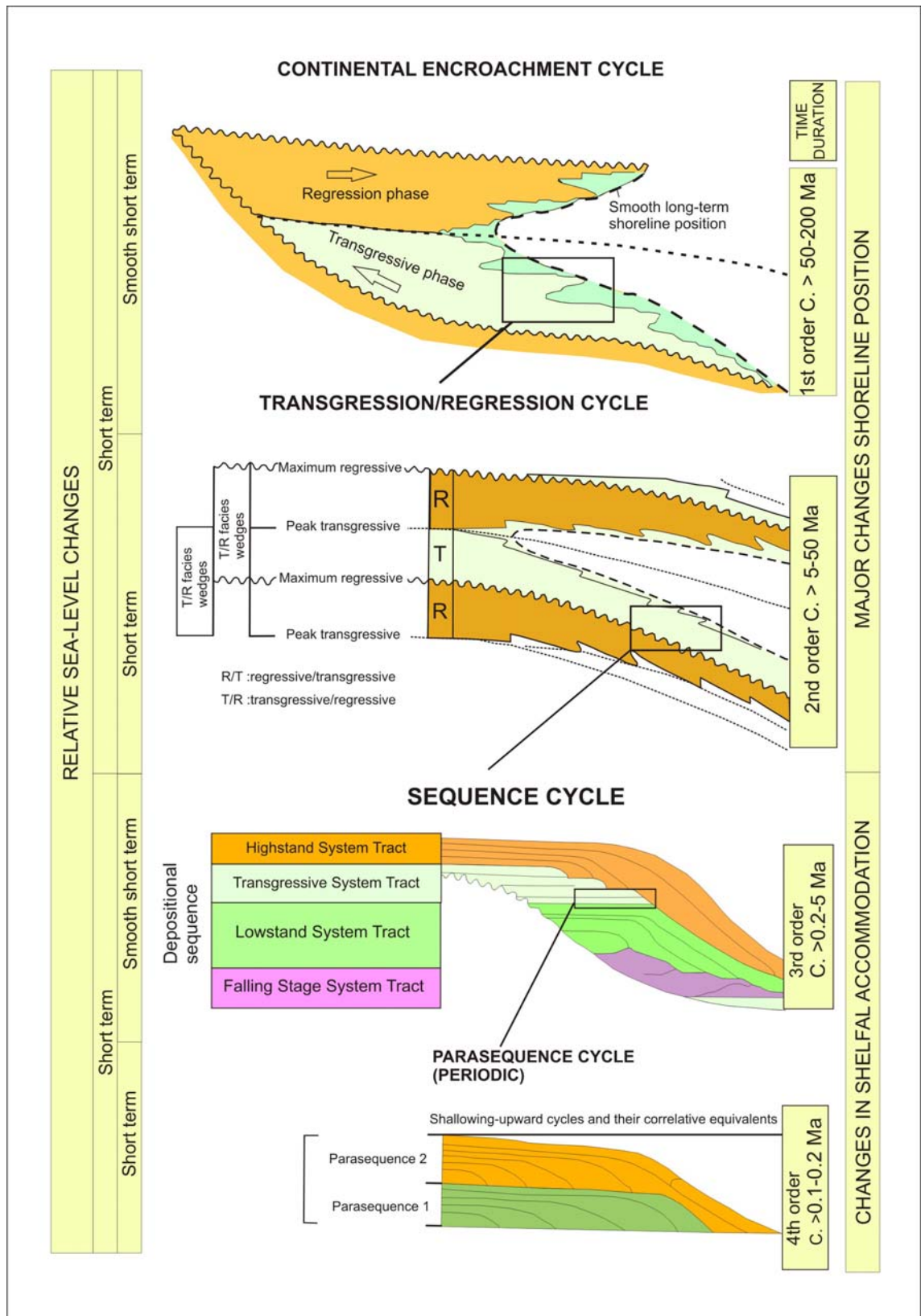
Figure 7.2. The hierarchy of stratigraphical cycles (after Coe *et al*., 2002).

The transgressive systems tract (TST) deposits will have retrogradational (accommodation space greater than sedimentation rate resulting in landward-stepping units) or progradational (accommodation space less than sedimentation rate, so basin-ward stepping units) geometries. If the succession is dominated by metre-scale cycles (parasequences) then these will be quite thick, perhaps showing a thickening-up pattern, and will often lack or have restricted tidal-flat facies. A maximum flooding surface (MFS) documents the change from the TST to the highstand systems tract (HST). The maximum flooding surface represents the maximum landward extent of deep-water deposition. The HST (sometimes referred to as the regressive systems tract, RST) is deposited during the late stage of sea-level rise, stillstand and early sea-level fall. Accommodation space decreases due to a decreasing rate of relative sea-level rise and increasing sedimentation rates. The HST has a prograding geometry that downlaps on to the MFS. Where a succession is dominated by parasequences, then these are typically thin, perhaps showing a thinning upward pattern, and are often dominated by peritidal facies with well-developed exposure surfaces.

7.3. Sequence stratigraphic analysis of the Gialo Formation

The Gialo Formation, ~1100 ft (~300 metres) thick, approximately corresponds to the Middle Eocene time-interval. Unfortunately there is no new stratigraphic information available from this study on the main part of the formation, just the data from the cores from the top ~240 ft of the formation. According to the Haq *et al.* (1987) curve, there was a major sea-level fall and subaerial exposure at the Middle/Upper Eocene boundary which corresponds to their TB3.6/TB4.1 cycle boundary (Figure 7.3). The top of the Gialo Formation occurs at this position so that exposure and sequence boundary formation is likely there too. The Upper Eocene begins with a drowning event (see Figure 7.3) and the deposition of the Augila Shale. At the base of the Gialo, also close to the base of the Middle Eocene, there is another major sea-level fall and rise on the Haq *et al.* (1987) curve. This sea-level event may well have been the one that terminated sedimentation of the Gir Formation (Lower Eocene) and heralded the start of Gialo deposition.

In terms of the upper part of Middle Eocene, there are minor sea-level changes recorded on the Haq *et al.* (1987) curve in Figure 7.3. These might well be expected to be recorded in the core of the Gialo Formation, although the biostratigraphy of the Gialo

Formation is not sufficiently accurate to be able to make correlations with the Haq *et al*. curve.
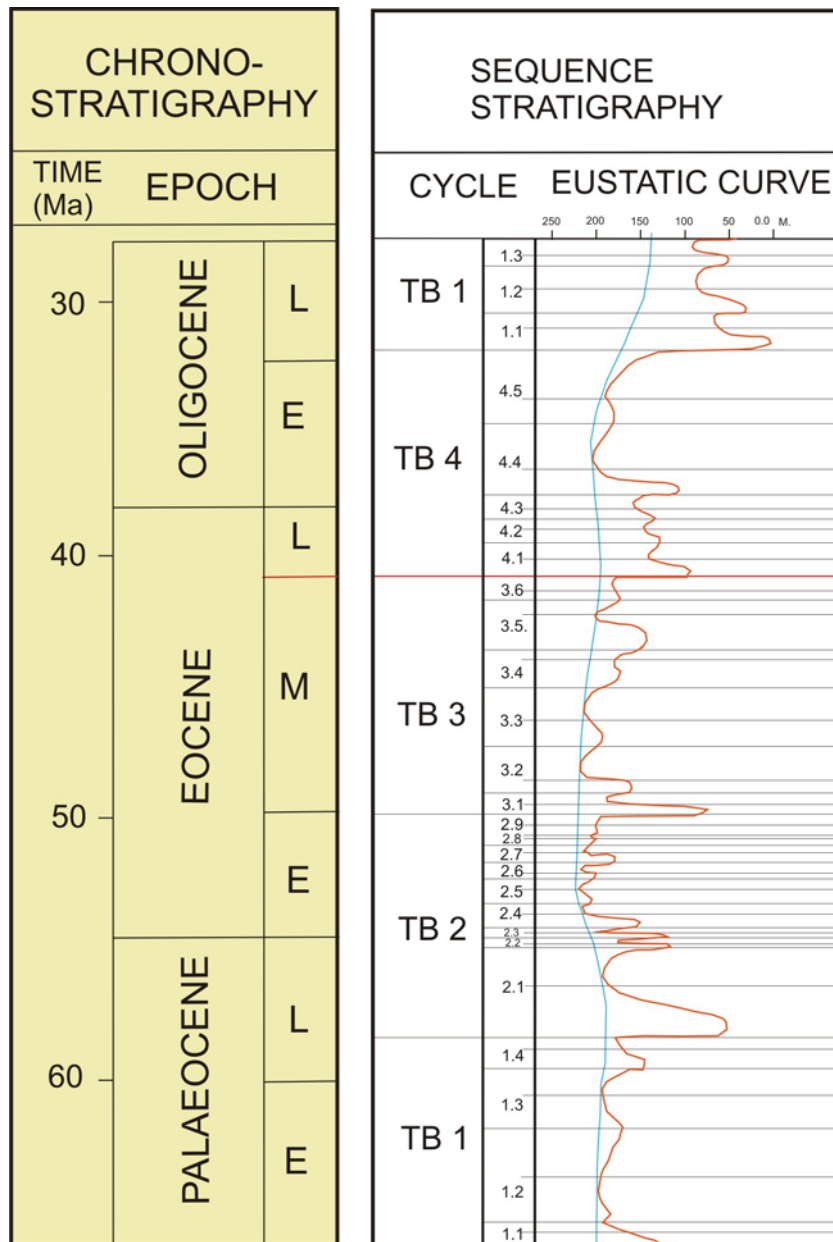
Figure 7.3. Global sea-level curve for the Cenozoic (after Haq *et al*., 1987).

7.3.1. Intra-formation-scale sequence stratigraphic analysis of the Gialo Formation

Core description and petrographic investigation of thin-sections from the studied wells of the Gialo Formation reveal facies cycles on a 5-40 feet (metre to 10-metre) scale (shown on Figures 7.4 to 7.8). These are mostly shallowing-upward, regressive successions of facies, deduced from a coarsening-up nature through increase in

occurrence of larger benthic foraminifera and decreasing quantities of lime mud. Deepening-upward, transgressive, facies packages also occur, recognised primarily by upward increasing lime mud content and presence of planktonic foraminifera towards the top. The shallowing-upward and deepening-upward facies patterns would have resulted from changes in relative sea-level and migrations of facies belts.

Overall in the upper, cored part of the Gialo, there seems to be a broad trend of increasing presence of larger foraminifer, in coarser grained packstone and rudstone towards the top of the formation. This is well seen in the logs of well 4-01-6 (Figure 7.4) and H6-6 (Figure 7.6). This is most likely to indicate an overall shallowing of the depositional environment towards the end of the Gialo deposition in these areas; that is a highstand (or regressive) systems tract. Unfortunately there is no core available from the uppermost 5-40 ft of the Gialo but the shallowing is likely to have continued up to the top of the formation itself, with this upper surface representing a sequence boundary, as noted above.

OOOO1-6 well (core thickness 119 ft, see Figure 7.4):

In this core, four facies cycles (parasequences) are recognised each around 20-30 ft (6-10 m) thick. In the lowest part of the core, the presence of abundant elongate *Discocyclina* wackestone/floatstone with whole and fragmented nummulites suggests deposition in the deeper-water part of the photic zone. This sediment is interpreted as the deposit of a distal fore-bank setting. Above this package, the facies shows an increase in water depth, with planktonic foraminifera mudstone/wackestone containing common small echinoid fragments. This facies was deposited under open-marine conditions and is inferred to have been deposited under deeper-water conditions than the underlying *Discocyclina*-rich deposits. This is then overlain by nummulithoclastic wackestone-packstone/floatstone and rudstone, interpreted to have formed through extensive transportation and redeposition to areas of low to moderate-energy back-bank and bank environments. The succession of facies from the open-marine facies to the foraminiferal packstone/float-rud-stone (i.e. depth 5240-5220 ft), is interpreted as a shallowing upward regressive unit.

Two further regressive facies cycles occur in the middle part of the core where there are nummulithoclastic packstone/rudstone and wackestone/floatstone microfacies

with upward increasing foraminfera size and abundance. The top of the core is also represented by nummulitic facies, also interpreted as regressive deposits as the amount of lime mud decreases upwards. These shallow-water facies are dominated by A and B-form nummulite floatstone/rudstone grading into packstone/rudstone. The A-form nummulites are inferred to have been deposited under shallower-water conditions than the larger B-forms.

O3-6 well (core thickness 248 ft, see Figure 7.5):

Six facies cycles are recognised in this core, with three showing deepening upward facies successions passing to shallowing-upward units, and three simply shallowing-up units. The lower part of this cored interval starts with lime mudstone/wackestone facies containing planktonic foraminifera and common small echinoid fragments. The presence of planktonic foraminifera and mud-rich microfacies indicates deposition under open-marine conditions. This facies grades upwards to large, elongate *Discocyclina* with flat B-form nummulite wackestone/floatstone. This sediment is interpreted as a fore-bank deposit. The presence of abundant elongated *Discocyclina* suggests deposition in the deeper-water part of the photic zone. This part of the section (5370-5340 ft) is interpreted as an aggrading (regressive) package. Above this unit the texture changes to small and large nummulite floatstone/rudstone dominated by B and A-forms and then a coarsening-upward, through change in texture from wackestone to floatstone/rudstone with decrease in micrite, suggests that this facies accumulated in shallower conditions than the underlying facies. These sediments were mostly deposited in a moderate to high-energy, back-bank to bank environment, and are interpreted as regressive deposits. The upper part of the core starts with wackestone/floatstone grading into floatstone/rudstone with common whole and fragmented *Operculina* and *Discocyclina* bioclastic rich mud. Moving upward to the uppermost part of the well, the texture changes to wackestone/floatstone and is composed of whole and mainly fragmented *Operculina* and *Discocyclina* bioclastic and highly micritic facies. These sediments were mostly deposited in a moderate energy, fore-bank environment. The changing texture upward from wackestone/packstone to wackestone/floatstone, and an increase in micrite upwards, are indicative of lower energy.

H6-6 well (core thickness 184 ft, see Figure 7.6):

Five shallowing-upward facies cycles are recognised in this core, and overall there is a clear coarsening/shallowing up of the succession. The lower part of the core starts with mudstone/wackestone with common planktonic foraminifera and minor small echinoid fragments. Above this the texture changes to wackestone/floatstone and mudstone/wackestone dominated by elongated *Discocyclina* and *Operculina*. The lime-mud facies was deposited under open-marine conditions and is inferred to have been deposited under deeper-water conditions than the *Discocyclina* and *Operculina*-rich deposits

The middle part is characterized by flat B-form nummulite and elongated *Discocyclina* wackestone/floatstone grading into floatstone/rudstone with minor echinoid fragments. This facies is interpreted as fore-bank. This package is overlain by bank, back-bank of nummulite and nummulithoclastic wackestone/floatstone with minor elongated *Discocyclina* and echinoid fragments. The uppermost unit is characterized by abundant A-B-form nummulite packstone/rudstone. This part of the section is interpreted as regressive deposits, with shallow-water facies. The A-form nummulites are inferred to have been deposited under shallower-water conditions than the larger B-forms.

H4-6 well (core thickness 128 ft, see Figure 7.7):

In this core, two deepening-up facies cycles can be recognised, as well as two shallowing-upward cycles. The lower part of the core starts with *Discocyclina*-nummulite wackestone, interpreted as forming in the lower part of a bank (fore-bank), and this grades upward into mudstone/wackestone with common planktonic foraminifera, suggesting increasing water depth. This passes upward into mudstone with common *Operculina-Discocyclina*. The changing texture upward from wackestone/floatstone to mudstone/wackestone and an increase in micrite upwards are indicative of lower energy and so this whole lower section is interpreted as a transgressive package. Moving upward the texture changes progressively to small and large nummulite wackestone/floatstone dominated by whole and fragmented nummulites. A coarsening-upward and change in texture with decrease in micrite suggest that this facies accumulated in shallower conditions than the underlying facies. These sediments were mostly deposited in a moderate to high-energy, bank to back-

bank environment, and so overall this is a regressive facies package (core depths 5065-4990 ft, Figure 7.7).

Mollusc and brachiopod fragments dominate the overlying bioclastic facies. This package is overlain by thick beds consisting of elongated *Discocyclina* and large, flat B-form nummulite floatstone/rudstone grading to packstone/rudstone with minor echinoid fragments. The presence of elongated *Discocyclina* and flat nummulites suggests deposition in the moderate depth part of the photic zone. The top part of this section consists mainly of small and large nummulite packstone/rudstone dominated by A and B-forms with minor echinoid fragments. Overall then, this part of the core represents a regressive facies cycle.

Above this package at the top of the core, the facies shows an increase in water depth with wackestone/floatstone grading to packstone nummulithoclastic debris-rich deposits. The uppermost unit is characterized by abundant large foraminifera such as elongated *Discocyclina* and *Operculina* with minor large B-form nummulites and echinoid fragments. The presence of elongated *Discocyclina* and large B-form nummulites suggests deposition in the moderate to deeper part of the photic zone (fore-bank) and so this is interpreted as a transgressive package.
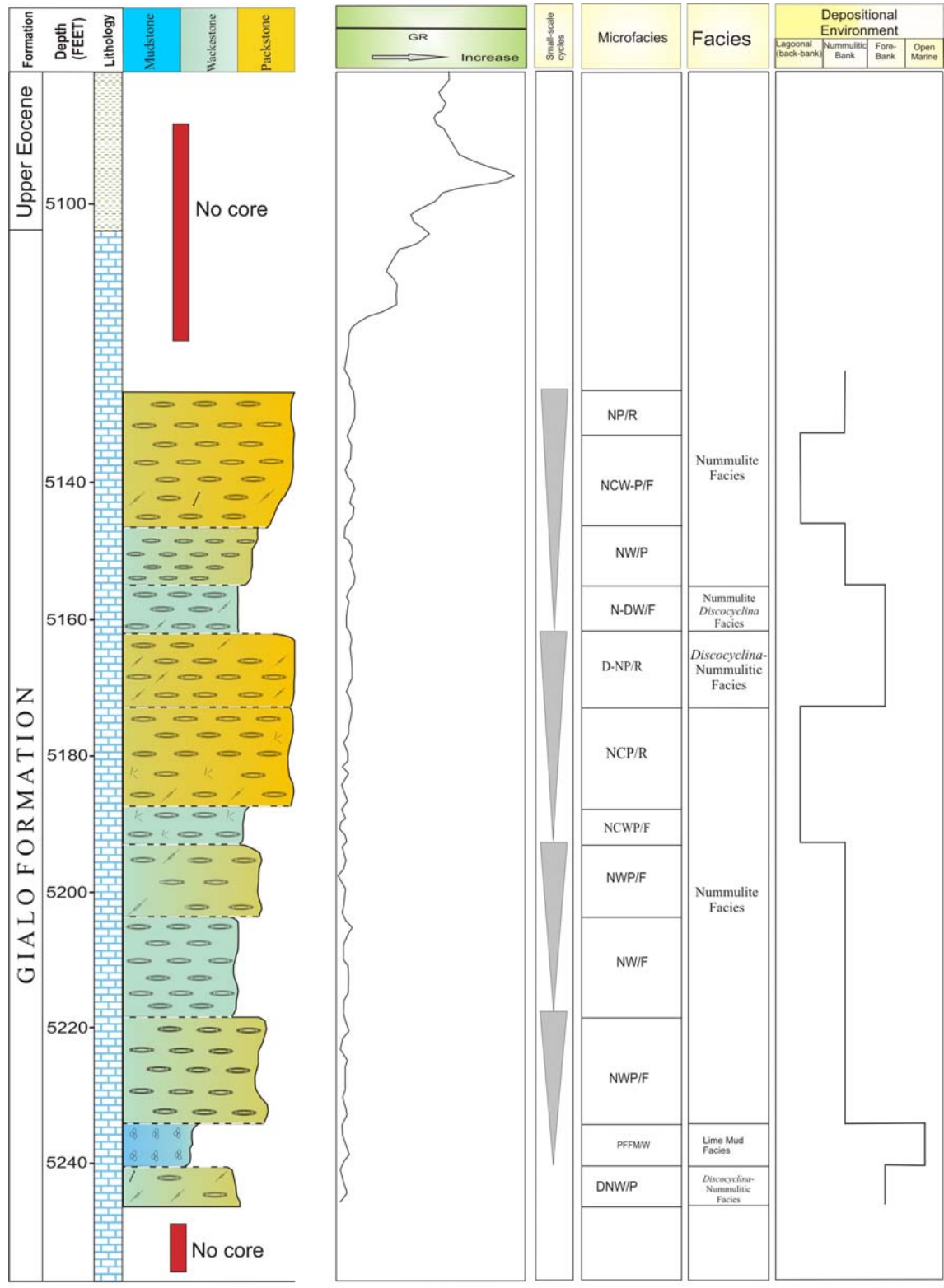
Figure 7.4. Lithological log and sequence stratigraphy of the Gialo Formation in well OOOO1-6.
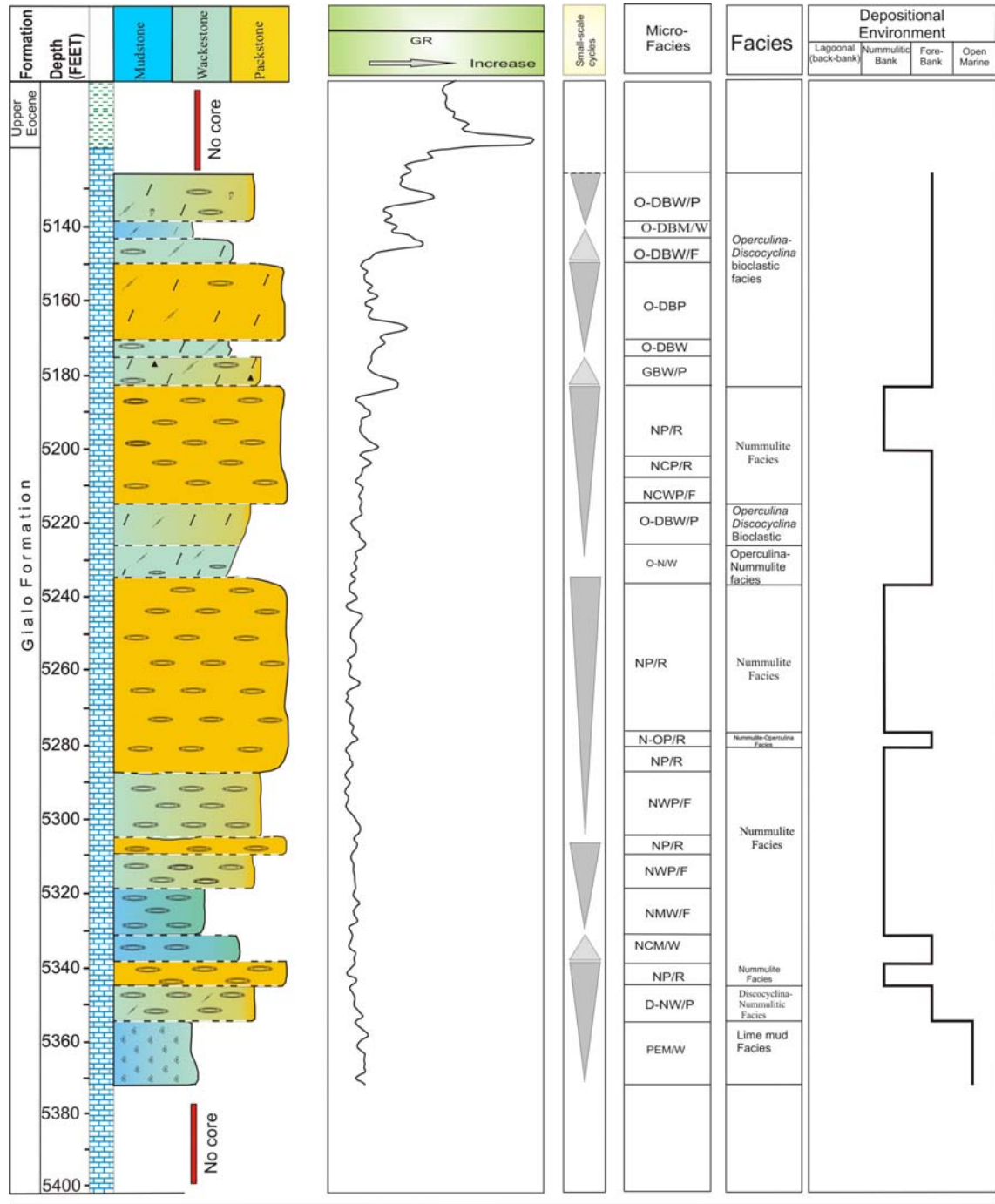
Figure 7.5. Lithological log and sequence stratigraphy of the Gialo Formation in well O3-6.
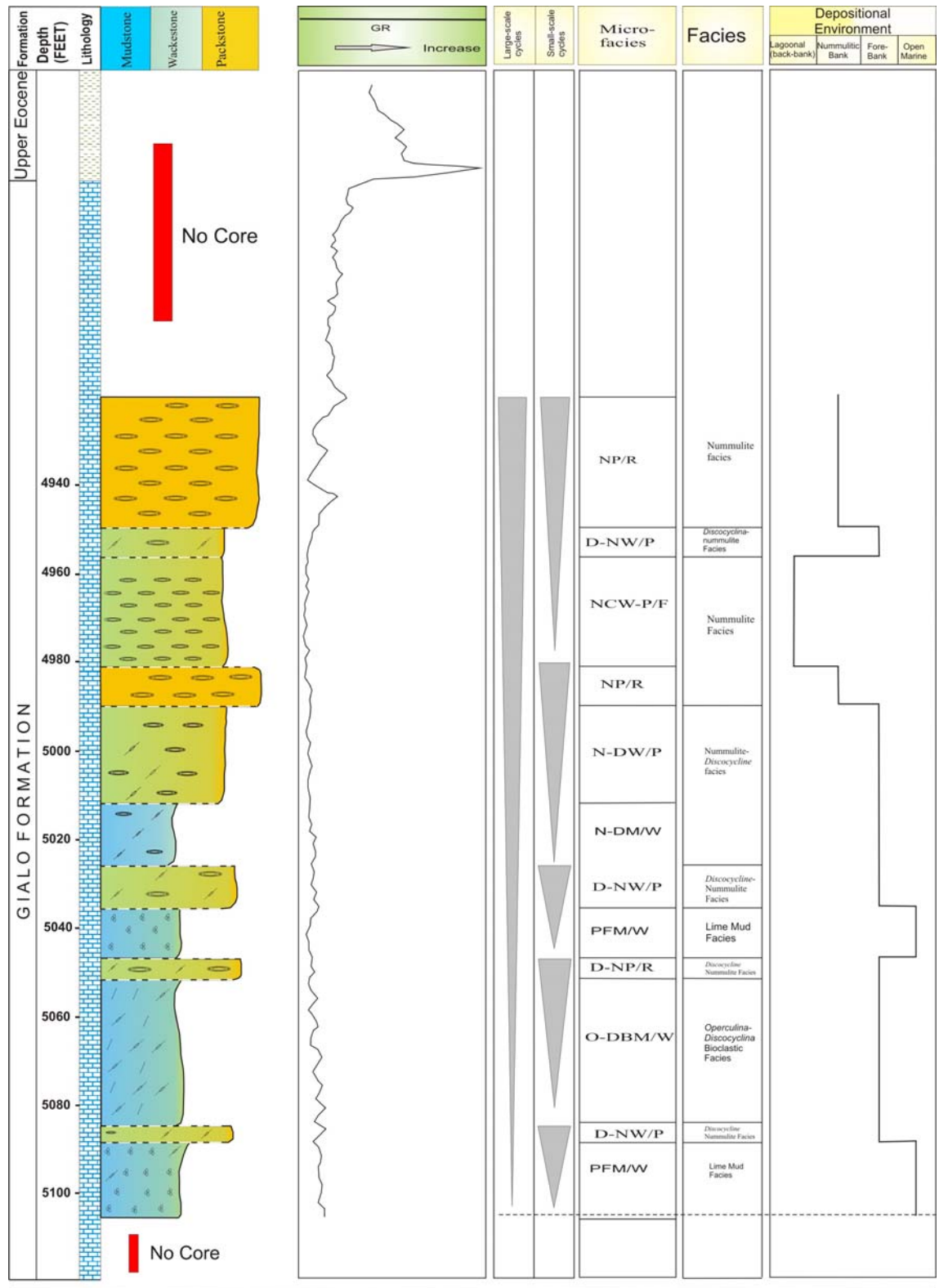
Figure 7.6. Lithological log and sequence stratigraphy of the Gialo Formation in well H6-6.
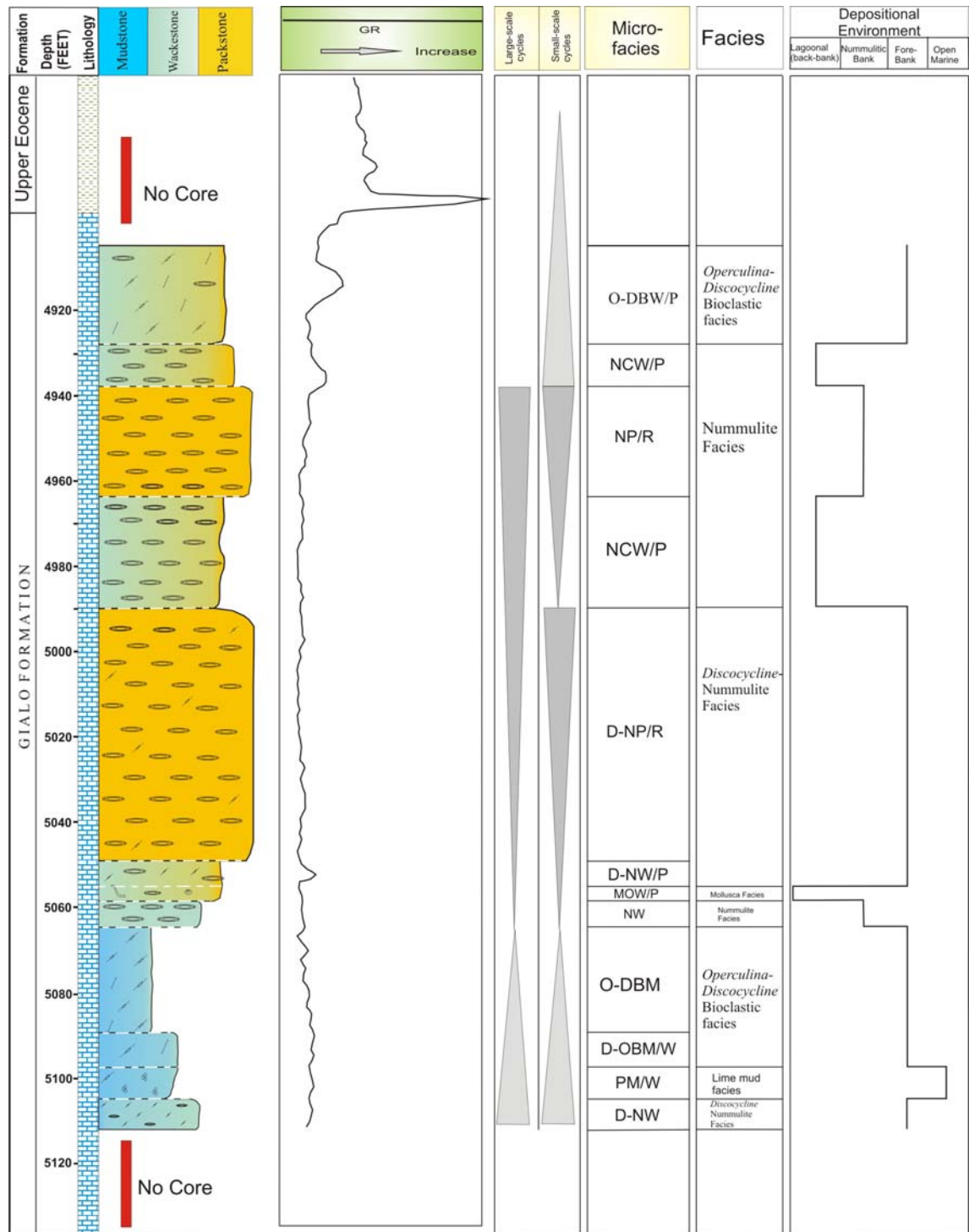
Figure 7.7. Lithological log and sequence stratigraphy of the Gialo Formation in well H4-6.
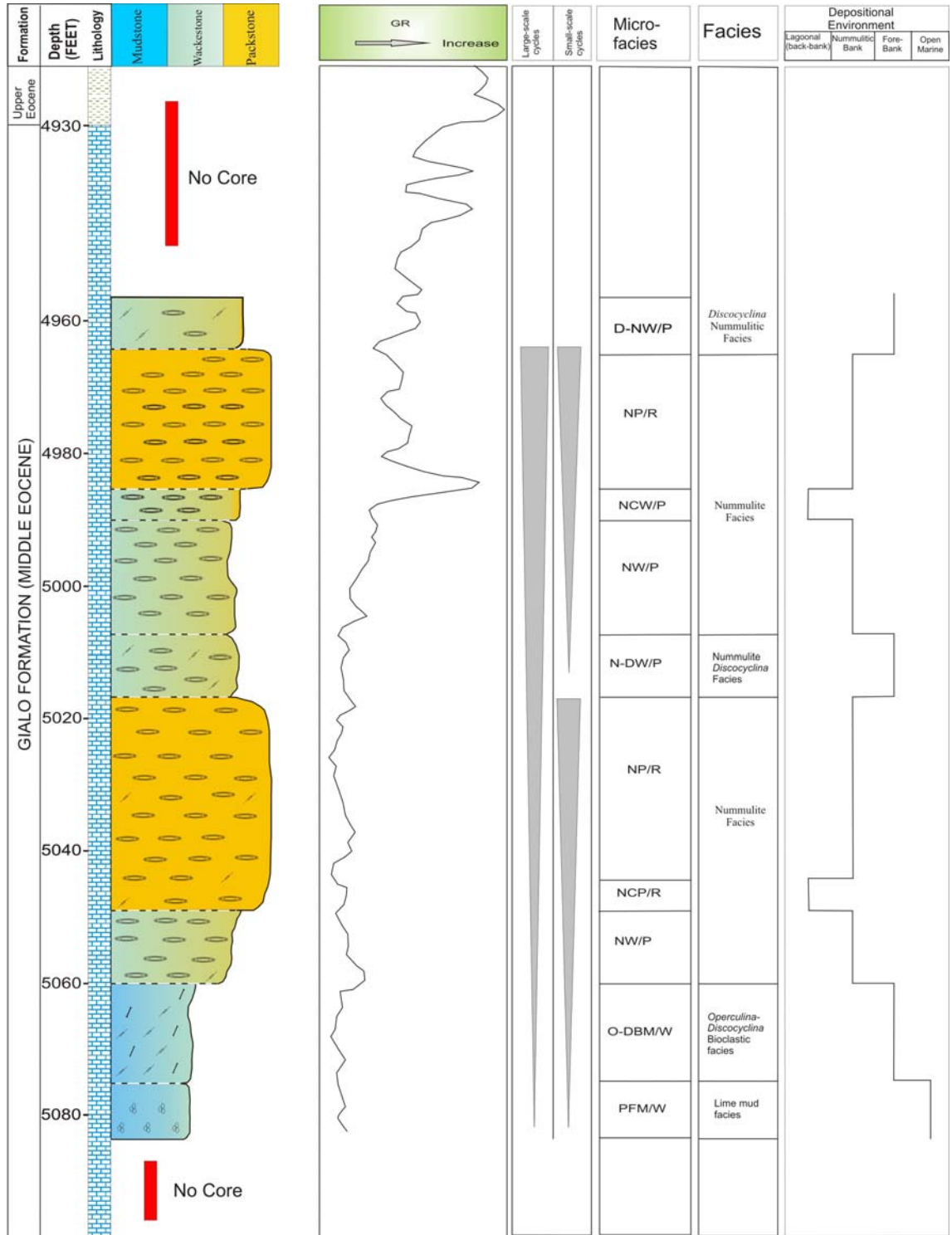
Figure 7.8. Lithological log and sequence stratigraphy of the Gialo Formation in well H10-6.
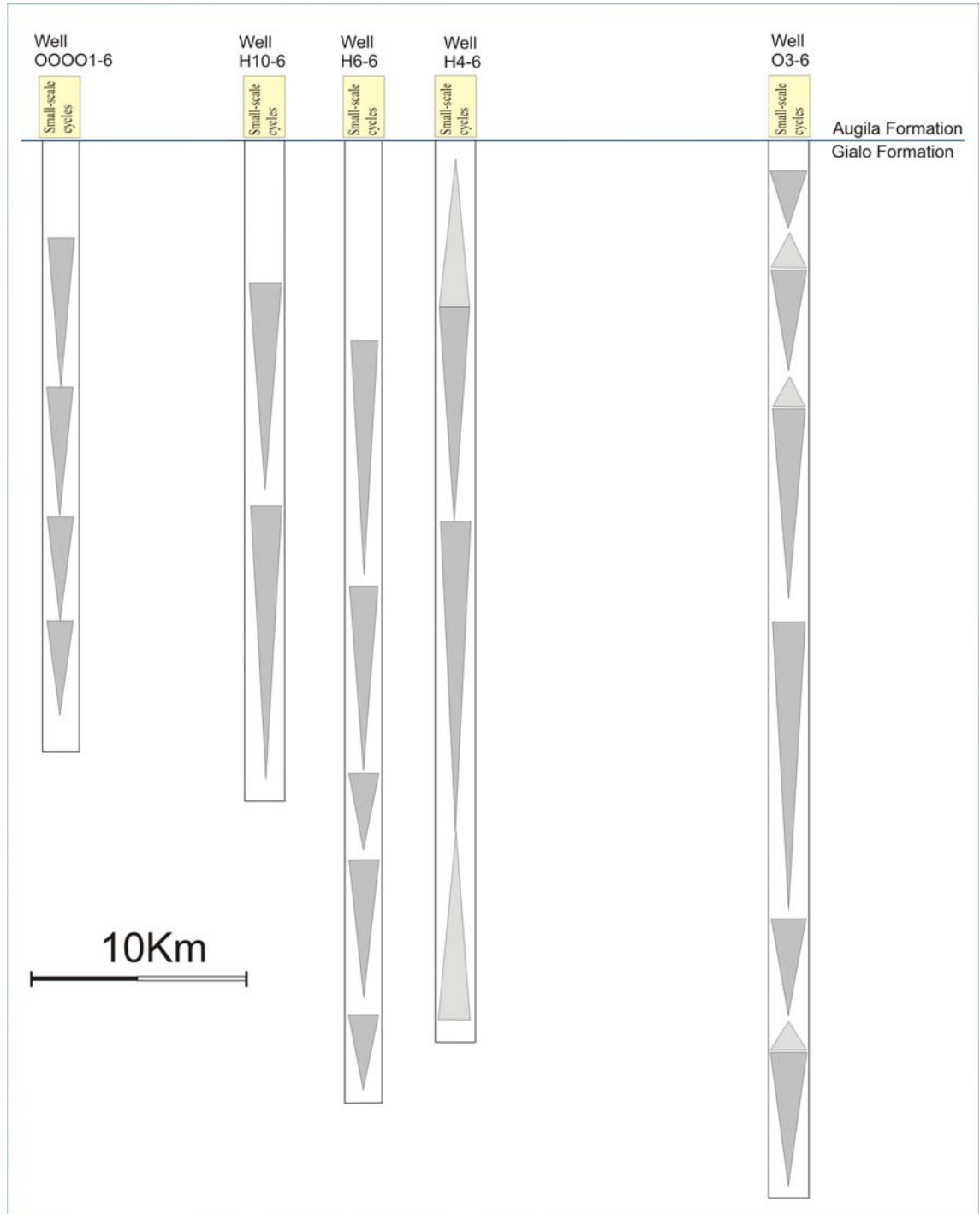
Figure 7.9. Small scale facies cycles within the upper part of Gialo Formation as seen from core material.

H10-6 well (core thickness 125 ft, see Figure 7.8):

Two shallowing-upward facies cycles are reconised in this core, each around 60 ft in thickness. The lower part of the core starts with mudstone/wackestone with common planktonic foraminifera, small echinoid fragments and is highly micritic. This

facies was deposited under open-marine conditions. Moving upward, *Operculina* and *Discocyclina* with minor small echinod fragments dominate the overlying bioclastic mudstone/wackestone. The presence of elongated *Discocyclina* and *Operculina* suggests deposition in the moderate to deep part of the photic zone. These sediments are interpreted as fore-bank facies; they grade upward into wackestone/packstone and packstone/rudstone nummulithoclastic debris-rich deposits, overlain by small and large nummulite floatstone/rudstone, locally packstone with minor *Discocyclina* and echinoid fragments. The abrasion and fragmentation of sediments resulted from the transport of sediments from palaeohighs and reaccumulation into intra or back-bank environments. Overall this package of 65 ft, at core depth 5080 – 5020 ft, is interpreted as a regressive cycle.

The upper part of the core (5015-4965 ft) starts with the presence of flattened nummulites and elongated *Discocyclina* with minor echinoid fragments. The presence of large B-form nummulites suggests deposition in the moderate to deep part of the photic zone. These sediments are interpreted as forming in the lower part of a bank (fore-bank). This facies grades upward into nummulite bank deposits which consist mainly of moderately sorted, flattened nummulite wackestone/packstone grading to packstone/rudstone. Overall this is another regressive package. The uppermost 10 ft of this core (depth 4965-4955 ft) consist of whole and fragmented *Discocyclina* and nummulite bioclastic wackestone/packstone, which suggest deposition in a moderate energy depositional setting, of deeper water than the underlying facies.

7.4. Discussion and correlation

Based on the microfacies types and their vertical arrangement described above, the Gialo Formation was wholly deposited in subtidal environments on a homoclinal-type ramp, with facies representative of the inner ramp, middle ramp and outer ramp. The palaeoslope dip was mainly directed to the south-east and as a result, the deeper-water facies are generally more abundant towards the south-east. The slope gradient between the platform and the adjacent basin was very low and the transition from shallow to deeper-water environments was very gradual. This is suggested by the lack of slumps and debris-flow deposits.

From the facies studies in Chapter 4, also referred to here, it is clear that similar facies occur in all wells. One difference of note though is that the *Operculina-Discocyclina* bioclastic wackestone/packstone, along with fragmented nummulitic packstone, is well developed in the Sahl Field (well O3-6), where it forms a reservoir unit This particular facies does not form such a thick, and porous, unit in the other studied fields. The analysis of the facies succession in the cores has shown that facies cycles can be recognised. There are different numbers and thicknesses of cycles in each core, even taking into account the different thicknesses of core (see Figure 7.9). In addition, there are no distinctive cycles, nor particular surfaces seen in core, that can be correlated from one well to the next. The distance apart of the cores is not great; they all occur within 10-30 km of each other.

There are some broad variations in terms of facies. In the **OOOO1-6** well, there are four main facies: nummulite, nummulite-*Discocyclina*, *Discocyclina*-nummulite and lime-mud facies. These facies are interpreted as having accumulated in bank, upper fore-bank, lower fore-bank and open-marine settings, respectively. In the **O3-6** well, there occur *Operculina-Discocyclina* bioclastic, nummulite, *Operculina*-nummulite, nummulite-*Operculina*, *Discocyclina*-nummulite and lime-mud facies. These facies are interpreted as accumulating in fore-bank, bank and open-marine settings mostly. In the **H6-6** well, five facies are present: nummulite, *Discocyclina*-nummulite, nummulite-*Discocyclina*, lime mud, and *Operculina-Discocyclina* bioclastic facies. These facies are interpreted as accumulating in bank, fore-bank, back-bank and open-marine environments. In the **H4-6** well, *Operculina-Discocyclina* bioclastic, nummulite, *Discocyclina*-nummulite, mollusc and lime-mud facies are present. These facies are interpreted as accumulating in fore-bank, back-bank, bank, lagoonal (back-bank), and open-marine settings. In comparison, six facies in well **H10-6** are recognized: *Operculina-Discocyclina* bioclastic, nummulite, *Operculina*-nummulite, nummulite-*Operculina, Discocyclina*-nummulite and lime-mud facies. These facies are interpreted as forming in fore-bank, bank and open marine settings (Figures. 7.4, 7.5, 7.6,7.7 and 7.8). The abundance of A-form and B-form in the nummulite facies are different from one well to another, and this is probably related to different water-depths. These differences in depositional settings are probably the result of variable palaeogeographic and palaeoenvironmental settings in the Sirt Basin and these make cross-formation

correlation difficult. The different vertical positions and numbers of transgressive-regressive cycles in each well also make formation-wide correlation problematic.

Difficulties were encountered in attempting to correlate between the five studied wells: 1) There are no core data for the upper contact with the Augila Formation and from the lower part of the studied wells, 2) well logs do not reflect facies very well; GR shows little, as is usual for clean carbonates, 3) cycles are not well defined in the cores and there are no diagnostic zone fossils within the deposits that can be used to subdivide the wells into different correlateable time-units, 4) units are of different thickness, and so do not correlate on this basis; this suggests that autocyclicity is the dominant depositional control, 5) the weak record of cyclicity in the upper part of this Middle Eocene succession suggests that fourth-order relative sea-level changes were not sufficiently strong across this platform to affect sedimentation across the platform as a whole, and finally 6) there are very different facies and inferred depositional environments for the studied wells (Figures 7.4, 7.5, 7.6,7.7 and 7.8). In terms of accommodation development, there is no evidence of exposure at the top of each facies package. Thus, it appears that the succession developed from slightly deeper to slightly shallower water, from lower energy to higher energy, up through the succession. There is no strong evidence for subaerial exposure, apart from some diagenetic textures which could be interpreted as meteoric.

As noted earlier, the Haq *et al.* (1987) curve (Figure 7.3) did recognise several high-frequency sequences in the upper part of the Middle Eocene. The number of packages recognized within the various wells of the Gialo Formation is up to 6 but unfortunately there is no way they can be correlated with the sequences identified by Haq *et al.*, 1987. Perhaps in the future with more detailed biostratigraphic and chemostratigraphic data, it may be possible to make correlations between wells and the 'global'chart.

The facies cycles identified in the core material are mostly shallowing-upward units passing from more muddy to more bioclastic-grainy sediments with increasing numbers of nummulites and other foraminifera. Since these cycles cannot be correlated it is most likely that they are the result of autocyclic or tectonic processes. The latter is actually unlikely since the platform does not seem to have been undergoing strong faulting at this time. There is no evidence of significant slopes nor of significant

thickness changes for the Gialo Formation itself. Movement on the bounding faults between the platforms and the troughs mostly took place during the Late Cretaceous. Thus it is most likely that autocyclic processes led to the formation of the facies packages and this would have taken place through migration of foraminiferal banks and shoals. Progradation would have led to foram-dominated packstones-grainstones formed in shallower water, building out over more muddy foram wacke-pack-stones, themselves prograding over deeper water open-marine facies. Lenticular, discontinuous cycles would have been formed, in a manner similar in many respects to the tidal-flat island model for peritidal carbonates in epeiric seas put forward by Pratt and James (1986). In many respects the Gialo depositional environment was similar to an epeiric sea, with very gentle ramps and migrating foraminiferal sand banks.

The origin of the deepening-upward facies cycles could be related autocyclic (sedimentary) or allocyclic processes. Against a background of regional subsidence, a local decrease in carbonate productivity could have led to a deepening-up succession of facies. Relative sea-level rises too could have led to local drowning of carbonate banks and these could have been brought about by eustatic fluctuations in sea level or local tectonic effects.

Studies of Gialo carbonates at outcrop in Cyrenaica by Bishop (1975), Moody (1987) and Keheila and El-Ayyat (1990) have recognised shallowing-upward cycles with nummulite banks occurring these. Also from outcrop in Cyrenaica, Bernasconi *et al*. (1991) showed that the uppermost nummulitic bank deposits in the Gialo were subjected to an extensive regression compared with bank facies in the middle and lowermost parts of the formation. They related this to the more extensive eustatic sea-level fall at the end of the Ypresian (Middle Eocene). For larger foraminiferal banks in the underlying Gir Formation (Lower Eocene), Ahmed (1992) concluded that their development occurred in two stages: first bank formation during phases of storm activity connected to eustatic sea-level rise, and then foraminiferal production decreased as eustasy peaked, i.e. when the rate of sea-level rise reached a minimum, and then the banks were flooded and drowned in a subsequent sea-level rise.

In general, the best reservoir quality in the Middle Eocene carbonates of the north-central Sirt Basin occurs in the mud-free foraminifera-bearing facies, which occurs towards the top of the formation and also in the upper part of the smaller scale

facies cycles. This facies is characterized by a pore system largely composed of primary intergranular pores and moldic pores which are related to dissolution. The foram packstones do form reservoir systems, and offer a range of subtle stratigraphic play types. In terms of reservoir potential, it would be useful to determine whether packstone units were deposited during transgressive or highstand (regressive) systems tracts, in terms of the potential for meteoric exposure. This is most likely to occur in the late HST and so create better porosities through leaching. To identify foraminiferal packstone reservoirs in Middle Eocene ramp systems, the use of detailed sequence stratigraphic and diagenetic models could be useful in the future, if there is sufficient core data available.

7.5. Summary

The facies in the upper part of the Gialo Formation are commonly arranged into shallowing-upward packages on the scale of several 10s of ft (up to 10 metres). These cycles grade up from mud-dominated to mud-poor sediments with changes in the number, size and species of foraminifera. Deepening-upward facies packages are also present. Cycle boundaries are insignificant in core; and are recognised by microfacies changes. There are no clear exposure horizons developed.

There is no strong evidence of eustasy, because it is difficult to make correlations between the cycles in the various wells, at least with the data available. The facies pattern is different from one well to another, which does suggest that there was a strong tectonic control, that is differential tectonic subsidence and/or fault control, or that deposition was controlled by autocyclic processes, for example the prograding of nummulite banks or other foram banks and shoals, which would then give rise to shallowing-upward packages. The lack of correlation in terms of cycle thickness, as well as facies, between wells, also suggests autocyclic processes. Third and fourth-order relative sea-level changes do not appear to have been a major control on deposition during this Middle Eocene time.

CHAPTER 8: CONCLUDING REMARKS

8.1. Summary and conclusions

This chapter brings together the main findings of each of the different parts of the thesis. It deals in turn with facies characteristics (both micro and macro), environment of deposition, geochemistry, diagenesis, petroleum and hydrocarbon potential, and sequence stratigraphy. For each of these topics, information is taken primarily from the Summary and Conclusions sections of each chapter, with an effort to weave these into a coherent story and to provide some synthesis between the different parts. Bibliographic references are given in the relevant chapters and are not repeated here.

Overall, this thesis is the first detailed study of Middle Eocene sedimentology in Central Sirt Basin. It thereby provides a wealth of new data on carbonate facies, their composition and depositional model. Standard lithostratigraphic sections for the fore-bank, bank and back-bank regions are identified, and a more complete assessment of hydrocarbon potential is made than was previously available.

The database available included core material from 5 wells and well data (wireline logs, porosity-permeability measurements). In addition, some seismic lines were available. Laboratory analysis has involved optical microscopy (175 thin-sections), SEM study (10 samples), and porosity-permeability determinations (230 samples). Results of all these analysis are fully documented in the appendices.

- **Structure and stratigraphy of the Sirt Basin** - A huge amount of data is available for the Sirt Basin as a result of oil exploration activities extending over more than forty years. Thousands of wells have been drilled and as a result the basin is far better known than any other area in Libya. The oldest rocks in the area are Late Precambrian to Early Cambrian and these have been penetrated on the basement highs (Dahra, Beda and Zelten Platforms and Messlah and Rakb Highs). The stratigraphic succession in the onshore Sirt Basin area is dominated by granitic basement, clastics, limestone, dolomite and evaporites ranging in age from Precambrian to Recent. The tectonic features of the Sirt Basin were formed

by large-scale subsidence and block faulting in response to latest Jurassic/early Cretaceous rifting, which then controlled the pattern of deposition during late Cretaceous and early Tertiary. The complex tectonic history of the Sirt Basin resulted in multiple reservoirs and conditions that favoured hydrocarbon generation, migration and accumulation.

- **Literature review on Eocene Nummulitic Accumulations and Palaeoenvironments** - Nummulites are Tertiary (Late Palaeocene to mid-Oligocene) benthic rotalid foraminifera which are particularly common throughout the Tethyan region. Nummulites with other larger foraminifera including nummulitids and alveolinids are believed to have lived symbiotically with photosynthetic algae and are therefore thought to have been restricted to warm (25ºC), clear, shallow waters (<120m) within the euphotic zone. Nummulites had alternating asexual and sexual generations, characterized respectively by small A-forms and large B-forms. In nummulitic banks, B-forms are often dominant in high-energy settings, whereas the A-forms and larger *Discocyclina* are dominant in deeper-water, lower energy settings. The distribution of these two morphotypes is in general controlled by the hydrodynamics of the depositional system. Nummulite tests may display breakage ranging from external damage to complete fragmentation (commonly referred to as nummulithoclastic debris). Studies of modern larger benthic foraminifera suggest that transport-induced abrasion is a likely candidate for the test damage. Larger benthic foraminifera are important contributors to modern and ancient tropical, shallow-marine sediments. Eocene nummulitic limestones are important hydrocarbon reservoirs in North Africa (Tunisia and Libya) with good porosity and permeability. Also they are potential exploration targets in Egypt, Italy, Oman and Pakistan.

- **Facies Analysis and Depositional Environments of the Gialo Formation** - The Middle Eocene Gialo Formation has been studied in five wells in the Assumood and Sahl fields, Concession 6, Sirt Basin. Detailed core description and petrographic study show that the Gialo Formation consists mainly of shallow-water carbonate and is characterized by facies and thickness variations

between the five wells. The vertical and lateral variation of the Gialo depositional facies was influenced by basin-floor architecture and other environmental controls. Sedimentological and petrological investigation of 175 thin-sections to document the main components (nummulite, *Discocyclina*, *Operculina* and planktonic foraminifera), distinguished seven separate sedimentary facies and twenty microfacies, including nummulite facies, *Discocyclina*-nummulite facies, mollusc facies, nummulite-D*iscocyclina* facies, *Operculina*-nummulite facies, *Operculina-Discocyclina* bioclastic facies and lime mudstone facies. These facies were predominantly deposited under shallow-marine conditions, within the photic zone, as indicated from their richness in phototrophic fauna and flora, and can best be ascribed to a carbonate ramp (Figure 4.16). Open-marine, fore-bank, main bank and lagoon (back-bank) environments are recognised. The nummulite packstone/rudstone facies dominated by A-forms with minor to common B-forms comprises the upper part of the bank. Fragmentation and abrasion of sediments resulted in the transport of sediments from the palaeohigh and redeposition in back-bank environments. The *Operculina-Discocyclina* bioclastic facies accumulated in a fore-bank setting. There is a pronounced gradation from coarser to finer debris down the ramp. Towards the north and northwest of the Sahl Field (towards the open Tethyan sea), mid-ramp, shallow-marine, moderate-high energy environments prevailed and low relief nummulitic shoals developed in the Assumood area. Sediments from shoals and the mid-ramp environment were fragmented and later transported during strorms and strong currents to a relatively deeper marine location in the outer ramp environment near the Sahl Field. Petrographic and petrophysical studies indicate that porosities and permeabilities in the Gialo Formation are the result, in part, of the depositional environments and conditions. Porosity is at a maximum in the nummulitic bank facies and lowest in the lime mud facies.

- **Diagenesis of the Gialo Formation -** Present-day reservoir characteristics of the Gialo Formation are the net result of modifications to the original depositional characteristics caused by diagenesis. The diagenetic processes took place on the seafloor, in the meteoric environment and under burial conditions. Rare micritization is recorded and micrite envelopes, when present, preserved

mouldic pores from collapsing. Lack of early seafloor cementation may have preserved intergranular porosity in the early burial stage, but then porosity was reduced through burial compaction. Grain breakage, grain penetration, plastic deformation and a few fine fractures were produced by mechanical compaction. Amongst these products, fracturing would have improved permeability, especially in mud-supported facies. Chemical compaction is more evident in grain-supported facies, causing partial grain dissolution and forming localized horizontally-discontinuous stylolites. Both of these processes are a source for burial calcite cement. Porosity in the lower parts of the Gialo Formation in Assumood and Sahl fields is partially to more than partially filled with burial ferroan and non-ferroan calcite cement. Meteoric and early burial diagenesis includes dissolution, drusy calcite and syntaxial overgrowth cements and neomorphism. Localized neomorphism enlarged the crystal size of lime mud ($<$ 4µm) to microspar ($<$ 10µm). Syntaxial overgrowth cements have developed and are mainly associated with crinoids fragments. These processes generally reduced matrix porosity in some facies.

Two generations of cement are revealed by cathodoluminescence (CL), dull luminescent and bright orange cement. The dull luminescent zone includes sparry (mainly drusy) calcite cement between grains and filling bioclastic cavities (e.g. nummulite chambers) and late syntaxial overgrowth calcite cements. Bright pink to orange zones represent mainly the microcrystalline calcite (micrite), early syntaxial overgrowth cements and bioclasts (nummulites). The cathodoluminescence behaviour of syntaxial overgrowth calcite shows two cement stages, an early overgrowth cement which is bright luminescent and probably formed in a meteoric to shallow-burial environment with manganese present, then a later overgrowth that is dull and therefore probably contains iron and less Mn which reduces the luminescence. Bright luminescence of the syntaxial overgrowths is indicative of precipitation from waters changing from oxic to suboxic/anoxic in character. Bioclasts (nummulite) have picked up manganese to become luminescent as a result of some early recrystallization and alteration. Dull sparry calcite cement which fills nummulite chambers is probably a burial cement.

The oxygen isotope values of the bioclasts vary from marine values to more negative values as a result of some alteration. The more negative oxygen of the cements suggests precipitation within the shallow-burial environment under the influence of meteoric water and / or precipitation at higher temperatures during further burial. The carbon isotopic signatures are typical marine values.

There is a strong relationship between porosity and the diagenetic processes that have affected the Gialo sediments. Generally the porosity in the Assumood and Sahl fields is either primary or secondary, enhanced by dissolution and fracturing of the sediments. Reduction in porosity in the investigated sediments is mainly due to cementation and compaction.

- **Petroleum Geology of the Gialo Formation** - The complex tectonic history of the Sirt Basin resulted in multiple reservoirs and conditions that favoured hydrocarbon generation, migration and accumulation. The gas was generated from the gas-prone Sirt Shale source rock in the northern Ajdabiya Trough and this migrated onto the Assumood Ridge from the northeast through late Cretaceous, Palaeocene and early Eocene carbonates, before being trapped beneath the Augila Shale (Upper Eocene), which is the principal regional seal in the area. The time-structure map shows that the contour density increases towards the north of the area, indicating steeper dips representing a carbonate bank in the Middle Eocene. The OOOO-6 structure (north part of the Assumood Field) is separated from the Assumood Field by a channel structure cut into the Gialo top surface.

    Dissimilarities in the type and quality of the Gialo reservoir facies across the Sirt Basin are attributed to vertical and lateral variations in depositional facies and their diagenetic history. Vertical and lateral variations of the Gialo depositional facies were governed by basin-floor architecture and environmental variables. Two broad facies groups are distinguished: (1) Platform facies: comprising shallow-marine dasycladacean, bryozoan, and nummulite-rich packstone and wackestone, which were deposited in inner to outer ramp facies belts. (2) Trough facies: comprising relatively deeper-marine, fine skeletal,

rarely nummulitic, lime mudstone. Each platform facies belt hosted distinctive reservoir facies: (a) inner-ramp dasycladacean-rich facies were affected by mineral-controlled meteoric dissolution, which brought about good, but patchy, moldic porosity in Jebel and S. Nasser Fields. (b) Mid-ramp nummulitic packstone facies are rarely cemented and contain good, well-connected, matrix and intragranular porosity in whole tests of nummulites in the Assumood Field. (c) Outer-ramp fragmented nummulitic packstone facies, with rarely cemented inter-and intragranular porosity, are good reservoirs in Sahl Field.

Reservoir quality in the Gialo Formation is a function of grain types, pore types, grain size, sorting, cementation and compaction, and it is difficult to predict areas of high reservoir quality. Exploration should be oriented to positioning a well into the main trend of the mid-ramp, nummulite accumulation. Different nummulite facies can be reservoirs depending on their diagenetic history. A diagenetic decrease in porosity must be distinguished from a lack of porosity because of an unfavourable depositional environment, so that exploration options can be adequately assessed. This integrated study has shown the presence of good reservoir rocks, hydrocarbon traps and the close proximity of potential source rocks, and this is significantly encouraging for further hydrocarbon exploration in the area. The study also helps with our understanding of the reservoir heterogeneity and its potential, on the basis of which current wells have been completed appropriately and successfully; the information should also aid in completing future wells productively.

- **Sequence Stratigraphy of the Gialo Formation** – The facies in the upper part of the Gialo Formation are commonly arranged into shallowing-upward packages on the scale of several 10s of ft (up to 10 metres). These cycles grade up from mud-dominated to mud-poor sediments with changes in the number, size and species of foraminifera. Deepening-upward facies packages are also present. Cycle boundaries are insignificant in core; and are recognised by microfacies changes. There are no clear exposure horizons developed.

There is no strong evidence of eustasy, because it is difficult to make correlations between the cycles in the various wells, at least with the data

available. The facies pattern is different from one well to another, which does suggest that there was a strong tectonic control, that is differential tectonic subsidence and/or fault control, or that deposition was controlled by autocyclic processes, for example the prograding of nummulite banks or other foram banks and shoals, which would then give rise to shallowing-upward packages. The lack of correlation in terms of cycle thickness, as well as facies, between wells, also suggests autocyclic processes. Third and fourth-order relative sea-level changes do not appear to have been a major control on deposition during this Middle Eocene time.

8.2. Future work

More wells (cores and wireline logs) from Jahama and Zelten Platforms should be used for further detailed study. The general lack of cored sections in wells drilled to date severely hampers sedimentological and sequence stratigraphic interpretations. It is therefore recommended that future wells be better cored in selected target intervals, for example the nummulite bank facies. The nummulite bank facies provide one of the key potential reservoir rocks in the area. More detailed studies of all core, outcrop, wireline log and seismic data available in this potential play area would be beneficial. A specific recommendation would be those areas in the trough (south east Sahl Field). Selection of surface sections (outcrop) in the Jabal Al-Akhdar area for detailed interdisciplinary study, including structural, stratigraphic and sedimentological aspects, would be useful. This would be particularly important for documenting structural style and complexities for extending coverage of facies distribution, and for examining the three dimensional geometry of particular facies associations and sequence stratigraphy.

REFERENCES

ABDULSAMAD, E.O., 1999. Stratigraphy and palaeogeography of Tertiary larger foraminifera from Al Jabal la Akhdar (Cyrenaica, NE Libya). *Gournale di Geol. Bologna*, **61**, 75-98.

ABDULSAMAD, E.O. and BARBIERI, R., 1999. Foraminiferal distribution and palaeoecological interpretation of the Eocene-Miocene carbonates at Al Jabal al Akhdar (northeast Libya). *Jour. Micropalaeont*., **18**, 45-65.

ABUGARES, I. Y., 1996. Sedimentology and hydrocarbon potential of the Gir Formation, Sirt Basin. *The Geology of the Sirt Basin*. Salem, M. J., Busrewil, M. T., Misallati, A.A. and Sola, M. A. (eds.), Elsevier, Amsterdam, **II,** 31-64.

ADAMS, C. G., LEE, D. E. and ROSEN, B. R., 1990. Conflicting isotopic and biotic evidence for tropical sea-surface temperatures during the Tertiary. *Palaeogeography, Palaeoclimatology, Palaeoecology,* **77,** 289-313.

AHLBRANDT, T. S., 2002. The Sirt Basin province of Libya- Sirte-Zelten total petroleum system: *U.S. Geological Survey Bulletin*, **2202-F**, 1-26.

AHMED, S. S., 1992. Depositional environment, geochemistry and diagenesis of Palaeocene and Early Eocene carbonates of Agedabya-Augila Trough, Sirt Basin, Libya. Msc. Thesis. University of Glasgow, 185pp.

AIGNER, T., 1982. Event stratification in nummulite accumulations and in shell beds from the Eocene of Egypt. In: Einsele, G. and Seilacher, A. (eds.), *Cyclic and Event Stratification,* Springer-Verlag, 248-262.

AIGNER, T., 1983. Facies and origin of nummulitic build-ups: an example from the Giza Pyramids Plateau (Middle Eocene, Egypt). *Neues Jahrbuch Geol. Palaont. Abh.,* **166,** 347-368.

ALEXANDERSSON, T., 1978. Destructive diagenesis of carbonate sediments in the eastern Skagerrak, North sea. *Geology*, **6**, 324-327.

ALLAN, J. R. and MATTHEWS, R. K., 1982. Isotope signatures associated with early meteoric diagenesis. *Sedimentology*, **29**, 797-817.

ALLAN, J. R. and WIGGINS, W. D., 1993. Dolomite reservoirs: Geochemical techniques for evaluating origin and distribution. *AAPG*, Continuing education course note, **36**, 129pp.

AMIEUX, P., 1982. La Cathodoluminescence: method d'eutude sedimentolgique des carbonate. *Bull. Centres. Rech. Explor*. Elf-Aqu, **6**, 437-483.

ANDERSON, T. F. and ARTHUR, M. A., 1983. Stable isotopes of oxygen and carbon and their application to sedimentological and paleoenvironmental problems. In: Arther, M. A. and Anderson, T. F. (eds.), Stable Isotopes in Sedimentary Geology. *SEPM.,* short course, 10, 1.1-1.151.

ANKETELL, J.M., 1996. Structural history of the Sirt Basin and its relationships to the Sabratah Basin and Cyrenaican Platform, Northern Libya. In: Salem, M.J., EL-Hawat, A.S. and Sbeta, A.M. (eds.), The Geology of Sirt Basin. *Amsterdam, Elsevier*, **III**, 57–88.

ANKETELL, J. M. and GHELLALI, S. M., 1991. A palaeogeological map of the pre-Tertiary surface in the Jafarah plain and its implication to the structural history of northern Libya. In: Salem, M. J., Sbeta, A. M. and Bakbak, M. R. (eds.), *The Geology of Libya*, **VI**, 2381-2406.

ANKETELL, J.M. and MRIHEEL, I.Y., 2000. Depositional environment and diagenesis of the Eocene Jdeir Formation, Gabes-Tripoli Basin, Western Offshore Libya. *Journal of Petroleum Geology,* **23**, 425-447.

ARNI, P., 1965. L'évolution des nummulitinae en tant que facteur de modification des depots littoraux. *Coloque International de Micropaléontologie* (Daker), Mémoires du BRGM, **32**, 7-20.

ARNI, P. and E. LANTERNO., 1972. Considérations paléoécologiques et interprétation des calcaires de l'Éocène du Véronais. *Archives de Sciences* (Geneve) **25**:251–283.

ARNI, P. and LANTERNO, E., 1976. Observations paleoecologiques dans I'Eocene du Gargano (Italie meridionale). *Archives Science Genéve,* **29**, 287-314.

BACK, W., HANSHAW, B.B., PYLE, T.E., PLUMMER, L.N. and WEIDIE, A.E., 1979. Geochemical significance of ground-water discharge and carbonate solution to the formation of Caleta Xei Ha, Quintana Roo, Mexico. *Water Resources Res.* **15**, 1531-1535.

BACK, W., HANSHAW, B. B. and VAN DRIEL, J., 1984. Role of groundwater in shaping the eastern coastline of the Yucatan Peninsula, Mexico. In: Lafleur, R. G. (ed.), Groundwater as a Geographic Agent, 157-172.

BAILEY, H. W., DUNGWORTH, G., HARDY, M., SCULL, D. and VAUGHAN, R. D., 1989. A Fresh Approach to the Metlaoui. *Actes des IIétme Journées de Géolologie Tunisienne appliquée a la recherche des Hydrocarbures,* 281-307.

BAIRD, W. D., ABURAWI, R. M. and BAILEY, J. N., 1996. Geohistory and Petroleum in the central Sirt Basin. In: Salem, M. J., Busrewil, M. T., Misallati, A.A. and Sola, M. A. (eds.), *The Geology of the Sirt Basin*. Elsevier, Amsterdam, III, 3-56.

BALL, L., BOEBE, M., SADLER, P., CORBETT, P., and LEWIS, J., 1996. Permeability prediction in a braided fluvial reservoir: A probe permeameter study on the Pre-Upper Cretaceous-B Sandstone, as Sarah Field, Sirt Basin, Libya. In: Salem, M. J., Busrewil, M. T., Misallati, A.A. and Sola, M. A. (eds.), *The Geology of the Sirt Basin*. Elsevier, Amsterdam, **I**, 185-194.

BARIC, G., SPANIC, D., and MARICIC, M., 1996. Geochemical characterization of source rocks in NC-157 Block (Zelten Platform), Sirt Basin. In: Salem, M. J., EL-Hawat, S. A. and Sbeta, M. A. (eds.), *The Geology of Sirt Basin*: Amsterdam, Elsevier, **ll**, 541-553.

BARR, F. T. and BERGGREN, W. A., 1980. Lower Tertiary biostratigraphy and tectonics of Northeastern Libya. In: Salem, M. J. and Busrewil, M. T. (eds.), *Geology of Libya*. Al-Fateh University, Tripoli, Libya, **I**, 163-191.

BARR, F. T. and WEEGAR, A. A., 1972**.** Stratigraphic nomenclature of the Sirt Basin, Libya: *Petroleum Exploration Society of Libya*, 179pp.

BATES, R. L. and JACKSON, J. A., 1980. Glossary of Geology. 2nd edition, Am. Geol. Inst., Virginia, 75lpp.

BATHURST, R. G. C., 1975. Carbonate sediments and their diagenesis. Elsevier, Amsterdam, 2nd Edition, 658pp.

BATHURST, R. G. C., 1986. Carbonate diagenesis and reservoir development: conservation, destruction and creation of pores. *Quart. J. Colorado Sch. Mines*, **81**, 1-25.

BEAVINGTON-PENNEY, S. J., 2002. Characterisation of selected Eocene nummulites accumulations. Ph.D. thesis. University of Wales, Cardiff.

BEAVINGTON-PENNEY, S. J., 2004. Analysis of the effects of abrasion on the test of Palaeonummulites venosus: implications for the origin of nummulithoclastic sediments. *Palaios*, **19**, 143-155.

BEAVINGTON-PENNEY, S. J. and RACEY, A., 2004. Ecology of extant nummulitids and other large benthonic foraminifera: applications in palaeoenvironmental analysis. *Earth. Sci. Rev.*, **67**, 219-265.

BEAVINGTON-PENNEY, S. J., WRIGHT, V. P. and RACEY, A., 2005. Sediment production and dispersal on foraminifera-dominated early Tertiary ramps: the Eocene El Garia Formation, Tunisia. *Sedimentology,* **52,** 537-569.

BEBFIELD, A. C. and WRIGHT, E. P., 1980. Post-Eocene sedimentation in the eastern Sirt Basin, Libya. In: Salem, M. J. and Busrewil, T. M. (eds.), Geology of Libya. Academic Press, London, **II**, 463-499.

BEEUNAS, M.A. and KNAUTH, L.P., 1985. Preserved stable isotopic signature of subaerial diagenesis in the 1.2-b.y. Mescal Limestone, central Arizona. Implications for the timing and development of a terrestrial plant cover. *Bull. Geol. Soc. Am.* **96**,737-745

BELAZI, H. S., 1989. The geology of the Nafoora Oil Field, Sirt Basin, Libya. *Journal of Petroleum Geology*, **12**, 353-366.

BELLINI, E. and MASSA, D., 1980. A stratigraphic contribution to the Palaeozoic of the southern basins of Libya. *In:* Salem, M. J. and Busrewil, M. T. (eds.), *The geology of Libya*: London, Academic Press, **3**, 3–57.

BENFIELD, A.C. and WRIGHT, E.P., 1980. Post-Eocene sedimentation in the eastern Sirt Basin, Libya. *In:* Salem, M. J. and Busrewil, M. T. (eds.), *The Geology of Libya*. Academic Press, London, II, 463-499.

BERNASCONI, A., POLIANI, G. and DAKSHE, A., 1991. Sedimentology, petrography and diagenesis of Metlaoui Group in the offshore Northwest of Tripoli. In: Salem, M. J. and Belaid, M. N. (eds), *Geology of Libya,* 1907- 1928.

BERNER, R. A., 1970. Sedimentology of pyrite formation. *Am. Journ. Sci.*, **268**, 1-23.

BEZAN, M. A. and EMIL, K. M., 1996. Oligocene sediments of Sirt Basin and their hydrocarbon potential. In: Salem, M. J., Busrewil, M. T., Misallati, A. A. and Sola, M. A. (eds.), *The Geology of the Sirt Basin*. Elsevier, Amsterdam, **I**, 119-127.

BEZAN, M. A., 1996. The Paleocene Sequence in Sirt Basin. In: Salem, M. J., Busrewil, M. T., Misallati, A. A. and Sola, M. A. (eds.), *The Geology of the Sirt Basin*. Elsevier, Amsterdam, **I**, 97-118.

BIGNOT, G., 1972. Recherches stratigraphiques sur les calcaires du Crétace Supérieur de l'Eocéne d'Istrie et des régions voisines. Essai de révision de Liburnien. *Travaux du Laboratoire de Micropaleontologie,* **2**, 353.

BISHOP, W. F., 1975. Geology of Tunisia and adjacent parts **of** Algeria and Libya. *Bull. AAPG*, **59**, 413-450.

BISHOP, W.F., 1985. Eocene and Upper Cretaceous carbonate reservoirs in East Central Tunisia. *Oil and Gas Journal*, Dec **2**, 137-142.

BLONDEAU, A., 1972. Les nummulites. Vuibert, Paris, 254pp.

BONNEFOUS, J., 1972. Geology of the quartzitic "Gargaf Formation" in the Sirt Basin, Libya. *Bull. Cent. Rech. Pau.*, *SNPA*, **6** (2), 225-261.

BOSENCE, D., PROCTER, E., AURELL, M., BEL KAHLA, A., BOUDAGHER-FADEL, M., CASAGLIA, F., CIRILLI, S., MEHDIE, M.., NIETO, L., REY, J., SCHERREIKS, R., SOUSSI, M. and WALTHAM, D., 2009. A dominant tectonic signal in high-frequency, peritidal carbonate cycles? A regional analysis of

Liassic platforms from western Tethys. *Journal Sedimentary Research*, **79**, 389-415.

BRADY, T.J., CAMPBELL, N. D. J. and MAHER, C. E., 1980. Intisar 'D' Oil Field, Libya. In: Halbouty, M. T. (ed.), Giant Oil and Gas Fields of the Decade 1968-1978. *AAPG.,* Memoir, **30**, 543-564.

BROWN, J. R. and FISHER, W.L., 1977. Seismic stratigraphic interpretation of depositional systems: examples from Brazilian rift and pull apart basins. In: Payton, C.E. (ed.), Seismic Stratigraphy — Applications to Hydrocarbon Exploration. *AAPG.*, Memoir, **26,** 213–248.

BURKE, K. and DEWEY, J., 1974. Two plates in Africa during the Cretaceous. *Nature*, **249**, 313-316.

BUXTON, M.W.M. and PEDLEY, M.H., 1989. A standardised model for Tethyan Tertiary carbonate ramps. *Journal of Geological Society London,* **146**, 746-748.

CARROLL, D. 1958. Role of clay minerals in the transport of iron. *Geochim. Cosmochim. Acta*, **14**, 1-27.

CATUNEANU, O., 2006. Principles of Sequence Stratigraphy. Elsevier, Amsterdam, 375pp.

CATUNEANU, O., ABREU, V., BHATTACHARYA, J.P., BLUM, M.D., DALRYMPLE, R.W., ERIKSSON, P.G., FIELDING, C.R., FISHER, W.L., GALLOWAY, W.E., GIBLING, M.R., GILES, K.A., HOLBROOK, J.M., JORDAN, R., KENDALL, C.G.ST.C., MACURDA, B., MARTINSEN, O.J., MIALL, A.D., NEAL, J.E., NUMMEDAL, D., POMAR, L., POSAMENTIER, H.W., PRATT, B.R., SARG, J.F., SHANLEY, K.W., STEEL, R.J., STRASSER, A., TUCKER, M.E. and WINKER, C., 2009. Towards the standardization of sequence stratigraphy. *Earth-Science Reviews*, **92**, 1-33.

CHILINGAR, G. V., BISSEL, H. J. and WOLF, K. H., 1979. Diagenesis of carbonate sediments and epigenesis (or catagenesis) of limestones. In: Larsen, G. and Chilingar, V. G. (eds.), *Diagenesis in Sediments and Sedimentary Rocks.* Elsevier, Amsterdam, 249-422.

CHOQUETTE, P. W. and JAMES, N. P., 1987. Diagenesis in limestones – 3, the deep burial environment. *Geoscience Canada*, **14**, 3-35.

CHOQUETTE, P. W. and PRAY, L. C., 1970. Geologic nomenclature and classification of porosity in sedimentary carbonates. *Bull. AAPG.*, **54**, 207-250.

CLIFFORD, H. J., GRUND, R. and MUSRATI, H., 1980. Geology of a stratigraphic giant: Messla Oil Field. In: HALBOUTY, M. T. (eds.), Giant oil and gas fields of the decade (1968-1978). *AAPG.*, memoir, **30**, 507-524.

COE, A., BOSENCE, D., CHURCH, K., FLINT, S., HOWELL, J. and WILSON, C., 2002. The sedimentary record of sea.-level change. The Open University, Walton Hall, 285pp.

CONANT, L. C. and GOUDARZI, G. H., 1967. Stratigraphic and tectonic framework of Libya. *Bull. AAPG.*, **51**, 719-730.

CORFIELD, R. M., 1995. An introduction to the techniques, limitations and landmarks of carbonate oxygen isotope palaeothermometry. In: BOSENCE, D. V. J and ALLISON, P. A., (eds.). Marine Palaeoenvironmental Analysis from Fossils. *Geological Society, Special Publication,* **83**, 27-42.

CRAIG, D. H., 1961. Isotopic variations in meteoric waters. *Science,* **133**, 1702-1703.

CRAIN, E.R., 1986. The Log Analysis Handbook. Quantitative Log Analysis Methods, PennWell Publishing Company, Tulsa, Oklahoma, 648pp.

DICKSON, J. A. D., 1965. A modified staining technique for carbonates in thin section. *Nature*, 205:597.

DICKSON, J. A. D., 1966. Carbonate identification and genesis as revealed by staining: *Journal of Sedimentary Petrology*, **36**, 491-505.

DICKSON, J. A. D. and COLEMAN, M. L., 1980. Changes in carbon and oxygen isotope composition during limestone diagenesis. *Sedimentology,* **27**, 107-118.

DRUCKMAN, Y. and MOORE, C.H., 1985**.** Late subsurface secondary porosity in a Jurassic grainstone reservoir, Smackover Formation, Mt. Vernon field, southern

Arkansas. In: Roehl, O. P. and Choquette, W. P. (eds.), Carbonate Petroleum Reservoirs. Springer-Verlag, Berlin, 369-384.

DUNHAM, R. J., 1962. Classification of carbonate rocks according to depositional texture. In: Ham, W. E. (ed), Classification of carbonate rocks. *AAPG.*, Tulsa, Okla, 108-121.

DUNHAM, R. J., 1969. Early vadose silt in Townsend Mount (reef), New Mexico. In: Friedman, G. M. (ed.), Depositional environments in carbonate rocks: A symposium. Special Publication of the Society of Economic Palaeontologists and Mineralogists. Tulsa, Oklahoma, **14**, 139-181.

DUNHAM, R. J., 1971. Meniscus cements. In: BRICKER, O. P. (ed.), Carbonate cement. *AAPG.,* Studies in Geology, **19**, John Hopkins University Press, Baltimore, 296-300.

EICHENSEER, H. and LUTERBACHER, H., 1992. The marine Paleogene of the Tremp Region (NE Spain), depositional sequence, facies history, biostratigraphy and controlling factors. *Facies, 27*, 119-152.

EL-ALAMI, M., 1996. Habitate of oil Abu Attifel area, Sirt Basin, Libya. In: Salem, M. J., Busrewil, M. T., Misallati, A.A. and Sola, M. A. (eds.), *The Geology of the Sirt Basin*. Elsevier, Amsterdam, **II**, 337-347.

EL-ALAMI, M., RAHOMA, S. and BUTT, A. A., 1989. Hydrocarbon habitat in the Sirt Basin, Northern Libya. *Petrol. Res. Jour*., **1**, 17-29.

EL-ARNAUTI, A. and SHELMANI, M., 1988. A contribution to the northeast Libyan subsurface stratigraphy with emphasis on Pre-Mesozoic. In: El-Arnaauti, A. (ed.), Subsurface Palynostratigraphy of Northeastern Libya.

EL BAKAI, T. M., 1996. Diagenesis and diagenetic history of the Lidam Formation in NW Sirt Basin. In: Salem, M. J., Busrewil, M. T., Misallati, A.A. and Sola, M. A. (eds.), *The Geology of the Sirt Basin*. Elsevier, Amsterdam, **II**, 83-98.

EL-GHOUL, A., 1996. An approach to locate subtle Waha structural traps on the Zelten Platform: geology and geophysics. In: Salem, M. J., Busrewil, M. T., Misallati, A.

A. And Sola, M. (eds), *The Geology of the Sirt Basin*. Elsevier, Amsterdam, **III**, 137-154.

EL-HAWAT, A. S., 1985. Submarine slope carbonate mass movement in response to global lowering of sea-level: Appollonia Formation Lower - Middle Eocene, northeast Libya. 6th European Regional Meeting of IAS. Lilda.

EL-HAWAT, A. S., 1992. The Nubian Sandstone sequence in Sirt Basin, Libya: sedimentary facies and events. In: Sadek. A. (ed.), *Geology of the Arab World*. Cairo Univ. **1**, 317-327.

EL-HAWAT, A. S., SANUSSI, R. B., SHELWI, S. A., FIGI, O. O., ZAYANI, A., MEGASSABI, M., BITAL-MAL, Y., AMMAR, A., SALEM, F. M. and AHMED, S., 1986a. Stratigraphy and sedimentation of Eocene nummulitic bank complexes, Darnah Formation, NE, Libya. 12th International Sedimentological Congress. *International Association of Sedimentologists.* Canberra, Australia.

EL-HAWAT. A.S. and SHELMANI, M.A., 1993. Short notes and guidebook on the geology of Al Jabal la Akhdar, Cyrenaica NE Libya. Interprint, Malta, 70 pp.

EMERY, D. and MYERS, K. J. (eds.) 1996. *Sequence Stratigraphy*. 297 pp. Oxford: Blackwell Science.

EVAMY, B. D., 1969. The precipitation environments and correlation of some calcite cement deduced from artificial stains. *Journal of Sedimentary Petrology*, **39**, 787-793.

FAIRCHILD, I. J., 1983. Chemical controls of cathodoluminescence of natural dolomite and calcite: new data and review. *Sedimentology*, **30,** 579-583.

FAIRCHILD, I. J., HENDRY, G., QUEST, M. and TUCKER, M., 1988. Chemical analysis of sedimentary rocks. *In:* Tucker, M. (ed). *Techniques in Sedimentology*. Oxford, Blackwell Scientific Publications. P. 274-354.

FISCHER, A. G. and BOTTJER, D. J., 1881. Orbital forcing and sedimentary sequences (introduction to special issue). *Journal of Sedimentary Petrology*, **61**, 1063-1069.

FLÜGEL, E., 1982. Microfacies analysis of limestone. Springer-Verlag, Berlin-Heidelberg-New York, 633p.

FLÜGEL, E., 2004. Microfacies of Carbonate Rocks: Analysis, Interpretation and Application. Springer-Verlag, Berlin-Heidelberg-New York, 976pp.

FOURNIE, D., 1975. L'analyse sequentialle et la sedimentologie de I'Ypresien de Tunisie. *Bulletin Centre Recherche, Pau-SNPA*, **9,** 27-75.

FUTYAN, A. and JAWZI, A.H., 1996. Petrography and reservoir quality of the Lower Cretaceous sandstone in the deep Mar Trough, Sirt Basin. *In:* Salem, M. J., EL-Hawat, A. S. and Sbeta, A. M. (eds.), *The geology of Sirt Basin*: Amsterdam, Elsevier, 287-308.

FRANK, T. C., LOHMANN, K. C. and MEYERS, W. J., 1995. Chronostratigraphic significance of cathodoluminescence zoning in syntaxial cement: Mississippian Lake Valley Formation, New Mexico. *Sedimentary Geology*, **105**, 29-50.

FRIEDMAN, G. M., 1965. Terminology of crystallization textures and fabrics in sedimentary rocks. *Journal of Sedimentary Petrology*, **35,** 643-655.

FUTERER, E., 1982. Experiments on the distinction between wave and current influenced shell accumulations. In: Einsele, G. and Seilacher, A. (eds.), *Cyclic Event Stratification,* Springer-Verlag, 175-179.

GALLOWAY, W.E., 1989. Genetic stratigraphic sequences in basin analysis, I. Architecture and genesis of flooding-surface bounded depositional units. *Bull. AAPG.,* **73,** 125–142.

GAMMUDI, M.A., 1996. The Ostracod fauna of the Miocene Maradah Formation exposed in the Eastern Sirt Basin, Libya. In: Salem, M. J., Busrewil, M. T., Misallati, A.A. and Sola, M. A. (eds.), *The Geology of the Sirt Basin*. Elsevier, Amsterdam, I, 391-418.

GEEL, T., 2000. Recognition of stratigraphic sequences in carbonate platform and slope deposits: empirical models based on microfacies analysis of Palaeogene deposits in southeastern Spain: *Palaeogeography, Palaeoclimatology, Palaeoecology*, **155**, 211-238.

GHORI. K. A. R., and MOHAMMED, R. A., 1996, The application of petroleum generation modelling to the eastern Sirt Basin, Libya. In: Salem, M. J., EL-Hawat, S. A. and Sbeta, M. A. (eds.), *The Geology of Sirt Basin*: Amsterdam, Elsevier, **ll**, 529-540.

GHOSE, B.K., 1977. Paleoecology of the Cenozoic reefal foraminifers and algae—a brief review, *Palaeogeography, Palaeoclimatology, Palaeoecology*, **22**, 231–256.

GILHAM, R.F. and BRISTOW, C.S., 1998. Facies architecture and geometry of a prograding carbonate ramp during the early stages of foreland basin evolution: Lower Eocene sequences, Sierra del Cadı´, SE Pyrenees, Spain. In: WRIGHT, V.P. and BURCHETTE, T.P. (eds.), Carbonate Ramps, *Geol. Soc. London Spec. Publ.*, *149,* 181–203.

GOLDHAMMER, R. K., DUNN, P. A. and HARDIE, L. A., 1990. Depositional cycles, composite sea-level changes, cycle stacking patterns, and the hierarchy of stratigraphic forcing: Examples from Alpine Triassic carbonates: *Geological Society of America Bulletin*, **102**, 535-562.

GONZALEZ, L. A. and LOHMANN, K. C., 1985. Carbon and oxygen isotopic composition in Holocene reefal carbonates. *Geology*, **13**, 811-814.

GOUDARZI, G. H., 1980. Structure of Libya. In: Salem, M. J. and Busrewil, M. T. (eds.), *The Geology of Libya*. Academic Press, Tripoli, **III**, 879-892.

GRAS, R. and THUSU, B., 1998. Trap architecture of the Early Cretaceous Sarir Sandstone in the eastern Sirt Basin, Libya. In: Macgregor, D.S., Moody, R.T.J., and Clark-Lowes, D.D. (eds.), Petroleum geology of North Africa: *Geological Society, Special Publication,* **132**, 317–334.

GUIRAUD, R. 1998. Mesozoic rifting and basin inversion along the northern African Tethyan margin. In: Macgregor, D. S., Moody, R. T. J., Clark Lowes. (eds.), Petroleum Geology of North Africa. Geol. Soc. Special Publication, **132**, 217-230.

GUIRAUD, R. and BELLION, Y., 1995. Late Carboniferous to Recent geodynamic evolution of West Gondwanian cratonic Tethyan margins. In: Nairn, A., Dercourt, J. and Verielynck, B. (eds.), Basins and Margins. *The Ocean*. The Tethys Ocean, Planum, New York, **8**, 101-124.

GUIRAUD, R. and BOSWORTH, W., 1997. Senonian basin inversion and rejuvenation of rifting in Africa and Arabia: synthesis and implications to plate-scale tectonics: *Tectonophysics*, **282**, 39-82.

GUIRAUD, R. and MAURIN J. C., 1992. Early Cretaceous rifts of western and central Africa: *An overview: Tectono-physics*, **213**, 153-168.

GUMATI, Y. D. and KANES, W. H., 1985. Early Tertiary subsidence and sedimentary facies, north Sirt Basin, Libya. *Bull. AAPG.*, **69**, 39-52.

GUMATI, Y. D. and NAIRN, A. E., 1991. Tectonic subsidence, the Sirt Basin, Libya. *Journal of Petroleum Geology*, **14**, 93-102.

GUMATI, Y. D. and S. SCHAMEL., 1988. Therma maturation history of the Sirt Basin, Libya: *Journal of Petroleum Geology*, **11**, 205-218.

GUMATI, Y. D., KANES, W. H. and SCHAMEL, S., 1996. An evaluation of the hydrocarbon potential of the sedimentary basins of Libya. *Journal of Petroleum Geology*, **19**, 95-112.

HALLETT, D., and EL GHOUL, M., 1996**.** Oil and gas potential of the deep troughs areas in the Sirt Basin, Libya in: Salem , M. J., EL-Hawat, A. S. and Sbeta, A. M. (eds.), *The geology of Sirt Basin*: Amsterdam, Elsevier, **7**, 455-484.

HALLETTT, D., 2002. *Petroleum Geology of Libya*. Amsterdam, Elsevier, 372-387.

HALLOCK, P., 1979. Trends in test shape with depth in large, symbiont-bearing foraminifera. *Journal of Foraminiferal Research,* **9**, 61-69.

HALLOCK, P., 1984. Distribution of larger foraminiferal assemblages on two Pacific coral reefs. *Journal of Foraminiferal Research*, **14**, 250-261.

HALLOCK, P. and GLENN, E. C., 1986. Larger foraminifera: A tool for palaeoenvironmental analysis of Cenozoic depositional facies. *Palaios,* **1**, 55-64.

HALLOCK, P. and HANSEN, H. J., 1979. Depth adaptation in Amphistegina: change in lamellar thickness. *Bulletin of the Geological Society of Denmark,* **27**, 99-104.

HALLOCK, P. and SCHLAGER, W., 1986. Nutrient excess and the demise of coral reefs and carbonate platforms. Palaios, **1**, 389-398.

HAMMUDA, O. S., 1973. Eocene biostratigraphy of Derna Area, northeast Libya. Ph.D Thesis. University of Colorado. USA., 427pp.

HANDFORD, C.R. and LOUCKS, R.G., 1993. Carbonate depositional sequences and systems tracts-responses of carbonate platforms to relative sea-level changes. In: Loucks, R.G. and Sarg, J.F. (eds.), Carbonate Sequence Stratigraphy. *AAPG.*, Memoir, **57**, 3–42.

HAQ, B.U., HARDENBOL, J. and VAIL, P.R., 1987. Chronology of fluctuating sea levels since the Triassic (250 million years ago to present). *Science,* **235**, 1156–1166.

HASLER, C. A. 2004. Geometry and internal discontinuities of a Ypresian carbonate reservoir (SIT oil field, Tunisia). *Terre et Environment*, **45**, 230pp.

HAYNES, J. R., 1965. Symbiosis wall structure and habitat in foraminifera. *Special Publication- Cushman Foundation for Foraminiferal Research,* **16,** 40-43.

HECKEL, P. H., 1985. Recent interpretations of the Late Paleozoic cyclothems: Proceedings of the Third Annual Field Conference, Mid-Content Section, *Society of Economic Paleontologists and Mineralogists,* 1-22.

HENSON, F. R. S., 1950. Cretaceous and Tertiary reef formation and associated sediments in Middle East. *Bull. AAPG.*, **34**, 215-238.

HOHENEGGER, J., YORDANOVA, E. and HATTA, A., 2000. Remarks on west Pacific nummulitidae (Foraminifera). *Journal of Foraminiferal Research,* **30**, 3-28.

HOLAIL, H., 1994. Diagenesis of the Middle Eocene "nummulite banks" of the Giza Pyramids Plateau, Egypt. Qatar Univ. Sci. J. **14**, 146-152.

HOLLAUS, S. S. and HOTTINGER, L., 1997. Temperature dependence of endosymbiotic relationships? Evidence from the depth range of Mediterranean Amphistegina lessonii (Foraminifera) truncated by the thermocline. *Eclogue Helvetiae,* **90**, 591-597.

HOTTINGER, L. and DREHER, D., 1974. Differentiation of protoplasm nummulitidae (Foraminifera) from Elat, Red Sea. *Marine Biology*, **25**, 41-61.

HOTTINGER, L., 1983. Processes determining the distribution of larger foraminifera in space and time. Utrecht Micropaleont. Bull **30**, 239–253.

HUDSON, J. D., 1977. Stable isotopes and limestone lithification. *Journal of the Geological Society of London*, **133**, 637-660.

HUDSON, J. D. and PALFRAMAN, D.F.D., 1969. The ecology and preservation of the Oxford clay fauna at Woodham, Buckinghamshire. *Quart. Journ. Geol. Soc London*, **124**, 387-418.

HUNT, D. and TUCKER, M.E., 1993. Sequence stratigraphy of carbonate shelves with an example from the mid-Cretaceous (Urgonian) of Southeast France. In: Posamentier, H.W., Summerhayes, C.P., Haq, B.U. and Allen, G.P. (eds.), Sequence Stratigraphy and Facies Associations. *International Association of Sedimentologists,* Special Publication, **18,** 307–341.

HUNT, D. and TUCKER, M.E., 1995. Stranded parasequences and the forced regressive wedge systems tract: deposition during base-level fall. *Sedimentary Geology,* **95**, 147-160.

IRWIN, H., CURTIS, C. D. and COLEMAN, M., 1977. Isotopic evidence for source of diagenetic carbonates formed during burial of organic-rich sediments. *Nature,* **269**, 209-213.

JAMES, N. P. and CHOQUETTE, P. W., 1983. Diagenesis 6. Limestone – the sea-floor diagenetic environment. *Geosciences Canada*, **10**, 162-180.

JAMES, N. P. and CHOQUETTE, P. W., 1984. Diagenesis 6. Limestone – the meteoric diagenetic environment. *Geosciences Canada*, **11**, 194-1161.

JAMES, N. P. and CHOQUETTE, P. W., 1988. *Paleokarasts*. Springer- Verlag, New York, 416pp..

JAMES, N. P. and CHOQUETTE, P. W., 1990b. Limestone – The meteoric diagenetic environment. In: McIlreath, A. and Morrow, D. W. (eds.), Diagenesis. Geoscience Canada Reprint Series, **4**, 35-73.

JAMES, N. P. and GINSBURG, R. N., 1979. The seaward margin of Belize barrier and atoll reefs. *International Association of Sedimentologists*, Special. Publication, **46**, 523-544.

JAMES, N. P. and KENDALL, A. C., 1992. Introduction to carbonate and evaporate facies models. In: Walker, R. G. and James, N. P. (eds.), Facies Models: Response to Sea Level Change. *Geological Association of Canada,* GeoTest 1, 265-275.

JONES, B. and DESTOCHERS, A., 1992. Shallow platform carbonates. In: Walker, R. G. and James, N. P. (eds.), Facies Models: Response to Sea Level Change, *Geological Association of Canada*, GeoText 1, 277-301.

JONES, R. W., 1999. Marine invertebrate (chiefly foraminifera) evidence for the palaeogeography of the Oligocene-Miocene of western Eurasia, and consequences for terrestrial vertebrate migration. In: Agusti, J., Andrews, P. and Rook, L. (eds.), Hominoid evolution and climatic change in Europe. Cambridge Univ. Press, **1**, 274-308.

JORRY, S., 2004. The Eocene nummulite carbonates (Central Tunisis and NE Libya), sedimentology, depositional environments and application to oil reservoir. phD. Thesis, Université De Genéve. Départment de Géologie et de Paléontologie.

JORRY, S., DAVAUD, E. and CALNE, B., 2003. Structurally controlled distribution of nummulite deposits: Example of the Ypresian El Garia Formation (Kersa Plateau, Central Tunisia). *Journal of Petroleum Geology*, **23**, 283-306.

KEHEILA, E. A. and EL-AYYAT, A. M., 1990. Lower Eocene carbonate facies, environments and sedimentary cycles in Upper Egypt: Evidence for global sea-level changes. *Palaeogeogr. Palaeoclimatol. Palaeoecol.*, **81**, 33-47.

KLETT, T.R., AHLBRANDT, T.S., SCHMOKER, J.W. and DOLTON, G.L., 1997. Ranking of the world's oil and gas provinces by known petroleum volumes: *U.S. Geological Survey Open-File Report* 97-463, CD-ROM.

KLITZSCH, E., 1970. Die Struckturgeschichte der Zentral-Sahara: Neue Erkenntnisse zum Bau und zur Palaeogeographie eines Tafellandes. *Geol. Rundsch.*, **59**, 459-527.

KLITZSCH, E., 1971. The structural development of the part of North Africa since Cambrian time. In: *The Geology of Libya*. Tripoli University, Faculty of Science, Tripoli, 253-262.

KOSCEC, G. B. and GHERRYO, S. S., 1996. Geology of reservoir performance of the Messlah Oil Field, Libya. In: Salem, M. J., Busrewil, M. T., Misallati, A.A. and Sola, M. A. (eds.), *The Geology of the Sirt Basin*. Elsevier, Amsterdam, **II,** 365-389.

KULKA, A., 1985. Sedimentological model in the Tatra Eocene. *Kwartalnik Geologiczny*, **29**, 31-64.

LANGER, M. R. and HOTTINGER, L., 2000. Biogeography of selected larger foraminifera. *Micropaleontology,* **26**, 126-215.

LAWRENCE, J. R. and WHITE, J. W. C., 1991. The elusive climate signal in the isotopic composition of precipitation. In: Taylor, H. P. and O'Neil, J. R. (eds.), *Geochemical Society Special Publication*, **3**, 169-185.

LEHRMANN, D.J. and GOLDHAMMER, R.K., 1999. Secular variation in parasequence and facies stacking patterns of platform carbonates: a guide to application of stacking patterns analysis in strata of diverse facies and settings. In: HARRIS, P.M., SALLER, A.H., SIMO, J.A (Eds). Advances in Carbonate Sequence Stratigraphy. *Society of Economic Paleontologists and Mineralogists Special Publication*, **63**, 187-225.

LOHMANN, K. C., 1988. Geochemical patterns of meteoric diagenetic systems and their application to studies of paleokarst. In: James, N. P. and Choquette, P. W. (eds.), *Paleokarst*. Springler-Verlag, New York, 58-80.

LONGMAN, M. W., 1980. Carbonate diagenetic textures from nearshore diagenetic environments. *Bull. AAPG.*, **64,** 461-487.

LONGMAN, M.W., 1982. Carbonate diagenesis as a control on stratigraphic traps. *Am. Ass. Petrol. Geol.* Educ. Course Note Series, 21, 159pp.

LOPATIN, N.V., 1971. Temperature and geologic time as factors in coalification: Akademiya Nauk Soyuz sovetskikh Sotsialisticheskikh Respublik Izvestiya, SSeriya Geologicheskaya, **3**, 95-106.

LOUCKS, R. G., and SARG, J. F., 1993 (eds.), Carbonate Sequence Stratigraphy – Recent Developments and Applications. *AAPG., Memoir*, **57**, 545.

LOUCKS, R. G., MOODY, R. T. J., BELLS, J. K. and BROWN, A. A., 1998. Regional depositional setting and pore network systems of the El Garia Formation (Metlaoui Group, Lower Eocene), offshore Tunisia. In: MacGregor, D. S., Moody, R. T. J. and Clark-Lowes, D. D. (eds.), Petroleum Geology of North Africa. *Geol. Soc., London, Special Publication,* **132**, 355-374.

MACHEI, H. G. and BURTON, E. A., 1991. Factors governing cathodoluminescence in calcite and dolomite. In: Barker, C. E. and Kopp, D. C. (eds.), Luminescence Microscopy: Quantitative and Qualitative Aspects. *Soc. Econ. Palaeont. Miner.*, Short Course, **25**, 37-57.

MACHEL, H. G., KROUSE, H. R. and SASSEN, R., 1995. Products and distinguishing criteria of bacterial and thermochemical sulphate reduction. *Applied Geochemistry*, **10**, 373-389.

MACINTYRE, I. G., PRUFERT-BEBOUT, L. and REID, R. P., 2000. The role of endolithic cyanobacteria in the formation of lithified laminae in Bahamian stromatolites. *Sedimentology*, **47**, 915-921.

MANSOUR, T. A., and MAGAIRYAH, I. A., 1996. Petroleum geology and stratigraphy of the southeastern part of the Sirt Basin. In: Salem, M. J., Busrewil, M. T., Misallati, A.A. and Sola, M. A. (eds.), *The Geology of the Sirt Basin*. Elsevier, Amsterdam, **II**, 485-528.

MARSHALL, J. D., 1988. Cathodoluminescence of Geological Materials. Unwin-Hyman, London, 146pp.

MARSHALL, J. D., 1992. Climatic and oceanographic isotopic signals from the carbonate rock record and their preservation. *Geological Magazine,* **129**, 143-160.

MASSA, D., and DELORT, T., 1984, Evolution du Bassin de Syrte (Libya) du Cambrien au Cretace Basal: *Bulletin Société Géologique de France*, Series 7, **26**, 1087–1096.

MCILREATH, I. A. and MORROW, D. W., 1990. Diagenesis. Geosci. Can. Rep. Ser. **4**.

MCQUILLAN, H., 1973. Small-scale fracture density in Asmari Formation of south west Iran and its relation to bed thickness and structural setting. *Bull. AAPG.,* **57,** 2367-2385.

MEGERISI, M. and MAMGAIN, V. D., 1980a. The Upper Creataceous-Tertiary Formations of Northern Libya. *In*: Salem, M. J. and Busrewil, M. T. (eds.), *The Geology of Libya*. Academic Press, London, **I**, 67-72.

MEYERS, W. J., 1978. Carbonate cements: their regional distribution and interpretation in Mississippian limestone of southwestern New Mexico. *Sedimentology*, **25**, 371-399.

MIALL, A. D., 1986. Eustatic sea level changes interpreted from seismic stratigraphy: a critique of the methology with particular reference to the North Sea Jurassic record. *Bull. AAPG*., **70**, 131-137.

MEYERS, W. J. 1991. Calcite cement stratigraphy, an overview. In: Barker, C. E. and Kopp, D. C. (eds.), Luminescence Microscopy: Quantitative and Qualitative Aspects. *Soc. Econ. Palaeont. Miner*., Short Course, **25**, 133-148.

MIALL, A. D. and TYLER, N., 1991. The three-dimentional facies architecture of terrigenous classtic sediments and its implications for hydrocarbon discovery and recovery: Society of Economic Paleontologists and Minerologists Concepts in Sedimentology and Paleontology, **3**, 309pp.

MILLER, J., 1988. Cathodoluminescence microscopy. In: Tucker, M. E. (ed.), *Techniques in Sedimentology*. Blackwell, Oxford, 394pp.

MILLIMAN, J. D., 1974. Marine Carbonate. Springer-Verlag, Berlin, 375pp.

MITCHUM JR., R.M., 1977. Seismic stratigraphy and global changes of sea level, part 11: glossary of terms used in seismic stratigraphy. In: Payton, C.E. (Ed.), Seismic

Stratigraphy - Applications to Hydrocarbon Exploration. Memoir, **26**. *AAPG.*, 205–212.

MOODY, R. T . J., 1987. The Ypresian carbonates of Tunisia- a model of foraminiferal facies distribution. In: Hart, M. B. (ed.), Micropalaeontology of carbonate environments. B.M.S. Series, Ellis Horwood, Chichester, 82-92.

MOODY, R. T. J. and GRANT, G. G., 1989. On the importance of bioclasts in the definition of a depositional model for the Metlaoui Carbonate Group. Actes des IIeme Journées de Géologie Tunisienne appliquée a la récherche des Hydrocarbures, 409 - 427.

MOORE, C. H., 1989. Carbonate diagenesis and porosity. Elsevier, 338pp.

MOORE, C. H., 2001. Carbonate Reservoirs. Elsevier, 444pp.

MORES, J. and MACKENZIE, F. T., 1990. Geochemistry of sedimentary carbonates. Elsevier, New York, 707pp.

MOUZUGHI, A. J. and TALEB, T. M., 1981. Tectonic elements of Libya, 1:2,000,000. National Oil Corporation, Libya.

MOZLEY, P.S., and BURNS, S.J., 1993. Oxygen and carbon isotopic composition of marine carbonate concretions*: an overview: Journal of Sedimentary Petrology*, 63, 73-83.

MURRAY, J. W., 1991. Ecology and distribution of benthonic foraminifera. In: Lee, J. J. and Anderson, R. O. (eds.), Biology of Foraminifera. Academic Press, London, 221-284.

NEMKOV, G. I., 1962. Remarks on the palaeoecology of nummulites. *Micropaleontology*, **6**, 64-72.

OLDERSHOW, A. E. and SCOFFIN, T.P., 1967. The source of ferroan and non-ferroan calcite cements in the Halkin and Wenlock Limestones. *Geological Journal*, **5**, 309-320.

PARRELLA, G., 1990. Evaluation of the minor reservoir of the Assumood Field. Geological note 178. (Sirte Oil Company internal report).

PARSONS, M.B., AZGAAR, A.M., and CURRY, J.J., 1980. Hydrocarbon occurrences in the Sirte Basin, Libya. In: Miall, A.D. (ed.). *Canadian Society Petroleum Geologists Memoir*, **6**, 723–732.

PHLEGER, F. B., 1960. Ecology and distribution of recent foraminifera. Johns Hopkins, Baltimore, Md. 297pp.

PICKFORD, S., 1992. Libya – A Hydrocarbon exploration evaluation. (NOC, Unpublished report).

PITMAN, W. C., 1978. Relationship between eustasy and stratigraphic sequences on passive margins: *Geology Society of America Bulletin*, **89**, 1389-1403.

PLINT, A.G. and NUMMEDAL, D., 2000. The falling stage systems tract: recognition and importance in sequence stratigraphic analysis. In: Hunt, D. and Gawthorpe, R.L. (eds.), Sedimentary Response to Forced Regression. Special Publication, **172.** *Geological Society of London*, 1–17.

POMERAL, C., 1981. Stratotypes of Paleogene stages. International Union of geological Science, Commission on stratigraphy, Memoir 2. *Bulletin d'Information des Géol. De Bassin du Paris.*

POSAMENTIER, H. W. and JAMES, D. P., 1993. An overview of sequence stratigraphic concepts: Used abuses. In: Posamentier, H. W. and Summerhayes, C. P. (eds.), *Sequence Stratigraphy and Facies Associations*, Oxford, Blackwell, 3-18.

POSAMENTIER, H.W. and VAIL, P.R., 1988. Eustatic controls on clastic deposition II — sequence and systems tract models. In: Wilgus, C.K., Hastings, B.S., Kendall, C.G.St.C., Posamentier, H.W., Ross, C.A. and Van Wagoner, J.C. (eds.), Sea Level Changes — An Integrated Approach. *Society of Economic Paleontologists and Mineralogists (SEPM),* Special Publication, **42,** 125–154.

PRATT, B.R.. and JAMES, N.P., 1986. The St George Group (Lower Ordovician) of western Newfoundland: tidal flat island model for carbonate sedimentation in shallow epeiric seas. *Sedimentology*, **33**, 313-343.

RACEY, A., 1988. Nummulitid biostratigraphy and Palaeogene palaeoenvironments, Sultanate of Oman. *PhD thesis*, University of London, 510pp.

RACEY, A., 1994. Biostratigraphy and palaeobiogeographic significance of Tertiary nummulitids (foraminifera) from northern Oman. In: Simmons, M.D. (ed.), Micropalaeontology and Hydrocarbon Exploration in the Middle East. Chapman and Hall, London, 343–370.

RACEY, A., 1995. Palaeoenvironmental significance of larger foraminiferal biofabrics from the Middle Eocene Seeb Limestone Formation of Oman: Implications for petroleum exploration. In: AL-Husseini, M.I. (ed.), *GE0'94 The Middle East Petroleum Geosciences,* published by Gulf-Petrolink, Bahrain, **II**, 793-8 10.

RACEY, A., 2001. A review of Eocene nummulite accumulations: Structure, formation and reservoir potential. *Journal of Petroleum Geology,* **24**, 79-100.

RACEY, A., BAILEY, H.W., BECKETT, D., GALLAGHER, L.T., HAMFTON, M.J. and McQUILKEN, J., 2001. The petroleum geology of the Early Eocene El Garia Formation in the Hasdrubal Field, Offshore Tunisia. *Journal of Petroleum Geology,* **24**, 29-53

RACZ, L., 1979. Paleocene carbonate development of Ras al Hamra, Oman. *Bulletin des Centres de Recherches Exploration-Production Elf-Aquitaine*, **3**, 767– 779.

READ, J. F., 1995. Overview of carbonate platform sequences, cycle stratigraphy and reservoirs in greenhouse and icehouse worlds. In: Read, J. F., Kerans, C. K. and Weber, L. J. (eds.), Milankovitch Sea-Level Changes, Cycles and Reservoirs on Carbonate Platforms in Greenhouse and Ice-house Worlds, SEPM Short Course Notes, **35**, 1-102.

REALI, S., PONCHI, P. and BORROMEO, O., 2003. Sedimentological model of the El Garia Formation (Jdeir Formation), NC41, offshore Libya. In: *The Geology of Northwest Libya*, **II**, 69-97.

REID, R. P. and MACINTYRE, I. G., 2000. Microboring versus recrystallization: Further insight into the micritization process. *Journal of Sedimentary Research*, **70**, 24-28.

REISS, Z. and HOTTINGER, L., 1984. The Gulf of Aqaba**.** Ecological Micropalaeontology. Springer- Verlag, 354pp.

RIDER, M. H., 1986. The Geological Interpretation of Well Logs. Blackie, Glasgow, 175pp.

ROBERTS, J.M., 1970. Amal field, Libya. In: Halbouty, M.T. (ed.), Geology of giant petroleum fields: *American Association of Petroleum Geologists* Memoir, **14**, 438–448.

ROBERSTON, A.H.F., 1977. The origin and diagenesis of cherts from Cyprus, *Sedimentology* **24**, 11-30.

ROOHI, M., 1996. Geological history and hydrocarbon migration pattern of the Az Zaahra-Al Hufrah Platform. In: Salem, M. J., Busrewil, M. T., Misallati, A.A. and Sola, M. A. (eds.), The Geology of the Sirt Basin. Elsevier, Amsterdam, **I**, 195-232.

ROSS, C. A., 1972. Biology and ecology of Marginopora vertebralis (foraminifera), great barrier reef. *Journal of Protozoology*, **19**, 181-192.

ROTTGER, R., 1972. Die kultur von heterostegina depressa (Foraminifera: Nummulitidae). *Marine Biology,* **15,** 150-159.

SARG, J.F., 1988. Carbonate sequence stratigraphy. In: Wilgus, C.K., Hastings, B.S., Kendall, C.G.St.C., Posamentier, H.W., Ross, C.A. and VanWagoner, J.C. (eds.), Sea Level Changes - An Integrated Approach. *Society of Economic Paleontologists and Mineralogists* (SEPM), Special Publication, **42**, 155–181.

SBETA, A. M., 1991. Petrography and facies of the Middle and Upper Eocene rocks (Tellil Group), Offshore Western Libya. In: Salem, M. J. and Belaid, M. N. (eds.), *The Geology of Libya*, **V**, 1929-1966.

SCHLAGER, W., 1992. Sedimentology and sequence stratigraphy of reefs and carbonate platforms. AAPG., Continuing Education Course Note, **34**, 71 pp.

SCHLAGER, W., 1989. Drowning unconformities on carbonate platforms. In: Crevello, P.D., Wilson, J.L., Sarg, J.F. and Read, J.F. (eds.), Controls on Carbonate

Platform and Basin Development. Society of Economic Paleontologists and Mineralogists (SEPM), Special Publication, **44**, 15–25.

SCHLAGER, W., 2005. Carbonate Sedimentology and Sequence Stratigraphy. *SEPM Concepts in Sedimentology and Paleontology*, **8**, 200 pp.

SCHOLLE, P. A. and ULMER-SCHOLLE, D. S., 2003. A Color Guide to the Petrography of Carbonate Rocks: *AAPG Memoir* **77**.

SELLEY, R. C., 1969. Near-shore marine and continental sediments of the Sirt Basin, Libya. *Quart. Journal of Geological Society of London*, **124**, 419-460.

SELLEY, R. C., 1971. Structural control of the Miocene sedimentation in the Sirt Basin. In: Gray, C. (ed.), *The Geology of Libya*, 99-106.

SGHAIR, A. M. A. and EL-ALAMI, M. A., 1996. Depositional environment and diagenetic history of the Maragh Formation, NE Sirt Basin, Libya. In: Salem, M. J., Busrewil, M. T., Misallati, A.A. and Sola, M. A. (eds.), *The Geology of the Sirt Basin*. Elsevier, Amsterdam, **II**, 263-271.

SHAABAN. M. N., 2004. Diagenesis of the Lower Eocene Thebes Formation, Gebel Rewagen area, Eastern Desert, Egypt. *Sedimentary Geology*, **165**, 53-65.

SHARP, Z., 2007. Principle of stable isotope geochemistry. *Prentice Hall*. 344pp.

SINCLAIR, H.D., SAYER, Z.R. and TUCKER, M.E., 1998. Carbonate sedimentation during early foreland basin subsidence: the Eocene succession of the French Alps. In: Wright, V.P. and Burchette, T.P. (eds.), Carbonate Ramps. *Geol. Soc. London Spec. Publ.*, **149**, 205–227.

SLOSS, L.L., 1963. Sequences in the cratonic interior of North America. *Geological Society of America Bulletin*, **74**, 93–114.

SPENCE, G.H. and TUCKER, M.E., 2007. A proposed integrated multi-signature model for peritidal cycles in carbonates. *Journal of Sedimentary Research*, **77**, 797-808.

STEINEN, R. P., 1974. Phreatic and vadose diagenetic modification of Pleistocene limestone: petrographic observations from subsurface of Barbados, West Indies. *Bull. AAPG.,* **58**, 1008-1024.

STRASSER, A., HILGEN, F.J. and HECKEL, P.H., 2006. Cyclostratigraphy – concepts, definitions and applications. *Newsletters Stratigraphy*, **42**, 75-114.

 STRASSER, A., PITTET, B., HILLGARTNER, H., and PASQUIER, J.-B., 1999. Depositional sequences in shallow carbonate-dominated sedimentary systems: concepts for a high-resolution analysis. *Sedimentary Geology*, **128**, 201-221.

TREVISANI, E. and PAPAZZONI, C. A., 1996. Palaeoenvironmental control on the morphology of Nummulites fabianii in the Late Priabonian parasequences of the Mortisa Sandstone (Venetian Alps, northern Italy). *Rivista Italiana Paleontologia Stratigrafia*, **102**, 263-366.

TUCKER, M. E., 1988. Techniques in Sedimentology. Blackwells, Oxford, 394pp.

TUCKER, M. E., 2001. Sedimentary Petrology: An Introduction to the Origin of Sedimentary Rocks. 3rd edition. Blackwell Science Publications, Oxford, 260pp.

TUCKER, M. E., 1993. Carbonate diagenesis and sequence stratigraphy. In: Wright, V.P. (ed.), Sedimentology Review. Blackwell Science Publications, Oxford, 51-72.

TUCKER. M. E. and BATHURST, R. G. C., 1990. Carbonate Diagenesis. Reprint Series, *International Association of Sedimentologists*, **1**, 312pp.

TUCKER M.E., CALVET, F. and HUNT, D., 1993. The sequence stratigraphy of carbonate ramps, with application to the Muschelkalk carbonate platforms of eastern Spain. In: Posamentier, H.W., Summerhayes, C.P., Haq, B.U. and Allen, G.P. (eds.), Sequence Stratigraphy and Facies Associations. *International Association of Sedimentologists,* Special Publication, **18,** 397–415.

TUCKER, M.E. and GARLAND, J., 2010. High-frequency cycles and their sequence stratigrphic context: Orbital forcing and tectonic controls on Devonian cyclicity, Belgium. *Geologica Belgica*, **13**, 213-240.

TUCKER. M. E. and WRIGHT, V. P., 1990. Carbonate Sedimentology. Blackwell Scientific Publication, Oxford, 482pp.

VAIL, P. R., MITCHUM, and THOMPSON, S., 1977. Seismic stratigraphy and global changes of sea level, part 3: relative changes of sea level from coastal onlap. In: Payton, C.E. (ed.), Seismic Stratigraphy - Applications to Hydrocarbon Exploration. *AAPG., Memoir*, **26,** 63–81.

VAIL, P.R., AUDEMARD, F., BOWMAN, S.A., EISNER, P.N. and PEREZ-CRUZ, C., 1991. The stratigraphic signatures of tectonics, eustasy and sedimentology- an overview. In: Einsele, G., Ricken, W. and Seilacher, A. (eds.), Cycles and Events in Stratigraphy. Springer-Verlag, Berlin, 617–659.

VAN DER MEER, F. and CLOETINGH, S., 1993a. Intraplate stresses and subsidence history of the Sirt Basin (Libya). *Tectonophysics*, **226**, 37-58.

VAN DER MEER, F. and CLOETINGH, S., 1993b. Late Cretaceous and Tertiary subsidence history of the Sirt Basin (Libya): an example of the use of backstripping analysis. ITC Journal, **93**, 68-76.

VAN HOUTEN, F. B., 1983. Sirt Basin, North-Central Libya. Cretaceous rifting over a fixed mantle hotspot. *Geology*, **11**, 115-118.

VAN WAGONER, J.C., 1995. Overview of sequence stratigraphy of foreland basin deposits: terminology, summary of papers, and glossary of sequence stratigraphy. In: Van Wagoner, J.C. and Bertram, G.T. (eds.), Sequence Stratigraphy of Foreland Basin Deposits: Outcrop and Subsurface Examples from the Cretaceous of North America. *AAPG*., Memoir, **64,** ix–xxi.

VAN WAGONER, J.C., MITCHUM JR., R.M., CAMPION, K.M. and RAHMANIAN, V.D., 1990. Siliciclastic sequence stratigraphy in well logs, core, and outcrops: concepts for high-resolution correlation of time and facies. *AAPG.*, *Methods in Exploration Series*, **7**, 55pp.

VAN WAGONER, J.C., POSAMENTIER, H.W., MITCHUM, R.M., VAIL, P.R., SARG, J.F., LOUTIT, T.S. and HARDENBOL, J., 1988. An overview of sequence stratigraphy and key definitions. In: Wilgus, C.K., Hastings, B.S., Kendall, C.G.St.C., Posamentier, H.W., Ross, C.A. and Van Wagoner, J.C. (eds.),

Sea Level Changes – An Integrated Approach. *Society of Economic Paleontologists and Mineralogists (SEPM)*, Special Publication, **42,** 39-45.

WALKER, R.G., 1992. Facies, facies models and modern stratigraphic concepts. In: Walker, R.G., and James, N.J., (eds.), Facies Models: Response to Sea Level Changes; Geological Association of Canada, St. John's, Newfoundland, 1-14.

WENNEKER, J. H. N., WALLACE, K. F. and ABUGARES, I. Y. 1996. The geology and hydrocarbons of the Sirt Basin: A synopsis. In: Salem, M. J., Mouzoughi, A. J. and Hammuda, O. S. (eds.), *The Geology of the Sirt Basin*. Amsterdam, Elsevier, **1,** 3-56.

WENTWORTH, C. K., 1922. A scale of grade and classes terms for clastic sediments. *J. Geol.*, **30**, 377-392.

WILLIAMS, J. J., 1972. Augila Field, Libya – depositional environment and diagenesis of sedimentary reservoir and description of igneous reservoir. *Mem. AAPG., Special publication*, **10**, 623-632.

WILSON, M. and GUIRAUD, R., 1998. Late Permian to Recent magmatic activity on the African-arabian margin of Tethys. In: Macgregor, D. S. Moody, R. T. J. and ClarkLowes, D. D. (eds.), Petroleum Geology of North Africa. *Geological Society, London*, Special Publication, **132**, 231-263.

WILSON, M. E. J., 1995. The Tonasa Limestone Formation, Sulawesi, Indonesia: Development of a Tertiary Carbonate Platform. PhD Thesis, University of London.

WILSON, M. E. J., 2002. Cenozoic carbonates in SE Asia: Implication for equatorial carbonate development. *Sedimentary Geology*, **147**, 295-428.

WILSON, M. E. J and EVANS, M. J., 2002. Sedimentology and diagenesis of Tertiary carbonates on the Mangkalihat Peninsula, Borneo: implications for subsurface reservoir quality. *Marine and Petroleum Geology*, **19**, 873-900.

WRIGHT, V. P., 1982. The recognition and interpretation of paleokarsts: two examples from the lower Carboniferous of South Wales. *Journal of Sedimentary Petrology*, **52**, 83-94.

WRIGHT, V. P., 1986. Facies sequences on a carbonate ramp: the Carboniferous Limestone of South Wales. *Sedimentology*, **33**, 221-241.

WRIGHT, V. P., 1992. A revised classifi cation of limestones: *Sedimentary Geology*, **76**, 177-185.

YORDANOVA EK, HOHENEGGER J., 2002. Taphonomy of large foraminifera: relationships between living individuals and empty tests on flat reef slopes (Sesok Island, Japan). *Facies*, **46**, 169-204.

ZIEGLER, P. A., CLOETINGH, S., GUIRAUD, R. and STAMPFLI, G. M., 2001. Peri-Tethyan platforms: constraints on dynamics of rifting and basin inversion. In: Ziegler, P. A., Cavazza, W., Robertson, A. H. F. and Crasquin-Soleau, S. Pre-Tethys Memoir 6: Pre-Tethyan Rift/Wrench Basin and Passive Margins. *Mem. Mus. Natn. Hist. Nat*., **186**, 9-49.

APPENDIX I

Appendix I.i. List of symbols for the facies description

Bioclasts	Symbol
Nummulite	
Discocyclina	
Operculina	
Planktonic foraminifera..	
Bivalve	
Gastropod	
Coralline algae	
Scaphopod	
Brachiopod	
Bryozoan	
Echinoid	

	Symbol
Pyrite	
Glauconite	▲

Sequence stratigraphy	Symbol
Shallowing-upward cycle	▽
Deepening-upward cycle	△

I.ii. Petrographic characteristics of the Gialo Formation in well OOOO1-6, showing the point counting data, grain types, cement, matrix and porosity.

I.iii. Petrographic characteristics of the Gialo Formation in well OOOO1-6, showing the point counting data (B-forms, A-forms, whole, fragments and grain size).

I.iv. Petrographic characteristics of the Gialo Formation in well H4-6, showing the point counting data, grain types, cement, matrix and porosity.

I.v. Petrographic characteristics of the Gialo Formation in well H4-6, showing the point counting data (B-forms, A-forms, whole, fragments and grain size).
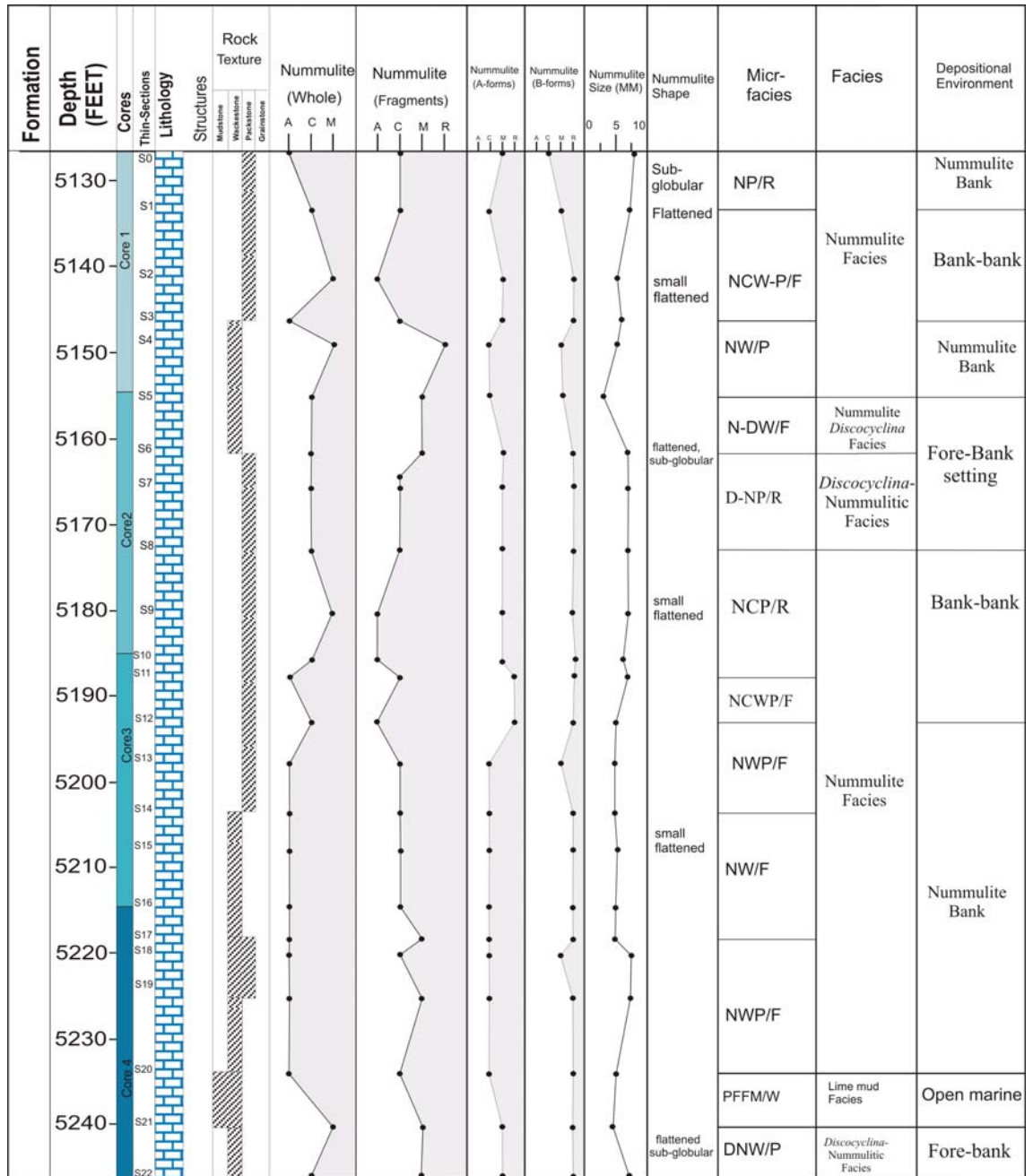
I.vi. Petrographic characteristics of the Gialo Formation in well H6-6, showing the point counting data, grain types, cement, matrix and porosity.

I.vii. Petrographic characteristics of the Gialo Formation in well H6-6, showing the point counting data (B-forms, A-forms, whole, fragments and grain size).

I.viii. Petrographic characteristics of the Gialo Formation in well H10-6, showing the point counting data, grain types, cement, matrix and porosity.

I.ix. Petrographic characteristics of the Gialo Formation in well H10-6, showing the point counting data (B-forms, A-forms, whole, fragments and grain size).
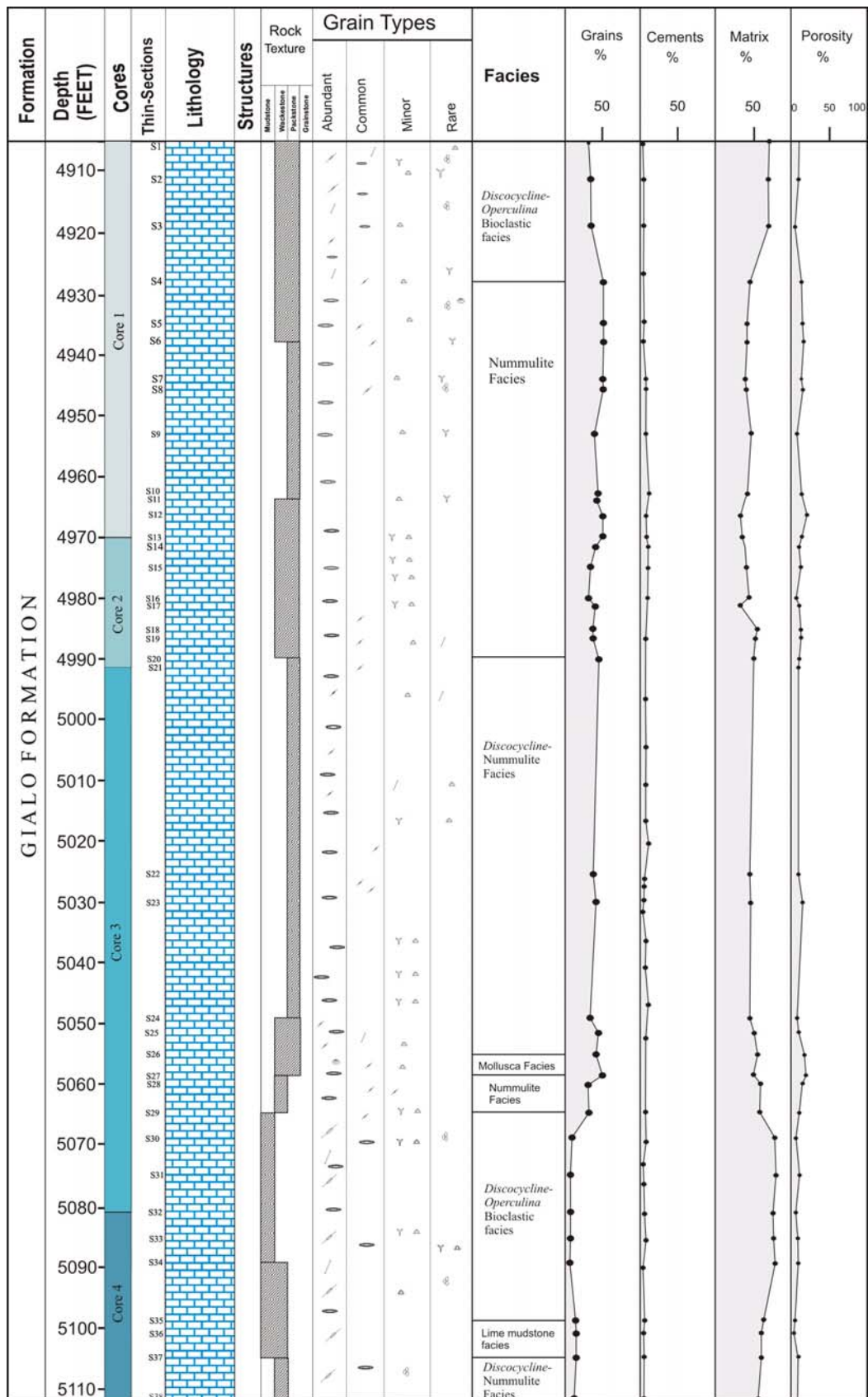
I.x. Petrographic characteristics of the Gialo Formation in well O3-6, showing the point counting data, grain types, cement, matrix and porosity.
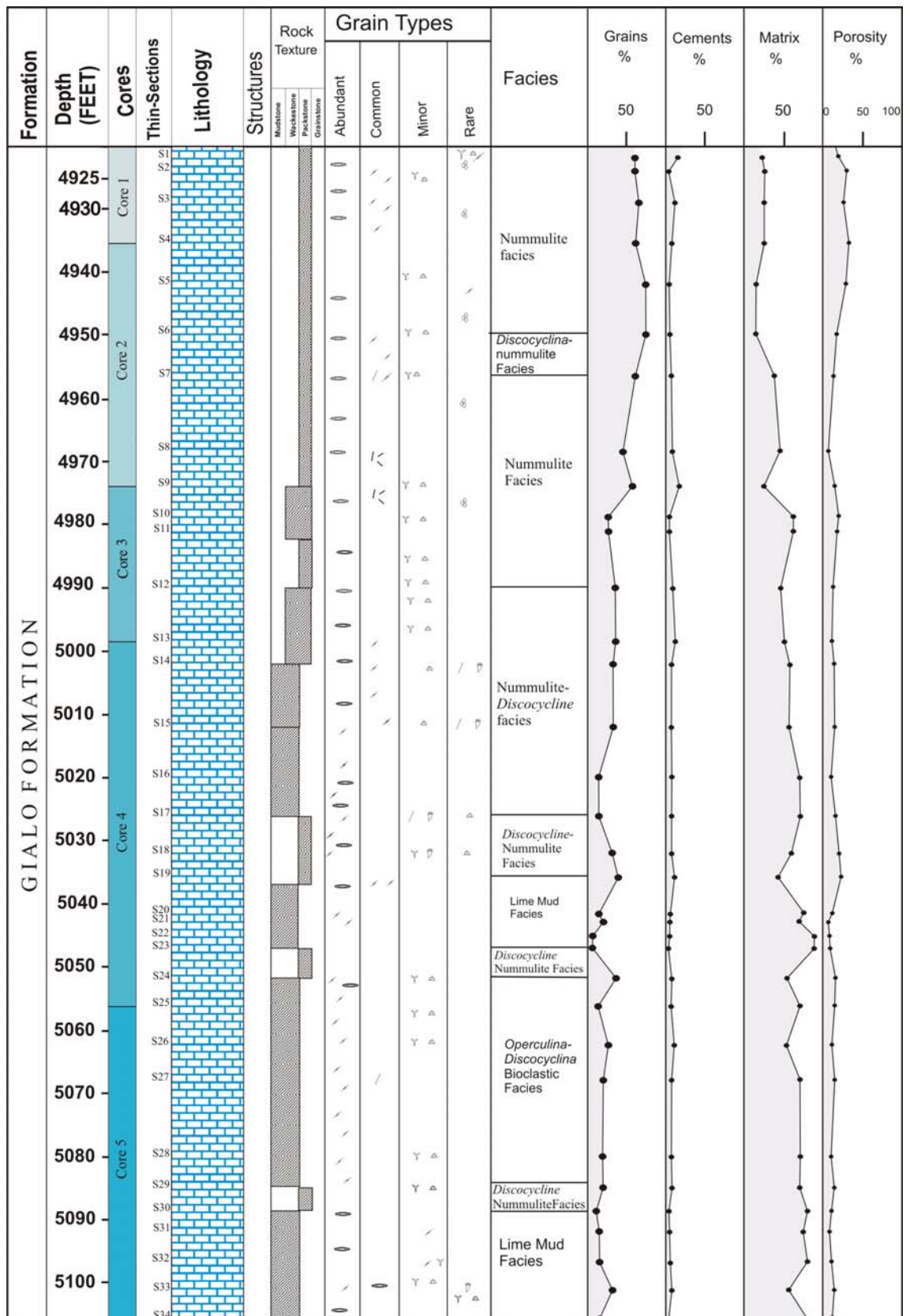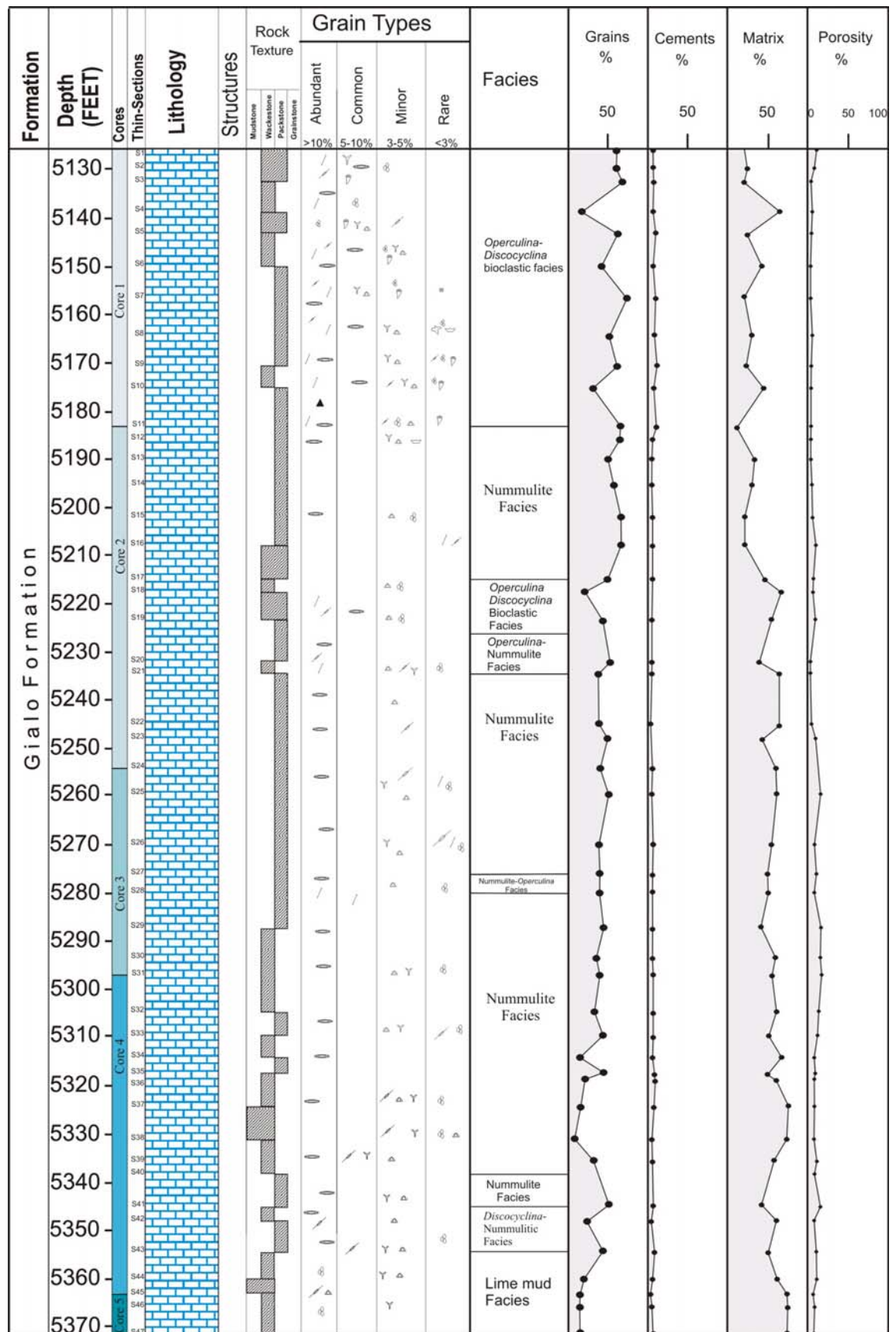
I.xi. Petrographic characteristics of the Gialo Formation in well O3-6, showing the point counting data (B-forms, A-forms, whole, fragments and grain size).
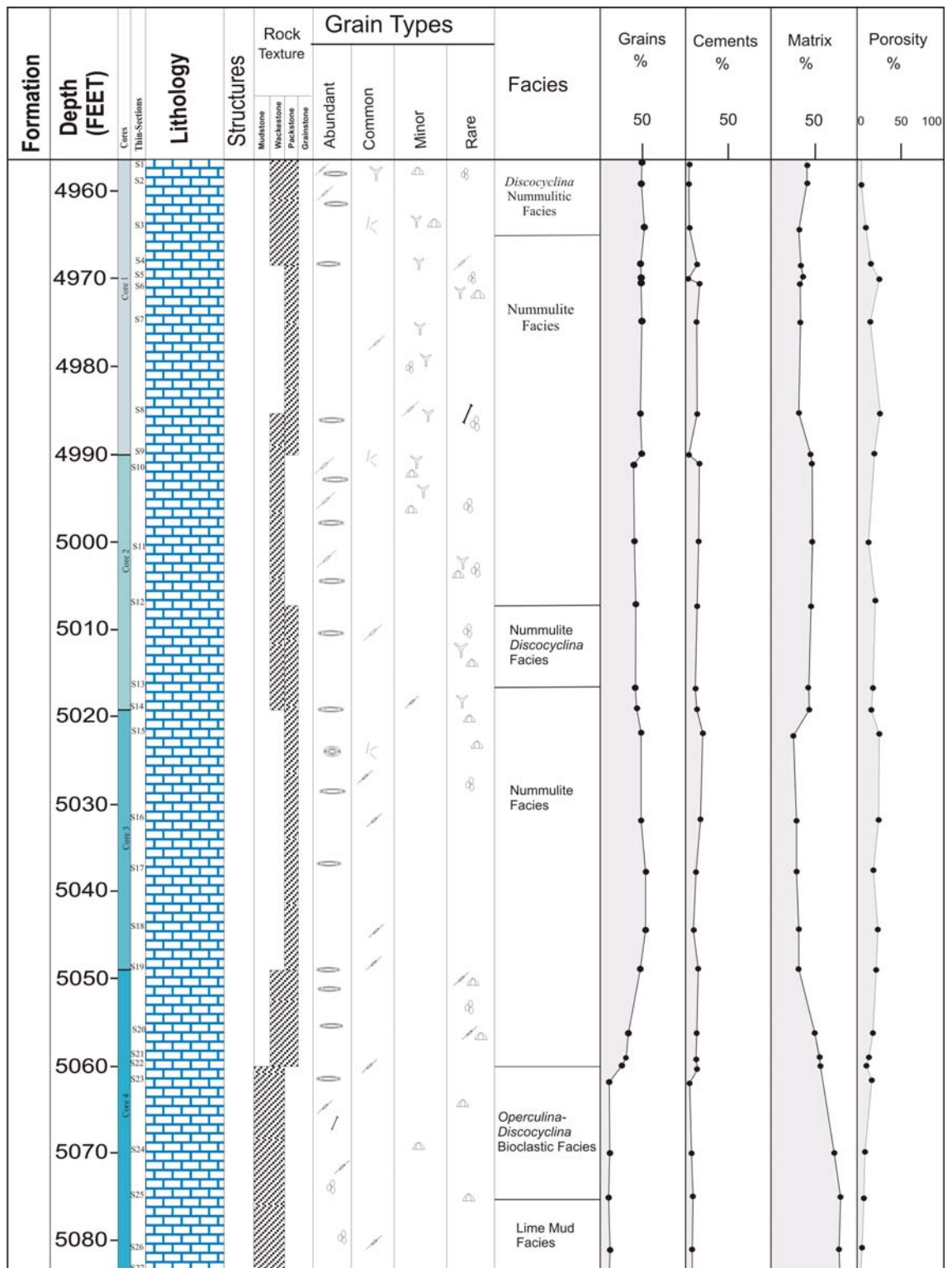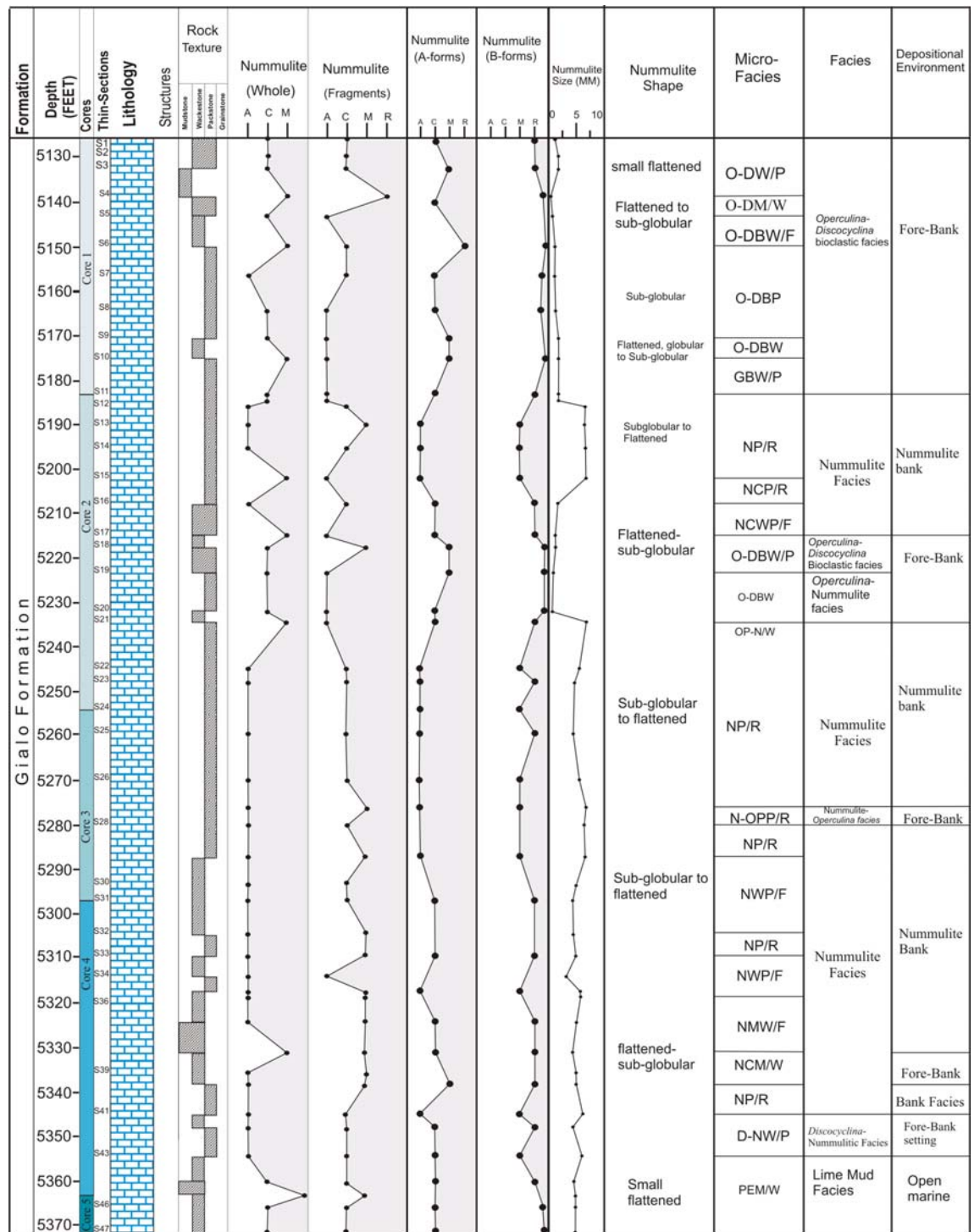
APPENDIX II

Appendix II. i. Sub-sea depth and two-way time (TWT) values of the top Gialo Formation.

Well	Depth (sub-sea) (Ft)	Two-way time (TWT) (ms)
DDD1-6	5165	1270
OOOO1-6	5000	1235
OOOO2-6	4950	1240
ZZ1	5220	1275
O15-6	5080	1250
O9-6	5100	1230
O4-6	5120	1240
O13-6	5009	1190
O3-6	4980	1195
O16-6	4990	1205
O5-6	5050	1225
O9-6	5100	1200
O12-6	5030	1210
O17-6	5000	1190
O2-6	4985	1195
O6-6	5040	1223
O10-6	5090	1240
O11-6	5020	1235
O7-6	5095	1235
01-6	5100	1238
O8-6	5100	1240
H12-6	4875	1176
H10-6	4750	1170
H2-6	5020	1210
H1-6	4725	1155
H9-6	4850	
H7-6	4750	1153

H8-6	4695	1152
H6-6	4693	1154
H4-6	4725	1158
H5-6	4730	1155
H3-6	4800	1170
H11-6	4750	1160

II.ii. Core porosity and permeability. Well OOOO1-6

Depth (FT)	Porosity (%)	Permeability (mD)	Depth (FT)	Porosity (%)	Permeability (mD)
5127	32.57	25.35	5188	29.55	89.91
5129	28.67	17.59	5191	34.53	25.41
5129	33.27	15.79	5192	26.88	32.15
5131	27.98	23.13	5197	27.32	12.56
5132	27.51	13.97	5197	27.34	21.60
5133	25.56	266.22	5199	28.77	22.51
5135	32.49	89.60	5201	21.45	52.62
5137	36.22	243.78	5202	17.72	0.72
5140	31.21	17.34	5203	25.01	9.81
5141	32.50	82.04	5205	26.49	5.27
5143	26.12	12.44	5207	23.65	2.36
5145	32.09	179.39	5208	25.59	8.57
5146	33.27	117.78	5210	24.03	2.80
5149	29.53	23.42	5210	20.45	5.07
5150	32.23	12.26	5212	17.21	0.28
5151	26.89	5.49	5213	19.22	2.64
5152	35.34	37.42	5215	25.63	4.10
5154	36.58	28.47	5216	22.82	6.23
5156	30.54	11.74	5218	18.68	1.74
5158	33.83	34.54	5219	18.69	2.10
5159	32.64	38.29	5221	20.60	3.34

5161	32.32	13.71	5222	20.73	2.08
5162	31.46	9.80	5224	17.88	2.55
5164	33.69	12.25	5224	20.59	2.71
5166	35.90	25.78	5226	20.70	3.17
5167	28.36	225.69	5228	20.06	1.97
5169	23.05	24.25	5231	22.55	3.95
5170	29.88	57.21	5232	17.11	1.31
5172	25.20	29.83	5234	17.77	1.51
5174	25.41	126.6	5235	19.38	1.29
5176	22.98	23.15	5237	19.27	1.29
5178	24.47	49.37	5238	18.88	1.11
5179	23.24	49.97	5240	19.61	1.04
5181	32.92	410.13	5241	16.94	1.26
5182	31.41	65.85	5242	13.37	0.69
5183	27.74	38.69	5244	17.65	1.62
5185	34.20	55.07	5244	14.97	1.09
5186	32.61	63.83	5245	14.96	0.7

II.iii. Core porosity and permeability. Well H4-6.

Depth (FT)	Porosity (%)	Permeability (mD)	Depth (FT)	Porosity (%)	Permeability (mD)
4906	34.20	122.00	4990	23.50	6.30
4912	35.50	132.00	4992	21.40	3.70
4919	32.00	70.00	5026	15.70	1.10
4928	27.30	39.00	5030	23.10	2.60
4930	24.00	157.00	5049	13.40	0.90
4938	24.00	55.00	5052	20.60	2.10
4944	21.00	9.20	5055	15.10	1.20
4946	18.50	47.80	5058	30.70	16.30
4953	27.90	53.90	5060	24.30	14.80
4963	21.30	19.10	5065	23.80	4.40

4964	9.10	0.90	5069	23.60	2.00
4966	10.00	0.70	5075	19.50	1.70
4970	10.10	0.50	5080	28.00	6.50
4971	14.00	4.30	5085	24.00	5.20
4975	20.10	0.60	5089	24.30	2.70
4980	11.40	1.10	5098	22.20	2.70
4981	23.00	4.90	5101	13.00	0.30
4985	19.80	2.80	5105	21.10	2.00
4987	25.20	6.70	5111	20.70	1.70

II.iv. Core porosity and permeability. Well H6-6.

Depth (FT)	Porosity (%)	Permeability (mD)	Depth (FT)	Porosity (%)	Permeability (mD)
4921	34.00	32.60	5037	20.60	1.80
4924	27.90	98.00	5041	22.90	1.70
4929	25.60	94.00	5042	23.20	1.90
4936	23.30	19.00	5045	24.40	2.60
4942	24.20	57.00	5047	21.60	1.00
4950	14.00	15.00	5051	19.80	0.80
4957	23.00	29.00	5056	27.60	2.90
4968	16.00	3.80	5062	19.40	4.50
4974	12.70	0.50	5068	25.80	4.90
4979	19.90	8.80	5080	26.40	4.80
4981	25.60	12.20	5085	21.70	1.90
4990	15.70	1.40	5089	25.10	4.30
4998	17.30	0.80	5092	21.30	1.40
5002	16.60	0.90	5097	18.90	0.90
5011	19.90	1.30	5101	15.00	0.20
5020	25.00	4.20	5106	20.30	1.10
5026	25.80	3.40	5109	21.90	1.30
5031	20.60	1.10	5113	17.90	0.70

II.v. Core porosity and permeability. Well H10-6.

Depth (FT)	Porosity (%)	Permeability (mD)	Depth (FT)	Porosity (%)	Permeability (mD)
4957	27.70	2212.00	5032	15.70	3.90
4959	27.80	24.50	5038	12.60	0.60
4964	22.90	4.90	5044	13.10	0.95
4968	24.20	17.10	5049	13.20	1.60
4985	11.80	1.80	5056	26.50	9.30
4990	18.50	4.80	5059	23.30	4.50
4991	16.20	1.50	5060	23.40	5.50
5000	22.90	10.90	5062	24.40	3.20
5007	9.90	0.62	5070	19.70	1.10
5015	12.10	1.86	5075	13.00	0.30
5019	17.20	2.50	5081	16.70	0.60
5022	12.30	68.90	5084	18.50	0.72

II.vi. Well data available

Well	OOOO1-6	O3-6	H4-6	H6-6	H10-6
KB (ft)	96'	148'	164'	194'	156'
TD	10,088'	5,535'	5,265'	5,270'	5,260'
Arida	NL	NL	2,770' (-2606')	NL	2,790' (-2634')
Augila	4,736' (-4640')	NL	4,480' (-4316')	4,425' (-4231')	4,489' (-4333')
Gialo	5,105' (-5009')	5,117' (-4969')	4,900' (-4736')	4,879' (-4685')	4,930' (-4774')

Gir	6,235' (-6139')	NDE	NDE	NDE	NDE
Kheir	7,205' (-7109')	NDE	NDE	NDE	NDE
Zelten	7,374' (-7278')	NDE	NDE	NDE	NDE
Harash	ND	NDE	NDE	NDE	NDE
Khalifa	7,892' (-7796')	NDE	NDE	NDE	NDE
Hagfa	8,177' (-8081')	NDE	NDE	NDE	NDE
Kalash	9,660' (-9564)	NDE	NDE	NDE	NDE
Waha	NP	NDE	NDE	NDE	NDE
Sirte Shale	NP	NDE	NDE	NDE	NDE
Sirte Dolomite	NP	NDE	NDE	NDE	NDE
Bahi/Gargaf	9,734' (-9638')	NDE	NDE	NDE	NDE

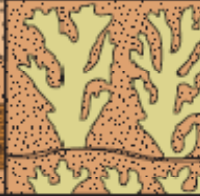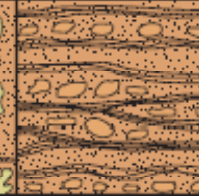NP: Not present

NL: Not logged
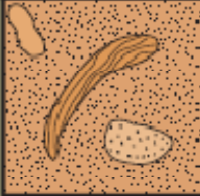
ND: Not differentiated

NDE: Not deep enough

APPENDIX III

III.i. Dunham (1962) Classification with Embry and Klovan (1971), James (1984) and Wright (1992) Modifications

Dunham's classification (1962) and its modification by Embry and Klovan (1971), James (1984) and Wright (1992) (Figures below) deal with depositional texture. For this reason, his scheme may be better suited for rock descriptions that employ a hand lens or binocular microscope. Embry and Klovan (1971) and James (1984) have modified Dunham's classification to include coarse grained carbonates. In their revised scheme, a wackestone in which the grains are greater than 2mm in size is termed a floatstone and a coarse grainstone is a rudstone. Both terms are extremely useful in the description of limestones. Wright (1992) introduced several useful new terms, including "cementstone", "condensed grainstone", and "fitted grainstone" for cement-rich or chemically compacted limestones.

Classification table of skeletal limestones (Embry and Klovan, 1971).

DEPOSITIONAL				BIOLOGICAL			DIAGENETIC			
Matrix-supported (clay & silt grade)		Grain-supported		In-situ organisms			Non-obliterative			Obliter-ative
<10% grains	> 10% grains	with matrix	no matrix	Encrusting binding organisms	Organisms acted to baffle	Rigid organisms dominant	Main component is cement	Many micro-stylolitic grain contacts	Mostly micro-stylolitic grain contacts	Crystals > 10 µm
Calci-mudstone	Wacke-stone	Pack-stone	Grain-stone	Bound-stone	Baffle-stone	Frame-stone	Cement-stone	Condensed grainstone	Fitted grainstone	Spar-stone
	Float-stone	Rud-stone								Crystals < 10 µm
	Grains >2mm									Microspar-stone

Biological

Major processes influencing limestone texture

Depositional   Diagenetic

Classification table of limestones (Wright, 1992).

III.ii. Porosity

Porosity in limestones is rather different from that in sandstones. It is much more erratic in type and distribution within a reservoir and is generally much lower than in sandstone reservoirs (Choquette and Pray, 1970). Carbonate reservoirs with as low porosity as 5-10% are known, while most sandstone reservoirs have values of 15-30%.

Because of the broad-spectrum of diagenesis that affects carbonate rocks, the final porosity in carbonates may or may not be related to depositional environments. Unlike other lithologies, the original primary porosity in carbonate may be totally destroyed during diagenesis but significant new secondary porosity may also be created.

A number of classifications of porosity are available (reviewed in Flügel, 1982) but the most widely used is that by Choquette and Pray (1970) (Figure below). The types of porosities encountered are quite varied. Interparticle, intraparticle, growth-

framework, shelter and fenestral porosities are depositional porosities. Porosity formed during diagenesis may be moldic, channel, intercrystalline, fracture or vuggy porosity. An additional type not included by Choquette and Pray (1970) is stylolitic porosity. While in many limestones stylolites represent zones of very low or zero porosity, they can act both as porosity and as important conduits for fluid migration (Longman, 1982).
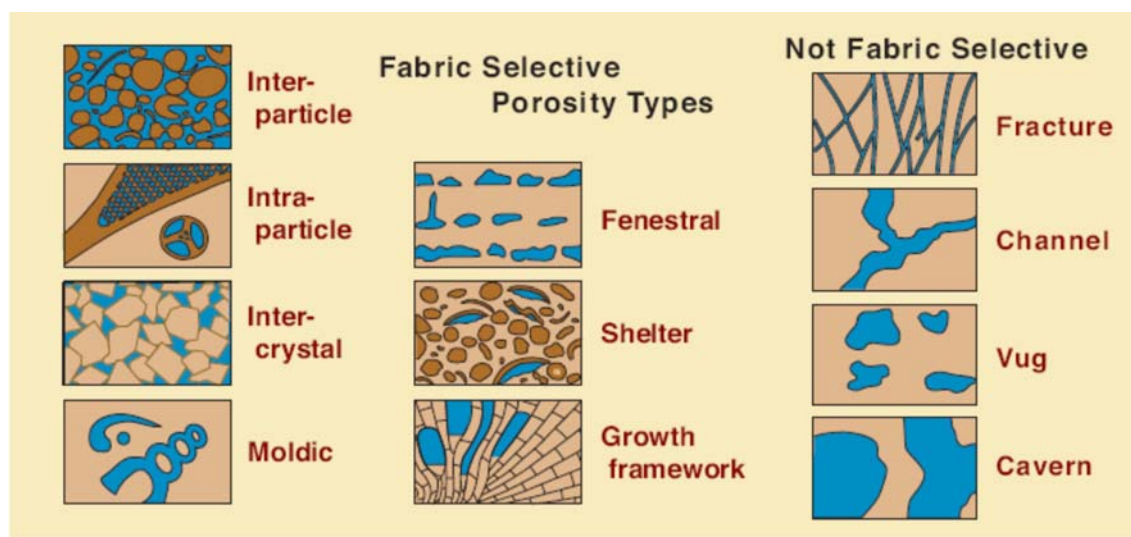
Basic fabric and non-fabric-selective porosity types (Choquette and Pray, 1970).

III.iii. Isotope methodology

Stable isotope geochemistry of carbonate rocks involves the measurement of $^{18}O/^{16}O$ and $^{13}C/^{12}C$ ratios, and comparing these to the ratios in a standard — typically VPDB (a belemnite) for carbonate rocks and/or SMOW (standard mean ocean water) for waters and for some carbonate and silicate rocks. Isotopic results are given as delta values (δ) between the isotopic ratio of the analyzed sample and that of the standard.

Interpretation of stable isotopic data is inherently complex because there are more variables than knowns. The $^{18}O/^{16}O$ incorporated into a calcite or dolomite, for example, is a function of water temperature; higher temperatures yield precipitates with more ^{16}O relative to ^{18}O and thus "lighter" or more negative ratios relative to the PDB standard. Unfortunately the $^{18}O/^{16}O$ ratios of precipitated carbonates are also a function of the $^{18}O/^{16}O$ ratios in the waters from which they precipitate. Thus, carbonates precipitated from fresh meteoric waters will also have "light" or negative isotopic ratios relative to VPDB. Further complications come from possible secular variations in the

isotopic chemistry of seawater, from isotopic fractionation in the biological precipitation of tests and shells (fractionation that varies even down to the species level), and from a wide range of isotopic water compositions (resulting from isotopic fractionation during repeated evaporation events) and from other factors.

Carbon isotopic variation is less dependent on temperature, but does depend on biological fractionation processes, the carbon isotopic composition of water (which also shows secular variations), organic and inorganic decomposition of organic matter, and the possible introduction of plant- or soil-derived CO_2.

The diagram below show the generalized isotope fields ($\delta^{18}O$ and $\delta^{13}C$) for a selection of carbonate components, sediments, limestones, dolomites and concretions and some of the factors that control the $\delta^{18}O$ (bottom) and $\delta^{13}C$ (right) compositions of precipitated carbonates, based on Hudson, 1977 and Moore, 1989, Source, Nelson and Smith, 1996).
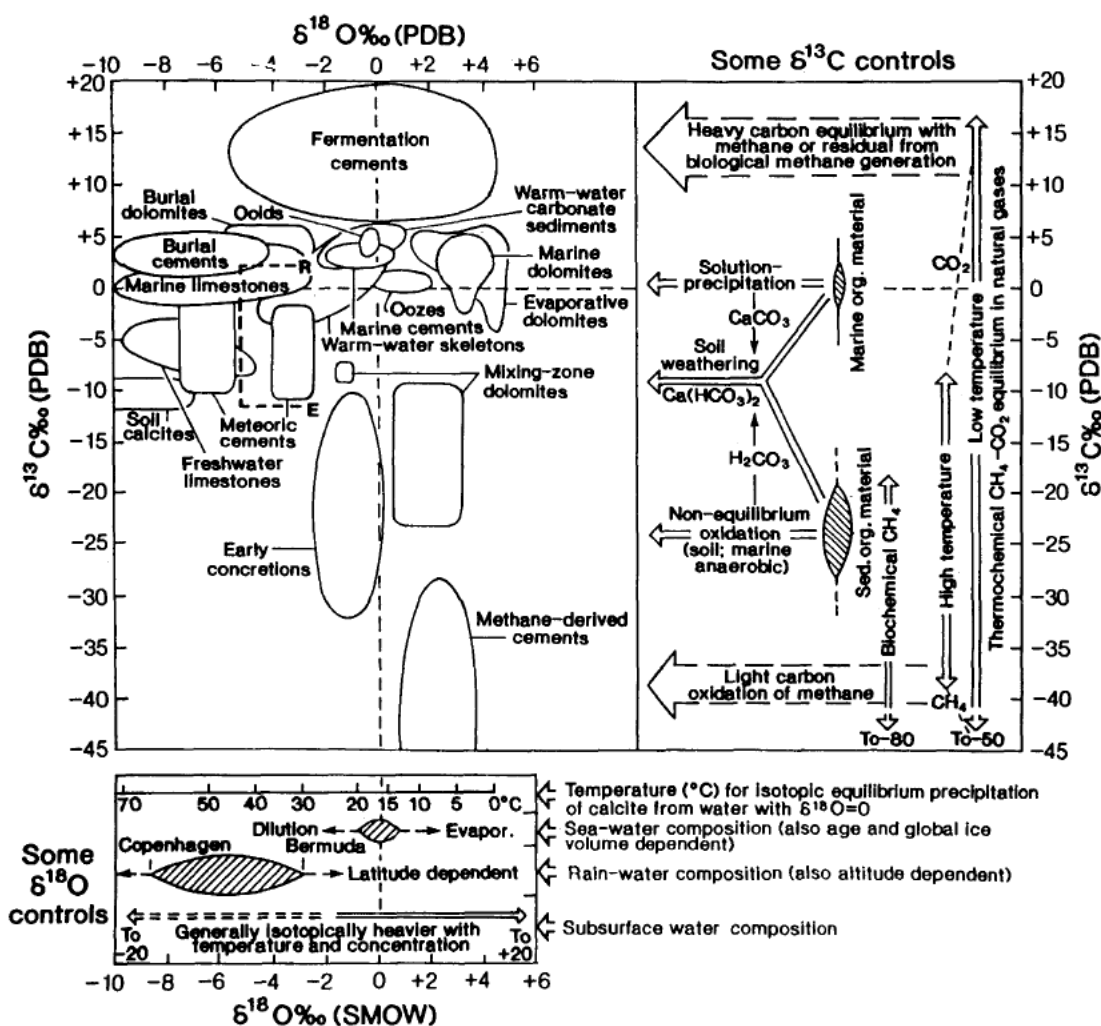
Twenty-two specimens were sampled for carbon and oxygen isotope analysis from different facies of the Gialo Formation after detailed petrographic study. A microscope and drill assembly was employed to extract powdered carbonate (including bioclasts, cements and micrite) from carefully selected areas of core. These included 14 samples of carbonate skeletons (nummulites, echinoid, brachiopods, bryozoa, *Discocyclina, Operculina* and mollusc) and 6 samples of different cements.

An aliquot of powdered sample (c. 10mg) was time reacted with anhydrous phosphoric acid in vacuo at $16^{o}C$ for 2 hours. This low temperature and short reaction time dissolves the calcite but leaves any dolomite present unreacted. The CO_2 liberated was separated from water vapour and collected for analysis.

Measurements were made on a VG Optima mass spectrometer. Overall analytical reproducibility for the samples was normally better than 0.1 for $\delta^{13}C$ and $\delta^{18}O$. Isotope values are reported as per mil deviations of the isotopic ratios ($^{13}C/^{12}C$ and $^{18}O/^{16}O$) from standards (VPDB for carbonates).

All geochemical analyses were carried out at the NERC Isotope Geoscience Laboratory (NIGL), British Geological Survey, Keyworth, Nottingham, under the direction of Dr. Melanie Leng.

Diagenetic trends of carbon and oxygen isotopic ratios in limestones

This diagram below (adapted from Lohmann, 1988) shows the effects of meteoric alteration in shifting rock chemistry to lighter $^{18}O/^{16}O$ ratios and variably lighter $^{13}C/^{12}C$ ratios (depending on the ratio of water to rock involved in the diagenesis). The "burial trend" arrow shows the extension of that alteration into the subsurface. The right-hand diagram (adapted from Irwin et al., 1977) shows the $^{13}C/^{12}C$ ratios in CO_2 liberated during burial diagenesis of organic matter. Some of that may be incorporated in burial-stage calcite cements.